FRIEDRICH-SCHILLER-
UNIVERSITÄT
JENA

Chemisch-Geowissenschaftliche Fakultät

Preparation of Functional Polymers and Block Copolymers *via* Post-Polymerization Modifications for Biomedical Applications

Dissertation

Zur Erlangung des akademischen Grades
doctor rerum naturalium
(Dr. rer. nat.)

vorgelegt dem Rat der Chemisch-Geowissenschaftlichen Fakultät der
Friedrich-Schiller Universität Jena

eingereicht von
M. Sc. Carsten Rössel
geboren am 11.10.1990 in Leipzig

Gutachter:

1. Prof. Dr. Felix H. Schacher (Friedrich-Schiller Universität Jena)
2. Prof. Dr. Ivan Vilotijević (Friedrich-Schiller Universität Jena)

Tag der öffentlichen Verteidigung: 20.10.2021

»Statt zu klagen, daß wir nicht alles haben,
was wir wollen,
sollten wir lieber dafür dankbar sein,
daß wir nicht alles bekommen,
was wir verdienen.«

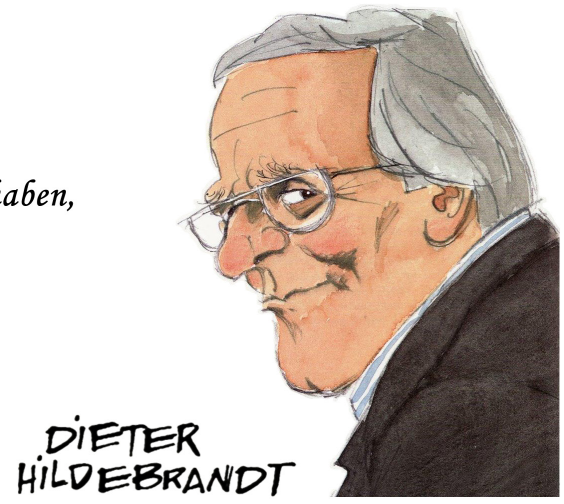

Zeichnung mit Genehmigung von Dieter Hanitzsch

Table of contents

1 Introduction

The term polymer composed of the two Greek words $\pi o \lambda \upsilon \varsigma$ (polus, meaning a lot of, many) and $\mu \varepsilon \rho o \varsigma$ (meros, meaning part, component).[1] In 1832, the Swedish chemist Jöns Jacob Berzelius suggested using the word polymeric in the context of isomers, which have the same composition but disparate properties. He wanted to distinguish between compounds with identical relative formulas, but a different absolute number of atoms, *e.g.* methylene (CH_2) and butene ($C_4H_8 = (CH_2)_4$).[2] In contrast to the actual definition, Berzelius' concept of repeating units refers to molecules with low molar masses. Later on in the 1920s, Hermann Staudinger postulated, in the context of natural rubber (polyterpene), the existence of macromolecules, which have high molecular weights and consist of covalently connected monomers.[3] At this time, it was known that rubber is based on isoprene, but most chemists believed that natural rubber were colloids of cyclic isoprene dimers or oligomers, which could be isolated by the purification of rubber.[4] Staudingers' conclusion about macromolecules involving covalent bonds was partially based on Samuel Shrowder Pickles' work, who presumed rubber consisted of a linear structure (Scheme 1.1).[5] Therefore, the early 20th century is considered the birth of macromolecular chemistry as a new research field despite the previous modification of polymers.[5–7]

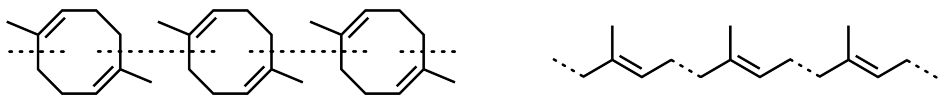

Scheme 1.1: Predicted structures of rubber by C. D. Harries[8] (left) and S. S. Pickles[9] (right).

Due to the evolution of polymer science, new materials were developed with definable features and used in nearly all areas of everyday life. Based on their low weight, plastics are applied in consumer packaging, for bottles, camping tableware, glass replacement, electrical device housing, and in the components of cars, trains and aircraft. Synthetic macromolecules are also found in contact lenses, detergents, textiles, as well as cosmetics such as toothpaste, shampoo and creams. The beneficial properties of these materials and their cheap production resulted in the extensive application of polymers. As a consequence of the switch from renewable materials such as wood to plastics in combination with a reduction in the lifespan of manufactured goods and usage as a disposable material, high amounts of waste are being generated. PlasticsEurope reported that Europe produced 61.8 megatons of plastic in 2018, of which 40% was used in packaging. At the same time, 29.1 megatons of plastic waste was collected in the European Union including Norway and Switzerland, whereby 39% was exported outside of these countries. Only 32.5% of the waste was recycled, 42.6% was incinerated for energy generation, and 24.9% was deposited

into landfill.[10] By improper management, plastic waste has leaked into the environment and a smaller part enters the oceans, *e.g.* in 2010 approximately 32 megatons of plastic debris was released into the surroundings, of which 8 megatons went into the ocean.[11, 12] An exploration in the North Sea revealed that only 15% of the plastic pollution floats on the water's surface, 15% returns to the coast, and 70% sinks to the seabed.[13] The Great Pacific Garbage Patch is one accumulation consisting of at least 79,000 tonnes of plastic on the surface of the water with an area of 1,600,000 km^2 between California and Hawaii in the North Pacific Gyre.[14] Such garbage patches are further observed in other major ocean gyres in the South Pacific, North Atlantic, South Atlantic, as well as the Indian Ocean, and additional plastic accumulations were found in enclosed seas such as the Mediterranean Sea and the Bay of Bengal.[15, 16] Under marine conditions, the synthetic material degrades or fragments into microplastics with a diameter below 5 mm by mechanical abrasion and UV light irradiation by sun exposure, which is retarded *via* surface fouling.[17, 18] In contrast to macroplastics that lead more to visible harm to animals, microplastic particles, with a micrometer size or lower, can be ingested by many marine species like plankton, coral, mollusks, fish, seabirds, and cetaceans. Microplastics negatively affect these marine animals in terms of their reproduction, growth, development and life expectancy.[19, 20] In this way, the synthetic material enters into the food chain and is taken up by terrestrial species. Another source of microplastics is the abrasion of tires, brake linings, synthetic fibers, and artificial turf resulting in air pollution with an expansive distribution, even to remote areas through deposition *via* rain and snow.[21, 22] Moreover, microplastics from the abrasion of synthetic textiles during laundry, as well as the industrial production of microbeads for personal care products, ends up in sewage sludge, which is used as fertilizer in agriculture, and which ultimately contaminates terrestrial and freshwater ecosystems.[22–24] Small synthetic polymer particles that predominantly consists of poly(ethylene), poly(propylene) and poly(vinyl chloride) have already been detected in beverages like water and beer, and so it is safe to assume that human food sources have also been contaminated with microplastics.[25] Currently, the impact of microplastics on human health is highly disputed. However, we have already witnessed an increased incidence of respiratory symptoms or pulmonary disease in industrial workers who inhale polymer particles over a long time period. Furthermore, different animal experiments have also revealed that the uptake of microplastics in water have toxic effects.[26, 27] Currently, a responsible handling and disposal of synthetic materials is required to protect the environment, and our delay in implementing appropriate protocols may have drastic consequences for us and the natural world. The use of biodegradable polymers, a rise in recycling, the reduction of disposable plastic products and packaging are slow changes currently underway.

1.1 Controlled Polymerization Techniques

The preparation of polymers by the addition of small molecules can occur *via* either a step-growth or chain-growth reaction. In a step-growth polymerization, bi- or multifunctional monomers are used, and a high conversion is necessary to reach high molar masses due to the formation of many dimers, trimers and oligomers at a moderate monomer consumption. In contrary to that, high degrees of polymerization are achieved at lower conversions by chain-growth reactions, because of a perpetual monomer addition to the reactive center from the initiator at the chain ends until deactivation.[28] Depending on the active species, the reactions can be divided into cationic, anionic, coordinative, or radical polymerization. Additionally, Michael Mojzesz Szwarc introduced the term living polymerization in 1956 as the absence of termination or side reactions, such that there is still an active chain end after complete conversion.[29, 30] This enables the addition of further monomers to prepare block copolymers as demonstrated by the anionic preparation of poly(styrene) and its block extension with isoprene.[30] At least through radical combination and disproportionation with an increased probability at high conversions, radical polymerizations are not living chain-growth reactions. However, radical polymerizations can be controlled *via* reversible deactivation or degenerative transfer. The equilibrium between active radicals and dormant species reduce the overall radical concentration resulting in a more than tenfold decrease in termination reactions.[31] Furthermore, a significantly faster initiation rate compared to the propagation rate in controlled radical polymerizations permits the formation of well-defined polymers with narrow molecular weight distributions below 1.3. By reactivation of the functional end group, block copolymers are accessible *via* controlled radical polymerization techniques. The three most common controlled radical polymerization methods are atom transfer radical polymerization (ATRP), nitroxide-mediated radical polymerization (NMP), and reversible addition-fragmentation chain transfer (RAFT) polymerization.

1.1.1 Reversible Addition-Fragmentation Chain Transfer Polymerization

The RAFT polymerization was first reported in 1998 as a controlled radical technique to prepare polymers with narrow molecular weight distributions and a linear increase in the molar mass with conversion using dithioesters.[32, 33] Nowadays, the RAFT polymerization is a well-understood and established technique. Due to the degenerative transfer, the number of active radicals resulting from the initiator and all dormant chains have an equal probability to grow. After the generation of radicals to start the polymerization, the initiator radical adds a monomer molecule and propagation can occur. At the beginning in the pre-equilibrium stage, the propagating radical adds to the RAFT agent at the reactive carbon-sulfur double bond to form an intermediate. The intermediate radical can fragment into the educts or a dormant species and a new radical for reinitiation as shown in Scheme 1.2. If the leaving group R of the chain transfer agent is homolytically cleaved from the intermediate radical, reinitiation occurs and another growing chain is formed. In the main equilibrium, the dormant chains with a RAFT end group are reactivated *via* the

attack of propagating radicals to the reactive thiocarbonyl moiety and fragmentation into growing radicals. The active polymer radicals react with the chain transfer moiety into the dormant form. At the end of the polymerization, a fraction of the polymer chains have no RAFT end group and can not be reactivated for a block extension. This is caused by the higher amount of propagating chains than available chain transfer agents through the use of a radical initiator and reinitiation of the RAFT agent. Dead chains also arise through termination reactions in the RAFT polymerization such as radical combination and disproportionation. A higher chain transfer agent to initiator ratio lead to a reduction in unfunctionalized chain ends, a lower active radical concentration, as well as the suppression of side reactions and decreased propagation rate.

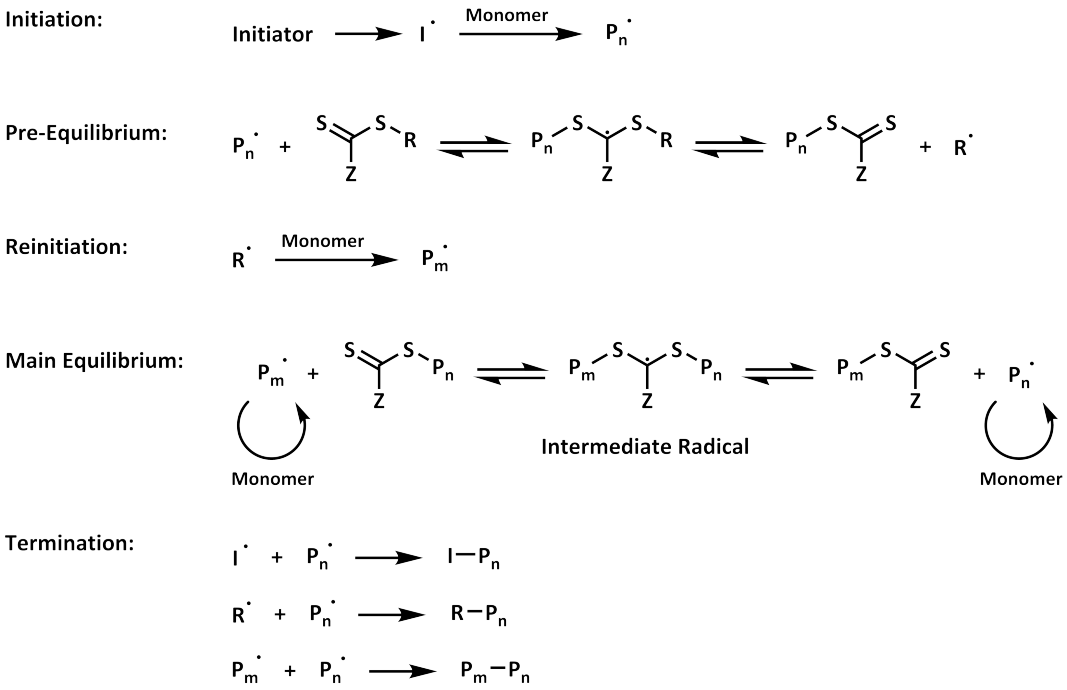

Scheme 1.2: Accepted mechanism of the RAFT polymerization using dithioesters as a chain transfer agent.[31, 33]

A variety of monomers including methacrylates, methacrylamides, acrylates, acrylamides, vinyl esters, vinyl amines, maleinimides, styrene, vinylpyridine, and acrylonitrile can be successfully polymerized in a controlled manner *via* the RAFT technique. Additionally, a variety of functionalities are tolerated, *e.g.* hydroxy groups, acids, heterocycles, aldehydes, and ketals, while mercaptans and unprotonated primary and secondary amines are not compatible with the chain transfer agent.[34–36] To afford well-defined polymers under controlled conditions, suitable RAFT agents have to be selected for the polymerizable olefins, which are simply distinguished by their reactivity into two classes. These classes are less activated monomers (LAMs) that include vinyl ethers or *N*-vinyl compounds, and more activated monomers (MAMs) such as methacrylic, acrylic and styrenic compounds. The substituent (Z) at the thiocarbonyl carbon of the RAFT agent influences the electron density at the sulfur of the thiocarbonyl group (Scheme 1.3). The reactivity of the thiocarbonyl moiety affects the addition rate of propagating radicals to the chain transfer agent, the

stability of the resulting intermediate radical after a radical addition, and their fragmentation rate. Propagating radicals in the polymerization of LAMs are highly reactive and easily add to the less reactive chain transfer agents, which form less stabilized intermediate radicals characterized by high fragmentation rates. To control the fast polymerization of LAMs, a RAFT agent with a high transfer constant is required, as well as the use of a less reactive chain transfer agent to favor the fragmentation of the intermediate radical with LAMs as a poor homolytical leaving group. In the case of MAMs, a decreased addition rate of the propagating radicals to the less reactive RAFT agent leads to a low transfer rate, broader molecular weight distributions, and a poorly controlled polymerization.[37, 38]

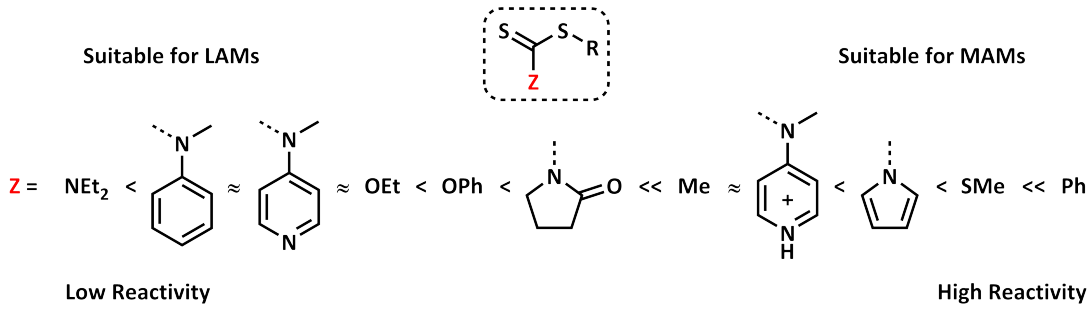

Scheme 1.3: Reactivity of typical thiocarbonyl moieties used as RAFT agents dependent on their substituent (Z) at the thiocarbonyl carbon.[34]

Furthermore, universal and stimuli-responsive or switchable RAFT agents have been developed to prepare well-defined copolymers with combinations of both monomer classes (Scheme 1.4). Chain transfer agents such as *N*-pyridin-4-yl-dithiocarbamates are suitable to control the radical polymerization of LAMs, and by protonation the electron density of the thiocarbonyl group is reduced, which enables the RAFT polymerization of MAMs with narrow dispersities. For the preparation of block copolymers containing MAMs and LAMs, the block comprising MAMs must be synthesized first due to the poor fragmentation of the propagating radicals of LAMs at the chain transfer agent in comparison to the terminal radicals of MAMs.[39] Universal RAFT agents with a moderately reactive thiocarbonyl moiety such as 4-chloro-3,5-dimethylpyrazole-1-carbodithioates are also suitable to control the polymerization of LAMs as well as MAMs, and also allow the preparation of statistical copolymers with both monomer classes. Derivatives of 3,5-dimethylpyrazole-1-carbodithioates are used to polymerize various monomers with narrow molecular weight distributions for acrylates, acrylamides, styrene and vinyl acetate, but high dispersities between 1.3 and 1.5 are observed for methacrylates.[40]

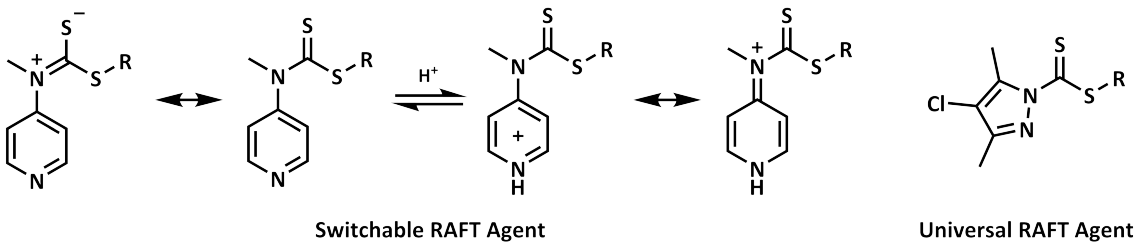

Scheme 1.4: Example of a switchable RAFT agent in comparison to a universal chain transfer agent.

In addition to the Z-substituent at the thiocarbonyl carbon of the RAFT agent, the R-group attached to the sulfur atom also influences the polymerization behavior. This group must be a much better homolytic leaving group than the propagating radical to prevent retardation and broader molecular weight distributions by slow reinitiation. Stabilization of the leaving radical moiety (R) through hyperconjugation by various groups and steric effects facilitates fragmentation as shown in Scheme 1.5. However, reinitiation of the leaving radical from the chain transfer agent must be faster than the propagation of growing chains in order to achieve a controlled RAFT polymerization without inhibition or retardation. Generally, tertiary alkyl radicals and benzylic radicals are inefficient at reinitiating most LAMs.[31]

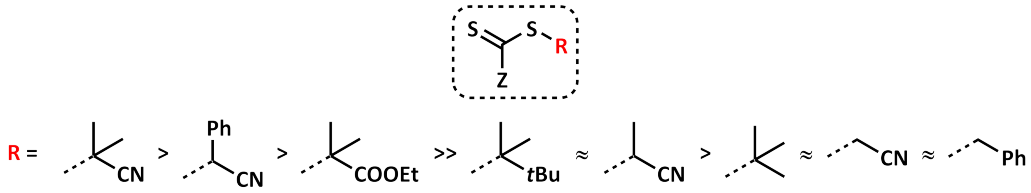

Scheme 1.5: Variation in the RAFT agent fragmentation rate with different R-substituents at the sulfur atom.[31]

After polymerization, the colored RAFT group can be modified to introduce a functional end group, to attach another polymer, or can be removed as some applications require (Scheme 1.6). One method to eliminate the thiocarbonylthio moiety is thermolysis in a temperature range of 120-200 °C.[41] The treatment of the polymer with hydrogen peroxide converts the RAFT end group into a hydroxy moiety, which enables further functionalization *via* a Steglich esterification.[42] A chain transfer moiety with an electron-withdrawing substituent (Z) can react as a dienophile in a hetero Diels-Alder reaction with a conjugated diene such as derivatives of cyclopentadiene to reversibly connect the polymer to surfaces or to couple two polymers together.[43]

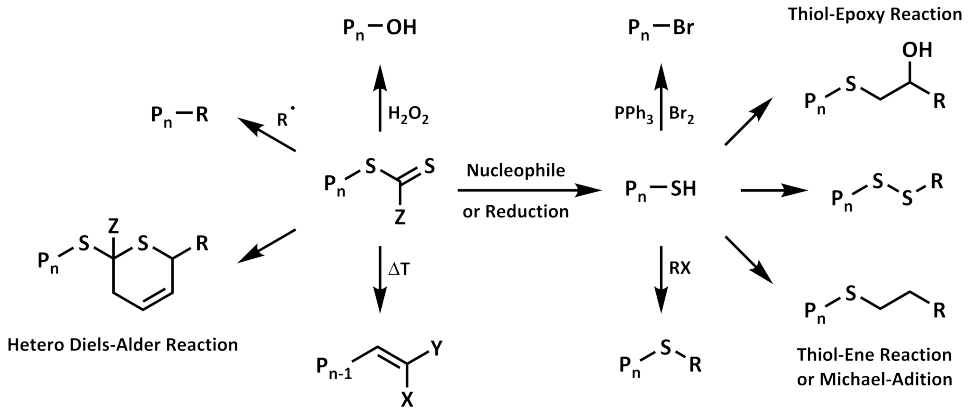

Scheme 1.6: Overview of the various transformations of a thiocarbonylthio end group following a RAFT polymerization.

Moreover, the RAFT end group can be replaced through a radical addition, fragmentation and termination by the combination of radicals using an excess of the radical initiator such as modified azo-initiators with functional groups.[41, 44] The thiocarbonylthio moi-

ety is also often transformed into a thiol by aminolysis, hydrolysis, or by reduction with sodium borohydride. Such thiol-terminated polymers can undergo a myriad of reactions: Michael addition, thiol-ene reaction, thiol-epoxy reaction, nucleophilic substitution with electrophiles, sulfur exchange reaction to a disulfide, bromination analogous to an Appel reaction, or oxidative chain coupling by disulfide formation (Scheme 1.6).[45, 46]

1.1.2 Anionic Ring-Opening Polymerization

In contrast to radical polymerizations, the number of functionalities amenable with anionic polymerizations are more limited. This is due to the basicity and nucleophilicity of the initiating or propagating anion. The reactivity of the anion depends on the kind of atom bearing a negative charge, the electron density of the anion that is influenced by the substituents, polarity and donating properties of the solvent, size and charge of the cation, temperature, concentration and the presence of additives such as salts or chelating agents.[47] These factors change the distance of the cation to the anion, or rather the equilibrium position between the different ion pair types as depicted in Scheme 1.7.

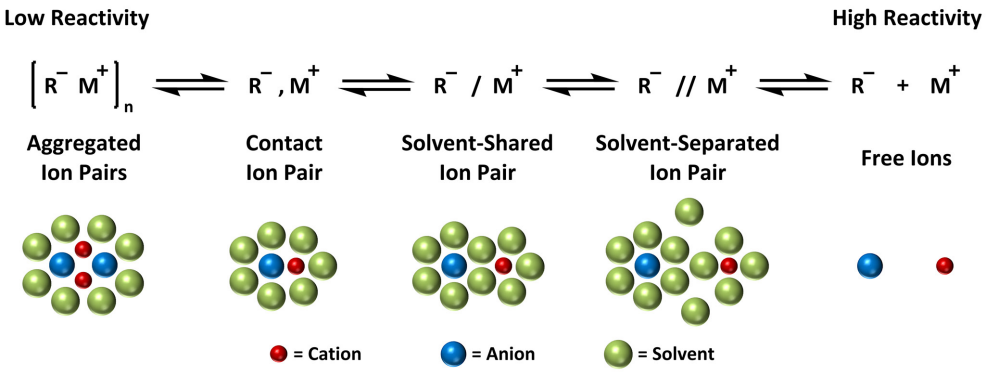

Scheme 1.7: Equilibrium of different ion associations and the corresponding schematic representation.[47, 48]

The anionic ring-opening polymerization is a special case of a chain growth reaction with nucleophilic moieties as the active center using cyclic monomers. This enables the anionic preparation of polymers containing heteroatoms along the backbone including polyether, polyester, polycarbonates, polyamides, polydepsipeptides, and polysiloxanes. Generally, the ring strain of the cyclic monomers facilitate the polymerization, as well as an electrophilic carbonyl carbon in the ring such as lactones, lactames, or cyclic carbonates. A variety of heterocyclic compounds are applied in anionic ring-opening polymerizations as shown in Scheme 1.8. However, cyclopropanes and cyclobutanes can only be anionically polymerized with electron-withdrawing substituents, which polarize the carbon-carbon bond and stabilize the propagating anion.[49]

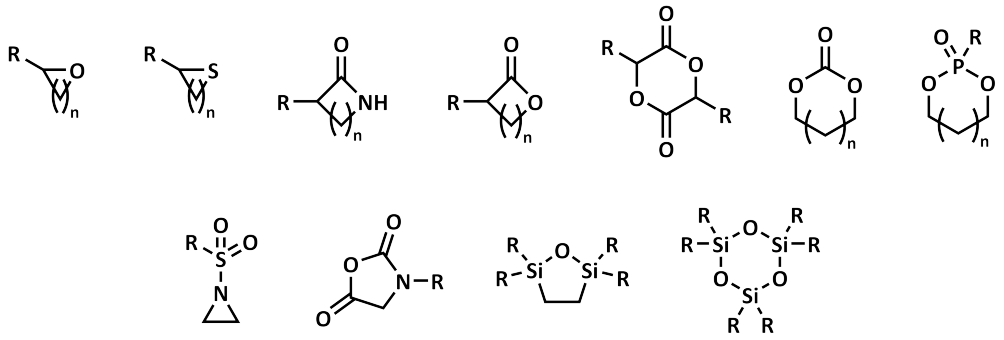

Scheme 1.8: Cyclic monomers polymerizable *via* anionic ring-opening polymerization.[49–52]

Polyethers prepared from epoxides are commonly used in cosmetics, food additives, pharmaceuticals, medical applications, lubricants, softeners, as well as surfactants, just to name a few examples. More than 33 megatons of polyethers are produced every year, which are mostly poly(ethylene oxide), poly(propylene oxide), and poly(butylene oxide). Besides the industrial production of these materials, academic research involves further monomers like higher alkene oxides, epichlorohydrine, glycidyl amines, and a variety of glycidyl ethers, which are synthesized and anionically polymerized for specific applications. The polymerization of oxiranes can be initiated with different nucleophiles including carbanions, oxyanions, thiolates, or secondary deprotonated amines that attack the monomer *via* an S_N2 reaction. After initiation, the propagating anion adds more epoxides until complete consumption of the monomer or termination occurs (Scheme 1.9). By using lithium as a counterion of the alkoxide initiator in the oxyanionic polymerization, it is only possible to add one monomer due to the strong bond between the lithium ions and alkoxide anions with a partial covalent character. Propagation with lithium counterions can be realized by using additives like phosphazene bases as a complexing agent to reduce the interaction between lithium cations and the initiated alkoxide chain ends and changing the ion association.[53, 54]

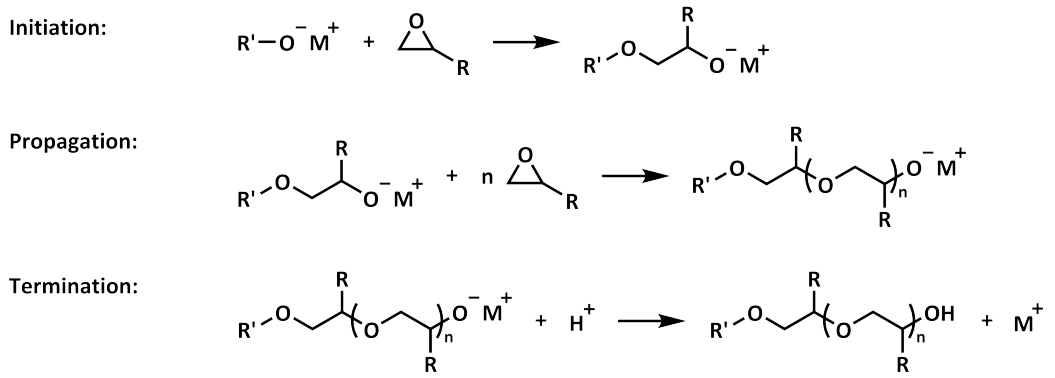

Scheme 1.9: The mechanism of an anionic ring-opening polymerization of epoxides initiated by a metal alkoxide.[49]

The conventional anionic ring-opening polymerization of substituted epoxides is restricted to a limited molecular weight range due to significant chain transfer reactions. Thereby, the anionic chain end abstracts a proton from a monomer and generates an allyl alkoxide as a new propagating species as shown in Scheme 1.10. The use of larger cations

such as cesium, the addition of crown ethers or cryptands to complex the cation, as well as phosphazene cations can reduce these side reactions. This is achieved by improving the ion pair separation, or rather through a larger distance between the anionic chain end, which results in a strong enhancement of the propagation rate.[49, 53, 55]

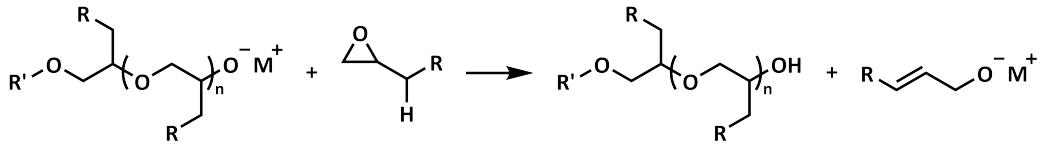

Scheme 1.10: The chain transfer reaction in a conventional anionic ring-opening polymerization *via* deprotonation of substituted epoxides at the methylene group next to the heterocycle.[53]

The anionic polymerization of epoxides can further be initiated by the attack of weaker nucleophiles such as a chloride, bromide, or azide in combination with a Lewis acid catalyst -typically triisobutylaluminium (triisobutylalan)- to activate the monomers and suppress transfer reactions. The coordination of oxiranes by Lewis acids enhances their reactivity and the polymerization rate through electron-withdrawing effects, which enables the preparation of polymers at low temperatures like 25 °C. Besides the activation of epoxides, the Lewis acid forms an "ate" complex with the weak nucleophile, which initiates an activated epoxide (Scheme 1.11). Contrary to the anionic ring-opening polymerization in the presence of additives to increase the reactivity of the propagating species, the basicity of the anionic chain end is reduced by the coordination of the Lewis acid, and transfer reactions are also prevented.[49, 53]

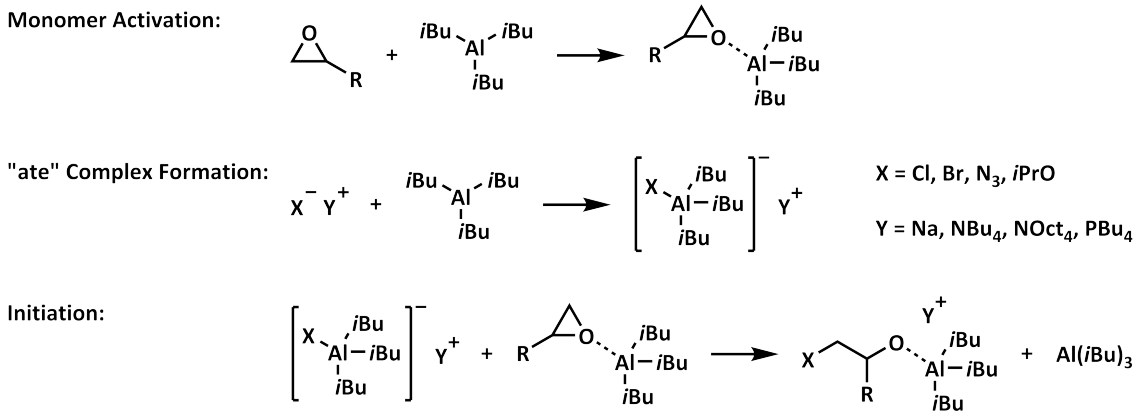

Scheme 1.11: The mechanism of initiation in the monomer activated anionic polymerization of epoxides with triisobutylaluminium.[53]

Termination of the polymerization with acidic compounds affords a hydroxy end group, which can be funtionalized *via* a nucleophilic substitution to form an ether, by esterification, a Michael addition, or by an Appel or Mitsunobu reaction. Instead of an additional reaction step to modify the end group of the polymer, such functional moieties can be introduced by the addition of reagents like alkyl halides, alkyl mesylates, acid chlorides, acid anhydrides, or Michael acceptors at the end of the oxyanionic polymerization.

1.2 Block Copolymers

A lot of industrially prepared macromolecules such as poly(ethylene) or poly(styrene) are linear homopolymers containing only one monomer unit. For a given application, the material properties of the polymer are highly important. The properties of a polymer, and hence their possible range of applications, can be further tuned by varying the polymer architecture and by the incorporation of other monomer units. Polymers can assume a variety of shapes as shown in Figure 1.1, and their topology influences the material properties. As an example, a cyclic polymer without end groups exhibits a smaller hydrodynamic radius, lower viscosity, and a higher glass transition temperature compared to its linear counterpart.[56]

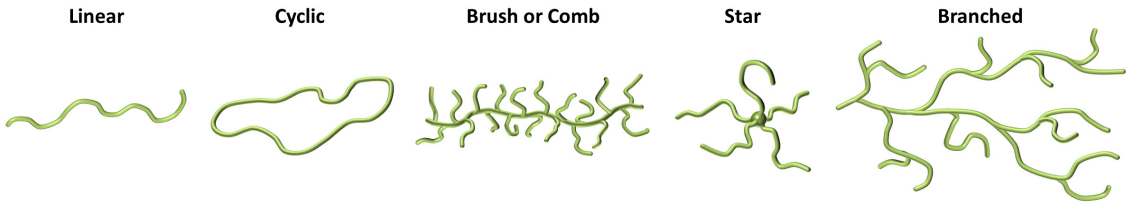

Figure 1.1: Schematic showing the possible polymer topologies that can be prepared.

As mentioned above, another method to adjust the properties of a polymeric material is through the preparation of copolymers, a polymer that consists of more than one monomer unit. The incorporation of different monomers into a polymer chain enables the desired properties of each monomer unit to be combined into one material. Besides the ratio of each monomer in the final product, the distribution of each monomer within the polymer chain also influences the material properties. The monomer distribution along the polymer chain depends on the reactivity ratio of each monomer. In the case of a two-monomer system, a copolymerization can afford either a statistical, gradient, or even an alternating distribution. The reactivity ratio is defined as the quotient of the rate constants of the homopropagation and crosspropagation of the monomer. An ideally random copolymer with an equal amount of the incorporated monomers is obtained if the product of both reactivity ratios is one. Alternating copolymers result when the product of the reactivity ratios approaches zero, which means the comonomers do not homopolymerize.[57] In the case where the two monomers have unequal reactivity ratios, gradient copolymers are usually obtained at high conversions due to a lower concentration of the preferential incorporation of one monomer over the other. Further compositions such as graft or block copolymers are accessible using controlled polymerization techniques as depicted in Figure 1.2. Additionally, even more complex macromolecular architectures are possible by combining different topologies and varying the composition of multiple monomers.

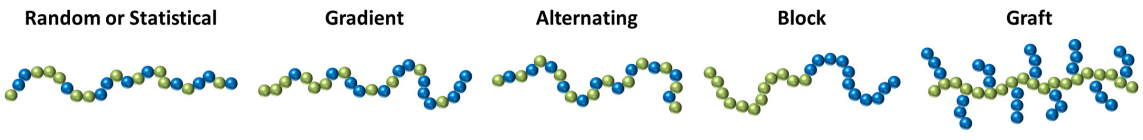

Figure 1.2: Possible compositions of copolymers with two different monomers.

Herein, we focus on linear diblock copolymers. The preparation of block copolymers enables the connection of two immiscible segments into a polymer chain, which can self-assemble in a variety of ordered nano- and microstructures. The phase separation is a result of the unfavorable mixing enthalpy of both segments in the polymer chain, as well as a small mixing entropy. This leads to the formation of microdomains with diverse morphologies of the bulky diblock copolymers as spheres, cylinders, gyroids, or lamellae (Figure 1.3). The morphology achieved depends on the molecular weight, ratio of the two blocks, and the Flory-Huggins interaction parameter (χ), which describes the difference in energy between the mixed phases of the block segments and the separated pure components.[58, 59]

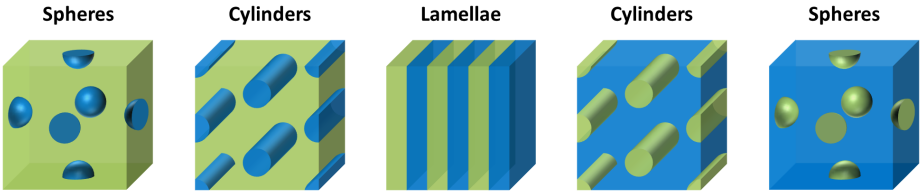

Figure 1.3: Various morphologies formed by the phase separation of diblock copolymers with increasing weight fraction of the blue component.

Furthermore, diblock copolymers containing a solvophobic and solvophilic segment can self-assemble in selective solvents into spherical micelles, cylinders, vesicles, and even into more complex structures at a certain concentration.[58] The self-assembled structure in water can be estimated using the packing parameter according to the theory of amphiphilic molecules published by J. N. Israelachvili *et al.*[60] The packing parameter p is defined by the equation: $p = V \cdot (a \cdot l)^{-1}$, where V is defined as the core volume, a as the area of the interface, and l as the length of the hydrophobic segment. From this parameter, the morphology can be predicted for the assembled structure with spheres for $p \leq 0.\bar{3}$, cylindrical micelles for $0.\bar{3} \leq p \leq 0.5$, and polymersomes in the case of $0.5 \leq p \leq 1.0$ (Figure 1.4).[58, 61, 62] Dilution of the block copolymer solution below the critical micelle concentration leads to the disassembly of the aggregated structures.

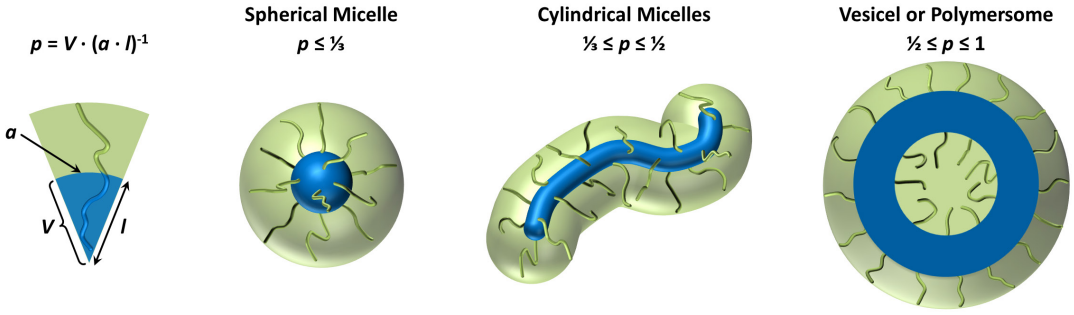

Figure 1.4: Different self-assembled structures of amphiphilic diblock copolymers in a selective solvent with packing parameter for varying block length ratios.

Self-assembled block copolymers can be applied as thin films in nanopatterning, which are used to prepare semiconductive materials.[63] Immobilization of metals or metal salts by block copolymers containing Lewis base functionalities have also been investigated for

heterogeneous catalysis to improve the efficiency of the catalytic reaction and the recovery of the catalyst without loss of its high activity.[64–66] Furthermore, amphiphilic block copolymers have been investigated as nanocarriers for drugs aiming to improve the therapeutic effectiveness of the drug whilst alleviating its side effects. The active ingredient can thereby be encapsulated in the self-assembled structures or attached to one block of the polymer. To release a drug linked to the polymer, cleavage of the connecting bond is required by applying an appropriate stimulus such as a change in the pH or redox potential.[67] To stabilize the nanocarrier structure from disassembling under shear forces in the blood stream and the probable dilution below the critical micelle concentration, the core can further be cross-linked.

1.3 Polymer Analogous Reactions

Polymer analogous reactions are the transformation of one or more functional groups along the macromolecule without changing the degree of polymerization.[68] In contrast to the reactions of small molecules, side products can generally not be separated from the polymer following the polymer modification. In the case of more than one functional group along the polymer chain, a high chemoselectivity is required for a polymer analogous reaction and high conversions for an efficient modification.[69] The polymerization techniques do not tolerate several functional groups and some can complicate the polymerization procedure especially during the preparation of copolymers. As examples, carbon-carbon double bonds are not tolerated in radical polymerizations, and amino or hydroxy groups are not compatible with anionic polymerization. Such moieties that are incompatible during polymerization can be introduced along the macromolecule in a post-polymerization modification as well as by the transformation of derivatives of groups to obtain the functional material, *e.g.* the conversion of esters into carboxylic acids. A further option is the use of monomers with protected functional groups, which can be cleaved after the polymerization. Depending on the initiator used to prepare the polymer, it is possible to functionalize the head group to a desired moiety by the attachment of small molecules. The development of controlled polymerization techniques further enables the macromolecular end group to be modified. This is described in more detail in Section 1.1.1, focusing on the modification of polymers prepared *via* RAFT polymerization.

A famous example of such a polymer analogous reaction is the preparation of poly(vinyl alcohol) starting from vinyl acetate. This is because the direct polymerization of vinyl alcohol is not possible due to the keto–enol tautomerism (Scheme 1.12). Therefore, poly(vinyl acetate) is converted into poly(vinyl alcohol) *via* an alkaline hydrolysis of the ester moieties.[70] During the saponification of poly(vinyl acetate), the polymer changes from being hydrophobic in character to being hydrophilic in character.

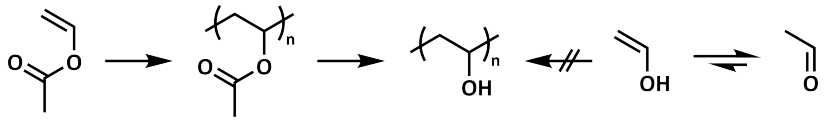

Scheme 1.12: Preparation of poly(vinyl alcohol) *via* polymer analogous saponification, which is not accessible by the polymerization of the repeating unit.

Changes in the solubility of the macromolecule can influence the polymer analogous reaction and reduce the degree of functionalization. Additionally, the post-polymerization modification of the polymer repeating unit is further affected by possible intramolecular interactions, generation of charges, and an inhomogeneity in solution of the reacting moieties compared to a small molecule reaction, caused by the linkage to the polymer backbone and spatial proximity. This can result in an acceleration or retardation of the polymer analogous reaction.[69] Besides ester hydrolysis to obtain acids and the cleavage of protecting groups, there are a vast array of chemical reactions that are used to prepare functional polymers including the quarternization of amines and alkylation of azoles to afford cationic charges along the polymer chain. A post-polymerization modification allows

the attachment of different moieties to the repeating unit of the precursor polymer resulting in functionalized macromolecules with the same degree of polymerization. Polymers prepared with monomers containing an active ester group such as *N*-hydroxysuccinimide or pentafluorophenyl esters can be substituted with various primary amines as shown in Scheme 1.13.[71]

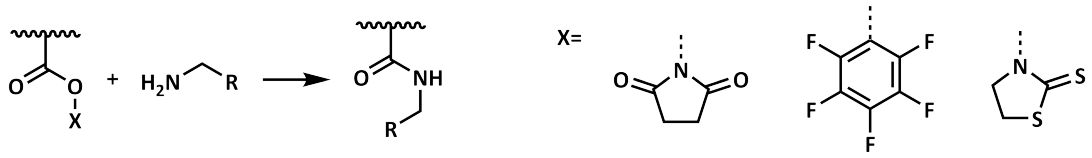

Scheme 1.13: Polymer analogous substitution of active ester moieties using primary amines.

Furthermore, epoxide pendent groups can be modified by a nucleophilic addition of azide, amines, and thiols, or functionalized with water using acids or bases as catalysts (Scheme 1.14). The azide-epoxy, amine-epoxy, thiol-epoxy reactions, and hydrolysis of the epoxide afford a hydroxy group, which can be used for a second post-polymerization modification such as an esterification.[72] On the other hand, a polymer containing amino groups is modifiable *via* a Michael addition of activated carbon-carbon double bonds such as acrylonitrile, acrylates, acrylamides, or vinyl sulfones.

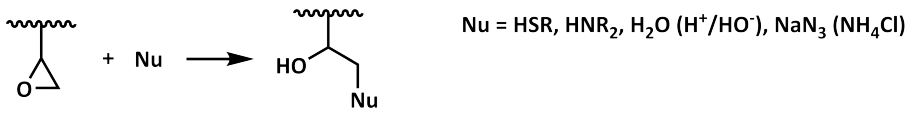

Scheme 1.14: Post-polymerization modification of polymer pendent epoxide groups using various nucleophiles.[72]

Cycloaddition reactions are also used to attach desired groups along the polymer backbone. The polymer analogous reaction requires macromolecules containing functionalities with a reactive double bond such as an azide, furan, dienes, anthracene, maleimide, norbornene, or a dithioester. The most frequently applied cycloadditions for post-polymerization modifications are the Diels-Alder reaction and 1,3-dipolar cycloadditions (Scheme 1.15) especially the azide-alkyne Huisgen cycloaddition.[73]

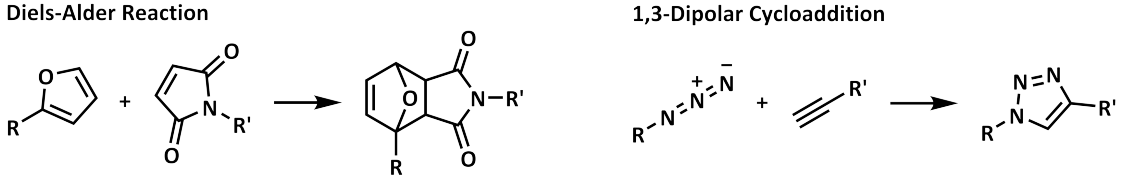

Scheme 1.15: Two examples of frequently used polymer analogous cycloadditions to modify polymers.

A further method to functionalize polymers is the thiol-ene reaction of polymer pendent carbon-carbon double bonds. Such hydrothiolations form thioethers by an anti-Markovnikov addition of the mercaptan to the olefin moiety. The thiol-ene reaction can either proceed by a radical mechanism or *via* a thiol-Michael addition in the case of activated carbon-carbon double bond with an electron withdrawing substituent. The radical

hydrothiolation is often used for post-polymerization modification of polymers as shown in Scheme 1.16. Thermal as well as photo-initiators are applied to initiate the thiol-ene reaction. The initiating radical reacts with a thiol to form a thiyl radical that subsequently adds to a carbon-carbon double bond. Next, a radical transfer of the formed intermediate carbon radical to a second thiol occurs to afford the product and a new thiyl radical, which can further add to an unsaturated carbon-carbon bond. The thiol-ene reaction can be terminated by the coupling of radicals that form disulfides. A rather unlikely side reaction is the intra- and intermolecular addition of the intermediate carbon radical to an olefinic moiety. Such an intramolecular cyclization was observed by the thiol-ene reaction of poly(butadiene) due to the small distance between the carbon-carbon double bonds.[74, 75]

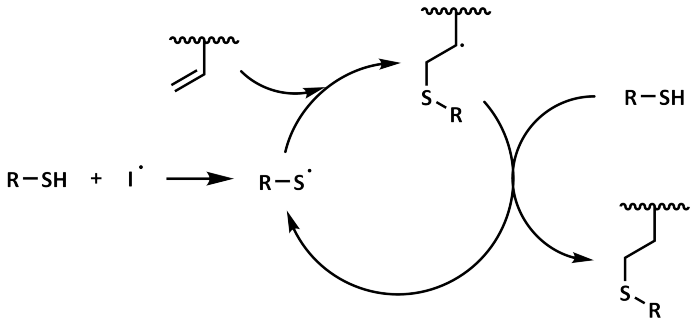

Scheme 1.16: Depiction of the reaction steps in a radical thiol-ene reaction to modify polymers.[74]

Until mow, a series of polymers, with the exception of poly(butadiene), were quantitatively modified *via* a thiol-ene reaction without any indications of side reactions such as cyclization. The macromolecules can be functionalized with a wide range of thiols and a variety of mercaptans, which are commercially available.[74]

1.4 Polyelectrolytes and Polyampholytes

Charged polymers are a class of macromolecules with ionic or ionizable groups. A prominent subclass of ionic polymers are polyelectrolytes, which contain a high amount of charged moieties or chargeable groups along the polymer backbone.[76] Polyelectrolytes can be further divided according to the charge into either polyanions or polycations, as well as by the ionic moiety as either strong or weak electrolytes (Scheme 1.17).[77]

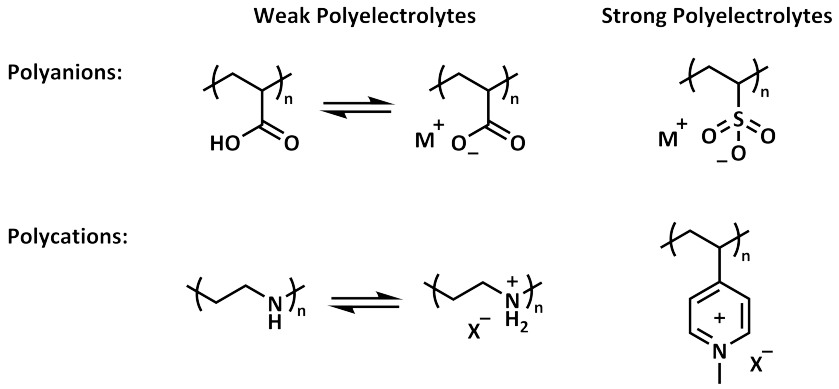

Scheme 1.17: Classification of polyelectrolytes into either weak or strong polyanions or polycations.

Polyanions typically contain carboxylates, phosphonates, and sulfonates as the ionizable or ionic groups. In contrast to the anionic moieties, polycations can consist of a variety of charged and chargeable groups that are based on amines, nitrogen-containing heterocycles, phosphonium, and sulfonium moieties. Whilst strong polyelectrolytes possess a permanent charge, the ionization of weak polycations and polyanions depend on the pH value of the solution, and the dissociation constant of the chargeable group. Therefore, several weak polyelectrolytes are stimuli-responsive materials that can be switched between a hydrophilic and a predominantly hydrophobic state by protonation and deprotonation. Examples of such polycations are poly(2-(dimethylamino)ethyl methacrylate), poly(*N*-vinylimidazole), and poly(2-vinylpyridine). The pH-responsive polyelectrolytes are interesting materials for use in biomedical applications as biosensors (*e.g.* poly(4-vinylphenylboronic acid) in glucose sensors) or as drug delivery systems with a controllable release due to changes in the pH in the body (*e.g.* methyl methacrylic acid-based polymers for colonic drug delivery).[78] Polycations have been investigated and used to complex and deliver nucleic acids as non-viral vectors in gene therapy. Cationic poly(ionic liquid)s such as poly(3-butyl-1-vinylimidazolium L-prolinate) were also successfully explored for gene transfection with low toxicities.[79] Polymeric ionic liquids are a special type of strong polyelectrolytes that consist of charged monomers with a melting point below 100 °C.[80] Due to their enhanced ion mobility, poly(ionic liquid)s can be used in electrical devices as electrolytes with a high conductivity, *e.g.* in fuel cells, batteries, or transistors. Furthermore, poly(ionic liquid)s can be used as dispersants, antimicrobial materials, and in the field of catalysis.[81] Polyelectrolytes are also added as stabilizers in cosmetics and pharmaceuticals, and are implemented in water purification as flocculants and coagulants.[82]

Another type of charged polymer are polyampholytes that contain both anionic and cationic groups along the polymer chain. A special subclass of polyampholytes are polyzwitterions with a negative and positive charge in the same repeating unit, which are both ionized over a wide pH range (Figure 1.5). In contrast to polyzwitterions with a net neutral charge, many polyampholytes exhibit an overall net charge with the exception of several weak polyampholytes in a narrow pH range near the isoelectric point.[83]

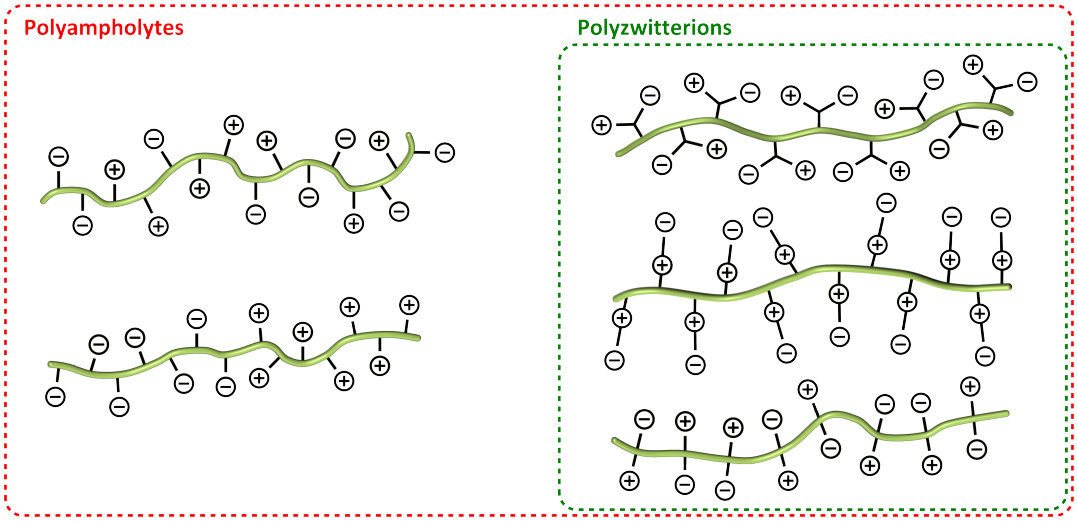

Figure 1.5: Simplified representation of several possible polyampholyte structures, including polyzwitterions.[83]

Due to the strong Coulomb interactions within polyzwitterions, the addition of a critical salt concentration of a low molar mass electrolyte is necessary to promote their solubility in water. The added electrolyte disrupts the intra- and intermolecular electrostatic interactions of the polymer and enhances its solubility. Besides its improved solubility, the antipolyelectrolyte effect observed for polyzwitterions in aqueous solutions also results in an increased solution viscosity with increasing salt concentration and a stretching of the polymer coil. However, polyzwitterions do not typically exhibit a polyelectrolyte effect as other polyampholytes do, which experience a reduced solubility at higher salt concentrations. Hydrophilic polyzwitterions exhibit superior antifouling properties and can be used as coatings or for hydrogels. Further fields of application of polyzwitterions include sewage treatment, paper reinforcement, and cosmetic formulations.[83–85]

1.4.1 Polyelectrolytes for Gene Delivery

Nucleic acids such as deoxyribonucleic acid (DNA) and ribonucleic acid (RNA) play an important role in living organisms and contain the genetic information. Simply put, the DNA in the cell nucleus is transcribed by an RNA polymerase into messenger RNA (mRNA), which is further transported into the cytoplasm where it is translated into a protein by a ribosome. A minor part of mRNA is non-coding RNA that influences gene expression, *e.g.* small inhibitory RNA (siRNA) and microRNA.[86] Nucleic acids are used in gene therapy to treat a variety of diseases including cancer and monogenic disorders. This is achieved *via* the replacement of defective genes, as well as by suppressing or inducing

the translation of proteins with their special functions.[87] A carrier or vector is required for the delivery of nucleic acids to protect them against a possible degradation in the blood by nucleases.[88] Hence, efficient virus-based carriers were developed, which have the disadvantage of a possible immune response and toxicity.[87, 88] Therefore, various non-viral vectors have been explored that are more biocompatible and cheaper to produce. However, they also exhibit a reduced transfection efficiency. Non-viral vectors are carriers containing cationic moieties that are required for the complexation of polyanionic oligo- and polynucleotides through electrostatic interactions. Several examples of non-viral vectors such as lipid-based carriers and polyelectrolytes are shown in Scheme 1.18.[88]

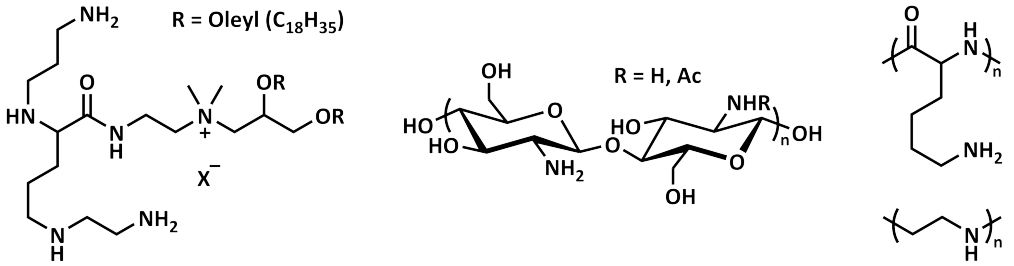

Scheme 1.18: A cationic lipid and polycations as examples of non-viral vectors for gene delivery.[88]

Numerous polyelectrolytes with different architectures and various cationic moieties were explored as non-viral vectors.[89] Block copolymers are often used as gene carriers through the formation of core-shell polyplex micelles with nucleic acids. The shell material, typically poly(ethylene oxide), of such polyplex micelles prevent undesired interactions in the biological environment, increase the circulation time in the blood, and tune the uptake into cells by using specific targeting moieties.[90, 91] The polyplex micelles in the blood stream are internalized into the cells by endocytosis. Several mechanisms of cellular uptake are known including phagocytosis, macropinocytosis, caveolae- or clathrin-mediated endocytosis, as well as a caveolae- and clathrin-independent endocytosis.[92] After cell internalization, the polyplex micelle is surrounded by a lipid membrane in an endosome. In the endosome, the pH value decreases from 7.4 to 6.5-5.5 by proton pumps, and later to 5.5-4.5 in the lysosome.[93] An endosomal escape of the polyplex micelle is required to achieve a therapeutic effect of the nucleic acid before an exocytosis or possible enzymatic degradation in the lysosome. Several hypotheses concerning the release of the polyplex from the endosome have been discussed from the proton sponge theory, to a polyplex-mediated or polymer-mediated membrane disruption.[94] The polyplex micelles dissociate in the cytoplasm, which may be caused by the presence of charged biomolecules.[94, 95] The delivered and released nucleic acids can either act in the cytoplasm or in the nucleus, which requires the nucleic acids to be further transported through the nuclear envelope as shown in Figure 1.6. In the case of plasmid DNA (pDNA) as a gene therapeutic, an uptake into the nucleus can take place during cell division or through a nuclear transport system. The active transport of nucleic acids through a nuclear pore complex requires the attachment of nuclear localization signals at the pDNA. Once in the nucleus, the pDNA is transcribed into mRNA and further translated into the desired protein. After gene expression, the

synthesized functional protein can have a therapeutic effect. An opposing strategy in gene therapy is the silencing of genes by transcription of pDNA into non-coding RNA such as siRNA, microRNA, or short hairpin RNA. The double-stranded siRNA in the cytoplasm, for example, binds to the RNA-induced silencing complex (RISC) and is cleaved into a single-stranded short RNA to release the second RNA strand. The active RISC containing the single-strand RNA interacts specifically to the complementary base-pairs of the target mRNA to induce its degradation. That results in the suppression of proteins and their function, or in gene silencing, resulting in a therapeutic effect. Such interfering RNA as siRNA can also be delivered using non-viral vectors without the nucleus membrane as an additional barrier. A further option is the delivery of mRNA as a prodrug to obtain a specific protein in the cell.[96, 97]

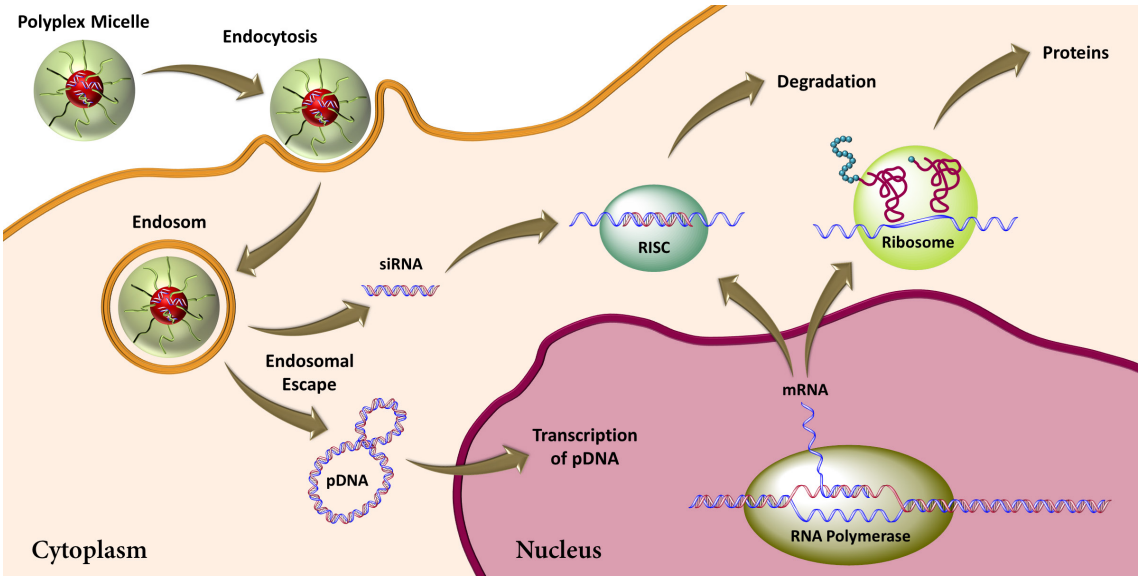

Figure 1.6: Schematic illustration of the polyplex micelle uptake, release of the nucleic acid, and the effect on gene expression.

1.5 Thesis Outline

The research in this thesis focuses predominately on the preparation and characterization of polymers and block copolymers containing ionizable or charged moieties. In the first part of this thesis, the synthesis and polymerization of various monomers is described, which are converted into polyelectrolytes and polyampholytes with a high charge density later on. Such functional materials are highly versatile, finding use as surfactants, in heterogeneous catalysis, or in biomedical applications. In the second part of this thesis, polyether-based block copolymers are prepared by anionic ring-opening polymerization for use in gene and drug delivery.

Acrylate-based polyelectrolytes and polyampholytes that were developed and characterized are described in the first part of this thesis. First, the weak polycation poly(ethyl 2-(imidazol-1-yl)acrylate) was prepared free radically, which then can be converted into a polyampholyte by ester hydrolysis. Alkylation of the polymer allows further functional groups to be attached in order to tune the properties of the polyelectrolyte, and may result in the formation of a poly(ionic liquid). Such polycations are interesting materials that are capable of binding to metal ions for use in heterogeneous catalysis or as non-viral vectors for gene delivery. The ester cleavage of poly(ethyl 2-(imidazol-1-yl)acrylate) affords a pH-responsive polyampholyte and further a polyzwitterion in combination with alkylation. The obtained polyampholytes can be applied as coatings, pH-responsive polymers for drug delivery, or perhaps to adsorb and activate carbon dioxide for reactions.[98] Furthermore, the monomer ethyl 2-(imidazol-1-yl)acrylate could be polymerized using the RAFT technique to prepare amphiphilic block copolymers, as some of these applications require self-assembled structures. A variation of the imidazole substitution from position 1 to 2 or 4 may further improve the properties of the material. This enables an alkylation without loss of the pH responsivity or an additional functionalization. The exchange of the carboxylate by a phosphonate of poly(ethyl 2-(imidazol-1-yl)acrylate) is also possible in order to obtain a polyampholyte after a post-polymerization modification as an antifouling surface coating. To investigate these new materials, the synthesis and polymerization of ethyl 2-(imidazol-2-yl)acrylate, ethyl 2-(imidazol-4-yl)acrylate, and diethyl 1-(imidazol-1-yl)vinylphosphonate was carried out.

However, the preparation of polyampholytes with different cationic groups such as poly(ethyl 2-(imidazol-1-yl)acrylate) and poly(dehydroalanine) requires the synthesis of the corresponding monomer. An ethyl 2-(hydroxymethyl)acrylate-based system could circumvent this problem *via* polymer analogous reactions. The hydroxy group can be transformed into cationic moieties by substitution after activation *via* a chlorination or sulfonylation. Additionally, a polymerization under controlled conditions *via* RAFT was attempted in order to prepare block copolymers, which is challenging for monomers such as ethyl 2-(imidazol-1-yl)acrylate and methyl 2-((*tert*-butoxycarbonyl)amino)acrylate.

In the second part of this thesis, a polyether-based system is investigated for use in gene and drug delivery. The preparation of the desired block copolymers was carried out by anionic-ring-opening polymerization of glycidyl ethers starting from poly(ethylene oxide) as macroinitiator. Poly(ethylene oxide) is used as a hydrophilic block that forms the

corona when the block copolymers self-assemble in water and mostly suppresses protein adsorption.[99] For the delivery of polynucleotides, allyl glycidyl ether was selected as the monomer for the second block, which can be functionalized with cationic groups *via* a thiol-ene reaction. A variation of the poly(allyl glycidyl ether) segment in the diblock copolymer and modification with cysteamine was carried out in order to investigate how it influences the gene delivery behavior. Moreover, functional thiols were prepared in order to compare the type of cationic groups and their effect on stability, uptake, and transfection efficiency of the polyplex micelles. Using a sequential anionic ring-opening polymerization, triblock terpolymers consisting of poly(ethylene oxide)-*block*-poly(allyl glycidyl ether)-*block*-poly(*tert*-butyl glycidyl ether) can be prepared as described by Barthel *et al.*[100] A further development of this amphiphilic polyether-based system for use in drug delivery was targeted by varying the third block. By increasing the number of repeating units in the third segment, the self-assembly into worm-like micelles may be possible, which could lead to an increase in the blood circulation time and improved uptake behavior.[101] The triblock terpolymers can be further modified in the middle segment with cationic moieties by a thiol-ene reaction to also deliver olignucleotides as siRNA besides guest molecules in the core. In order to stabilize the micellar structure, the reversible crosslinking of the core was attempted to prevent disassembly by dilution below the critical micelle concentration or change in the shape through shear forces in the blood stream.

2 Results and Discussion

2.1 Synthesis and Polymerization of Ethyl 2-(imidazol-yl)acrylates

The polyampholyte poly(dehydroalanine) with a high charge density was prepared from poly(methyl 2-((*tert*-butoxycarbonyl)amino)acrylate), which can also be converted into a polyelectrolyte by cleavage of the methyl ester or *tert*-butoxycarbonyl group.[102] Derivatives of poly(methyl 2-((*tert*-butoxycarbonyl)amino)acrylate) were applied as coatings and surfactants of nanoparticles in the field of biomedicine and for carbon nanotubes for use in biosensors.[103–106] Furthermore, poly(ethyl 2-(pyridin-2-yl)acrylate) and poly(ethyl 2-(pyrimidin-2-yl)acrylate) were prepared and modified in the research group of F. H. Schacher. To further improve the properties and expand their repertoire of applications, the cationic moiety of poly(dehydroalanine) was changed from an amine to an imidazole as shown in Scheme 2.1.

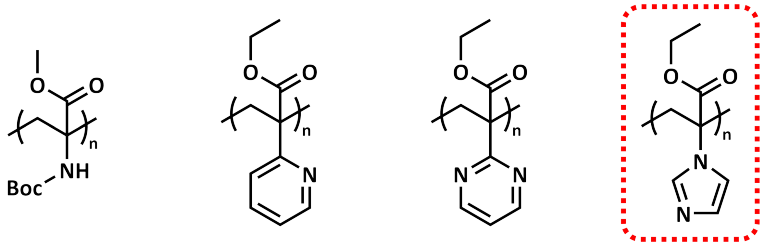

Scheme 2.1: Modifiable polymers used to access polyelectrolytes and polyampholytes.

A simple polymer containing an azole is poly(*N*-vinylimidazole). Poly(*N*-vinylimidazole) has been modified into a strong polycation, poly(ionic liquid), and polyzwitterion for applications in gene delivery, heterogenous catalysis, coatings, surfactants, and much more.[98, 107–114] Herein, the development of polyampholytes and the polyelectrolyte precursor is reported in order to design new materials that combine the properties of acrylic acid and alkylated *N*-vinylimidazole into a single ampholytic polymer. Hence, the polymer can be also used in carbon dioxide adsorption and utilization.[98]

2.1.1 Poly(ethyl 2-(imidazol-1-yl)acrylate) and its Modifications

The synthesis of ethyl 2-(imidazol-1-yl)acrylate (**1**) was first described by Yavari and Norouzi-Arasi *via* the nucleophilic α-addition of imidazole to ethyl propiolate using triphenylphosphine as a mediator at 0 °C to room temperature with a high yield of 87% (Scheme 2.2).[115] Under similar reaction conditions, Trost and Drake synthesized protected dehydroamino acids from ethyl alkynoates and sulfonamides or phthalimide in good yields.[116] Due to the low nucleophilicity of amides and imides, the reaction mixtures had to be heated to 105 °C with 10 mol% triphenylphosphine, as well as sodium acetate and acetic acid as additives.

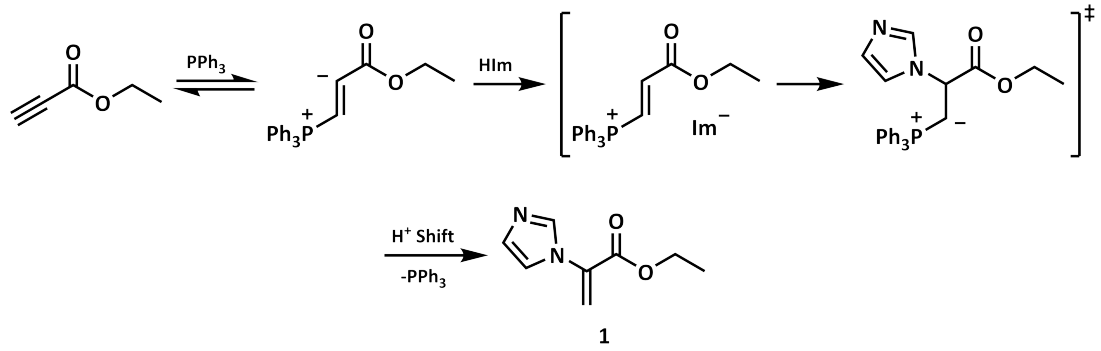

Scheme 2.2: Proposed mechanism of the triphenylphosphine-mediated synthesis of ethyl 2-(imidazol-1-yl)acrylate (**1**).[115, 116]

The preparation of **1** with 10 mol% triphenylphosphine diminished the yield from 83% to 44%. However, a further addition of acetic acid and sodium acetate resulted in an increase in the yield obtained, achieving a moderate yield of 64%. The use of a buffer reduces the nucleophilicity of imidazole by partial protonation, and influences the proton transfer steps of the reaction. A Michael addition can also occur as a side reaction with a low amount of phosphine. This was verified by the synthesis of ethyl 3-(imidazol-1-yl)acrylate (**2**) with ethyl propiolate and imidazole in chloroform (Scheme 2.3). A yield of 93% of **2** was obtained as a mixture of *E* and *Z* isomers. Additionally, a small quantity of pure ethyl (*E*)-3-(imidazol-1-yl)acrylate was isolated.

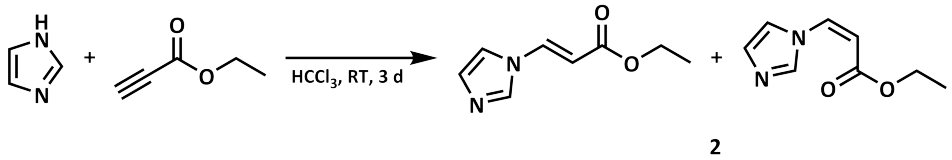

Scheme 2.3: Synthesis of ethyl 3-(imidazol-1-yl)acrylate (**2**) *via* Michael addition.

Balogh *et al.* reported the reaction of imidazole and ethyl propiolate in toluene under reflux for 2.5 hours to afford **2** in quantitative yields. Moreover, the preparation of the methyl ester derivative in chloroform at room temperature was described with a yield of 41% after 10 hours.[117] This procedure resulted in the presence of 13% methyl 3,3-di(imidazol-1-yl)propanoate as a side product due to a doubled Michael addition. This side reaction was

confirmed by the ^{1}H NMR spectroscopy (Figure 2.1) of **1** prepared with 10 mol% triphenylphosphine after column chromatography. This side product was not observed in the ^{1}H NMR spectra when acetic acid and sodium acetate were used.

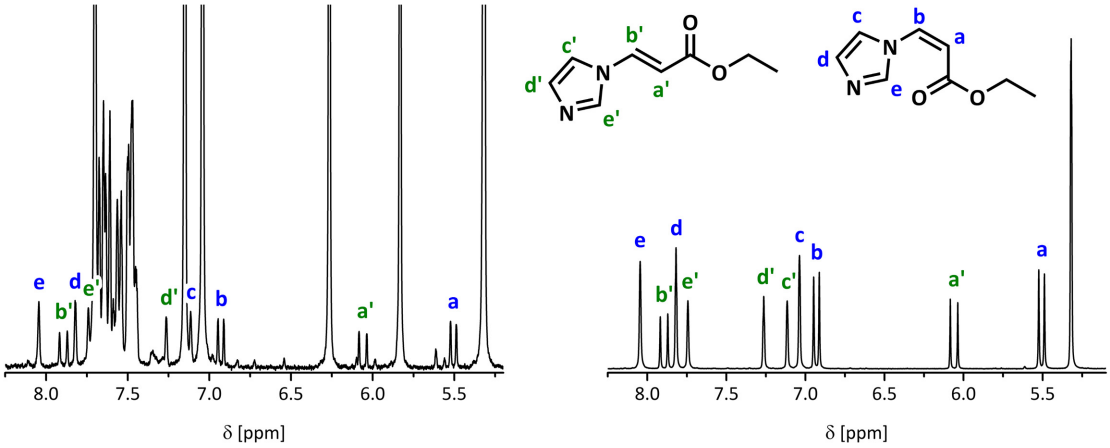

Figure 2.1: ^{1}H NMR spectra of ethyl 2-(imidazol-1-yl)acrylate (**1**) prepared with 10 mol% triphenylphosphine (left) and ethyl (*E*/*Z*)-3-(imidazol-1-yl)acrylate (**2**) (right) in CD_2Cl_2.

The synthesis of **1** with 20 mol% triphenylphosphine and the acetate buffer resulted in a high yield of 83%. However, the desired product was obtained with a yield of only 30% in a larger batch using 25 mol% triphenylphosphine and at a temperature of -20 °C instead of 0 °C. In catalyzed reactions, typically 5 mol% or less of the catalyst is used, with a maximum of 10 mol% in certain cases. Here, the phosphine acts as a mediator due to the use of ≥0.2 equivalents compared to ethyl propiolate, and the preparation of **1** under catalytic conditions may be possible with further optimization. Despite this, the described preparation of **1** was successfully scaled up from 2 mmol to 148 mmol imidazole as starting material by cooling the reaction mixture to -30 °C.

Ethyl 2-(imidazol-1-yl)acrylate (**1**) was first free radically homopolymerized with acetic acid in various solvents based on the proposed propagation inhibition by radical addition to the 2 position of the imidazole group of *N*-vinylimidazole by Santanakrishnan and Hutchinson (Scheme 2.4).[118] Additionally, examples of the radical polymerization of *N*-vinylimidazole and imidazole-containing methacrylates are described in the literature as alkylated or protonated imidazole moieties.[98, 119–125]

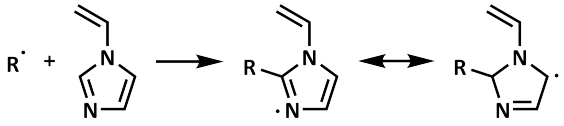

Scheme 2.4: Proposed propagation inhibition by radical addition to the 2 position of the imidazole moiety of *N*-vinylimidazole.[118]

The free radical polymerization of **1** with 5 equivalents of acetic acid in hexafluoroisopropanol, 2,2,2-trifluoroethanol, isopropanol, water, or pure acetic acid afforded oligomers of low molar mass. The achievable molecular weight was increased by using *N*,*N*-dimethylformamide and dimethyl sulfoxide as solvent (Table 2.1). To explore the polymerization

behavior of **1** depending on the protonation of the imidazole moiety, **1** was further polymerized with and without 1.1 equivalents of hydrochloric acid in *N*,*N*-dimethylformamide and dimethyl sulfoxide. Compared to the polymerization using acetic acid, the molar mass decreased when a stronger protonating agent was added, and highly increased by polymerizing the unprotonated monomer **1** (Figure 2.2). A radical addition to the imidazole group, which is known to inhibit the polymerization, was not observed. Furthermore, the preparation of imidazole-containing polymers by the radical polymerization of non-alkylated monomers without acids is described for some examples in the literature.[126–131] In contrast to *N*-vinylimidazole, **1** has a more reactive carbon-carbon double bond caused by the electron withdrawing ester moiety. Protonation of the electron donating imidazole ring alters the character of this moiety to be an electron withdrawing group, which stabilizes the initiated monomeric radical and growing oligoradical. The protonation of **1** may also lead to a lower propagation rate and perhaps a higher radical transfer to monomer rate.

Table 2.1: SEC data of poly(ethyl 2-(imidazol-1-yl)acrylate) (**3**) obtained by free radical polymerization.

Entry	Solvent	Additive	$\overline{M}_n$ [a)]	$Đ$ [a)]	$\overline{M}_n$ [b)]	$Đ$ [b)]
1	HFIP	HOAc	1,400 g·mol^{-1}	1.43	-	-
2	TFE	HOAc	1,400 g·mol^{-1}	1.47	-	-
3	*i*PrOH	HOAc	1,500 g·mol^{-1}	1.43	-	-
4	Water	HOAc	1,200 g·mol^{-1}	1.32	-	-
5	HOAc	-	1,500 g·mol^{-1}	1.34	-	-
6	DMSO	HOAc	2,700 g·mol^{-1}	1.53	-	-
7	DMF	HOAc	2,700 g·mol^{-1}	1.39	-	-
8	DMSO	HCl	1,000 g·mol^{-1}	1.52	-	-
9	DMF	HCl	2,100 g·mol^{-1}	1.37	-	-
10	DMSO	-	13,300 g·mol^{-1}	1.45	30,200 g·mol^{-1}	1.45
11	DMF	-	10,000 g·mol^{-1}	1.54	20,600 g·mol^{-1}	1.45
12	MeCN	-	8,600 g·mol^{-1}	1.48	17,000 g·mol^{-1}	1.42
13	THF	-	8,700 g·mol^{-1}	1.49	16,500 g·mol^{-1}	1.56
14	Anisole	-	11,500 g·mol^{-1}	1.65	23,800 g·mol^{-1}	1.53
15	Benzene	-	13,400 g·mol^{-1}	1.59	29,400 g·mol^{-1}	1.51

[a)] SEC (Water, P2VP calibration), [b)] SEC (DMAc, PMMA calibration).

The absence of acids in the polymerization resulted in an uncharged polymer with an enhanced solubility in organic solvents, which facilitates the alkylation of the aromatic heterocycle. Additionally, poly(ethyl 2-(imidazol-1-yl)acrylate) (**3**) was prepared in less polar solvents and analyzed by SEC in *N*,*N*-dimethylacetamide (Figure 2.2). Lower molar masses were achieved in acetonitrile and tetrahydrofuran because of the poor solubility of the polymer. Benzene, a suitable solvent for various compounds, afforded a macromolecule with high molecular weight. Due to safety considerations, benzene was replaced by less toxic anisole, which resulted in a slight decrease in the polymer molar mass. In comparison to the aqueous SEC, a molar mass approximately double that when using a *N*,*N*-dimethylacetamide SEC system, which is in closer agreement to the reality based on published measurements with a multi-angle light scattering detector.[132]

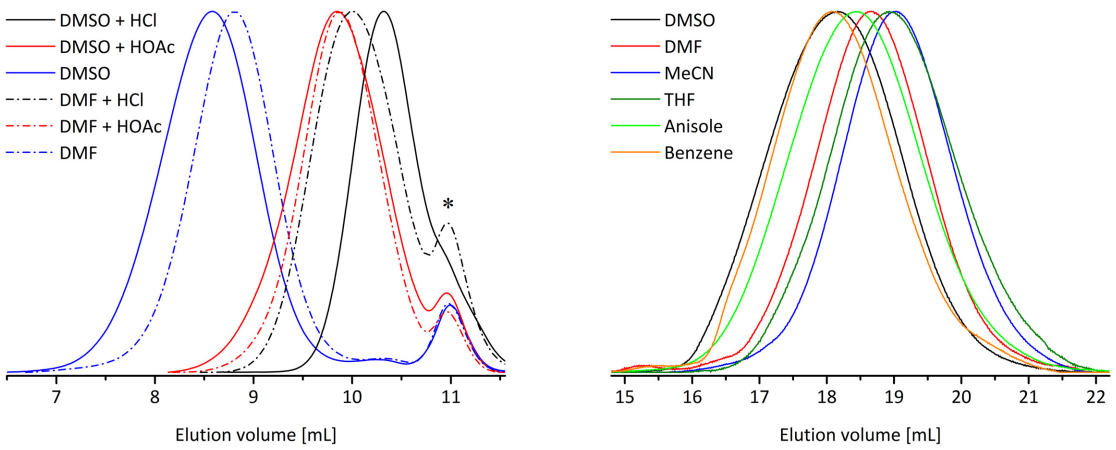

Figure 2.2: SEC elugrams in water (l, ∗ system peak) and DMAc (right) of poly(ethyl 2-(imidazol-1-yl)acrylate) (**3**) prepared *via* free radical polymerization.

The weak polyelectrolyte **3** was converted into a strong polycation *via* alkylation and further into a polyampholyte through hydrolysis of the ethyl ester (Scheme 2.5). The combination of both post-polymerization modifications resulted in a polyampholyte similar to the poly(carboxybetaine) based on *N*-vinylimidazole, which were functionalized with bromoacetic acid.

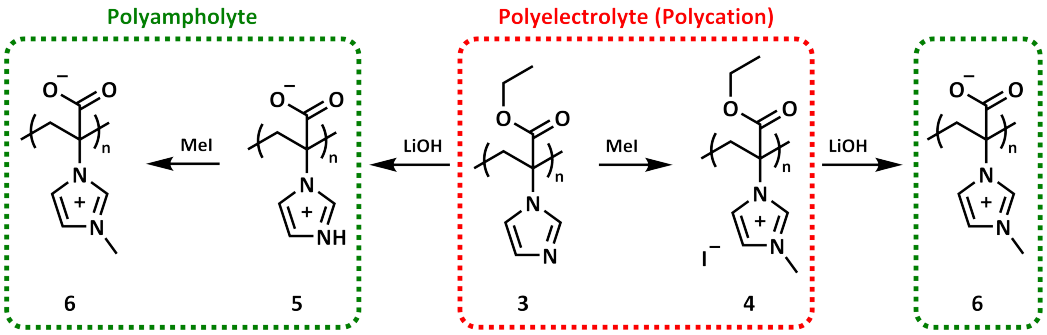

Scheme 2.5: Conversion of poly(ethyl 2-(imidazol-1-yl)acrylate) (**3**) into a strong polyelectrolyte and polyampholytes.

The uncharged polymer **3** represents a weak polycation that can be charged upon protonation of the imidazole moiety at a pH value below 6 by increasing the overall hydrophilicity. Besides acids, alkylation of the heterocycle can introduce a permanent cationic charge and different functionalities to modify the properties of the material. First, **3** was transformed into poly(ethyl 2-(3-methylimidazolium-1-yl iodide)acrylate) (**4**) with a fivefold excess of methyl iodide in methanol with a degree of methylation over 90%. The ^{1}H NMR spectrum depicted in Figure 2.3 shows the signal of the methyl group at a chemical shift of 4.3 ppm. The signals of the imidazole group are shifted downfield due to the cationic charge. In the solid state carbon MAS spectrum the signals at the 4 and 5 position of the imidazole ring are no longer separated as they are now chemically equivalent following alkylation. The preparation of poly(2-(3-methylimidazolium-1-yl)acrylate) (**6**) through

the ester hydrolysis of **4** with lithium hydroxide in a 1:1 mixture of water and methanol succeeded to 94%. A weak signal of the residual ethyl ester is visible in the ^{1}H NMR spectrum at 1.2-1.4 ppm.

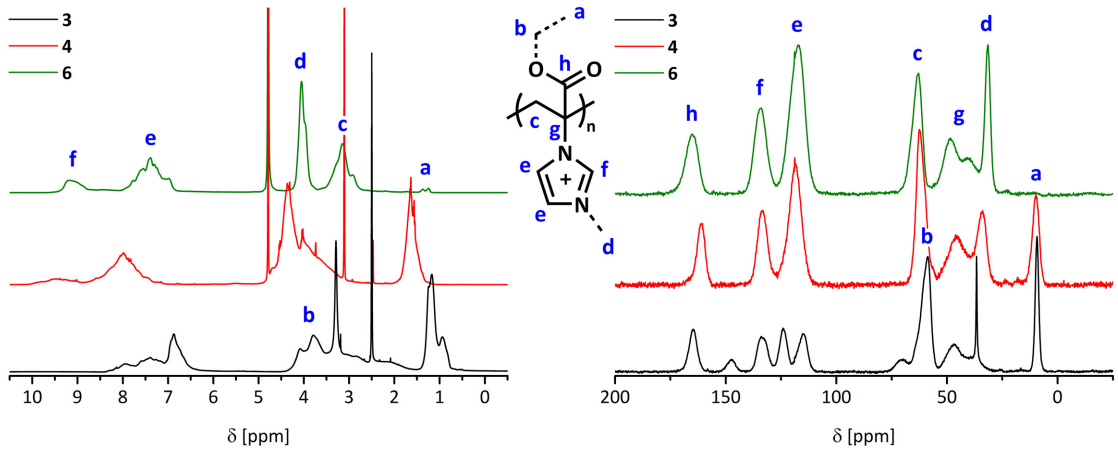

Figure 2.3: ^{1}H NMR spectra (left) in DMSO-d_6 and D_2O and ^{13}C ssMAS (right) of **3**, **4** containing methyl groups, and **6** after ester hydrolysis.

The SEC elugrams of polymers **3** and **4** show no noticeable changes due to their structural similarity, only differing in the substitution of a proton by a methyl group (Figure 2.4). The presence of the carboxylic acid moiety in **6** results in a smaller hydrodynamic volume and a lower molar mass as expected (Table 2.2).

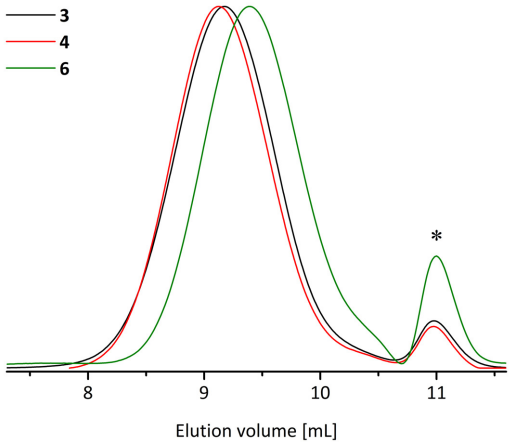

Figure 2.4: SEC elugrams in water (∗ system peak) of **3**, **4**, and **6**.

Table 2.2: SEC data in water of **3**, **4**, and **6**.

Polymer	$\overline{M}_n$ [a)]	$Đ$ [a)]
3	6,500 g·mol^{-1}	1.40
4	6,500 g·mol^{-1}	1.38
6	4,800 g·mol^{-1}	1.57

a) P2VP calibration.

In addition to the methylation, **3** was modified with *n*-butyl bromide, *n*-hexyl bromide, lauryl bromide, and benzyl bromide in the bachelor thesis of M. Riske under my supervision. The reactions were carried out in methanol at 50 °C for 48 hours with an excess of the bromides, and *N*,*N*-dimethylformamide was used as solvent for lauryl bromide. Using alkyl bromides, which are poorer leaving groups compared to iodides, degrees of modification between 32-65% were achieved. To increase the conversion of the polymeric imidazole groups, a higher reaction temperature could be applied, in addition to using the corre-

sponding mesylates as alkylating agents instead of alkyl bromides. However, the moderate to low conversions altered the solubility of the polymers from hydrophobic into hydrophilic at neutral pH with the exception of the polymer reacted with lauryl bromide despite the cationic charges. Poly(ethyl 2-(3-laurylimidazoilum-1-yl bromide)acrylate) can act as a phase transfer catalyst, which allows water-soluble anionic compounds to be dissolved in organic solvents like the dye Brilliant Blue FCF in dichloromethane.[133] Furthermore, polyionic liquids based on *N*-vinylimidazole are applied as dispersants of carbon nanotubes for the preparation of electrochemical sensors. In cooperation with J. B. Max, multi-walled carbon nanotubes were suspended with the synthesized polycations as well as the polyampholyte **6** in water.[134] In Figure 2.5, the TEM micrographs of various carbon nanotubes mixtures with and without dispersants in water are shown. The dispersants used include poly(1-butyl-3-vinylimidazolium bromide),[125] poly(dehydroalanine) functionalized with 1,2-epoxyoctane,[105] and the modifications of **3**[133]. In the absence of any dispersant, the carbon nanotubes visibly aggregate, and the addition of all polymers resulted in homogeneous and stable dispersions by π-π stacking of the imidazolium cations, van der Waals forces between the alkyl chains, and perhaps cation-π interactions to the aromatic carbon scaffold.[135, 136] A positive surface charge is generated by the adsorption of the polycations and a neutral charge with the polyampholytes depending on the pH. In comparison to the polyampholytes based on poly(dehydroalanine) and **3**, **6** does not precipitate at low pH values, nor does the composite material. Furthermore, the properties can be tuned by attaching functional groups (-CH_2-R) to the imidazole ring instead of methylation.

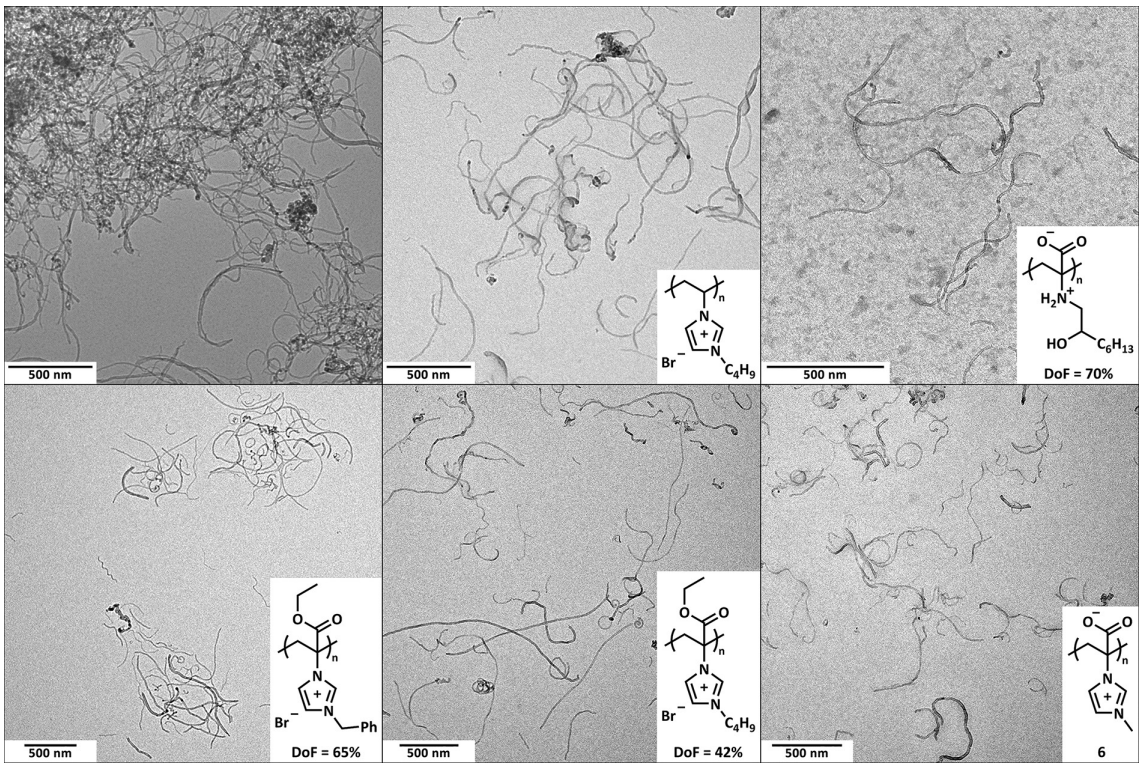

Figure 2.5: TEM micrographs of multi-walled carbon nanotube suspensions ($0.5\,g{\cdot}L^{-1}$) without and with dispersants ($2.5\,g{\cdot}L^{-1}$) in water.

Another polyampholyte is accessible *via* alkaline ester hydrolysis of **3** and was prepared with lithium hydroxide in a 1:1 mixture of water and methanol. The resulting poly(2-(imidazolium-1-yl)acrylate) (**5**) contains 8% residual ethyl ester groups according to ^{1}H NMR, with a shift to lower molar masses visible by SEC (Figure 2.7). This polyampholyte (**5**) is predominantly negatively charged in aqueous solutions at a pH above 6.8 and insoluble in a pH range between 6.8 and 2.2. In contrast to a similar weak polyampholyte poly(dehydroalanine), **5** dissolves again under strongly acidic conditions as a polycation.[102] M. von der Lühe and P. Biehl used poly(dehydroalanine) to coat magnetic iron oxide nanoparticles for possible medical applications in magnetic resonance imaging, hyperthermia, or drug delivery systems, and developed coatings with the polyampholyte **5**. An increased stability under acidic conditions was observed, and a neutral zeta potential was measured at a higher pH of 6.5 for the new hybrid material.[137, 138]

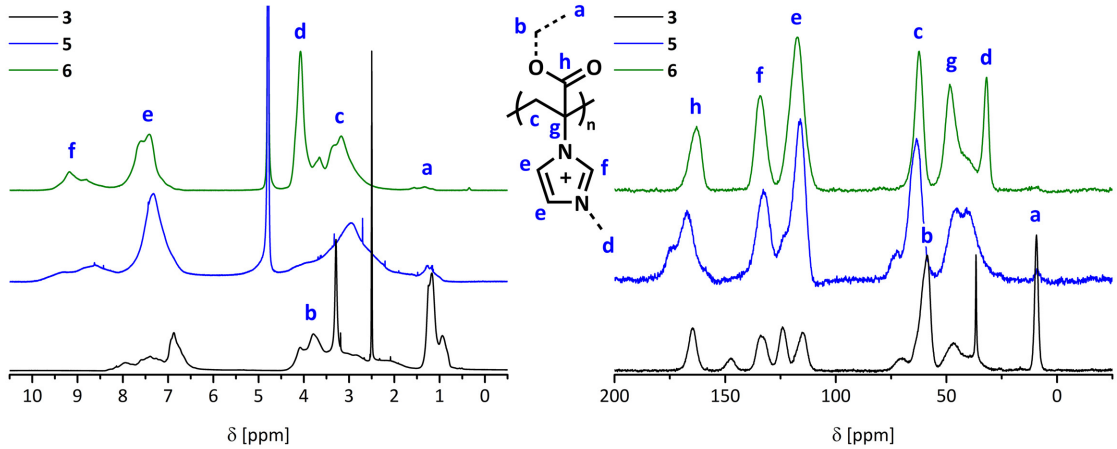

Figure 2.6: ^{1}H NMR spectra (left) in DMSO-d_6 and D_2O and ^{13}C ssMAS (right) of **3**, **5** with carboxylic acid groups, and **6** after methylation.

Furthermore, **5** was transformed into **6** similarly to the preparation of **4** with methyl iodide at 65 °C. The methylation occurred to 83% completion, and the ^{1}H NMR and ^{13}C ssMAS spectra in Figure 2.6 show, in addition to the low intensity signals of residual ethyl ester, a significant peak for the methyl group. A partial esterification could not be excluded for the reaction with the strong methylation agent, and the synthetic route to **6** starting from alkylation of **3** is preferable. Analogous to **3** and **4**, the SEC elugrams of **5** and **6** do not exhibit remarkable changes after methylation (Figure 2.7). The modification of **5** with protonated imidazole rings in the SEC eluent into **6** containing methylimidazolium moieties resulted in a negligible change in the hydrodynamic volume due to the similar size of both cationic groups. However, the hydrolysis of the ester group to a carboxylic acid increased the polarity and hydrophilicity of the polymer and influenced the conformation of the macromolecular chains in solution, leading to higher elution volumes and lower molar masses (Table 2.3).

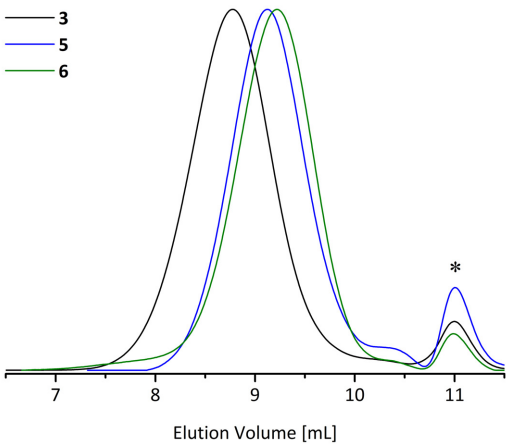

Figure 2.7: SEC elugrams in water (∗ system peak) of **3**, **5**, and **6**.

Table 2.3: SEC data in water of **3**, **5**, and **6**.

Polymer	$\overline{M}_n$ [a)]	$Đ$ [a)]
3	10,600 g·mol^{-1}	1.44
5	6,600 g·mol^{-1}	1.37
6	6,800 g·mol^{-1}	1.45

[a)] P2VP calibration.

Batchelor *et al.* free radically copolymerized acrylonitrile and methyl 2-(imidazol-1-yl)acrylate in a 5:1 ratio as a new plasticizer to prepare carbon fibers.[139] Controlled radical polymerization techniques access block copolymers of **1** and its derivatives, which can be applied as a drug delivery system or to immobilize metals for heterogeneous catalysis. The polymerization *via* nitroxide-mediated radical polymerization (NMP) requires high temperatures, while atom transfer radical polymerization (ATRP) may be challenging due to the potential competition between the ligand for the transition metal and the polymer. Nevertheless, an ATRP was explored by N. A. Hempel in a scientific internship under my supervision. In an ATRP reacts the copper(I) bromide complex reversibly with alkyl bromides as deactivated chain ends or the initiator to a copper(II) bromide complex and a propagating carbon radical. The ATRP equilibrium of the propagating (active) and dormant (inactive) species is characterized by the constant K_{ATRP}, and this influences the polymerization control. Solvents with a high polarity, such as *N*,*N*-dimethylformamide or dimethyl sulfoxide, stabilize the propagating species. This leads to a higher ATRP equilibrium constant, an increase in the radical concentration as well as side reactions.[140] Based on this knowledge, anisole was used for the polymerization of **1** mediated with a copper(I) bromide complex and initiated with methyl α-bromoisobutyrate (Scheme 2.6).

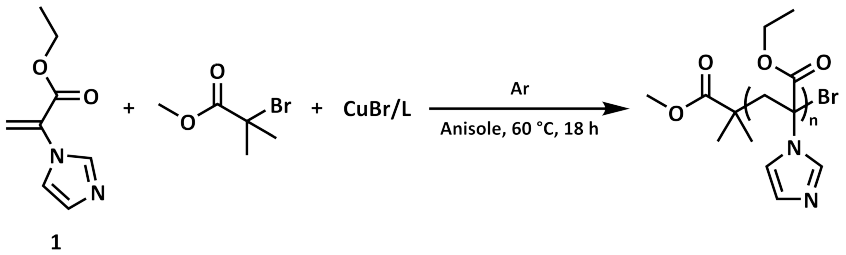

Scheme 2.6: Polymerization of ethyl 2-(imidazol-1-yl)acrylate (**1**) *via* ATRP.

For the ATRP of **1**, a ligand with a high stability constant should be chosen due to the competition with the imidazole moiety of the monomer and polymer. Additionally, the ratio between the complex stability constants for copper(II) to copper(I) is specific for

the ligands, and a higher quotient results in an increased K_{ATRP} value.[141] Consequently, four tetradentate ligands were investigated for the polymerization of **1** as depicted in Scheme 2.7.

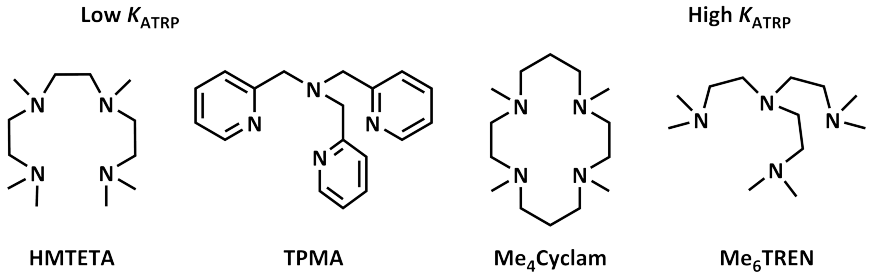

Scheme 2.7: The tetradentate ligands investigated for the ATRP of ethyl 2-(imidazol-1-yl)acrylate (**1**).

HMTETA has the lowest K_{ATRP} and complex stability with copper ions compared to the other ligands investigated, and only afforded oligomers (Figure 2.8). The ATRP using the ligand Me$_4$Cyclam, which has the lowest deactivation constant, afforded a polymer with a broad molecular weight distribution, which was caused by the higher radical concentration. TPMA and Me$_6$TREN also have a high activation rate, but with a corresponding 100-fold increase in the deactivation rate in contrast to Me$_4$Cyclam.[142] The pyridine-based ligand TPMA leads to a high dispersity of 2.45 (Table 2.4). This likely arises from the coupling of propagating radicals as indicated from the multimodal distribution observed by SEC analysis. The ATRP with Me$_6$TREN resulted in the highest number average molar mass and lowest molecular weight distribution, with a small low molar mass shoulder observed in the SEC elugram. These lower molecular weight species are likely to be dead chains that formed early in the polymerization as a consequence of side reactions.

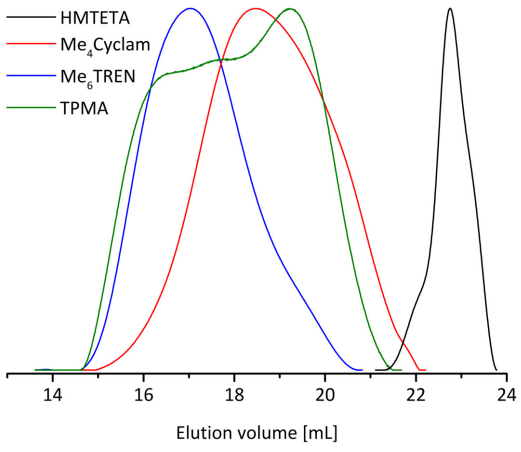

Figure 2.8: SEC elugrams in DMAc of ATRP of **1** with investigated ligands.

Table 2.4: SEC data in DMAc of ATRP of **1** with investigated ligands.

Ligand	$\overline{M}_n$ [a)]	$Đ$ [a)]
HMTETA	600 g·mol^{-1}	1.09
Me$_4$Cyclam	5,500 g·mol^{-1}	1.98
Me$_6$TREN	17,200 g·mol^{-1}	1.61
TPMA	10,000 g·mol^{-1}	2.45

a) PMMA calibration.

To obtain a deeper understanding of the polymerization, the ATRP of **1** was carried out with Me$_6$TREN and monitored over 5 hours by SEC and NMR spectroscopy using trioxane as an internal standard. After half an hour, the polymerization stopped at a conversion of 28%, and neither an increase in the molar mass nor a change of the monomer

concentration were detected. While it may be possible to further optimize the ATRP of **1** by changing the temperature, the addition of small amounts of copper(II) bromide, or using copper(I) chloride, we decided that ATRP was likely an unsuitable technique. Despite the poor control over the polymerization of **1** *via* ATRP achieved, a chain extension from a poly(pentafluorophenyl methacrylate) (PPFPMA) block was performed in order to incorporate the desired block of **1** to form the target block copolymer. A PPFPMA block permits a substitution of the active ester with amines in a post-polymerization modification to obtain hydrophobic or hydrophilic side chains. A block extension of PPFPMA with methyl methacrylate (MMA) *via* ATRP succeeded and the SEC analysis shows an increase in the molar mass by approximately 900 g·mol^{-1} and corresponding decrease in dispersity from 1.37 to 1.21 (Figure 2.9). In parallel to MMA, **1** was polymerized using PPFPMA as a macroinitiator, and a slight shift is visible in the SEC elugrams. According to the SEC data using a PMMA calibration, the molar mass after block extension of the PPFPMA macroinitiator only increased by 1,400 g·mol^{-1}. As such, it was only possible to add a few monomer units under the polymerization conditions used.

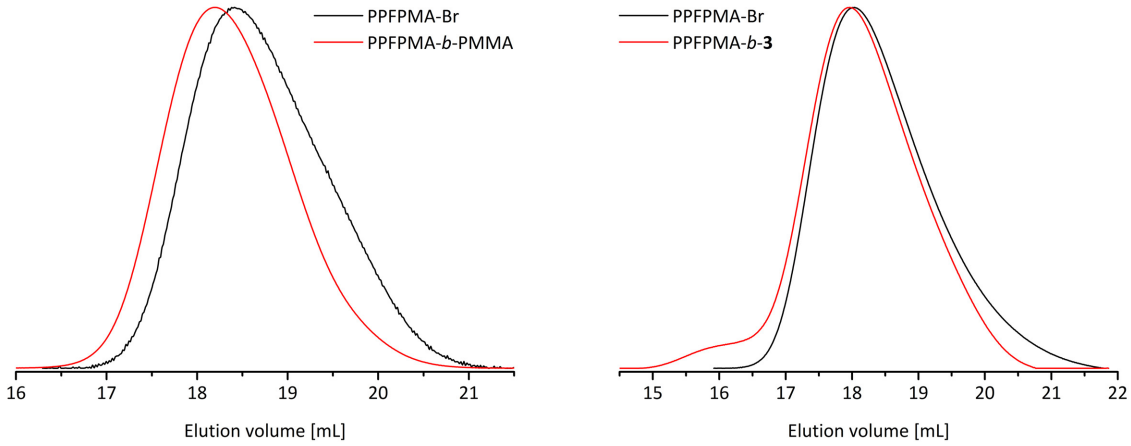

Figure 2.9: SEC elugrams in DMAc of PPFPMA before and after block extension with MMA (left) and **1** (right) *via* ATRP.

Another promising controlled radical polymerization technique is the RAFT polymerization, which offers a number of advantages from a tolerance to many functional groups, and a lower level of complexity compared to ATRP. To obtain a well-controlled polymerization, the choice of the chain transfer agent, with varying addition and fragmentation rates of radicals to the thiocarbonylthio moiety, dependent on the electron density, strongly influence the polymerization behavior. Three different RAFT agents were selected to polymerize the more active monomer **1** (Scheme 2.8). To find the appropriate conditions for a RAFT polymerization, a monomer to chain transfer agent to initiator ratio of 400:4:1 was used in solution at 70 °C for 24 hours.

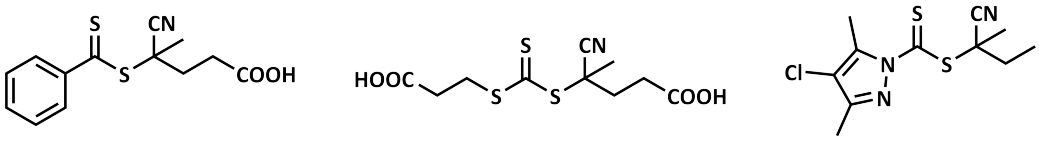

Scheme 2.8: Various chain transfer agents investigated for the RAFT polymerization of ethyl 2-(imidazol-1-yl)acrylate (**1**).

In our initial study, the polymerization of **1** *via* RAFT was investigated using various RAFT agents in *N*,*N*-dimethylformamide. When CPADB was employed as the RAFT agent, oligomers were formed as observed by SEC at an elution volume of 21.0 to 22.5 mL, and which was accompanied by a polymeric shoulder (Figure 2.10). In contrast to CPADB, which is unsuitable to control the polymerization of **1**, low amounts of oligomers and a clear polymer peak are visible in the SEC elugram when CPATTC is used as the chain transfer agent. Furthermore, the universal chain transfer agent CPzDB leads to a narrower molecular weight distribution and fewer side reactions than the trithiocarbonate, resulting in a more symmetric SEC trace. In addition to the RAFT agent, the solvent can influence the polymerization behavior. Consequently, *N*,*N*-dimethylformamide was exchanged with dimethyl sulfoxide and anisole, based on the results of free radical preparations of **3**. Besides the monomer and solvent peaks present in the reaction mixture at an elution volume of 22.5-24.0 mL, a bimodal distribution was observed by SEC when dimethyl sulfoxide was used as solvent. While using anisole as solvent resulted in a narrower dispersity and a well-separated polymer peak shifted to a lower elution volume.

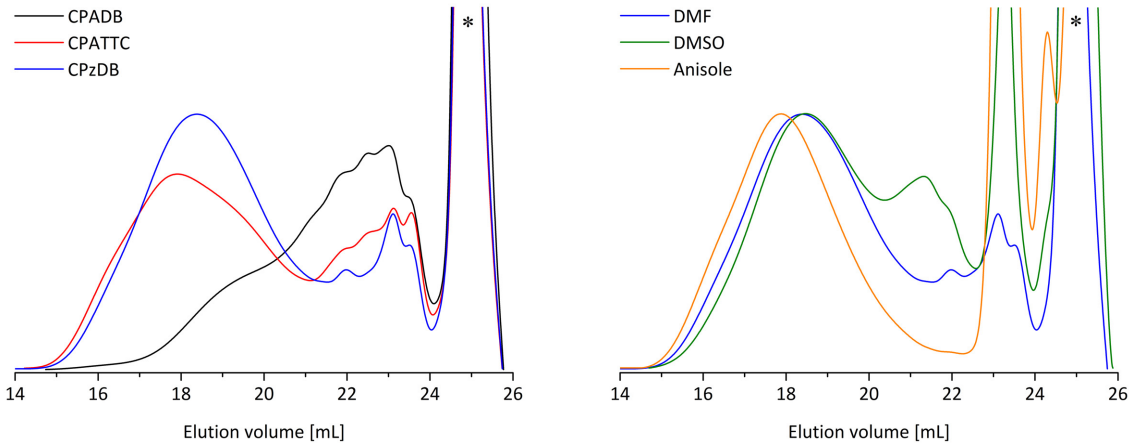

Figure 2.10: SEC elugrams in DMAc (∗ system peak) from the RAFT polymerization of **1** with investigated chain transfer agents (left) and CPzDB in suitable solvents (right).

The RAFT polymerization of **1** with CPzDB in anisole (Scheme 2.9) produced a polymer with a broad molecular weight distribution of 1.79. A kinetic study was performed to elucidate the origins of the high disperity, and therefore assist in further optimizations.

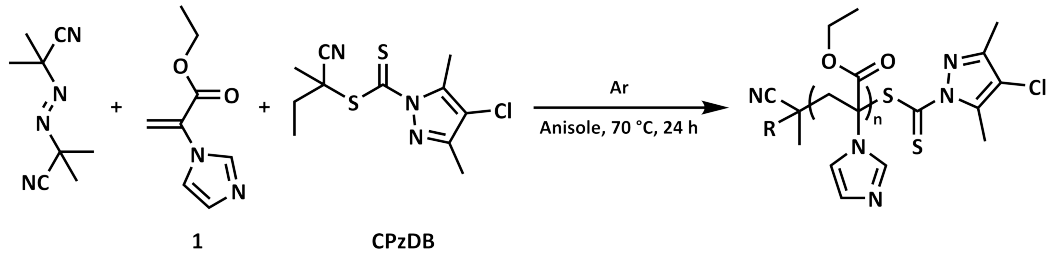

Scheme 2.9: Polymerization of ethyl 2-(imidazol-1-yl)acrylate (**1**) *via* RAFT.

To determine the monomer conversion by NMR spectroscopy, trioxane was added to the polymerization mixture as an internal standard, and changes in the molar mass and molecular weight distribution were measured by SEC in DMAc. The SEC peak maximum shifts to lower elution volumes with increasing polymerization time, but a shift of the peak end at an elution volume of 22.2 mL occurred after two hours (Figure 2.11). This could hint at slow reinitiation in the pre-equilibrium of the RAFT polymerization, resulting in the generation of new propagating chains over a long time period. Furthermore, a slight high molecular weight shoulder appeared after 8 hours, caused by reactions such as the combination of propagating radicals. The plot showing the molar mass with conversion increases nearly linearly between 1 to 8 hours or from 4 to 33% conversion, after which a sudden increase is observed. This may arise from the Trommsdorff-Norrish effect where higher viscosities cause an acceleration in the propagation rate. This effect is caused by the decreased mobility of the active radical chain ends resulting in a lower termination rate, and a poorer heat transport, leading to a rise in the reaction temperature.[143] At the beginning of the polymerization the molecular weight distribution decreases and remains constant until a conversion of 23% is reached. At higher monomer consumptions, a rise in the viscosity of the mixture is possible, which leads to broader molecular weight distributions. In this case, the increase in the dispersity resulted from the higher viscosity, as well as other undesired radical reactions.

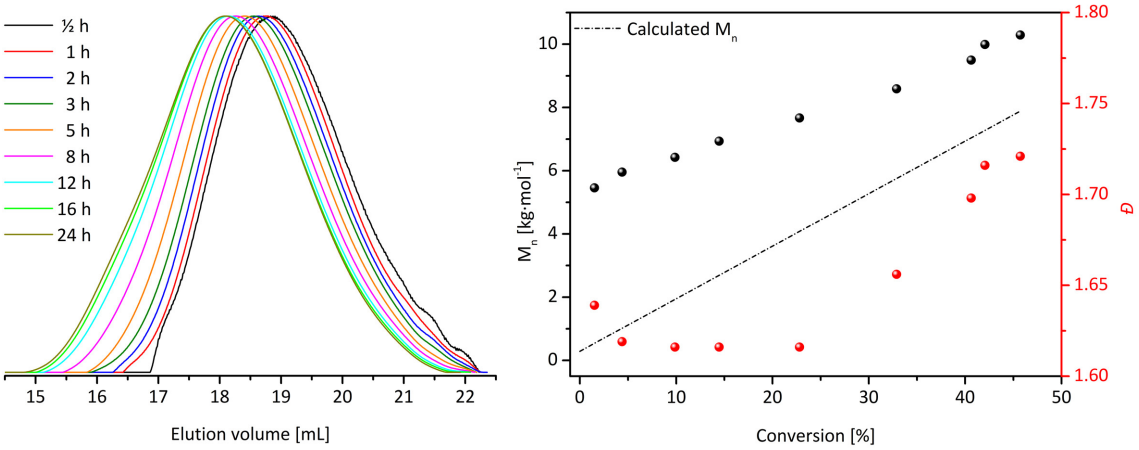

Figure 2.11: SEC elugrams in DMAc (left) and corresponding SEC data using a PMMA calibration with increasing conversion (right) of the RAFT polymerization of **1**.

Controlled radical polymerizations are pseudo-first-order reactions that form macromolecules by the addition of monomers to propagating radicals. The bimolecular reaction follows first-order kinetics due to the immense excess of monomer and a deviation occurs at higher conversion of the monomer. The kinetic plot of an idealized pseudo-first-order polymerization is depicted in Figure 2.12 with a theoretical linear curve for negligible changes in the monomer concentration, as well as curves including termination reactions and slow initiation. Compared to the kinetic plot of the polymerization of **1**, a linear slope between 0.5-3 hours is visible, and a retardation at half an hour. It is difficult to draw conclusions about the origin of the poor control observed in the RAFT polymerization of **1**. The well-controlled polymerization of ethyl 2-(hydroxymethyl)acrylate, which will be presented later in Section 2.2 (Figure 2.28), displays similar kinetic behavior. Both kinetic plots differ in the consumption of the monomer at the end of the linear slope, which is very low for **1** with approximately 23% monomer conversion, and which is much higher in the case of ethyl 2-(hydroxymethyl)acrylate with 68% monomer conversion.

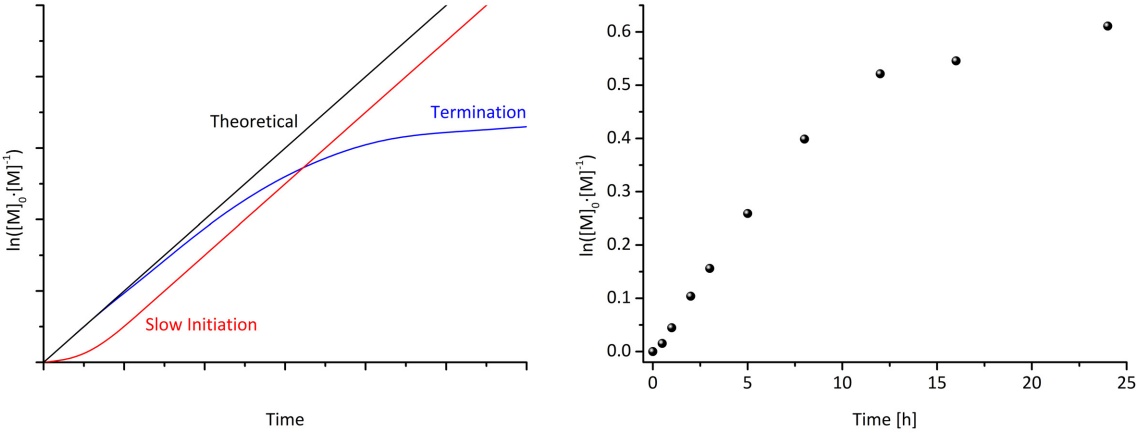

Figure 2.12: First-order kinetic plot in theory[144, 145] (left) in comparison to the RAFT polymerization (right) of **1**.

After initiation in the pre-equilibrium of the RAFT polymerization, an intermediate radical **8** is formed by the addition of the chain transfer agent CPzDB. This intermediate radical can then either fragment into the educts or into the dormant chain **9** and radical **10**, which is the homolytic leaving group of the RAFT agent (Scheme 2.10). In the pre-equilibrium or initialization, the cleavage of **10** from the intermediate **8** should be faster than **7** for an efficient reinitiation and to prevent retardation. In this example, the monomer-based radical **7** is also stabilized by the functional groups, wherefore the fragmentation of **8** into **10** is not favored. A better leaving group of the chain transfer agent could solve the problem, but the preparation of such a RAFT agent requires several steps and may be dangerous. Generally, the homolytic leaving group is introduced to the chain transfer agent by the reaction of an azo initiator containing the desired moiety with a disulfide precursor of the RAFT agent like **11** (Scheme 2.11).[146–148] To access the desired RAFT agent, it is necessary to synthesize an azo compound, which poses unknown decomposition and explosive risks. The observed retardation of the polymerization may be circumvented by polymerizing at higher temperatures according to other studies.[145]

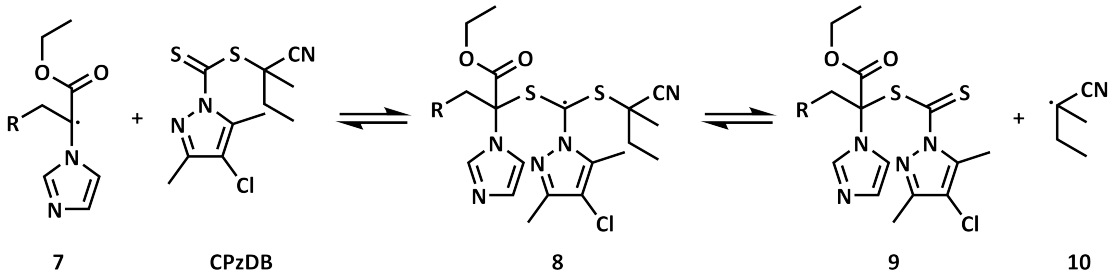

Scheme 2.10: Pre-equilibrium between oligomeric radicals (**7**) and the chain transfer agent, CPzDB, in the RAFT polymerization of **1**.

Another kinetic study of the RAFT polymerization of **1** was carried out at a higher temperature of 85 °C for 5 hours, but no significant improvements were observed. A macro-RAFT agent with poly(ethylene oxide) was synthesized in three steps (Scheme 2.11) to assess whether the poor control arises due to slow reinitiation, and the reaction was monitored *via* SEC measurements over the course of the polymerization. First, the disulfide **11** was reacted with 4,4'-azobis(4-cyanovaleric acid) to afford the RAFT agent **12** with a carboxylic acid at the leaving group. For the preparation of the chain transfer agent in good yield, two equivalents of the azo initiator was used due to the radical initiation efficiency of approximately 50-70%.[149–151] To attach the polymer, the carbonyl group was activated by conversion to an *N*-hydroxysuccinimide ester *via* a Steglich esterification. The moderate yield of **13** may be improved by the addition of 4-dimethylaminopyridine as catalyst, and using the alcohol in a slight excess of 0.1 equivalents to the carboxylic acid.[152]

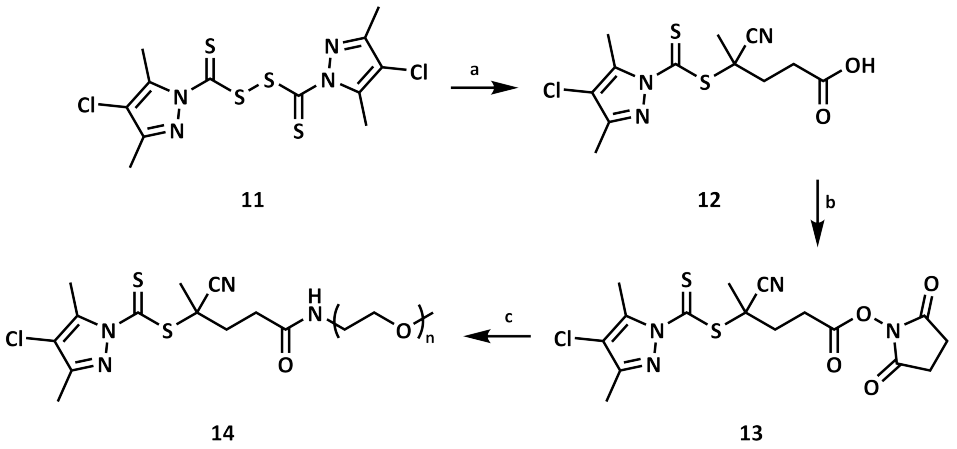

Scheme 2.11: Synthesis of a poly(ethylene oxide)-based macro-RAFT agent. Conditions: a) ACVA, 1,4-dioxane, 75 °C, 21 h, 80%. b) NHS, DCC, DCM, RT, 16 h, 48%. c) mPEO-NH_2, DCM, RT, 22 h, 92%.

After confirming the structure of **13** by NMR and UHPLC/HRMS, it was substituted by α-methoxy-ω-amino poly(ethylene oxide), and a stable amide bond was formed. The macro-RAFT agent **14** was purified by precipitation in diethyl ether and a functionalization of 87% was achieved according to ^{1}H NMR analysis (Figure 2.13). The SEC elugrams show a complete shift to higher molar masses caused by the high degree of modification of the polymer.

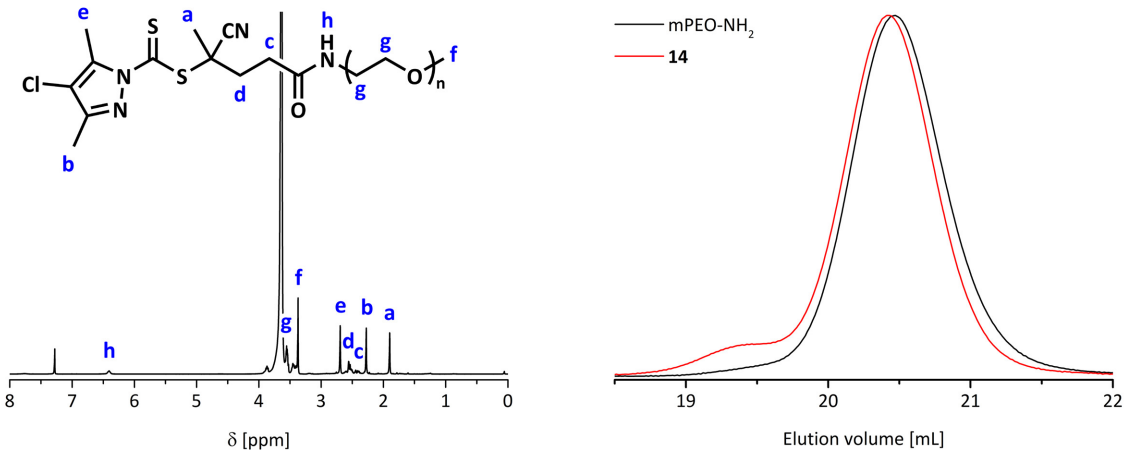

Figure 2.13: ^{1}H NMR spectrum (left) in $CDCl_3$ of the macro-RAFT agent **14** and SEC elugram in DMAc of **14** and its polymer precursor (right).

The RAFT polymerization of **1** with the macromolecular chain transfer agent **14** in anisole at 70 °C was monitored by SEC. After two hours, another polymer peak at a lower elution volume appeared and an intense signal for the macro-RAFT agent is visible (Figure 2.14). A residual peak of **14** of lower intensity was also observed after 9 hours, and is evidence of very slow reinitiation. A further reason for the observed retardation may be slow fragmentation or transfer rates of the RAFT agent due to the stability of the intermediate radical **8**.

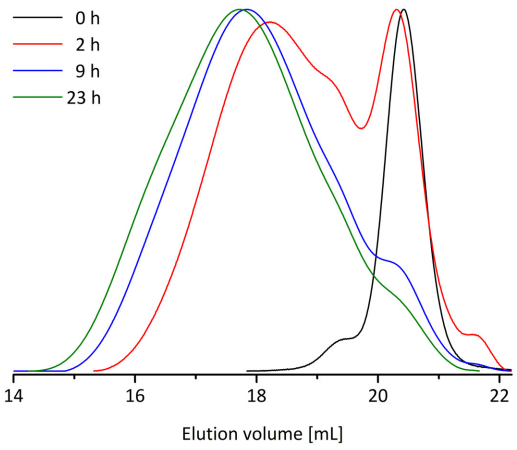

Figure 2.14: SEC elugrams in DMAc of the polymerization of **1** using the macro-RAFT agent **14** in anisole at 70 °C.

While a controlled radical polymerization of **1** was not achieved *via* RAFT, a controlled copolymerization with up to 15% acrylonitrile may be possible. One publication describes the controlled radical polymerization using a disulfide precursor of a trithiocarbonate with a photocatalyst, which could be used to polymerize **1**.[153] The use of the disulfide precursor of the RAFT agent is advantageous, generating the chain transfer agent *in situ* with a monomer-based leaving group. This method may also allow to determine whether the observed retardation is caused from slow fragmentation or slow reinitiation, which should not be observed. As an alternative approach to prepare block

copolymers with **1**, a free radical polymerization can be attempted using a macromolecular azo initiator or functionalized azo initiator followed by post-polymerization modification as shown in Scheme 2.12. The synthesis of the active ester of 4,4'-azobis(4-cyanopentanoic acid) with *N*-hydroxysuccinimide, and its substitution with various amines including pyrenylmethylamine,[154] *N*-6-aminohexyl biotinamide,[155] and peptides[156] is described in the literature.

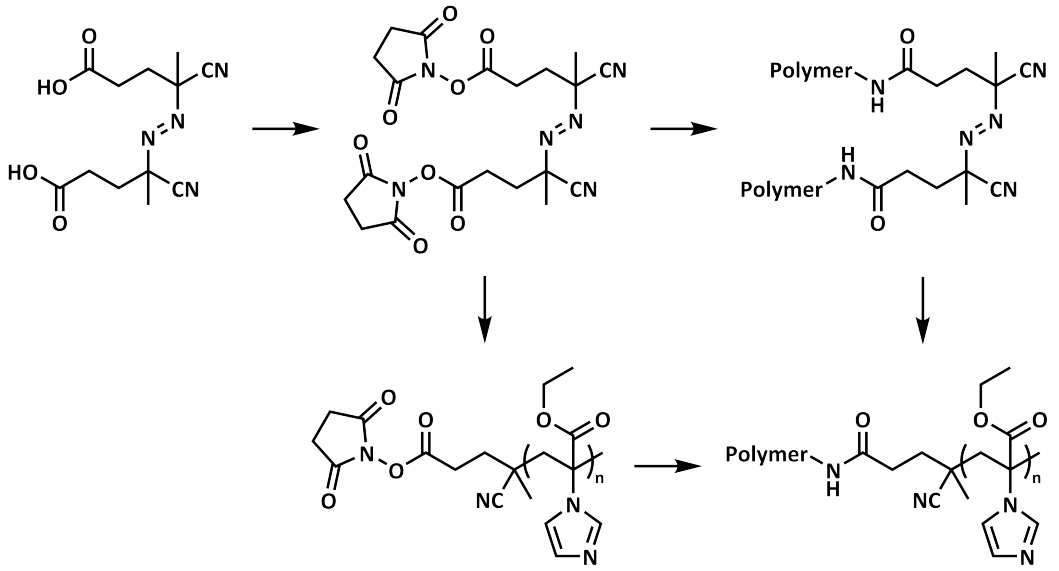

Scheme 2.12: Preparation of block copolymers *via* free radical polymerization using a macromolecular azo initiator or an initiator with active ester groups, and their post-polymerization modification.

2.1.2 Ethyl 2-(imidazol-2-yl)acrylate

The variation of the imidazole substitution of poly(ethyl 2-(imidazol-1-yl)acrylate) (**3**) to the position 2 enables an alkylation without loss of the pH responsivity of the heteroaromatic ring. Furthermore, a second functionalization of the imidazole moiety is possible to afford a strong polycation with a higher stability under alkaline conditions as an *N*-heterocyclic carbene can not be formed by abstraction of a proton at the 2 position of the imidazole. This restricts the field of application, as the use to bind metals for catalysis may no longer exist, and the fixation of carbon dioxide is unfeasible as demonstrated for copolymers consisting of acrylic acid and alkylated *N*-vinylimidazole.[98]

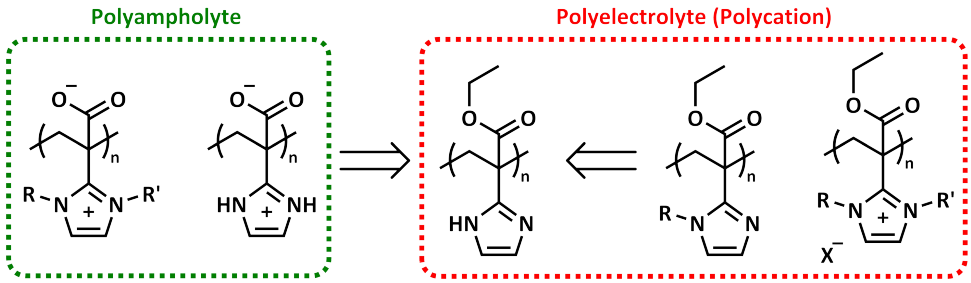

Scheme 2.13: Possible modifications of poly(ethyl 2-(imidazol-2-yl)acrylate).

One disadvantage of poly(ethyl 2-(imidazol-1-yl)acrylate) is that the synthesis of this monomer requires several steps compared to **1**, which is directly accessible by the addition of imidazole to ethyl propiolate. Additionally, a protecting group (PG) was used to decrease the polarity and simplify the purification by column chromatography. The polymerizable double bond is introduced last *via* the Wittig reaction of an oxoacetate or by α-methylenation of an acetate (Scheme 2.14). The precursors can be prepared by acylation with an acyl transfer of protected imidazoles, and by the preparation of the heterocycle.

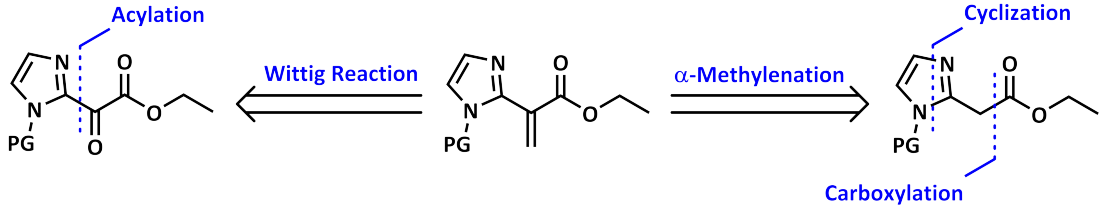

Scheme 2.14: Synthetic approaches to prepare the protected ethyl 2-(imidazol-2-yl)acrylate.

The synthesis of ethyl 2-(1-(2-(trimethylsilyl)ethoxy)methylimidazol-2-yl)oxoacetate (**16**), followed by the conversion into ethyl 2-(1-(2-(trimethylsilyl)ethoxy)methylimidazol-2-yl)acrylate (**17**) *via* the Wittig reaction requires a substitution of the acidic proton of the imidazole ring at the nitrogen. The presence of an acidic proton in the educt prevents an acyl transfer and may quench the phosphonium ylide (Scheme 2.15). A 2-(trimethylsilyl)ethoxymethyl moiety (SEM) was used as a protecting group due to its low steric hindrance for subsequent polymerization, and which can be cleaved easily with fluoride

or under acidic conditions. First, imidazole was deprotonated with sodium hydride before SEM chloride was added to afford 1-(2-(trimethylsilyl)ethoxy)methylimidazole (**15**) in good yield.

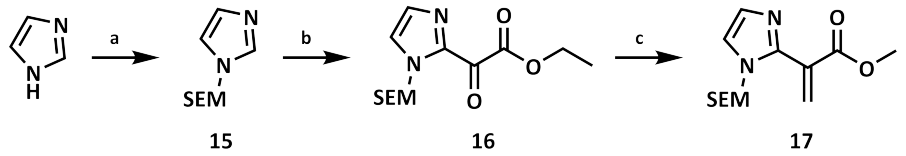

Scheme 2.15: Synthesis of **17** *via* the Wittig reaction. Conditions: a) NaH, SEMCl, THF, 0 °C to RT, 21 h, 78%. b) EtOCOCOCl, DIPEA, DCM, -20 °C to RT, 16 h, 93%. c) $MePPh_3Br$, KHMDS, THF, -77 °C to RT, 6 h.

In the second step, ethyl chlorooxoacetate was added to **15** to form an imidazolium cation (Scheme 2.16). Due to the positive charge, the C-H acidity at the 2 position of the heterocycle is increased, and the proton can be easily abstracted. The deprotonation with Hünig's base resulted in a properly zwitterionic or *N*-heterocyclic carbene intermediate, and an acyl transfer occurred. As reported for various alkylated imidazoles, **16** was also obtained in high yield. The structure was confirmed by NMR spectroscopy and mass spectrometry.[157]

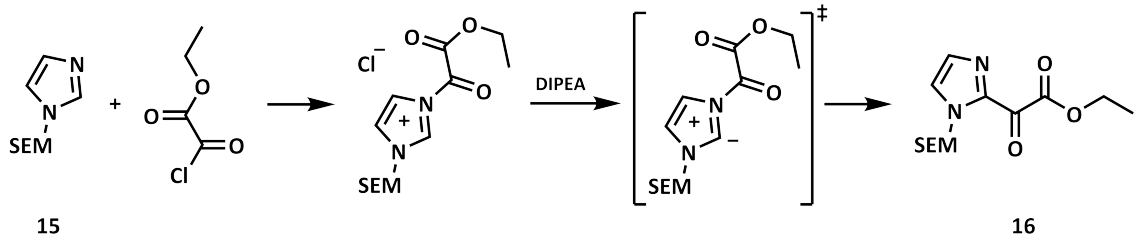

Scheme 2.16: Acylation of **15**, followed by deprotonation of the adduct to synthesize **16** by an acyl transfer.

For the Wittig olefination, methylenetriphenylphosphorane was prepared by the treatment of methyltriphenylphosphonium bromide with potassium bis(trimethylsilyl)amide. Afterwards, a solution of **16** was added to the yellow mixture at -77 °C. The color of the suspension changed from yellow to bright beige, which indicated the consumption of the phosphonium ylide. The desired product could not be isolated by column chromatography, but it could be identified by ^{1}H NMR spectroscopy (Figure 2.15).

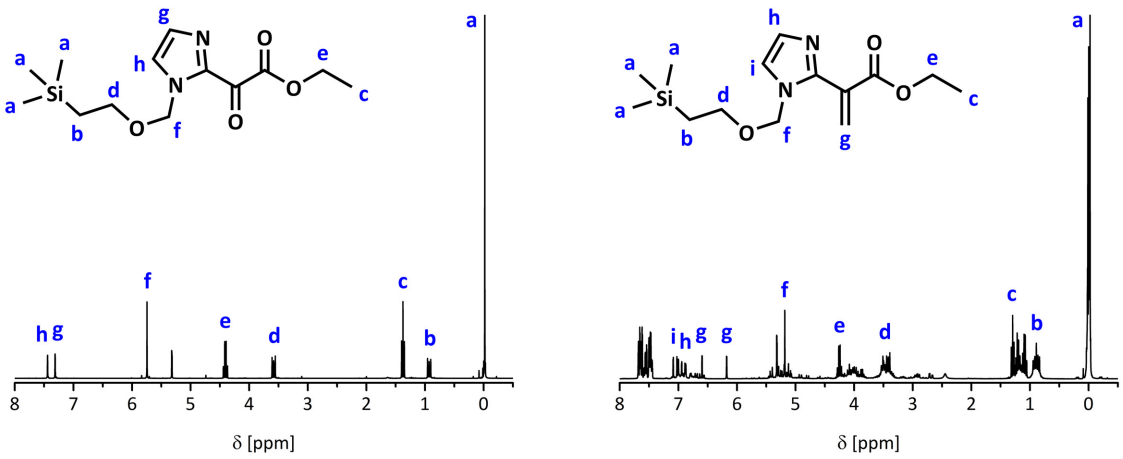

Figure 2.15: ^{1}H NMR spectra of **16** (left) and **17** (right) in CD_2Cl_2.

The increased polarity of **17** compared to **16** complicated the separation from the byproduct triphenylphosphine oxide. Generally, the Wittig olefination reacts with carbonyl moieties and tolerates various functional groups like esters. The expected signals of **17** are clearly visible in the NMR spectrum. Additional peaks associated with triphenylphosphine oxide are also visible, in addition to other peaks at approximately 7 ppm, which indicate side products were also formed. Conversely, the synthesis of **17** *via* α-methylenation affords the desired product in the absence of any byproducts, which simplifies the purification. Therefore, 2-methylimidazole was protected with a benzyl group (Bn) as described in the literature[158] or with a methoxymethyl group (MOM) for the preparation of ethyl 2-(imidazol-2-yl)acetate (**19**) (Scheme 2.17).

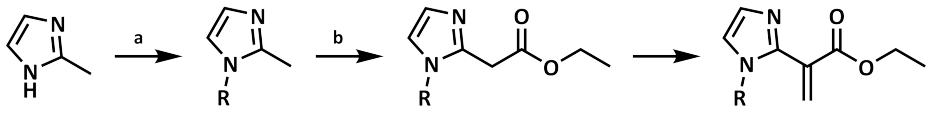

Scheme 2.17: Synthesis of protected ethyl 2-(imidazol-2-yl)acetate *via* α-methylenation. Conditions: a) NaH, RX, THF, -15 °C to RT, 23 h, >75%. b) ClCOOEt, DIPEA, MeCN, 0 °C to RT, 19 h, >10%.

In initial attempts to prepare **19**, the less expensive MOM group was used to protect 2-methylimidazole instead of the SEM moiety, and the benzyl group was used as a reference in the subsequent reaction. To attach the protecting moieties, the corresponding halides were substituted by 2-methylimidazolide, which was generated with sodium hydride. Similarly to the first synthetic route explored (Scheme 2.16), the ethyl ester was introduced by carboxylation with ethyl chloroformate using a trialkylamine as base. As reported for 2-methyl-1-benzylimidazole (**18b**),[158] the desired products were obtained in low yields due to the formation of a side product with two ester moieties, which was isolated and analyzed by NMR spectroscopy. The conversion of 2-methyl-1-(methoxymethyl)imidazole

(**18a**) with two equivialents of ethyl chloroformate and Hünig's base in acetonitrile resulted in a 1.0:1.4 mixture of ethyl 2-(1-(methoxymethyl)imidazol-2-yl)acetate (**19a**) and diethyl 2-(1-(methoxymethyl)imidazol-2-yl)malonate (**21a**) according to analysis by ^{1}H NMR spectroscopy (Figure 2.16).

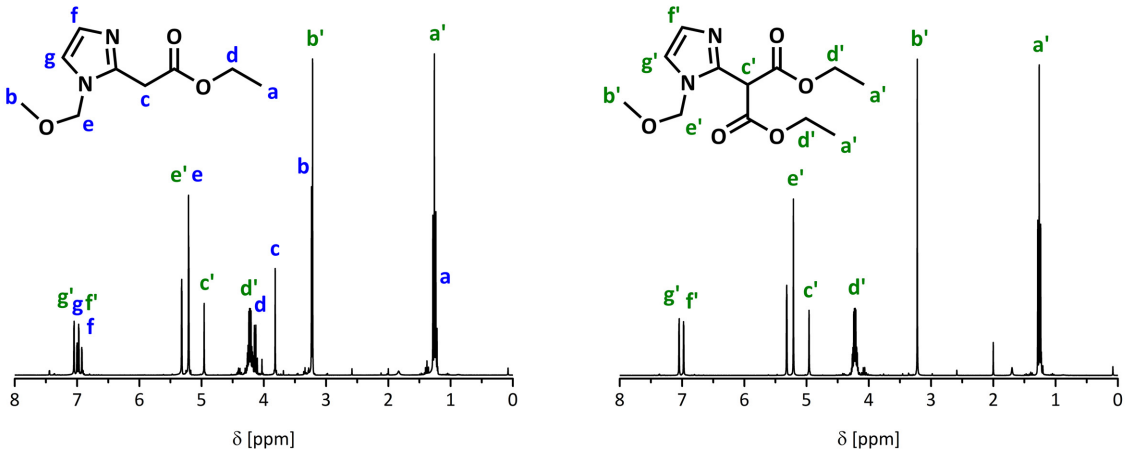

Figure 2.16: ^{1}H NMR spectra of the product mixture (left) and the isolated side product (**21a**) (right) from the carboxylation of **18a** in CD_2Cl_2.

Possible reactions to afford the diethyl malonate derivative **21** are depicted in Scheme 2.18. The imidazole was carboxylated at the nitrogen to form an imidazolium cation. The methyl group was deprotonated by the trialkylamine, and then a transfer of the ethyl ester to the desired product **19** occurred. Instead of the acyl transfer, a further ethyl chloroformate molecule could be added after the deprotonation to afford **20**, which reacts to the side product **21**. Furthermore, the product **19** can be carboxylated to **20** and an abstraction of a proton at the α-position of the ethyl ester is preferred in comparison to the carboxylated educt, caused by the stabilization of the anion by the ester group. For the second intermediate **22**, a transfer of the ethyl ester can occur, resulting in the formation of the side product diethyl malonate **21**. Furthermore, the product **19**, a malonate derivative, may be deprotonated to **23**, which can react with ethyl chloroformate to form **21** as a side product.

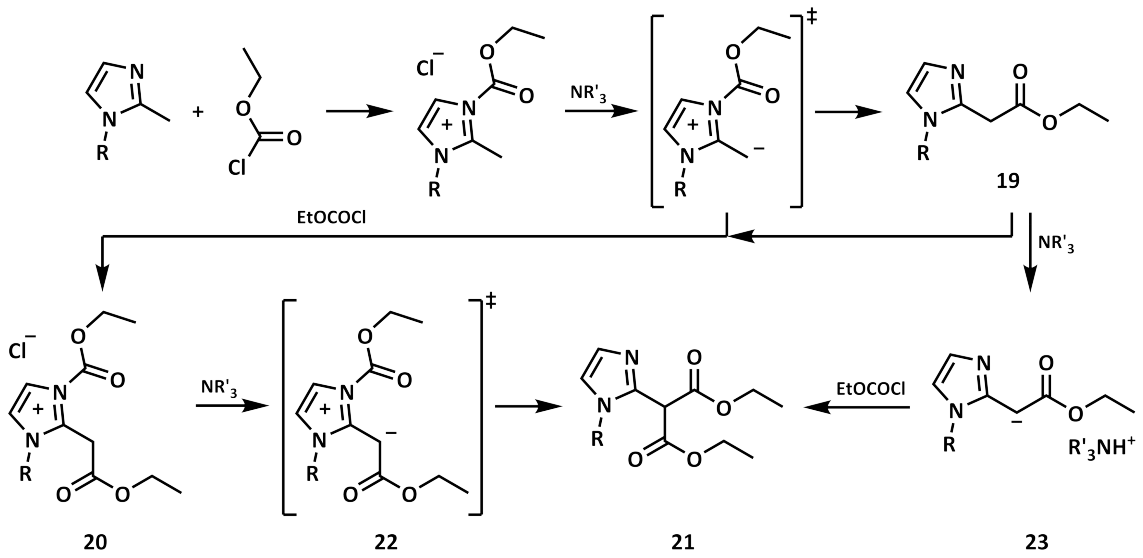

Scheme 2.18: Possible carboxylation reactions of alkylated 2-methylimidazoles with ethyl chloroformate.

A reaction with stoichiometric amounts of ethyl chloroformate and Hünig's base in dichloromethane resulted in a decreased yield to below 10% from 30% in the case of **19a**. The substituent at the 1 position of 2-methylimidazole influences the ratio of product (**19**) to side product (**21**) being formed. Due to steric effects of the protecting group at the imidazole ring, the α-position of the ethyl ester could be shielded, preventing the formation of the diethyl malonate derivative (**21**). For 2-methyl-1-tritylimidazole, only ethyl 2-(1-tritylimidazol-2-yl)acetate (**19**) was obtained in a poor yield of 8%. The exchange of the trityl moiety by a benzyl or MOM group with a lower steric hindrance leads to the formation of a mixture with the double carboxylated side product (**21**). In the case of **18a** with a MOM moiety, higher quantities of the diethyl malonate derivative (**21**) were produced in comparison to **18b** with a benzyl group. To achieve ethyl 2-(imidazol-2-yl)acetate (**24**) with an improved yield, another pathway was explored where cyclization of ethyl 3-ethoxy-3-iminopropionate hydrochloride with aminoacetaldehyde diethyl acetal was performed with non-aqueous hydrogen chloride (Scheme 2.19). The reaction has been described in the literature for different substituted α-aminoketals with yields between 35 and 72%.[159]

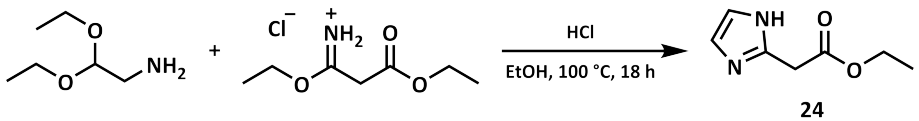

Scheme 2.19: Synthesis of ethyl 2-(imidazol-2-yl)acetate (**24**) *via* cyclization.

By the addition of aminoacetaldehyde diethyl acetal to ethyl 3-ethoxy-3-iminopropionate hydrochloride and heating to 100 °C for 5 hours, an amidine was formed. A hydrogen chloride solution in 1,4-dioxane was then added to cleave the acetal group. An intramolecular cyclization occurred by the reaction of the aldehyde with the amidine to afford **24** in a moderate yield of 50%. During purification *via* column chromatography, a smaller second product was isolated and characterized. In combination with mass spectrometry and

one- and two-dimensional NMR spectroscopy, the side product was identified as ethyl 2-(1-(diethoxymethylimidazol-2-yl)acetate (**25**). Compared to the ^{1}H NMR spectrum of **24**, the side product in Figure 2.17 shows additional signals with an ABX_3 pattern for the diastereotopic methylene groups of the acetal due to the prochiral center, and two separated signals for the aromatic imidazole protons, which is caused by the alkyl chain at the nitrogen.

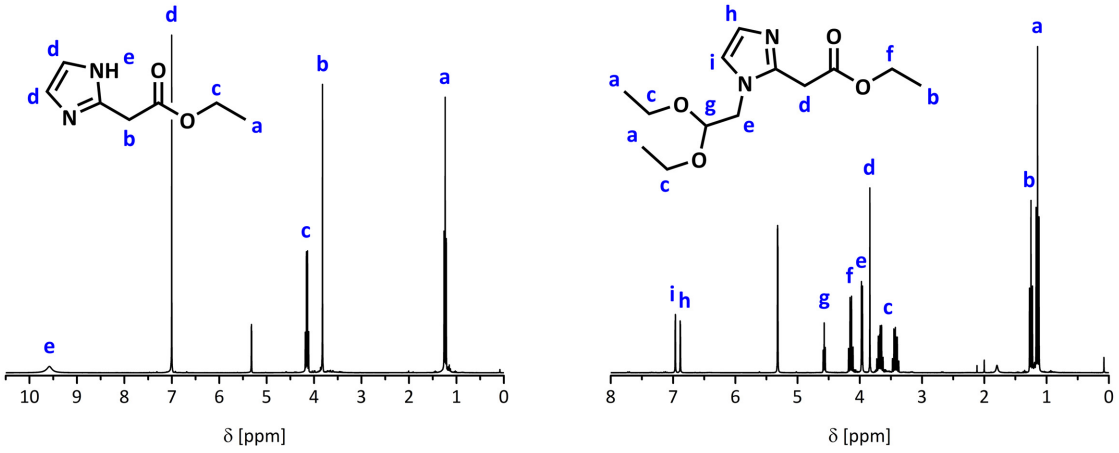

Figure 2.17: ^{1}H NMR spectra of ethyl 2-(imidazol-2-yl)acetate (**24**) (left) and the isolated side product (**25**) (right) in CD_2Cl_2.

The reaction of ethyl imidates with amines has already been described in the literature.[160–164] Hence, it is well-known that an amidine moiety can be formed by elimination of the ethoxy group as ethanol and carboximidates by the removal of nitrogen as an ammonium salt. In Scheme 2.20, both possibilities are depicted, which could explain the formation of the side product.

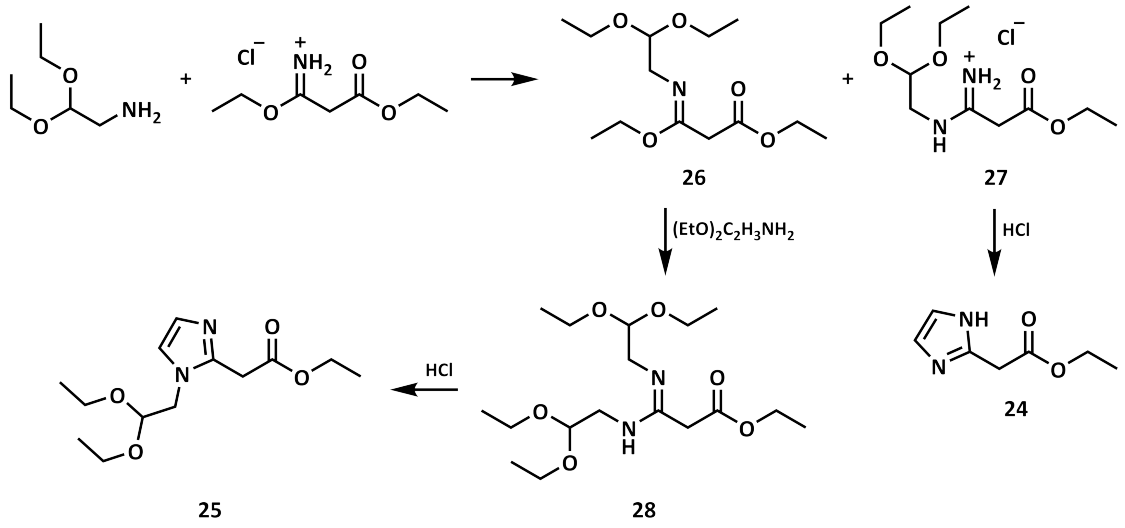

Scheme 2.20: Proposed reactions steps in the synthesis of ethyl 2-(imidazol-2-yl)acetate (**24**) and side product (**25**) *via* cyclization.

The reaction of ethyl 3-ethoxy-3-iminopropionate hydrochloride with aminoacetaldehyde diethyl acetal to the amidine (**27**) is preferred, but a carboximidate (**26**) may also be

produced. The formed carboximidate could be substituted by another aminoacetaldehyde diethyl acetal to form the amidine (**28**) with two acetal moieties, where one is cleaved by adding hydrogen chloride, followed by cyclization to imidazole. The consumption of two aminoacetaldehyde diethyl acetal molecules for one ethyl 3-ethoxy-3-iminopropionate hydrochloride diminished the yield to 50%, and higher quantities of **24** could be achieved using a slight excess of the amine. Next, **24** was deprotonated with sodium hydride and substituted by SEM chloride before it was converted into the monomer ethyl 2-(1-(2-(trimethylsilyl)ethoxy)methylimidazol-2-yl)acrylate (**30**) (Scheme 2.21).

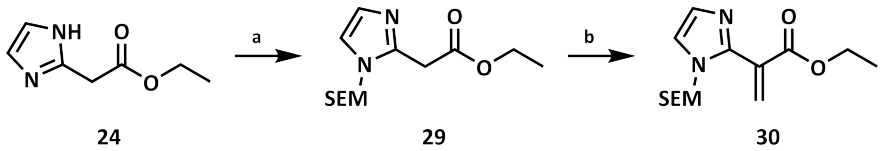

Scheme 2.21: Synthesis of **30** in two steps *via* α-methylenation. Conditions: a) NaH, SEMCl, THF, 0 °C to RT, 18 h, 75%. b) CH_2O, K_2CO_3, TBAB, MeCN, 60 °C, 16 h.

In contrast to the Wittig olefination with triphenylphosphine oxide as a byproduct, the impurities produced by α-methylenation with potassium carbonate, paraformaldehyde and a phase transfer catalyst can be removed by extraction as well as paraformaldehyde by column chromatography. After purification, **30** was obtained with a yield below 5% containing impurities and could not be used for polymerization similarly to the Wittig reaction. The broad peaks observed in the ^{1}H NMR spectrum of the crude product **30** in Figure 2.18 could indicate an autopolymerization of the monomer. Large amounts of the material were also lost by column chromatography, possibly through reactions of the strong Micheal acceptor with the silica, analogous to the synthesis of a similar monomer ethyl 2-(pyridin-2-yl)acrylate with the same problem. It is expected that the product **30** could be successfully isolated by a combination of HPLC and lyophilization. However, this route is unsuitable to purify the product on a larger gram scale.

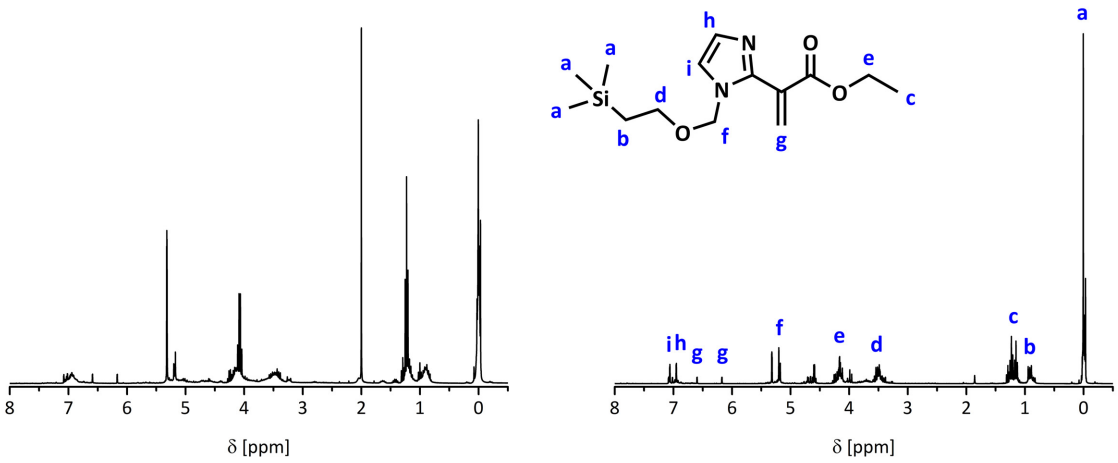

Figure 2.18: ^{1}H NMR spectra of **30** in CD_2Cl_2 before (left) and after (right) purification by column chromatography.

2.1.3 Poly(ethyl 2-(imidazol-4-yl)acrylate)

A further variation of the imidazole substitution of poly(ethyl 2-(imidazol-1-yl)acrylate) (**3**) to improve its characteristics for various applications is the attachment of the imidazole ring at the 4 or 5 position to the polymer backbone. An alkylation of poly(ethyl 2-(imidazol-4-yl)acrylate) allows to adjust its properties with the introduction of additional functional groups whilst preserving its pH response. A second alkylation affords a polycation, which can behave as a polyionic liquid that could be applied as a surfactant or for heterogeneous catalysis with immobilized transition metals within the polymer. Contrary to **3**, the 2 position of the imidazole is less sterically hindered in the alkylated poly(ethyl 2-(imidazol-4-yl)acrylate), and is therefore more suitable for use in catalysis. Furthermore, polyampholytes can be accessed by hydrolyzing the ester moiety, and used to coat magnetic iron oxide nanoparticles for biomedical applications, or in water treatment to remove metal ions through complexation.

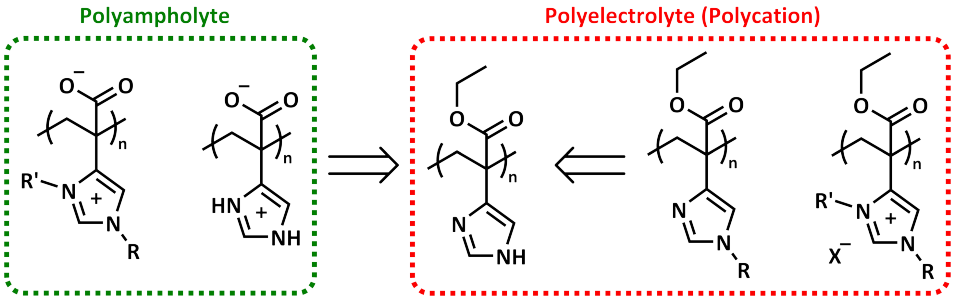

Scheme 2.22: Possible modifications of poly(ethyl 2-(imidazol-4-yl)acrylate).

To access poly(ethyl 2-(imidazol-4-yl)acrylate) and its derivatives, a multi-step synthesis of the monomer is necessary. Moreover, a protecting group is required to prevent side reactions by the formation of the carbon-carbon double bond *via* α-methylenation, and to reduce the polarity for an easier purification. Two synthetic routes were used to prepare ethyl 2-(imidazol-4-yl)acetate as a precursor to the monomer as shown in Scheme 2.23. One option is to synthesize the imidazole ring by cyclization, and another option is to transform a side group of the imidazole into an ester.

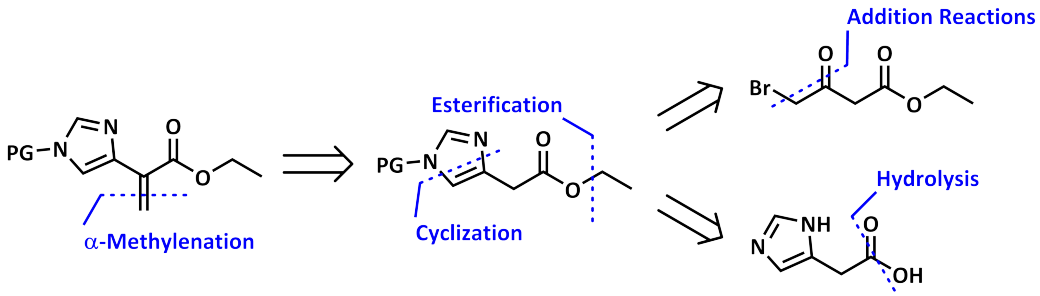

Scheme 2.23: Synthetic approaches to prepare the protected ethyl 2-(imidazol-4-yl)acrylate.

In accordance to literature, crotonyl chloride was converted into ethyl but-3-enoate (**31**) with ethanol and triethylamine in diethyl ether, instead of *n*-pentane, and further oxidized with *meta*-chloroperoxybenzoic acid to ethyl 2-(oxiran-2-yl)acetate (**32**) in good yields

(Scheme 2.24).[165, 166] The ring-opening of the epoxide to a bromohydrin occurred using lithium bromide and acetic acid to afford high quantities of ethyl 4-bromo-3-hydroxybutyrate (**33**).

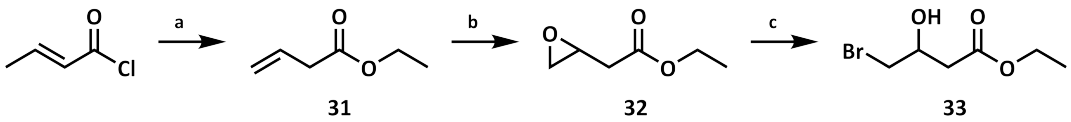

Scheme 2.24: Synthesis of ethyl 4-bromo-3-hydroxybutyrate. Conditions: a) EtOH, NEt_3, Et_2O, 0 °C to RT, 12 h, 77%. b) *m*CPBA, DCM, 0 °C to RT, 20 h, 73%. c) LiBr, HOAc, THF, 0 °C to RT, 19 h, 92%.

To prepare an imidazole moiety *via* cyclization, the α-bromoketone was synthesized by selective oxidation of the bromohydrin (**33**) under mild conditions with the Dess-Martin periodinane, and only a moderate yield of 46% was achieved (Scheme 2.25).

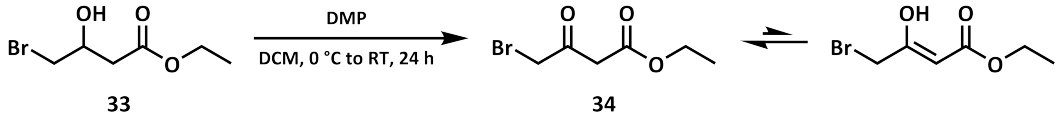

Scheme 2.25: Synthesis of ethyl 4-bromo-3-oxybutyrate (**34**) *via* a Dess-Martin oxidation.

In the ^{1}H NMR spectrum of the product ethyl 4-bromo-3-oxybutyrate (**34**) in Figure 2.19, additional signals associated with the enol tautomer are observed. The enol form of **34** is stabilized by intramolecular hydrogen bonding to the carbonyl oxygen of the ethyl ester. From the NMR spectrum, a keto-enol ratio of 1.0:0.3 was calculated, and a possible second enol species may be visible with the double bond to the brominated carbon atom. However, this species could not be definitively identified due to the low intensity of the signals.

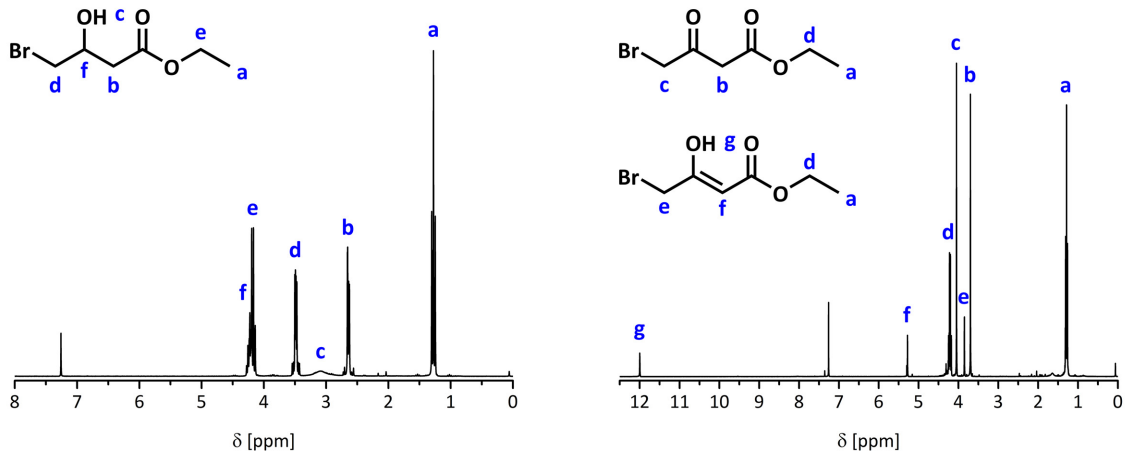

Figure 2.19: ^{1}H NMR spectra of ethyl 4-bromo-3-hydroxybutyrate (**33**) (left) and ethyl 4-bromo-3-oxybutyrate (**34**) (right) in $CDCl_3$.

A large variety of imidazole derivatives with aromatic, as well as aliphatic, substitutions at the 4 and 5 position can be prepared by the Bredereck synthesis from α-hydroxy- or α-haloketones using formamide as solvent and an ammonia source.[167] The conversion of

ethyl 4-bromo-2,2-dimethyl-3-oxobutyrate and formamide into ethyl 2-(imidazol-4/5-yl)-2-methylpropionate is described by Matsunaga *et al.* with a poor yield of 20%, which can be attributed to side reactions of the ester moiety.[168] The same reaction with **34** afforded no product, which may result from keto-enol tautomerism. Another method to transform α-bromoketones into imidazoles is the substitution with amidines. Therefore, a suspension of **34**, formamidine hydrochloride and potassium carbonate in *N*,*N*-dimethylformamide was heated to 100 °C for 15 hours. However, the desired product was not obtained as before.

Another approach to prepare ethyl 2-(imidazol-4/5-yl)acetate (**37**), besides the heterocycle synthesis, is to modify the substituent at the imidazole in histidine (Scheme 2.26). The conversion of the amino acid into ethyl 2-(1-tritylimidazol-4-yl)acetate, as well as individual reaction steps, are described in the literature.[169–172] The reaction conditions used here were slightly modified. To remove the additional carbon atom of the histidine scaffold between the carboxylic acid and imidazole ring, a decarboxylation and oxidation of the α-carbon and amine into a nitrile was performed using sodium hypochlorite in the first step.

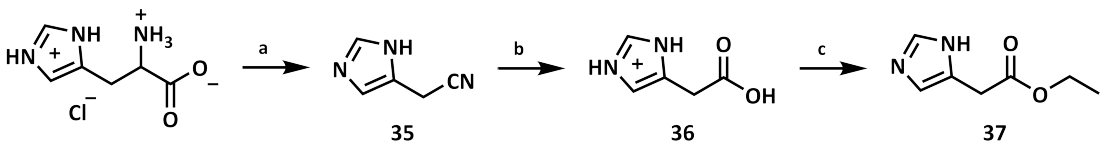

Scheme 2.26: Synthesis of ethyl 2-(imidazol-4/5-yl)acetate (**37**). Conditions: a) NaOCl, H_2O, -10 °C to RT, 22 h, 68%. b) 6 M HCl, H_2O, 110 °C, 5 h, 63%. c) AcCl, EtOH, -15 °C to RT, 4 h, 75%.

The hydrolysis of 2-(imidazol-4/5-yl)acetonitrile (**35**) to a carboxylic acid was carried out using hydrochloric acid under reflux, achieving a moderate yield after recrystallization from methanol. The prepared 2-(imidazol-4-yl)acetic acid hydrochloride (**36**) was then esterified with acetyl chloride in ethanol. Due to the protonated imidazole moiety, the carboxylic acid of **36** formed an asymmetric anhydride by the reaction with acetyl chloride at 0 °C. This asymmetric anhydride then reacted with ethanol to form **37** after the mixture warmed to room temperature. For the α-methylenation, the imidazole ring was substituted with trityl chloride or SEM chloride to prevent side reactions and to improve the separation by column chromatography, due to its reduced polarity. The crude ethyl ester (**37**) was used to synthesize ethyl 2-(1-tritylimidazol-4-yl)acetate (**38**) by the addition of trityl chloride and triethylamine as base. Whereas, the protection with the SEM group using sodium hydride required a purification of the educt, and afforded a regioisomeric mixture of ethyl 2-(1-(2-(trimethylsilyl)ethoxy)methylimidazol-4/5-yl)acetate (**39**) as depicted in Scheme 2.27.

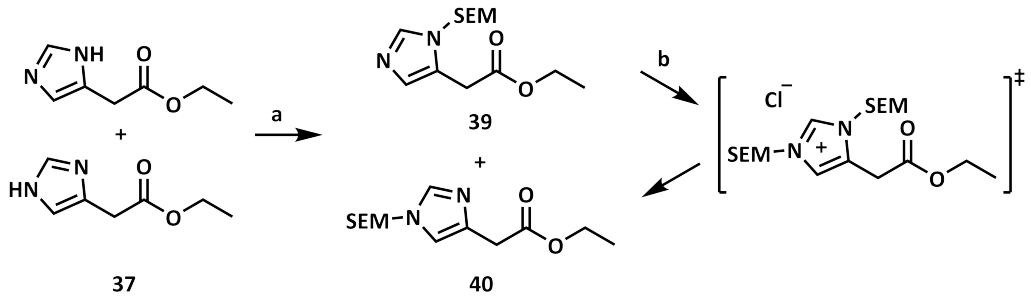

Scheme 2.27: Synthesis of ethyl 2-(1-(2-(trimethylsilyl)ethoxy)methylimidazol-4-yl)acetate (**40**). Conditions: a) NaH, SEMCl, THF, 0 °C to RT, 17 h, 68%. b) SEMCl, THF, 70 °C, 72 h, 84%.

The mixture of regioisomers was converted into the favored ethyl 2-(1-(2-(trimethylsilyl)ethoxy)methylimidazol-4-yl)acetate (**40**) by the addition of 10 mol% SEM chloride and heating to 70 °C. A high yield of 84% was achieved as expected from the synthesis of similar compounds.[173, 174] After isomerization, the structure of the isomer was confirmed by selective one dimensional nuclear Overhauser effect ^{1}H NMR spectroscopy. To prepare the monomers, the carbon-carbon double bond was introduced for a radical polymerization *via* an α-methylenation with paraformaldehyde, potassium carbonate and tetra-*n*-butylammonium bromide as a phase transfer catalyst. Ethyl 2-(1-tritylimidazol-4-yl)acrylate (**41**) was synthesized with a yield of 38% as pale yellowish crystals. These crystals were characterized by X-ray analysis, NMR spectroscopy and mass spectrometry (Figure 2.20). Ethyl 2-(1-(2-(trimethylsilyl)ethoxy)methylimidazol-4-yl)acrylate (**42**) was synthesized with a yield of 26% as a pale yellow oil, which did not crystallize, and they were analyzed by NMR spectroscopy and high resolution mass spectrometry. Similarly to **1**, an oil, autopolymerization of **42** was observed after a few months at -24 °C, but the crystalline monomers **1** and **41** were stable over one year at the same temperature.

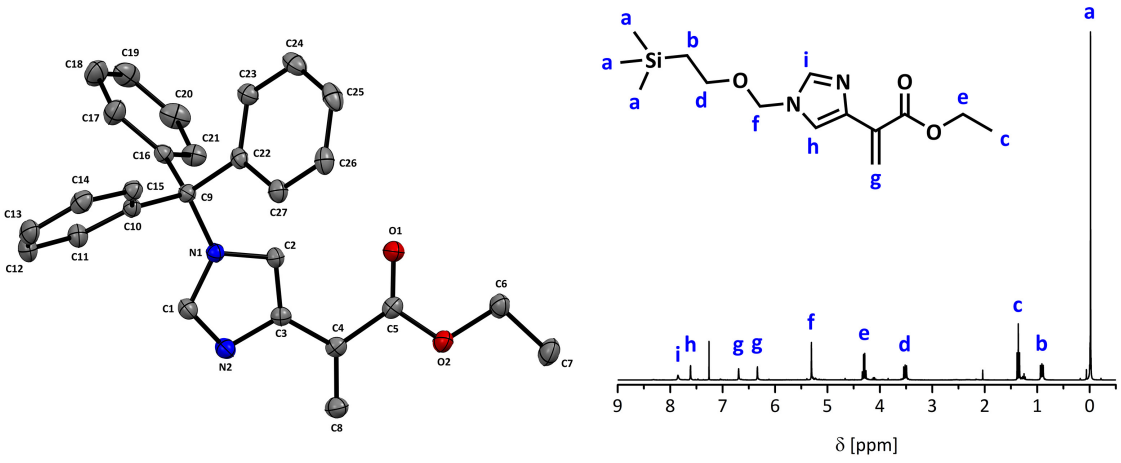

Figure 2.20: Molecular structure of ethyl 2-(1-tritylimidazol-4-yl)acrylate (**41**) (left) and the ^{1}H NMR spectrum of ethyl 2-(1-(2-(trimethylsilyl)ethoxy)methylimidazol-4-yl)acrylate (**42**) (right) in $CDCl_3$.

Both monomers were free radically polymerized at 70 °C with azobisisobutyronitrile as initiator resulting in high molecular weights (Table 2.5). The purification of poly(ethyl 2-(1-tritylimidazol-4-yl)acrylate) (**43**) and poly(ethyl 2-(1-(2-(trimethylsilyl)ethoxy)methylimidazol-4-yl)acrylate) (**44**) *via* dialysis afforded low quantities for analysis, which may be the result of damaged dialysis membranes caused by freezing in the refrigerator. Hence, cleavage of the polymer protecting groups and other modifications were not attempted. However, as **41** is the more promising monomer for further research, developing an effective polymer purification procedure by precipitation is necessary.

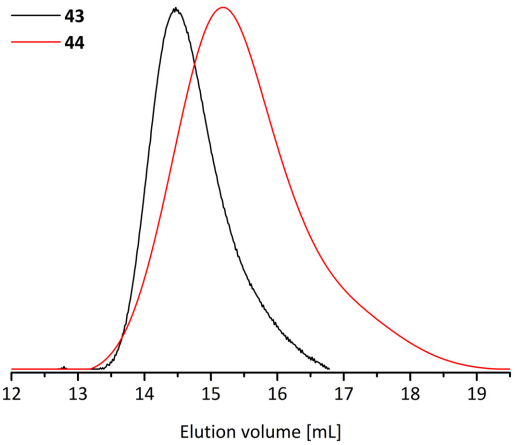

Figure 2.21: SEC elugrams in DMAc of **43** and **44**.

Table 2.5: SEC data in DMAc of **43** and **44**.

Polymer	$\overline{M}_n$ [a)]	$Đ$ [a)]
43	157,900 g·mol^{-1}	1.25
44	67,600 g·mol^{-1}	1.68

[a)] PMMA calibration.

2.1.4 Poly(diethyl 1-(imidazol-1-yl)vinylphosphonate)

The polyampholyte poly(2-(imidazolium-1-yl)acrylate) (**5**) was used to coat iron oxide nanoparticles. By changing the anchoring carboxylate group to a phosphonate group, the polymer could bind to the metal surface more effectively. Based on the stronger interaction with metal ions, such an ampholytic polymer is more suitable for use in water treatment or as an antifouling coating on metal surfaces. Furthermore, the solubility in aqueous media may be enhanced over the entire pH range due to the higher acidity and additional negative charge of the diprotic phosphonic acid derivative. Therefore, poly(dietly 1-(imidazol-1-yl)vinylphosphonate) (**45**) and its derivatives should be developed as shown in Scheme 2.28 starting with the preparation of the monomer.

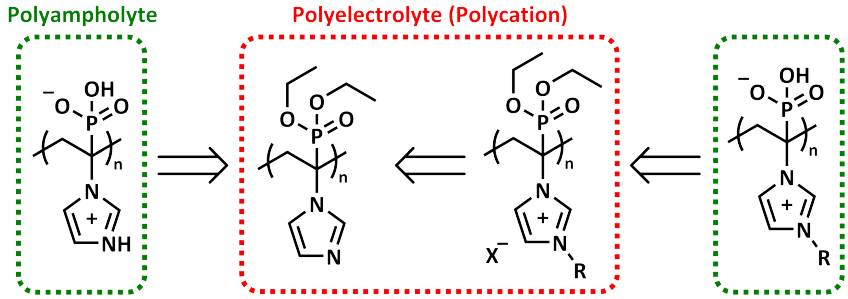

Scheme 2.28: Possible modifications of poly(diethyl 1-(imidazol-1-yl)vinylphosphonate).

Similar to **1**, the synthesis of diethyl 1-(imidazol-1-yl)vinylphosphonate (**46**) carried out by an addition reaction of imidazole to an activated acetylene derivative with a phosphonate group. First, diethyl ethynylphosphonate (**45**) was prepared *via* two different approaches as depicted in Scheme 2.29.

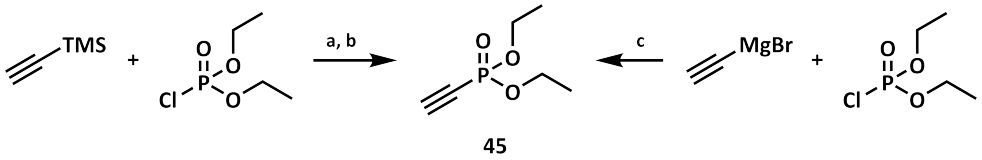

Scheme 2.29: Synthesis of diethyl ethynylphosphonate (**45**). Conditions: a) EtMgBr, Et_2O, -10 °C to RT, 6 h. b) TBAF, DCM, 0 °C to RT, 2 h. c) THF, -15 °C to RT, 3 h.

The synthesis of **45** has been reported *via* deprotonation of trimethylsilylacetylene, reacting with diethyl chlorophosphate, and followed by cleavage of the silyl group. A moderate yield of 45% was reported using *n*-butyllithium as base, and a yield of 84% using ethylmagnesium bromide.[175, 176] After conversion of trimethylsilylacetylene with ethylmagnesium bromide and diethyl chlorophosphate into diethyl 2-(trimethylsilyl)ethynylphosphonate, the trimethylsilyl moiety of the crude product was removed with tetra-*n*-butylammonium fluoride in dichloromethane to afford **45** with a low yield of 25%. The reaction using *n*-butyllithium instead of the Grignard reagent as base resulted in lower quantities of the product. A direct synthesis of **45** in one step by adding ethynylmagnesium bromide to diethyl chlorophosphate has been reported with yields between 24 and 38%.[177, 178] Under these conditions, the product was obtained with a yield of 22%, and the side products could

be easily removed by column chromatography. With imidazole and triphenylphosphine as a mediator, diethyl ethynylphosphonate was converted to **46** in a moderate yield of 48% (Scheme 2.30).

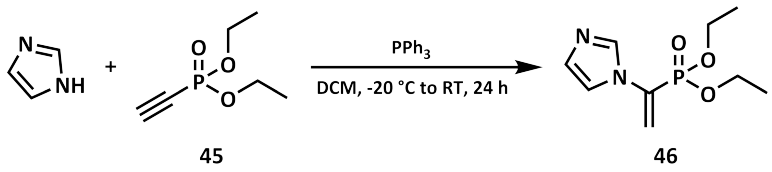

Scheme 2.30: Synthesis of diethyl 1-(imidazol-1-yl)vinylphosphonate (**46**) *via* triphenylphosphine-mediated nucleophilic α-addition.

The structure of the monomer was confirmed by mass spectrometry and NMR spectroscopy. Due to the phosphorus atom with a nuclear spin of 0.5 and magnetic interactions with other nuclei, the ^{1}H NMR spectrum of **46** shows a higher splitting for the protons at the ethyl esters and methylene group (Figure 2.22). Additionally, doublets were observed in the proton decoupled ^{13}C NMR spectrum, and the single signal in the ^{31}P NMR spectrum is shifted compared to the educt.

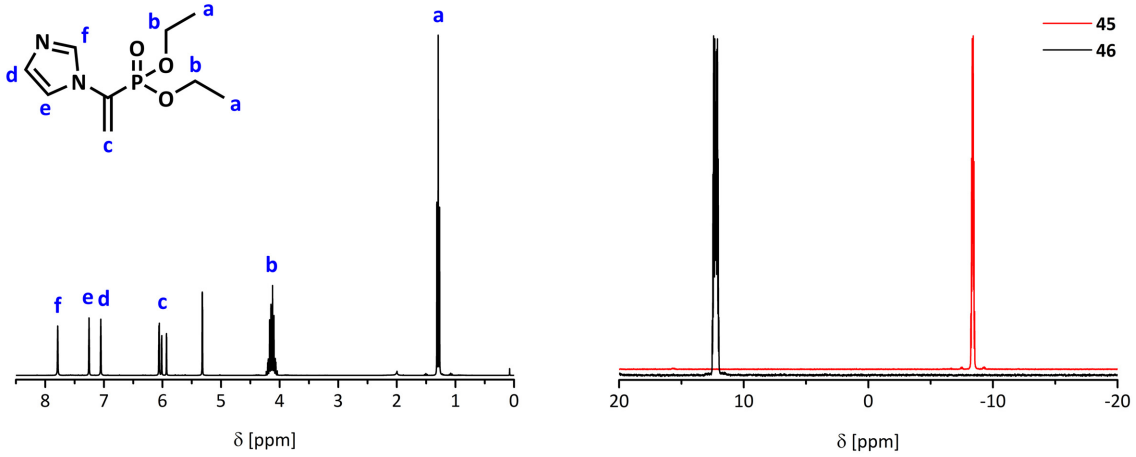

Figure 2.22: ^{1}H NMR spectrum of **46** (left) in CD_2Cl_2 and ^{31}P NMR spectra of **45** and **46** (right).

The polymerization of **46** was done free radically with azobisisobutyronitrile at 70 °C under solvent-free conditions and was purified by dialysis to afford low quantities of the polymer as a yellow solid. The same dialysis membrane was used as before, and which may have been damaged. The removal of the polar monomer from the polymer by precipitation is challenging due to their similar solubilities. Based on the SEC elugram in chloroform with a high molecular weight of 125,900 g·mol^{-1} and a dispersity of 6.74 against a PMMA calibration, a higher conversion is assumed as expected from the yield of the polymer. The NMR spectra of poly(diethyl 1-(imidazol-1-yl)vinylphosphonate) (**47**) show broad signals that are typical for polymers, and several broad peaks in the ^{31}P NMR spectrum, which could be caused by the tacticity of the polymer (Figure 2.23). In order to investigate

possible modifications of **47**, larger quantities of the polymer are necessary, and purification by dialysis can be reattempted. Another promising purification technique that can be applied is preparative SEC.

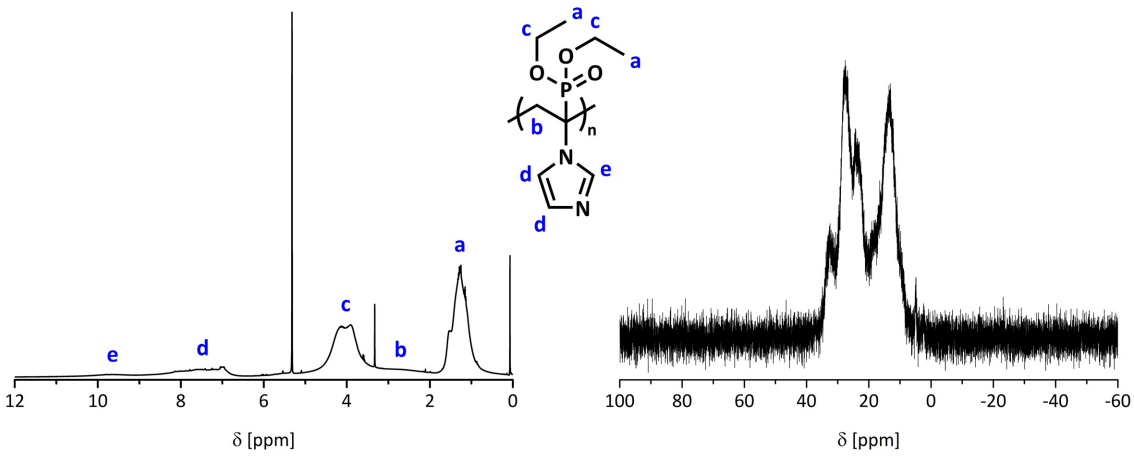

Figure 2.23: ^{1}H NMR (left) and ^{31}P NMR spectra (right) of poly(diethyl 1-(imidazol-1-yl)vinylphosphonate) (**47**) in CD_2Cl_2.

2.2 Poly(ethyl 2-(hydroxymethyl)acrylates) and Derivatives

In general, the preparation of polyampholytes with a high charge density and their precursors, *e.g.* poly(dehydroalanine) and poly(2-(imidazol-1-yl)acrylate), requires the synthesis of each monomer. Such monomers proved challenging to polymerize *via* controlled polymerization methods. To circumvent this problem, polyampholytes can be prepared by the polymerization and modification of ethyl 2-(chloromethyl)acrylate or ethyl 2-(hydroxymethyl)acrylate. Polyelectrolytes can be obtained by the substitution of the activated hydroxy groups and halides at such polymers using several amines or azoles, which can further be converted into polyampholytes by the cleavage of the ester moiety as shown in Scheme 2.31. Two synthetic approaches were explored involving the conversion of the monomer or polymer hydroxy moieties into a good leaving group.

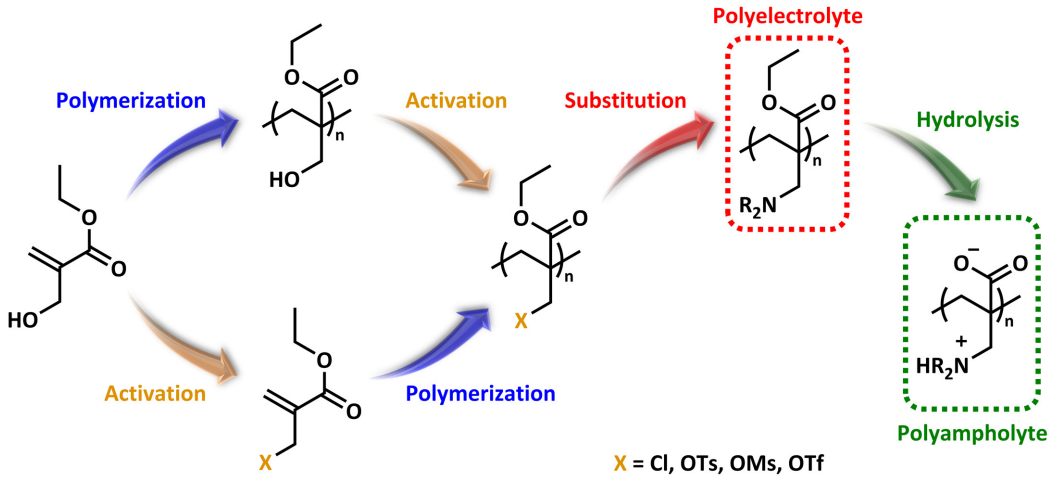

Scheme 2.31: Possible preparation methods and substitution of modified poly(ethyl 2-(hydroxymethyl)acrylate).

The radical homopolymerization of ethyl 2-(halomethyl)acrylate has already been described in the literature.[179, 180] The researchers found that only the fluoride and chloride derivatives formed a polymer. Furthermore, the synthesis of poly(ethyl 2-(chloromethyl)acrylate) and its subsequent substitution with stearyl mercaptan and 2-ethyl-2-oxazoline has been reported, as well as the copolymerization of ethyl 2-(chloromethyl)acrylate and styrene.[181, 182] To use poly(ethyl 2-(chloromethyl)acrylate) for the preparation of polyampholytes *via* substitution, the monomer was synthesized in two steps as depicted in Scheme 2.32.

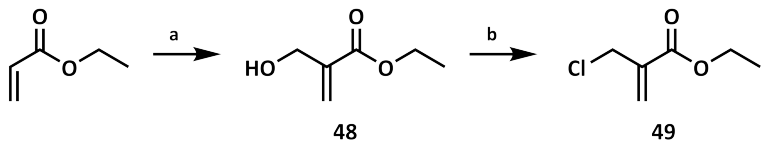

Scheme 2.32: Synthesis of ethyl 2-(chloromethyl)acrylate (**49**). Conditions: a) DABCO, H_2CO, MeCN, H_2O, 50 °C, 59 h, 44%. b) $SOCl_2$, RT, 18 h, 59%.

Ethyl acrylate was converted into ethyl 2-(hydroxymethyl)acrylate (**48**) by a literature procedure *via* the Morita-Baylis-Hillman reaction using formaldehyde and triethylenediamine as a nucleophilic catalyst.[183] Next, the hydroxy group was replaced by chloride using thionyl chloride to synthesize ethyl 2-(chloromethyl)acrylate (**49**). The product was obtained in a high purity for the subsequent polymerization by column chromatography and distillation. Based on previous reports on polymerizing **49** under various conditions, poly(ethyl 2-(chloromethyl)acrylate) (**50**) was prepared free radically under solvent-free conditions, as well as in benzene and anisole before attempting the controlled RAFT technique (Figure 2.24).

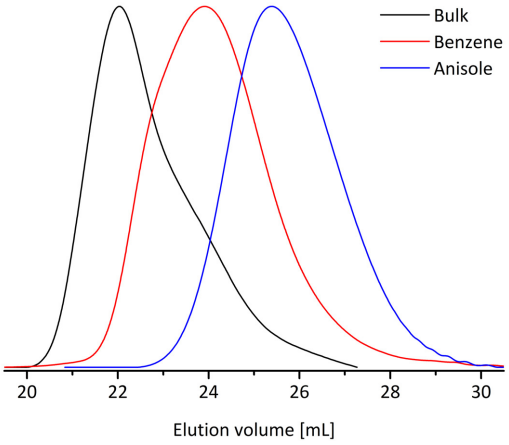

Figure 2.24: SEC elugrams in THF of **50** obtained by radical polymerization.

Table 2.6: SEC data in THF of **50** obtained by radical polymerization.

Solvent	$\overline{M}_n$ [a)]	$Đ$ [a)]
Bulk	14,100 g·mol^{-1}	1.67
Benzene	6,600 g·mol^{-1}	1.73
Anisole	3,300 g·mol^{-1}	1.38

a) PMMA calibration.

The polymerization of **49** using benzene as solvent resulted in a significantly lower molar mass compared to the preparation of **50** under solvent-free conditions, as well as a diminished yield from 78 to 32%. Moreover, the polymerization of **49** in anisole was attempted due to its lower toxicity compared to benzene. This resulted in a further decrease in the molecular weight achieved from 6,600 g·mol^{-1} in benzene to 3,300 g·mol^{-1} in anisole (Table 2.6). Due to the successful formation of polymer, a RAFT polymerization was attempted despite the possible transfer reactions of the chloride at the allyl position. Chain transfer constants (C_{tr}) of similar compounds like 2-(chloromethyl)acrylonitrile and bromide derivatives are given for the polymerization of methyl methacrylate in Scheme 2.33.[34, 184]

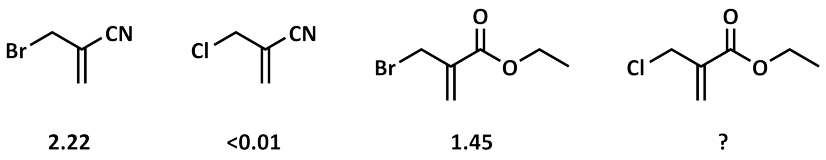

Scheme 2.33: Chain transfer constants of various allyl halides for the polymerization of methyl methacrylate with AIBN at 60 °C.[184]

The transfer constant is the quotient of the transfer rate constant to the propagation rate constant, and high values represent an efficient transfer. While the bromide derivatives afforded chain transfer predominantly, a copolymerization was observed for 2-(chloromethyl)acrylonitrile with a low transfer constant.[34, 184] Based on this data, a low transfer constant is also expected for **49**, which may influence the RAFT polymerization. In a first attempt, the monomer was polymerized using azobisisobutyronitrile as a thermal initiator in the presence of a suitable RAFT agent, 2-cyano-2-propyl benzodithioate, at 65 °C. However, under these conditions no polymer was formed. The use of the universal chain transfer agent CPzDB afforded the polymer **50** with a molecular weight of 6,500 g·mol^{-1}, which is half of that achieved using free radical polymerization. The SEC elugram in Figure 2.25 shows a slight higher molecular weight shoulder and a dispersity of 1.5. The polymerization was repeated with benzene as solvent resulting in a polymer with a decreased molar mass as anticipated from the free radical polymerizations, as well as a broader molecular weight distribution and a second peak at higher elution volumes. In both RAFT polymerizations of **49**, the SEC curves strongly suggest side reactions occur, which is further supported by the poor yields of below 15%. A radical transfer through the chloride is suspected as the predominant side reaction. The controlled radical polymerization of **49** *via* RAFT was not achieved, and it is simply unfeasible under the conditions explored to obtain high monomer conversions with narrow distributions or block extensions.

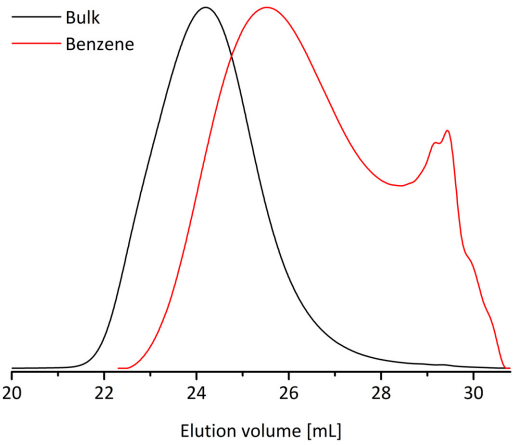

Figure 2.25: SEC elugrams in THF of **50** obtained by RAFT polymerization.

Table 2.7: SEC data in THF of **50** obtained by RAFT polymerization.

Solvent	$\overline{M}_n$ [a)]	$Đ$ [a)]
Bulk	6,500 g·mol^{-1}	1.53
Benzene	1,800 g·mol^{-1}	2.06

[a)] PMMA calibration.

An alternative monomer with a good leaving group is ethyl 2-((tosyloxy)methyl)acrylate (**51**), which was synthesized by tosylation of **48** (Scheme 2.34). Therefore, **48** was deprotonated with sodium hydride, and tosyl chloride added analogous to a similar literature procedure to afford the monomer **51** in a moderate yield of 63%.[185]

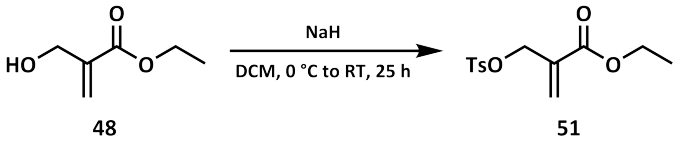

48 51

Scheme 2.34: Synthesis of ethyl 2-((tosyloxy)methyl)acrylate (**51**) by tosylation.

The monomer **51** was polymerized *via* RAFT in tetrahydrofuran at 40 °C. As a chain transfer agent, CPADB was used in a 3:1 ratio to the initiator 2,2'-azobis(4-methoxy-2,4-dimethylvaleronitrile). Additionally, trioxane was used as an internal standard to determine the monomer conversion by NMR spectroscopy, and the chain-growth was further monitored by SEC. A fast polymerization was observed in the beginning with a monomer consumption of 34% after 30 minutes, and 74% after 8 hours. At approximately 5 hours the viscosity of the reaction mixture increased and the pink color of the dithiobenzoate became brighter. The polymerization was terminated after 12 hours to afford the polymer as a white solid by precipitation. The white color of poly(ethyl 2-((tosyloxy)methyl)acrylate) indicates that the polymer has no ditihobenzoate end group, and that the RAFT agent degraded during the polymerization. The SEC analysis of the RAFT polymerization substantiates this assumption with a steady increase in the molecular weight distribution over the polymerization time as visible in Figure 2.26. However, the dispersities of the first two data points are not reliable due to the overlapping system peak starting from an elution volume of 21.5 mL. Whilst a slight increase in the molecular weight distribution occurred at higher viscosities, a distinct rise was detected as a result of the chain transfer agent degradation and inhomogeneities through poor mixing.

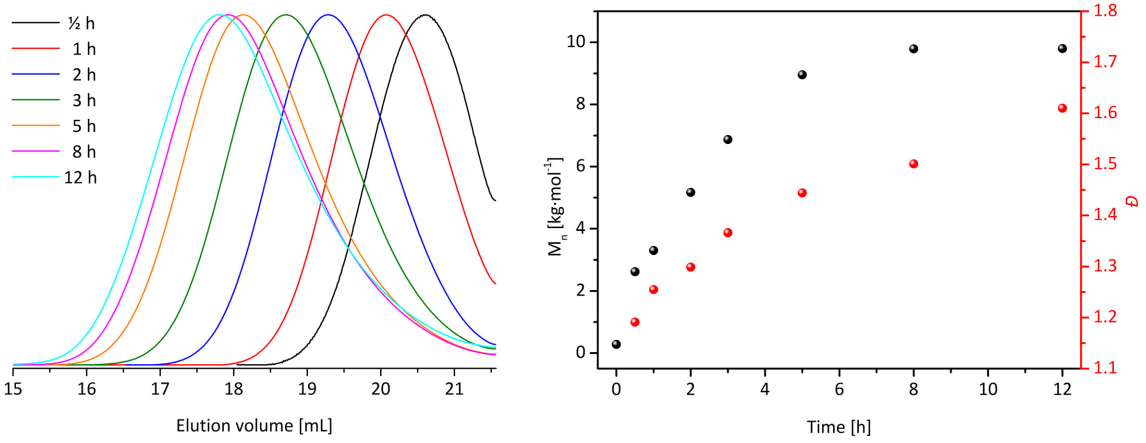

Figure 2.26: SEC elugrams in DMAc (left) and SEC data using a PMMA calibration with time (right) of the RAFT polymerization of ethyl 2-((tosyloxy)methyl)acrylate (**51**).

In a second attempt, a 10:1 ratio of the RAFT agent to initiator was used to reduce the radical concentration and hinder side reactions to improve the polymerization control. The reduced radical concentration leads to a slower consumption of **51**, with a monomer conversion of 45% after 12 hours instead of 70% as before. Similar to the first attempt, the molecular weight distribution increased over time and afforded higher dis-

persities at the same monomer conversions compared to the first RAFT polymerization. The precipitated polymer has a white color, again indicating the chain transfer agent degraded perhaps by a reaction of the dithioate moiety with the tosylated monomer. A trithiocarbonate could be used with a higher stability against nucleophiles, but the sulfur of the thiocarbonyl group may also react with the tosylate as an alkylation reagent. A RAFT polymerization of methacrylates with a leaving group at the 2 position is difficult as a consequence of side reactions including the degradation of the chain transfer agent or transfer reactions of the monomer. This is caused by the allylic position, and for a controlled radical polymerization there are only a few heteroatoms that are tolerated including oxygen. As a reported example, the ester moiety of ethyl 2-(aminomethyl)acrylate was substituted by the amine when polymerized free radically.[186] Furthermore, it has been reported that no propagation was observed for the radical initiation of ethyl 2-((*N*-benzyl-*N*-methylamino)methyl)acrylate.[187] Based on these findings, we aimed to polymerize **48** and modify its pendent hydroxy groups in a polymer analogous reaction to access polyelectrolytes. The preparation of poly(ethyl 2-(hydroxymethyl)acrylate) (**52**) with a narrow molecular weight distribution *via* RAFT is described by Peng and Joy.[188] They reported a lower monomer conversion by the increase in the chain transfer agent to monomer ratio from 3:1 to 5:1. To reduce the amount of dead chain ends, which are not terminated by a thiocarbonylthio group and could not be extended with a further block, a tenfold excess of the RAFT agent to initiator was used. Hence, the polymerization conditions were adjusted with a higher monomer concentration, the solvent was further changed from 1,4-dioxane to tetrahydrofuran, and the polymerization was initiated at 40 °C with 2,2'-azobis(4-methoxy-2,4-dimethylvaleronitrile) (Scheme 2.35).

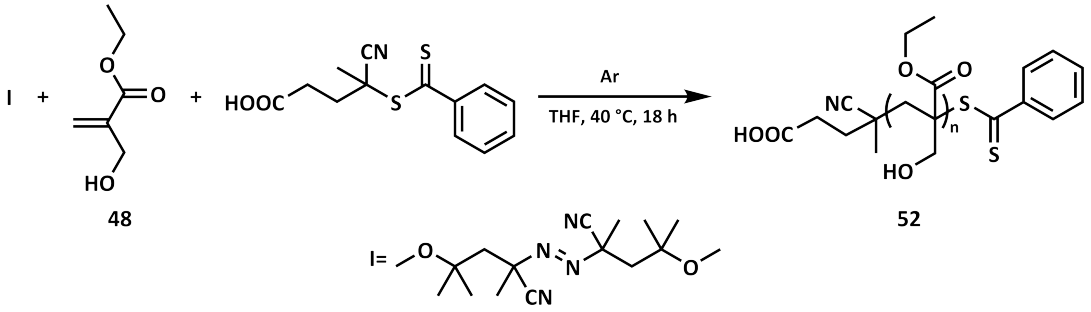

Scheme 2.35: RAFT polymerization of ethyl 2-(hydroxymethyl)acrylate (**48**).

In a kinetic investigation of the RAFT polymerization shown in Scheme 2.35, a monomer conversion up to 86% was achieved as determined by NMR spectroscopy using trioxane as an internal standard. Moreover, a narrow molecular weight distribution was observed by SEC analysis. The growth of the polymer with time is nicely visible in the SEC elugrams, with a small low molecular weight shoulder appearing after 30 minutes. This may be caused by moderately fast reinitiation (Figure 2.27). Another small shoulder, attributed to dead chains, appeared after 18 hours at higher molar masses. These dead chains likely arise from irreversible termination by coupling of propagating radicals, which is more likely at high conversion. The formation of these dead chains explains the observed deviation

from the linear increase in molar masses with conversion to higher molecular weights at the end. A reduction in the dispersity was observed until approximately 55% of the monomer **48** was consumed, and rose with the increasing viscosity at higher conversions.

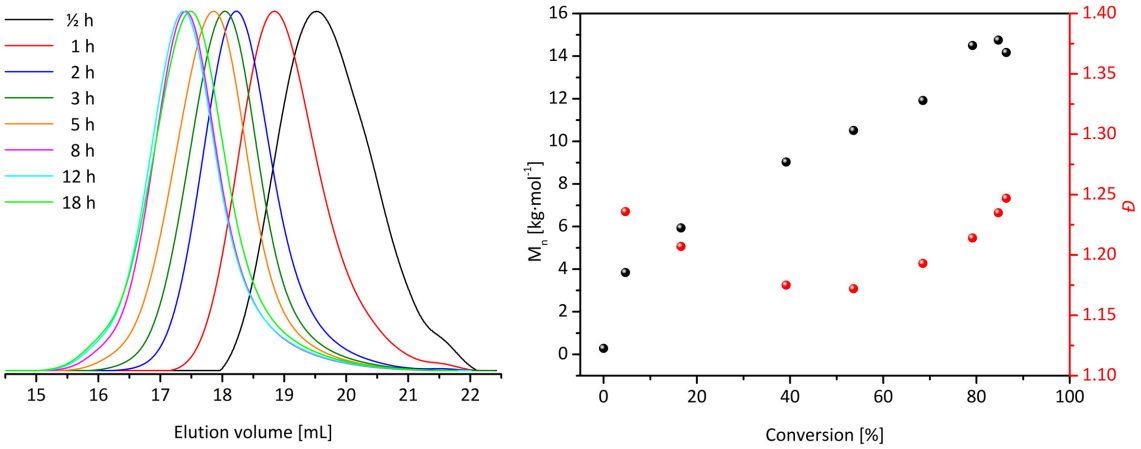

Figure 2.27: SEC elugrams in DMAc (left) and corresponding SEC data using a PMMA calibration with increasing conversion (right) from the RAFT polymerization of **48**.

In the conversion *versus* time plot shown in Figure 2.28, the increase in monomer conversion is negligible after 8 hours of polymerization. Hence, the reaction time can be reduced to prevent irreversible termination and broadening of the molecular weight distribution. Furthermore, the kinetic plot shows a retardation at the beginning of the polymerization before an almost linear slope is observed from 1 to 5 hours or until a conversion of 69% of **48** is reached. Afterwards, this curve flattens off due to the low excess of monomer, and the pseudo-first order reaction does not exhibit the characteristics of a first-order kinetic anymore.

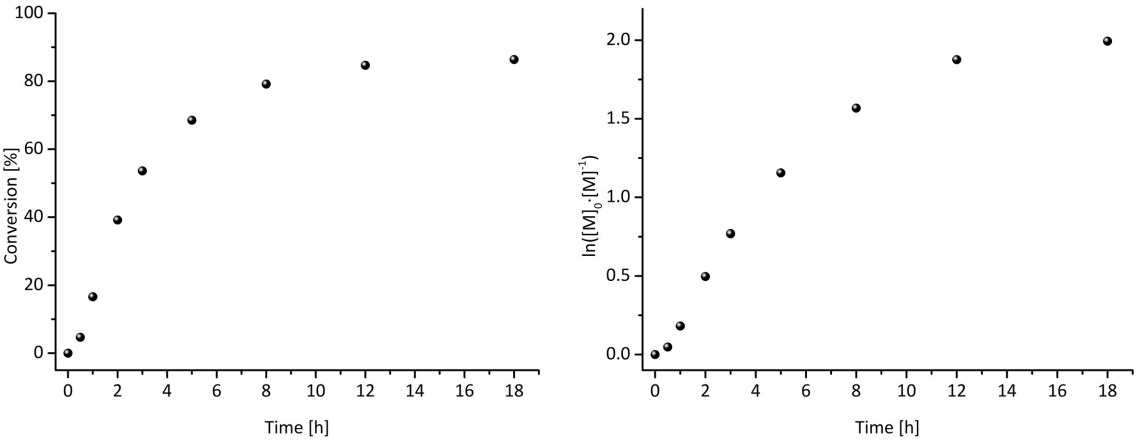

Figure 2.28: Conversion with time (left) and kinetic plot (right) of the RAFT polymerization of ethyl 2-(hydroxymethyl)acrylate (**48**).

Under the improved conditions, **48** was polymerized *via* RAFT in three batches. In the first batch, 5 g of monomer was used and yielded 71% of polymer (**52a**) as a pink solid. This reaction was repeated at a larger scale using 15 g of monomer to achieve approximately

11 g of the polymer (**52b**). A conversion of 78% was determined by NMR spectroscopy and an average chain length of 83 monomeric units was calculated. The third approach (**52c**) was performed similarly to the second batch, but a lower molar mass was observed, and only 50% of the monomer was consumed (Figure 2.29).

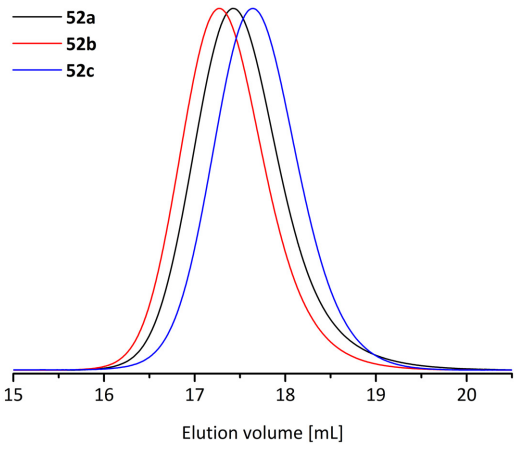

Figure 2.29: SEC elugrams in DMAc of **52** obtained by RAFT polymerization.

Table 2.8: SEC data in DMAC of **52** obtained by RAFT polymerization.

Polymer	$\overline{M}_n$ [a)]	$Đ$ [a)]
52a	18,300 g·mol^{-1}	1.13
52b	20,700 g·mol^{-1}	1.11
52c	16,700 g·mol^{-1}	1.11

a) PMMA calibration.

All three polymers have a narrow dispersity below 1.2 (Table 2.8). Since the SEC was calibrated using PMMA standards, the molecular weights are approximately 10,000 g·mol^{-1} higher than those calculated from NMR spectroscopy. Nevertheless, **52b** was used for a block extension, and first attempts to modify the polymer with amines were carried out using **52c**. With **52a**, the conversion into various polyampholytes by the attachment of amines and heterocycles in combination with the ester hydrolysis should be demonstrated. In accordance with our initial project goals to prepare polyelectrolytes and polyampholytes for use in advanced applications, such as heterogeneous catalysis and in drug or gene delivery, block copolymers containing **52** were successfully prepared that are capable of assembling into micellar structures as desired. Two diblock copolymers based on **52** were prepared with a hydrophilic poly(ethylene oxide) segment and a hydrophobic poly(*n*-butyl methacrylamide) segment. A simple method to obtain a block copolymer with poly(ethylene oxide) using the RAFT technique is the synthesis of a macro-RAFT agent as described in the literature instead of by polymer-polymer coupling.[189] The carboxylic acid of the chain transfer agent was converted into an active ester with *N*-hydroxysuccinimide and *N*,*N*'-dicyclohexylcarbodiimide in a moderate yield (Scheme 2.36). A higher conversion of the Steglich esterification can be reached by adding a catalytic amount of 4-dimethylaminopyridine, which suppresses side reactions.[152] The macro-RAFT agent **53** was obtained in high yields by acylation of α-methoxy-ω-amino poly(ethylene oxide) with the active ester and purified by precipitation in diethyl ether. The SEC analysis looks similar to the unfunctionalized polymer, and the molar mass and dispersity were nearly unchanged

according to SEC against PEO standards (Table 2.9). In contrast, the aromatic signals of the phenyl group and the amide proton are visible in the ^{1}H NMR spectrum, and a degree of functionalization over 95% was calculated.

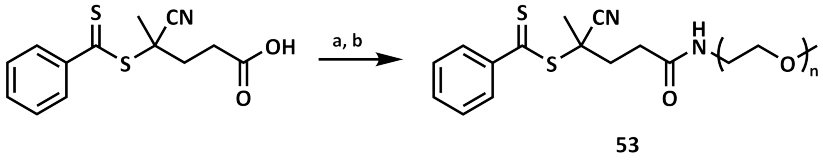

53

Scheme 2.36: Synthesis of a poly(ethylene oxide)-based macro-RAFT agent (**53**). Conditions: a) NHS, DCC, DCM, RT, 24 h, 63%. b) mPEO-NH_2, DCM, RT, 22 h, 89%.

A macro-RAFT agent can be synthesized by esterification in one step starting from α-methoxy-ω-hydroxy poly(ethylene oxide) and the chain transfer agent with a carboxylic acid. However, the disadvantage of the ester linkage is the possible aminolysis reaction, which can occur by post-polymerization modification with amines. Moreover, the ester linkage can be cleaved under basic conditions by the transformation of the polymer into a polyampholyte *via* hydrolysis of the ethyl ester at the monomeric units. The block copolymer poly(ethylene oxide)-*block*-poly(ethyl 2-(hydroxymethyl)acrylate) (**54**) was prepared using **53** according to the homopolymerization of **52** *via* RAFT, and purified by precipitation in cyclohexane and *n*-pentane to afford a pink solid. To determine the length of the poly(ethyl 2-(hydroxymethyl)acrylate) block by NMR spectroscopy, trioxane was added as an internal standard. A monomer to macro-RAFT agent ratio of 84:1 was calculated at the beginning of the reaction and a monomer conversion of 82% indicates the average block length consists of 69 repeating units. The SEC elugrams in Figure 2.30 show a clear shift to higher molar masses or lower elution volumes compared to **53**, accompanied by a narrow molecular weight distribution.

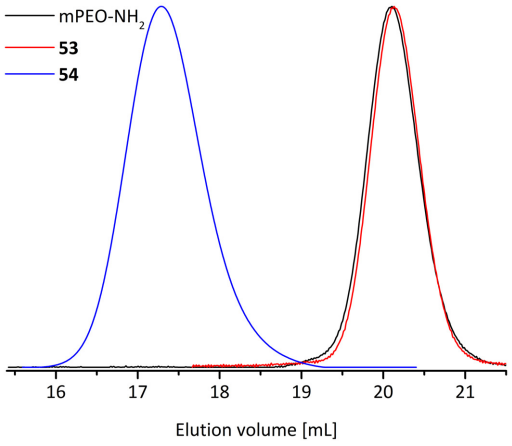

Figure 2.30: SEC elugrams in DMAc of **53**, **54** and precursor.

Table 2.9: SEC data in DMAC of **53**, **54** and precursor.

Polymer	$\overline{M}_n$ [a)]	$Đ$ [a)]
mPEO-NH_2	2,000 g·mol^{-1}	1.07
53	2,000 g·mol^{-1}	1.07
54	20,600 g·mol^{-1}	1.10

[a)] PMMA calibration.

For the preparation of a copolymer with **52b** containing a hydrophobic segment *via* block extension, *n*-butyl methacrylamide (**55**) was selected as the monomer. Besides the stability of the amide bond under the modification conditions, the polymerization of **55** is

well controlled by the RAFT technique using benzodithioate as a chain transfer agent in contrary to *n*-butyl acrylamide. The monomer was synthesized according to a literature procedure *via* the acylation of *n*-butylamine with methacryloyl chloride (Scheme 2.37).[190] To prevent a thermally initiated autopolymerization, hydroquinone was added to the reaction mixture, and the crude product was purified by distillation to obtain **55** as a colorless liquid in a good yield of 81%.

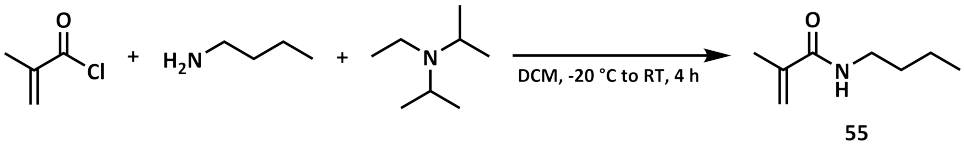

Scheme 2.37: Synthesis of *n*-butyl methacrylamide (**55**) by acylation.

The block extension with **55** was carried out using RAFT polymerization in THF at 40 °C using **52b** as a macromolecular chain transfer agent and trioxane as an internal standard (Scheme 2.31). Based on the ^{1}H NMR measurements, a monomer to RAFT agent ratio of 113:1 was determined and 37% of **55** was consumed after 12 hours. This corresponds to 42 repeating units for the hydrophobic second block and an increased molar mass by 5,900 g·mol^{-1}, which is in close agreement to the SEC data in Table 2.10 using a PMMA calibration.

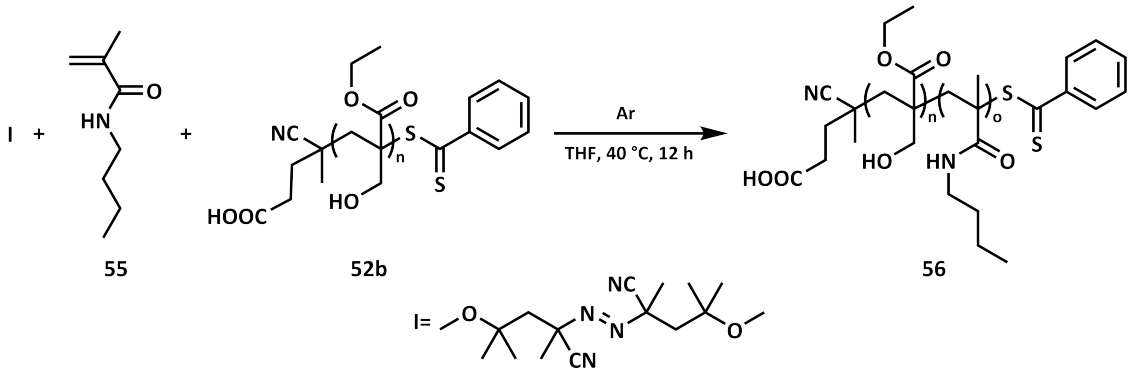

Scheme 2.38: Block extension of poly(ethyl 2-(hydroxymethyl)acrylate) (**52b**) with *n*-butyl methacrylamide (**55**).

Apart from the narrow dispersity and increased molar mass, the trace of **56** in the SEC elugram is not shifted to higher elution volumes, which may be a smaller overlapping curve from dead chain ends of **52b** without the dithiobenzoate moiety (Figure 2.31). The use of an initiator and reinitiation of the chain transfer agent resulted in a higher amount of propagating radicals compared to RAFT moieties, which afforded a minor part of dead polymer chains. The fraction of polymer chains that could not be reinitiated and grow in a block extension is defined by the initial RAFT agent to initiator ratio. The polymer **52b** was prepared with a tenfold excess of the chain transfer agent to initiator. This means that 91% of the polymers should possess a dithiobenzoate functionality in theory.

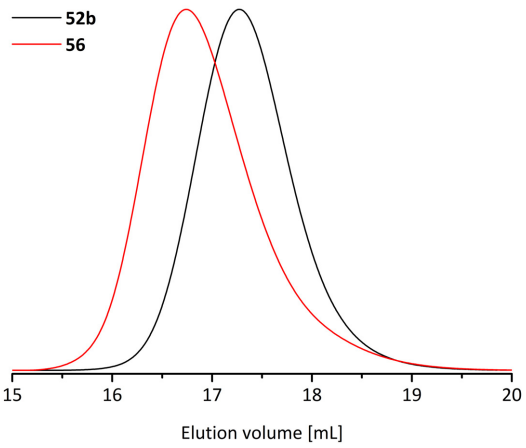

Figure 2.31: SEC elugrams in DMAc of **52b** and **56** prepared *via* RAFT.

Table 2.10: SEC data in DMAC of **52b** and **56**.

Polymer	$\overline{M}_n$ [a)]	$Đ$ [a)]
52b	20,700 g·mol^{-1}	1.11
56	26,400 g·mol^{-1}	1.17

[a)] PMMA calibration.

In the next steps, the hydroxy moieties of **52** were converted into good leaving groups for substitution with amines such as morpholine. Before attempting this modification on the prepared block copolymers, the homopolymer was modified to find the optimal conditions. An efficient bromination of the polymer hydroxy groups is described for poly(2-hydroxyethyl methacrylate) by Zhou *et al.* with an achieved degree of functionalization over 98% using XtalFluor-E, diazabicycloundecene and tetra-*n*-butylammonium bromide as shown in Scheme 2.39.[191] The reaction was performed with **52** in the bachelor thesis of F. Nagler under my supervision, and conversions lower than 10% were determined by elemental analysis.[192] A chlorination with thionyl chloride in dichloromethane over two days proceeded to less than 5%, and which could be improved by heating in toluene using pyridine as an additive. However, a high degree of functionalization may not be feasible.

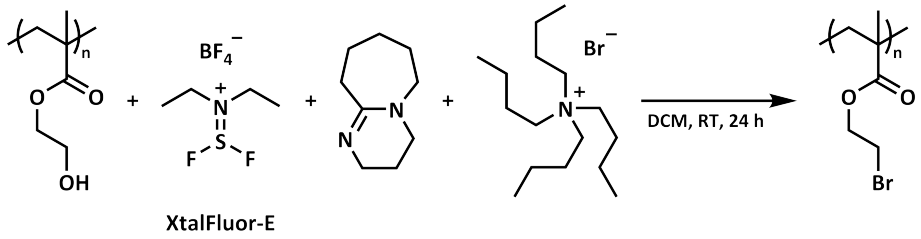

Scheme 2.39: Bromination of poly(2-hydroxyethyl methacrylate) with XtalFluor-E.[191]

Another type of good leaving group besides halides are sulfonates, and they can be prepared by esterification of the hydroxy moiety with sulfonyl chlorides. Tosyl chloride and mesyl chloride are often used for the transformation of alcohols into azides and amines *via* nucleophilic substitution. The tosylation of hyperbranched dendrimers containing 64 hydroxy groups and the following substitution with sodium azide in high yields is reported by Yamajala and Banerjee.[193] Poly(ethyl 2-(hydroxymethyl)acrylate) (**52a**) was modified under similar conditions with tosyl chloride with a moderate yield of 40% achieved (Scheme 2.40).

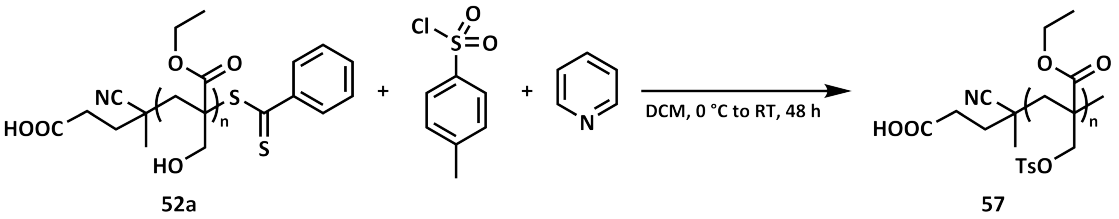

Scheme 2.40: Tosylation of poly(ethyl 2-(hydroxymethyl)acrylate) (**52a**).

The tosylation of poly(ethyl 2-(hydroxymethyl)acrylate) (**57**) was characterized by SEC in THF, ^{1}H NMR spectroscopy (Figure 2.32), and elemental analysis. According to elemental analysis, a mass fraction of 6.2% sulfur was detected instead of the calculated 11.3%. Based on both measurements, 45-56% of the hydroxy groups were tosylated. Furthermore, a shift in the SEC elugram in THF to lower elution volumes is observed, or rather an increase of the molar mass from 9,000 g·mol^{-1} to 13,800 g·mol^{-1} against a PMMA calibration.

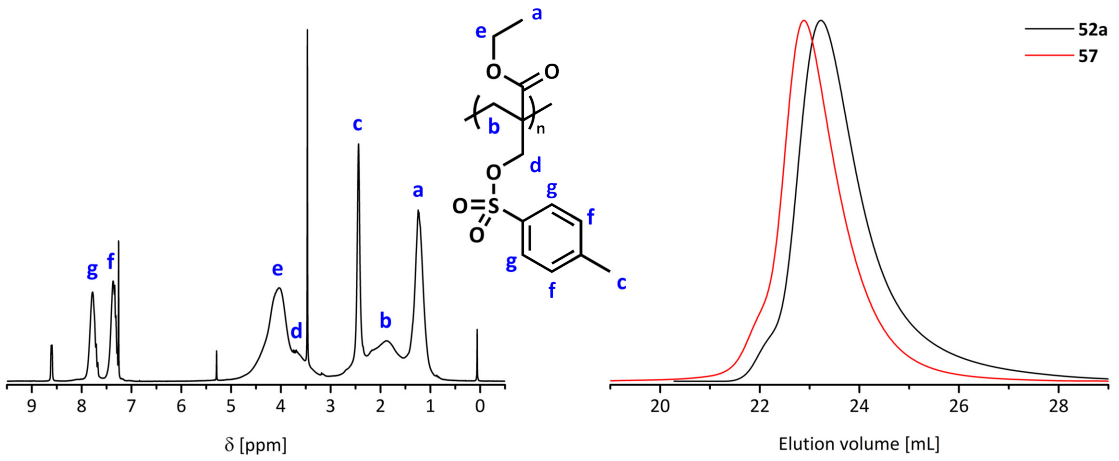

Figure 2.32: ^{1}H NMR spectrum in $CDCl_3$ (left) of tosylated poly(ethyl 2-(hydroxymethyl)acrylate) (**57**) and SEC elugram in THF before and after modification (right).

For the preparation of the sulfonic esters, pyridine was used as a base, and to further promote the reaction by the formation of *N*-tosylpyridiunium chloride with tosyl chloride. The intermediate *N*-tosylpyridiunium chloride has an increased electrophilicity and higher reactivity. A possible reason for the moderate conversion of **52a** into **57** is the steric hindrance of the hydroxy group near the polymer backbone with the ester moieties and the bulky tosyl group at a certain conversion. A less bulky leaving group with a similar reactivity and a better atom economy is the mesylate in comparison to the tosylate. The polymer was reacted with mesyl chloride, similarly to the tosylation under slightly varied conditions, with stronger cooling at the addition of the acid chloride and a reduced reaction time. The mesylated poly(ethyl 2-(hydroxymethyl)acrylate) (**58**) was prepared with a high yield of 96% as a white solid without the RAFT end group. A peak at 3.1 ppm in the ^{1}H NMR spectrum associated with the methyl group of the mesyl moiety was observed, and a conversion of 93% of the hydroxy groups was determined (Figure 2.33). Moreover, the elemental analysis afforded a slightly higher conversion of 96%, which was

calculated from the ratio of the sulfur mass fraction, which measured 15.0% compared to the theoretical 15.6%. That caused by a low amount of residual mesyl chloride in the polymer resulting in a measured chloride mass fraction of 0.4%. An increase in the molar mass from 6,100 to 10,400 g·mol^{-1} was observed by SEC analysis in THF using a PMMA calibration. Additionally, a shoulder at lower elution volumes is now visible, which may be the result of a side reaction with the polymer end group.

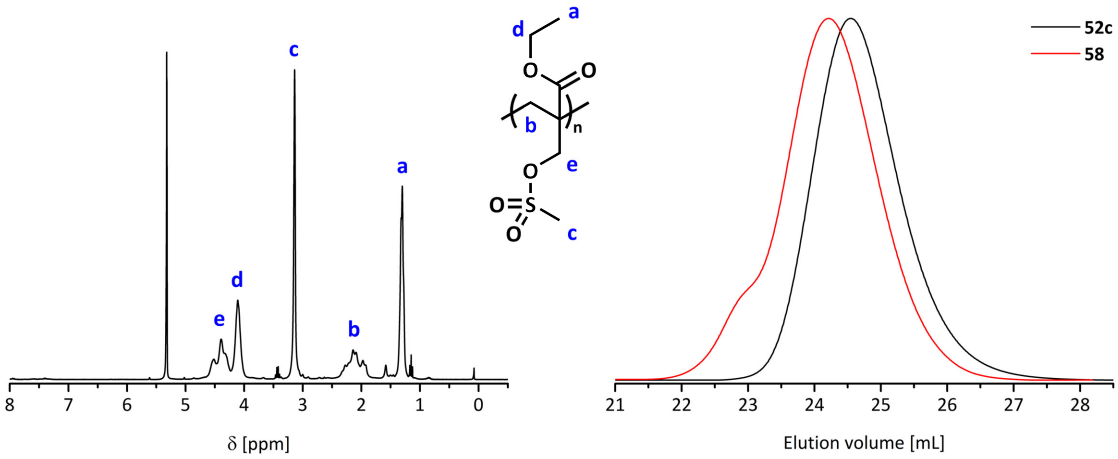

Figure 2.33: ^{1}H NMR spectrum in CD_2Cl_2 (left) of mesylated poly(ethyl 2-(hydroxymethyl)acrylate) (**58**) and corresponding SEC elugram in THF before and after modification (right).

After the successful mesylation, **58** was reacted with morpholine at 110 °C for two days to prepare poly(ethyl 2-(morpholinomethyl)acrylate) (**59**) by substitution (Scheme 2.41). The polymer was purified *via* dialysis before analyzing by ^{1}H NMR spectroscopy. A weak signal at 3.6 ppm, which is attributed to the methylene groups of morpholine, was observed. When performing the reaction of **58** with morpholine at a high temperature of 110 °C and over a long reaction time of two days, a conversion below 15% was obtained. For a higher degree of substitution, the nucleophilicity of the amine, or the reactivity of the leaving group, must be increased. Therefore, the mesyl group was replaced by the triflyl moiety as an excellent leaving group, and which also has a lower steric hindrance than the tosyl functionality.

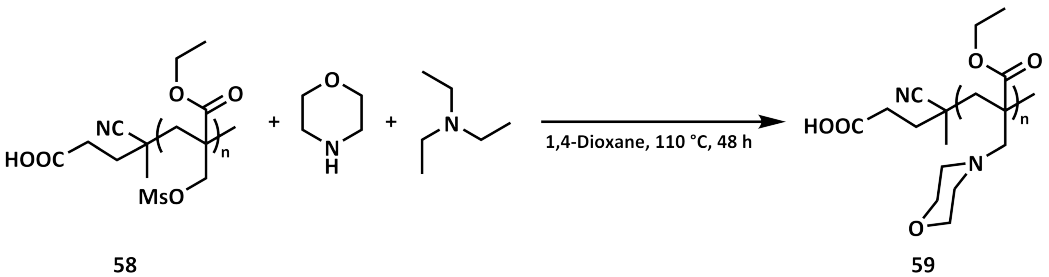

Scheme 2.41: Preparation of poly(ethyl 2-(morpholinomethyl)acrylate) **59** by the substitution of poly(ethyl 2-((mesyloxyo)methyl)acrylate) **58** with morpholine.

In the first attempt, **52a** was treated with triflyl chloride in dichloromethane with triethylamine instead of pyridine, which afforded poorly soluble and polar solids. Due to the high reactivity and lower stability of poly(ethyl 2-((triflyloxyo)methyl)acrylate) (**60**) compared to **58**, the triflated polymer was precipitated once and directly used for the preparation of **59** by substitution with morpholine in tetrahydrofuran at 70 °C. After 20 hours, the polymer was purified by dialysis against water. From the ^{1}H NMR spectrum of **59** (Figure 2.34), it was determined that the degree of functionalization of the polymer was 30-40%. This was confirmed by elemental analysis, where a nitrogen mass fraction of 2.7% instead of the calculated 7.0% was found.

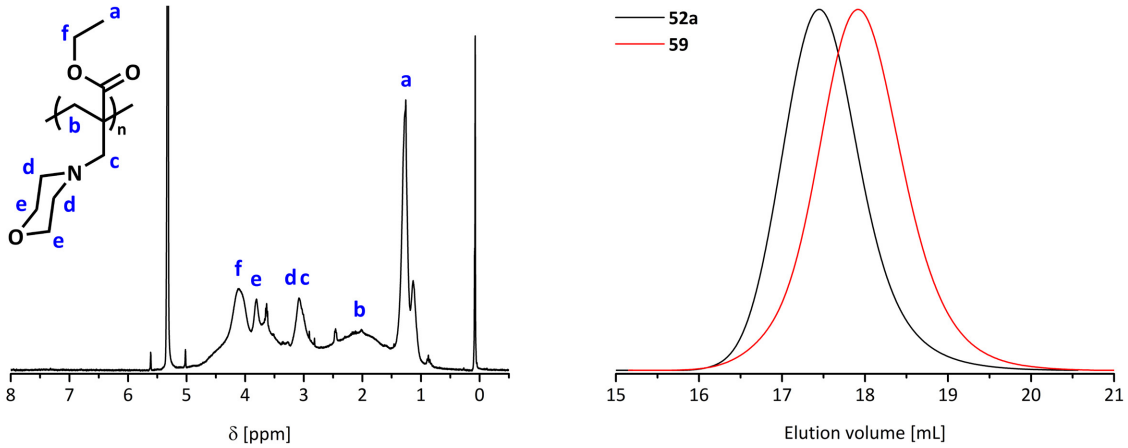

Figure 2.34: ^{1}H NMR spectrum in CD_2Cl_2 (left) and SEC elugram in DMAc (right) of substituted poly(ethyl 2-((triflyloxy)methyl)acrylate) (**59**).

In the SEC elugram, there is a clear change in the hydrodynamic volume with a shift to higher elution volumes compared to **52a** as shown in Figure 2.34. The hydroxy groups of the polymer **52a** form intra- and intermolecular hydrogen bonds and could be partially suppressed by the additive lithium chloride in the eluent. However, the molar mass was also approximately 10,000 g·mol^{-1} higher using a PMMA calibration, which does not fit perfectly, and which may indicate the polymer has formed aggregates in the eluent. After modification, the lower amount of hydroxy moieties may lead to a decreased aggregation and result in the smaller hydrodynamic volume of **59**. The modification efficiency of **60** can be improved by using a higher reaction temperature or an increased reaction time like in the substitution of **58**. To increase the nucleophilicity of amines by deprotonation is not recommended because it is possible that the ester moieties will undergo aminolysis. Alternative nucleophiles could be implemented such as thiolates, which are stronger Lewis bases. Azides could also be used, which can be converted into primary amines. Furthermore, varying the leaving group position from the allyl to homoallyl with an additional carbon atom between the functional group and the polymer backbone may simplify the polymerization of reactive monomers like **49**. Additionally, an increased distance to the polymer backbone facilitates its modification, but also enables an elimination reaction of

the leaving group. Another disadvantage of such a monomer with an additional carbon atom is the synthesis of the monomer, which requires more reaction steps as described by Luo *et al.* (Scheme 2.42).[194]

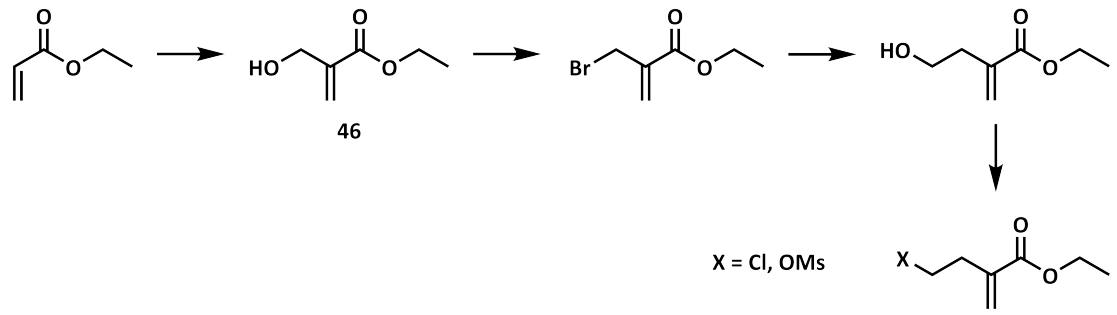

Scheme 2.42: Synthetic approach to ethyl 2-(2-hydroxyethyl)acrylate and other activated monomers.

2.3 Hydrophilic Polyethers for Gene Delivery

In the medical research field, polyelectrolytes, especially polycations, are explored for gene therapy to treat diseases like cystic fibrosis, cancer, and severe combined immunodeficiency with nucleic acids.[88, 195] The cationic polymers form polyplexes with the polyanions RNA or DNA to deliver the nucleic acid into the cells and protect them against enzymatic degradation. To find an efficient non-viral vector, several polymeric systems like peptides,[196, 197] polyesters,[198, 199] poly(oxazoline)s,[200, 201] poly(methacrylate)s[202, 203] and poly(acrylamide)s,[204, 205] as well as combinations[206–211] are investigated as linear or branched macromolecules that are hydrophilic or amphiphilic in character. Besides the complexation of the polynucleotides, protein aggregation or interactions with other biomacromolecules, which can lead to a dissociation of the polyplex in the blood, need to be avoided for cellular uptake. Consequently, polymers with an additional block to form a shell or corona in aqueous media exhibiting shielding properties are often used (Figure 2.35).[195]

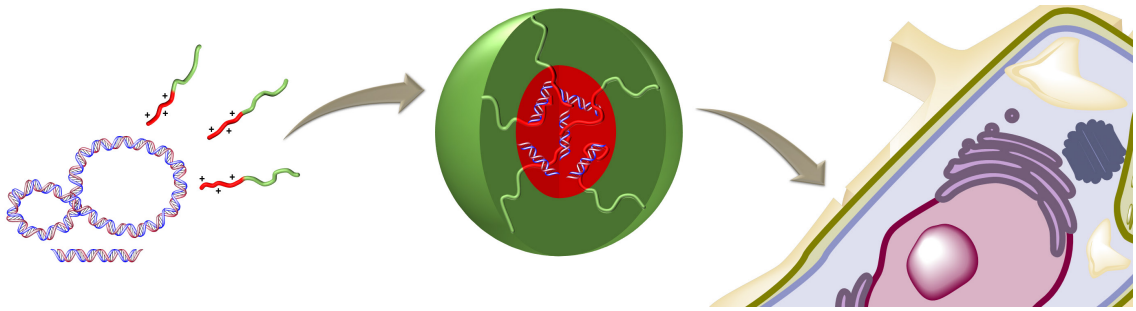

Figure 2.35: Polyplex formation of cationic polymers with nucleic acids and delivery into target cells.

Herein, a polyether system was developed with a poly(ethylene oxide) corona and a poly(allyl glycidyl ether) segment to attach the cationic moieties *via* a thiol-ene reaction. The diblock copolymer was prepared by anionic ring-opening polymerization of allyl glycidyl ether using poly(ethylene oxide) as a macroinitiator analogous to literature (Scheme 2.43).[100, 212, 213] Therefore, the melted α-methoxy-ω-hydroxy poly(ethylene oxide) was deprotonated with sodium hydride and the glycidyl ether was added for the addition reaction to achieve poly(ethylene oxide)-*block*-poly(allyl glycidyl ether) (**61**). The polymerization was quenched with methanol and the macromolecule was dried under vacuum at 100 °C.

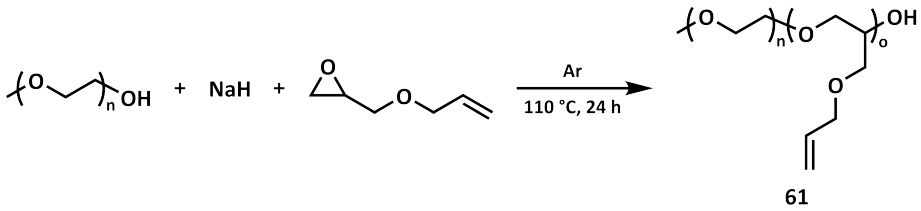

Scheme 2.43: Anionic ring-opening polymerization of allyl glycidyl ether using poly(ethylene oxide) as a macroinitiator.

A larger poly(allyl glycidyl ether) block allows the attachment of more cationic groups, and could lead to the formation of polyplexes with higher stability and a lower poly(ethylene oxide) corona density. Takeda *et al.* reported a reduction in the size of polyplex micelles of pDNA and poly(ethylene oxide)-*block*-poly(L-lysine) by increasing the length of the cationic block.[214] This arises due to a stronger condensation of the polynucleotide. Furthermore, they described that polyplexes with a larger cationic segment show a shorter circulation time in the blood through a poorer shielding of the changed corona structure. To find an optimal chain length, the ratio of the monomer to macroinitiator was varied in the polymerization to obtain the block copolymer **61** with an increased amount of modifiable carbon-carbon double bonds from 15 to 76 repeating units, whilst the poly(ethylene oxide) degree of polymerization was kept constant at 42. ^{1}H NMR spectroscopy was used to calculate the number of repeating units of the poly(allyl glycidyl ether) segment from the integral ratio of the allyl group and polymer backbone. The SEC measurements in chloroform revealed all polymers were characterized by a narrow molecular weight distribution below 1.3 (Table 2.11). Slightly broader dispersities were observed for **61d** and **61e** with the highest molar mass as a consequence of the solvent-free polymerization and increased viscosity.

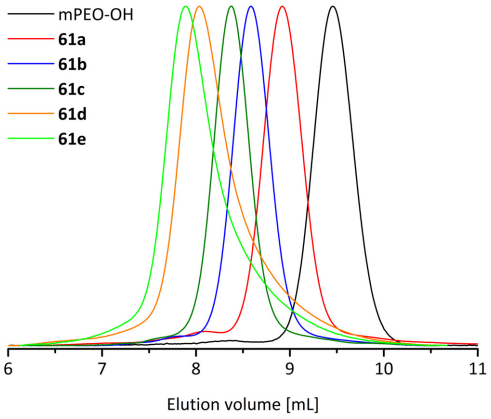

Figure 2.36: SEC elugrams in chloroform of **61** with increasing PAGE block length.

Table 2.11: SEC data in chloroform of **61** with increasing PAGE block length.

Polymer	DP[a)]	$\overline{M}_n$[b)]	$Đ$[b)]
mPEO-OH	0	1,900 g·mol^{-1}	1.04
61a	15	2,600 g·mol^{-1}	1.15
61b	29	3,400 g·mol^{-1}	1.06
61c	45	4,000 g·mol^{-1}	1.07
61d	60	4,500 g·mol^{-1}	1.25
61e	76	5,000 g·mol^{-1}	1.24

[a)] Determined by NMR, [b)] PEO calibration.

Miscellaneous functionalizations of poly(allyl glycidyl ether) homopolymer or copolymer with thiols in different solvents like methanol, *N*,*N*-dimethylformamide, tetrahydrofuran and solvent mixtures have been described in the literature by thermal or UV light radical initiation.[212, 215–218] The block copolymers series **61** were modified by a thiol-ene reaction with cysteamine hydrochloride to introduce primary amino groups using 2,2-dimethoxy-2-phenylacetophenone as a photoinitiator in an UV-cube (Scheme 2.44). A mixture of methanol and tetrahydrofuran was chosen to dissolve the highly polar thiol, the hydrophobic poly(allyl glycidyl ether) block and the resulting hydrophilic poly(ethylene oxide)-*block*-poly(3-((2-aminoethyl)thio)propyl glycidyl ether) (**62**).

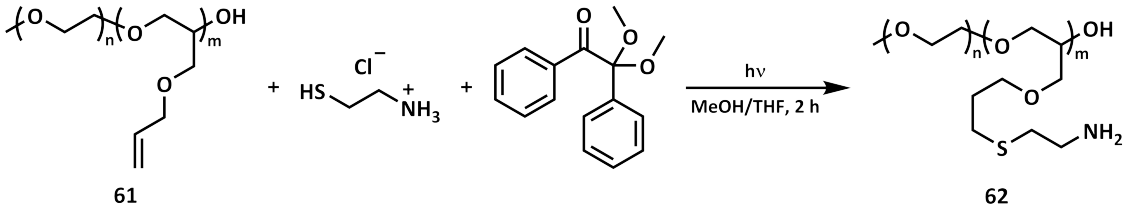

Scheme 2.44: Modification of **61** with cysteamine hydrochloride *via* a thiol-ene reaction.

After purification by dialysis, the polymers were analyzed *via* SEC in water under acidic conditions, and broader molecular weight distributions were detected. The SEC elugrams in Figure 2.37 show a tailing to lower elution volumes, which could be systemic and concentration-dependent. For **62c**, a more apparent tailing is observed, and may be an indication of carbon-carbon bond formation. Based on the same conditions of all five modifications, the appearance of intra- and interchain cross-linking in only one batch is unlikely. The SEC curve of **62c** does not exhibit a visible higher molecular weight shoulder as expected for the cross-linkage. An additional measurement of **62c** using a SEC system with *N*,*N*-dimethylacetamide as eluent showed a narrow dispersity of 1.1 and a number average molecular weight of 8,200 g·mol^{-1} using a PEO calibration.

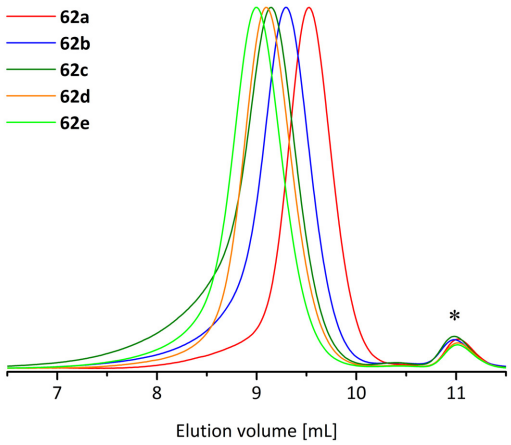

Figure 2.37: SEC elugrams in water (∗ system peak) of **62**.

Table 2.12: SEC data in water of modified **61**.

Polymer	$\overline{M}_n$ [a)]	$Đ$ [a)]
62a	4,600 g·mol^{-1}	1.31
62b	6,800 g·mol^{-1}	1.45
62c	8,700 g·mol^{-1}	1.87
62d	8,700 g·mol^{-1}	1.24
62e	10,200 g·mol^{-1}	1.34

a) P2VP calibration.

The ^{1}H NMR spectra of **62** show a complete disappearance of the allyl signals, indicating a degree of functionalization of over 99% with the thiol (Figure 2.38). In contrast to the methylene groups, the broad singlet of the amino protons from the attached cysteamine is not clearly visible in all ^{1}H NMR spectra. The proton signal of the amino group varies in width and height, which may be due to partial protonation or the water content in the deuterated dimethyl sulfoxide used.

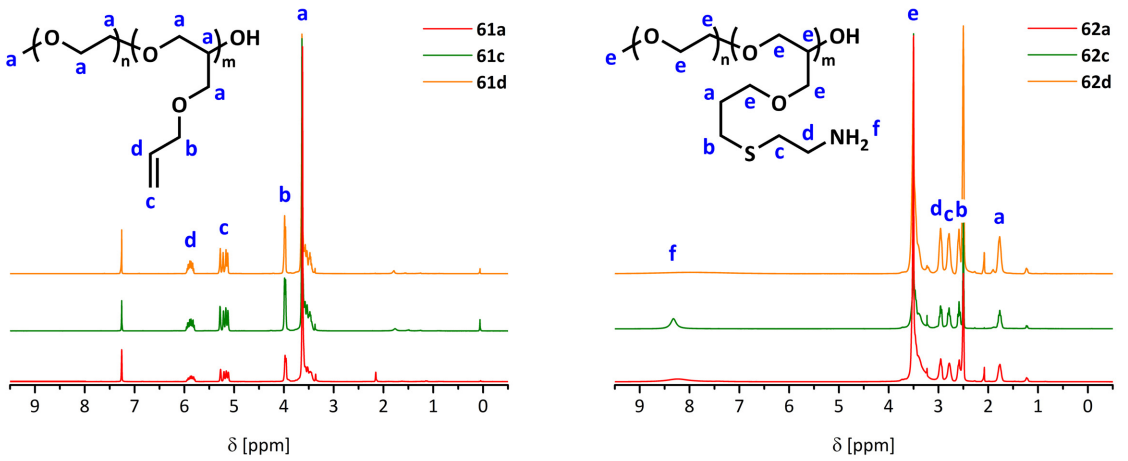

Figure 2.38: ^{1}H NMR spectra of **61** in $CDCl_3$ (left) and **62** in DMSO (right).

The formation of polyplex micelles with pDNA and the prepared polycations were performed by D. Hertz and A. Landmann, as well as the investigation of their stability, toxicity, and uptake behavior in cells using linear poly(ethylene imine) (PEI) as a reference. The interaction of the polymer **62** with pDNA was analyzed *via* an ethidium bromide displacement assay, as well as a heparin competition assay. In the first assay, the ethidium bromide has a strongly enhanced fluorescence by the intercalation in polynucleotides. The fluorescent dye can be displaced by adding polycations due to the formation of a polyplex with the nucleic acid. A reduced light emission of ethidium bromide was detected depending on the amount of added **62**, which is given as a ratio of nitrogen to phosphorous (N/P ratio), or more specifically as a charge ratio of the cationic moieties of the polymer to the anionic phosphate groups of the pDNA. Already at a N/P ratio of 2, the polycation binds almost completely with the nucleic acid, and the fluorescence decreases slightly with higher polymer concentrations in contrast to PEI (Figure 2.39). For all further characterization of the polyplex micelles, an N/P ratio of 15 was used. The stability of the polyplexes was examined using the multiple negatively charged polysaccharide heparin as a competitor to the nucleic acid, and ethidium bromide was used to detect the released pDNA *via* fluorescence. This heparin competition assay showed a higher stability of the polyplex micelles prepared with **62** compared to PEI at a lower heparin concentration up until 10 $mg \cdot ml^{-1}$. The polyplexes with **62** exhibit an enhanced stability as the number of repeating units containing amino groups increases.

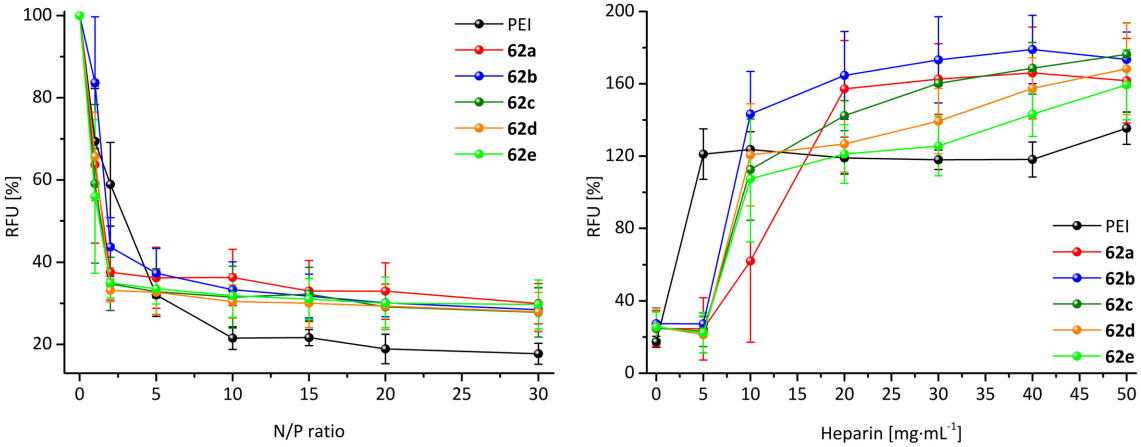

Figure 2.39: Ethidium bromide displacement (left) and heparin competition assay (right) of polyplex micelles with **62** and pDNA.

The cytotoxicity was indirectly evaluated by the loss of viable cells in a 3-(4,5-dimethylthiazol-2-yl)-2,5-diphenyltetrazolium bromide (MTT) assay. The dye MTT was reduced by L929 cells into the purple formazan, and the adsorption was measured after 24 hours. In Figure 2.40, a tendency for higher cytotoxicity with increasing cationic block length of the polymer was observed for polyplexes with **62**. To explore the delivery efficiency of the polyplex micelles, YOYO-1 labeled pDNA was used, and its fluorescence in the L929 cells was measured after two and four hours using Dulbecco's modified Eagle's medium with 10% fetal bovine serum. Nearly the same amount of pDNA was delivered into the cells with **62a** and **62b** in comparison to PEI, higher quantities in a similar range were detected using **62c**, **62d** and **62e** as carriers. Except in the case of **62b**, which exhibited a lower uptake as anticipated, a higher polymerization degree of the second block with amino groups results in an increased cytotoxicity and an improved cell penetration. In summary, a better carrier system of polynucleotides as PEI was achieved with **62** as non-viral vectors if the cationic segment contains more than 30 repeating units. Moreover, a modified poly(allyl glycidyl ether) block with higher degrees of polymerization showed small improvements in the delivery behavior.

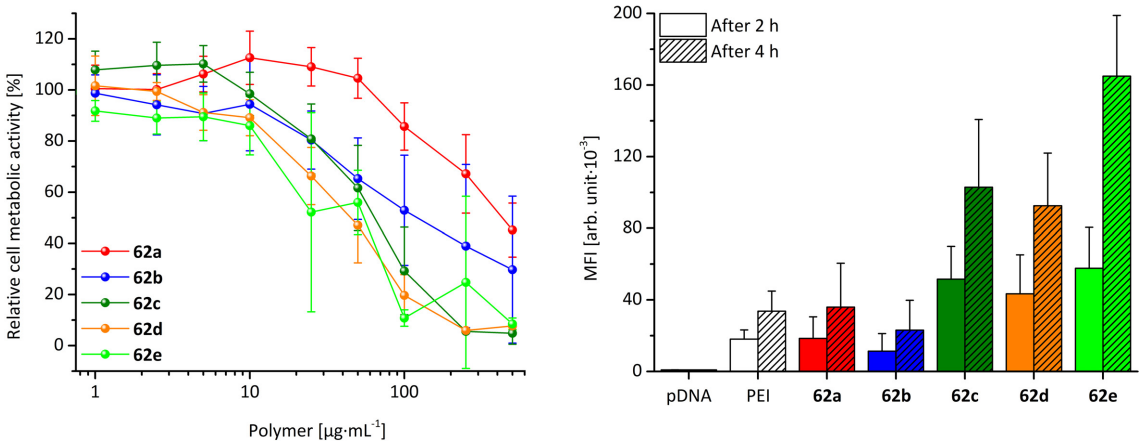

Figure 2.40: MTT assay (left) and uptake in L929 cells (right) of the polyplex micelles with **62** and pDNA.

Besides the amount of positive charges at the polymer chain, the type of cation has an important impact. The binding and release of the polynucleotides is influenced by the cation through the acid dissociation constant, the size of the ionic moiety, and the amount of possible hydrogen bonds. Actually, the comparison of the gene delivery behavior of only a few polymer pendent cationic groups has been described in the literature. As examples, tertiary amines and phosphonium ions, or primary amines and ethylenediamine moieties (*e.g.* $(C_2H_5N)n$, n= 2,3,4) were compared with each other, and imidazole or guanidine groups with primary, secondary, and tertiary amines, as well as their combinations.[219–221] To investigate the influence of a variety of nitrogen-based cationic moieties on the gene delivery behavior, thiols with the functionalities were prepared for the modification of **61**. The mercaptans with a primary and tertiary amine are commercially available as cysteamine and captamine hydrochlorides, as well as acetylthiocholine chloride as a precursor to the quaternary ammonium ion. Thiocholine chloride (**63**) was synthesized by the cleavage of the thioester under acidic conditions with a quantitative yield as reported in the literature (Scheme 2.45).[222]

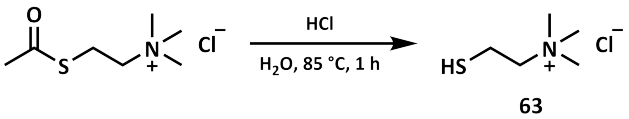

63

Scheme 2.45: Synthesis of thiocholine chloride (**63**) *via* acidic thioester hydrolysis.[222]

The mercaptan with a secondary amine was achieved in several steps from *N*-methylethanolamine according to a literature procedure (Scheme 2.46).[222] First, the amine was protected with a high yield of 94% using di-*tert*-butyl dicarbonate to prevent side reactions by the transformation of the alcohol into a thiol, and to decrease the polarity for purification by column chromatography. Next, the hydroxy group was converted into a good leaving group *via* mesylation and substituted by potassium thioacetate. Diminished yields were observed for the mesylation of 68%, and only 40% for the preparation of 2-(*N*-(*tert*-butoxycarbonyl)methylamino)ethyl thioacetate (**64**) when prepared at a larger scale at increased reaction times compared to the literature with an overall yield of 69%. One reason for the lower yield may be the limited solubility of the potassium thioacetate in *N*,*N*-dimethylformamide and the concentration can be reduced from 0.75 M to 0.3 M. The yield can be further improved by the addition of a phase transfer catalyst to increase the solubility of potassium thioacetate. The hydrolysis of the thioester was carried out using sodium methoxide and quenched with the acidic ion-exchange resin Dowex® 50WX8 to afford 2-(*N*-(*tert*-butoxycarbonyl)methylamino)ethanethiol (**65**) with a high yield of 93%. Due to the oxidation of the thiols to disulfides, small quantities of the mercaptan were prepared and stored at -24 °C until their use in the thiol-ene reaction.

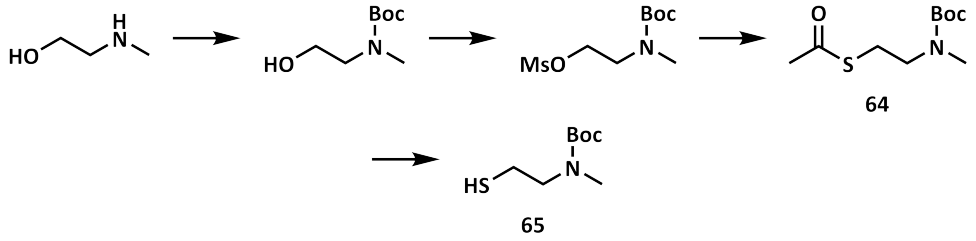

Scheme 2.46: Synthesis of 2-(*N*-(*tert*-butoxycarbonyl)methylamino)ethanethiol (**65**).[222]

Another cationic group is guanidine, which forms additional hydrogen bonds to the phosphate of polynucleotides and has a lower pK_b value. To access a thiol with a guanidine moiety, cysteamine hydrochloride was reacted with *N,N'*-bis-*tert*-butoxycarbonylthiourea and triethylamine similarly to the literature (Scheme 2.47).[223] In contrary to the reported procedure with a yield of 60%, *N,N'*-bis-(*tert*-butoxycarbonyl)-*N"*-2-mercaptoethylguanidine (**66**) was obtained with a yield of 94%. An explanation is the simplified purification method used of filtering the crude product through a short pad of silica instead of extraction and column chromatography to prevent the formation of disulfides. The use of cysteamine as a hydrochloride is another potential reason for the increased yield, because of its higher stability against oxidation. Cysteamine can also react to form cystamine under typical storage conditions to result in lower yields. Moreover, the purity of **66** was confirmed by NMR spectroscopy and a triplet signal associated with the thiol group is visible at a chemical shift of 1.42 ppm.

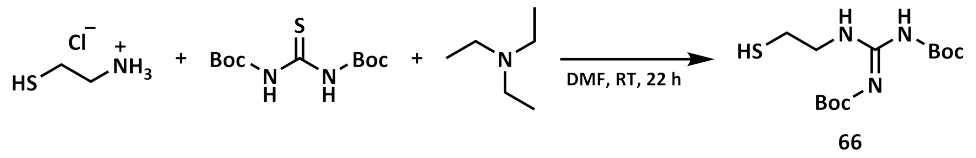

Scheme 2.47: Synthesis of *N,N'*-bis-(*tert*-butoxycarbonyl)-*N"*-2-mercaptoethylguanidine (**66**).[223]

Besides the guanidine group, the amidine moiety further represents a cationic functionality with a lower pK_b value than amines. Amidines can more strongly interact with the polynucleotides through hydrogen bonds like amines, but weaker than guanidine. Common routes to convert aliphatic nitriles into amidines are the treatment with amino(methyl)aluminum chloride or the Pinner reaction using acids followed by the addition of ammonia, which is also possible under alkaline conditions with activated nitriles.[224] Additionally, the nitrile can be transformed into a thioamide and substituted by ammonia after the introduction of a *tert*-butyloxycarbonyl group at the amide nitrogen, which decreases the polarity and simplifies the purification.[225, 226] Therefore, 3-((4-methoxybenzyl)oxy)propionitrile (**67a**) was synthesized *via* the Michael addition of anise alcohol to acrylonitrile, and reacted with ammonium sulfide in a mixture of triethylamine and pyridine to afford 3-((4-methoxybenzyl)oxy)propanethioamide (**68a**) (Scheme 2.48).[227, 228]

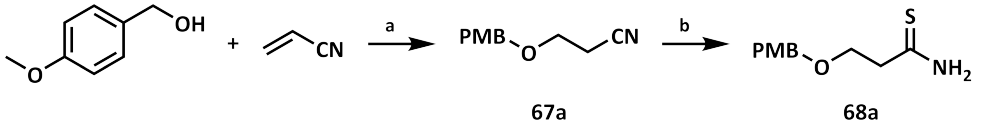

67a 68a

Scheme 2.48: Synthesis of 3-((4-methoxybenzyl)oxy)propanethioamide (**68a**). Conditions: a) NaOH, H_2O, 0 °C to RT, 7 h, 95%. b) NH_4S, NEt_3, C_5H_5N, 60 °C, 23 h, 80%.[227, 228]

Next, the thioamide **68a** was deprotonated twice with sodium hydride to protect the nitrogen with di-*tert*-butyl dicarbonate before its conversion into an amidine. The abstraction of the second proton of the thioamide is necessary because of the resonance stabilization leading to a higher probability of the negative charge at the sulfur as shown in Scheme 2.49.

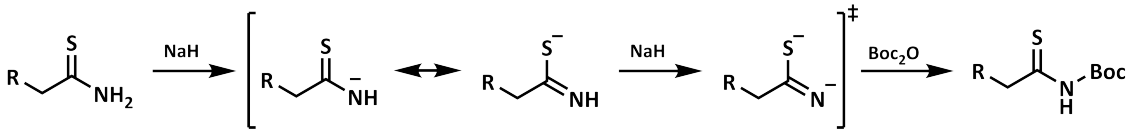

Scheme 2.49: Synthesis of *N*-*tert*-butyloxycarbonyl protected thioamides with possible intermediates.

The reaction of thioamides and *N*-*tert*-butyloxycarbonyl protected thioamides with primary amines or ammonia to amidines has been reported in high yields with mercury(II) chloride, zinc(II) chloride, as well as without any additive.[225, 226, 229] The conditions were verified in a small scale reaction using ammonia, with the exception of the highly toxic mercury salt. After 26 hours, samples of the reactions were diluted with ethyl acetate, extracted with water and analyzed by thin layer chromatography (CH:EA, 1:1) with **68a** and **69a** as references. For the treatment of **69a** with ammonia in the absence of thiophilic metal ions, a lower conversion was observed, and the formation of **68a** was detected in a side reaction by the elimination of *tert*-butyl carbamate. The zinc ion enhanced the cleavage of the sulfur through a coordinate bond and prevented the reverse reaction to **68a**. Furthermore, Spychała proposed a zinc complex with amines or ammonia as an intermediate, which could accelerate the nucleophilic attack at the thioamide.[229] The synthesis of *tert*-butyl (1-imino-3((4-methoxybenzyl)oxy)propyl)carbamate (**70a**) with ammonia and zinc(II) chloride afforded the product in high yield, and only required purification by filtration and extraction.

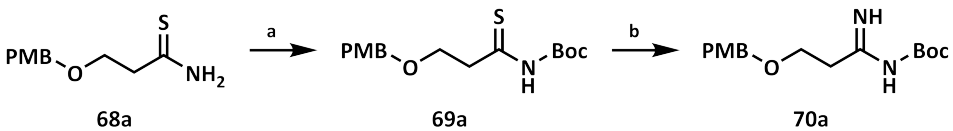

68a 69a 70a

Scheme 2.50: Synthesis of *tert*-butyl (1-imino-3((4-methoxybenzyl)oxy)propyl)carbamate (**70a**). Conditions: a) NaH, Boc_2O, THF, -20 °C to RT, 5 h, 79%. b) NH_3, $ZnCl_2$, MeOH, 0 °C to RT, 24 h, 91%.[225, 226, 229]

After confirmation of the structure by NMR spectroscopy and mass spectrometry, the 4-methoxybenzyl moiety of **70a** had to be removed to transform the hydroxy group into a thiol. A 4-methoxybenzyl ether can be cleaved by strong acids, by Lewis acids in combination with weak nucleophiles, *via* reduction like benzyl ethers, or by oxidation.[230, 231] Based on the functional groups present in **70a**, the often used oxidative deprotection with 2,3-dichloro-5,6-dicyano-1,4-benzoquinone was carried out in dichloromethane and sodium bicarbonate, but only the educt was observed by ^{1}H NMR spectroscopy. In a second attempt, the oxidizing agent ceric ammonium nitrate was applied in a mixture of water and acetonitrile to obtain the byproduct anise aldehyde after extraction. The cleavage of the protecting group succeeded with a high conversion compared to the first reaction using 2,3-dichloro-5,6-dicyano-1,4-benzoquinone, and signals of the educt **70a** were not detected by NMR spectroscopy. However, the resulting alcohol appears to be soluble in water, which complicated the purification from salts and side products. Alternatively, a silyl moiety was used to protect the hydroxy group, which can be easily cleaved with fluoride and purified by filtration through a silica pad. The preparation of 3-((*tert*-butyldimethylsilyl)oxy)propionitrile (**67b**) was carried out by a modified literature procedure with imidazole as a base and catalyst and was purified by distillation (Scheme 2.51).[232] In contrary to **68a**, 3-((*tert*-butyldimethylsilyl)oxy)propanethioamide (**68b**) was synthesized with hydrogen sulfide, which was bubbled into the reaction mixture for 1.5 hours.

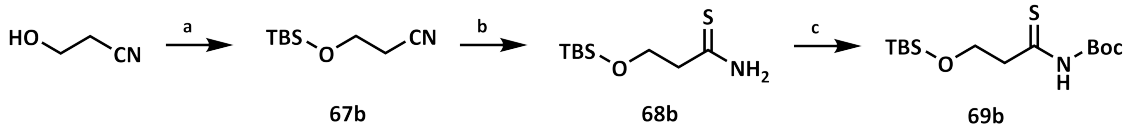

67b 68b 69b

Scheme 2.51: Synthesis of 3-((*tert*-butyldimethylsilyl)oxy)propanethioamide (**68b**). Conditions: a) TBSCl, HIm, THF, 0 °C to RT, 4 h, 91%. b) H_2S, NEt_3, C_5H_5N, 60 °C, 17 h, 71%. c) NaH, Boc_2O, THF, -30 °C to RT, 5 h, >99%.[225, 226, 232, 233]

Analogous to the conversion of **68a** into **70a**, the thioamide **68b** was reacted with sodium hydride and di-*tert*-butyl dicarbonate to *tert*-butyl (3-((*tert*-butyldimethylsilyl)oxy)propanethioyl)carbamate (**69b**), and further to *tert*-butyl (3-((*tert*-butyldimethylsilyl)oxy)-1-iminopropyl)carbamate (**70b**) in high yields. The silyl ether was cleaved by the treatment of **70b** with tetra-*n*-butylammonium fluoride in dichloromethane to afford *tert*-butyl (3-hydroxy-1-iminopropyl)carbamate (**71**) in a yield of 55% over five steps (Scheme 2.52). The product was purified by filtration through a short pad of silica to separate the product from salts before being dried under reduced pressure to remove the byproduct *tert*-butyldimethylsilyl fluoride.

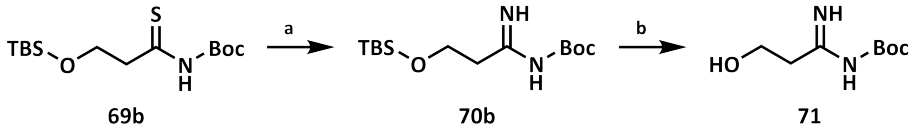

Scheme 2.52: Synthesis of *tert*-butyl (3-hydroxy-1-iminopropyl)carbamate (**71**). Conditions: a) NH_3, $ZnCl_2$, MeOH, 0 °C to RT, 2 h, 92%. b) TBAF, DCM, RT, 3 h, 92%.[225, 229]

In a first attempt, **71** was mesylated in dichloromethane with triethylamine. In the ^{1}H NMR spectrum of the mesylate, additional signals of a double bond were observed after extraction. Through the transformation of the hydroxy moiety into a good leaving group, an elimination is facilitated by the conjugation of the resulting carbon-carbon double bond with the amidine moiety. Hence, to a mixture of **71** and triethylamine, a slight excess of mesyl chloride was added, as well as thioacetic acid after one hour to prepare 3-((*tert*-butoxycarbonyl)amino)-3-iminopropyl thioacatate (**72**) *via* a substitution or Michael addition (Scheme 2.53).

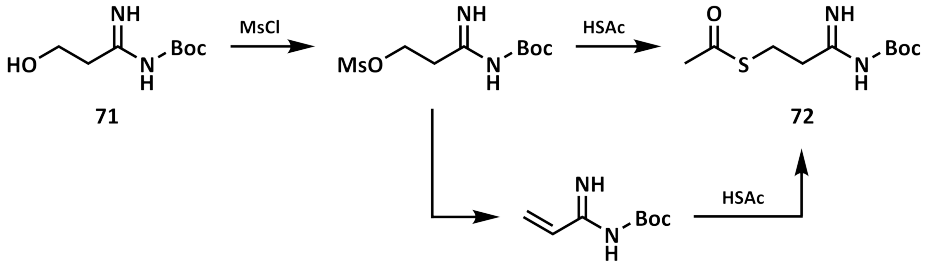

Scheme 2.53: Synthesis of 3-((*tert*-butoxycarbonyl)amino)-3-iminopropyl thioacatate (**72**).

Surprisingly, 3-((*tert*-butoxycarbonyl)amino)-3-oxopropyl thioacatate (**73**) with an amide moiety instead of amidine was obtained by the reaction to prepare **72**, and the desired product was not detected. The synthesis was repeated with a higher amount of triethylamine and a lower excess of thioacetic acid to afford **72** in a poor yield of 11%, in addition to **73**. Both compounds were distinguished by thin layer chromatography (CH:EE, 1:1) with a higher polarity and tailing of **72** compared to **73**. Furthermore, a change in the chemical shift of the methylene proton signals is visible in the ^{1}H NMR spectra depicted in Figure 2.41. In the case of **72**, a very broad singlet was observed at 9 ppm for the proton of the imino moiety. To identify the chemical formula and detect a difference between oxygen and nitrogen with a proton, the amidine and amide were characterized by ultra high performance liquid chromatography coupled with high resolution mass spectrometry.

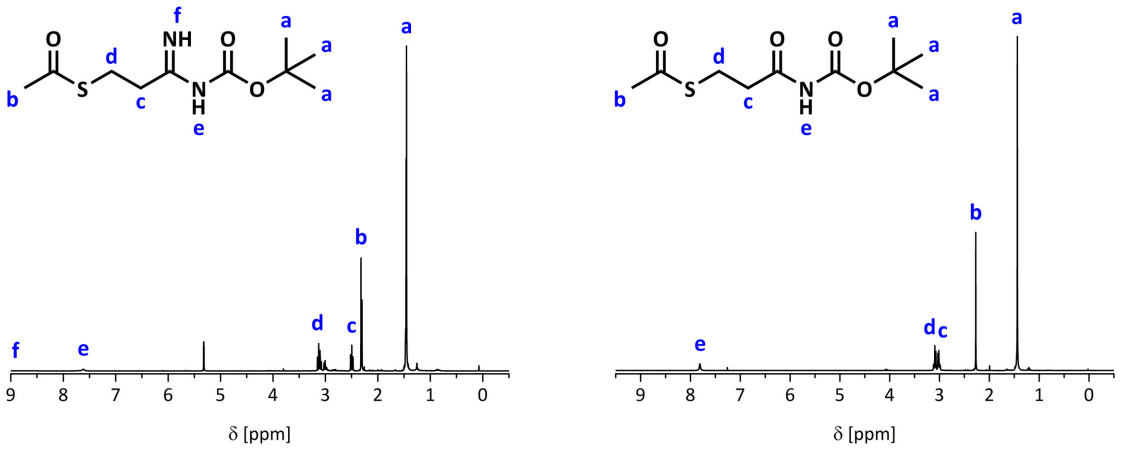

Figure 2.41: ^{1}H NMR spectra of **72** in $CDCl_3$ (left) and **73** in CD_2Cl_2 (right).

Moreover, the structure of **71** and **73** was confirmed by X-ray analysis to ensure that the educt **71** contains no amide (Figure 2.42). An amide could be formed by mesylation, whereby the hydroxy group and the imino moiety of the amidine can react with mesyl chloride. The mesylated imino group could be substituted by a hydroxide anion through the addition of an aqueous sodium bicarbonate solution to quench the reaction. The protection of the amidine with the electron withdrawing *tert*-butoxycarbonyl group increases the reactivity of the imino moiety and can facilitate its substitution. To optimize the synthesis of **72**, two equivalents of mesyl chloride can be used and the formation of an amide could be prevented by quenching of the reaction with non-aqueous ammonia at the end.

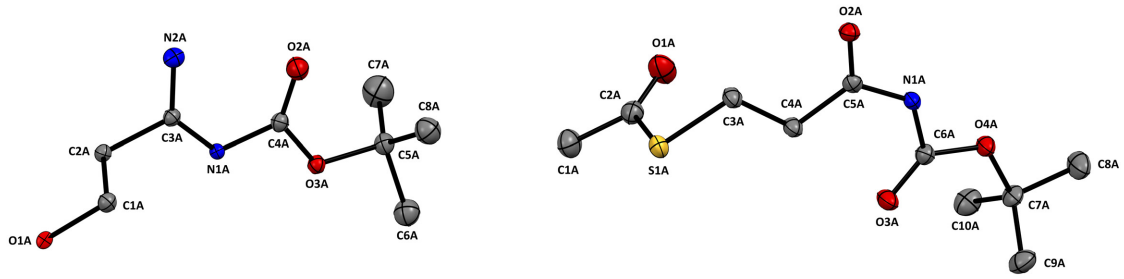

Figure 2.42: Molecular structures of **71** (left) and **73** (right) determined by X-ray analysis.

However, *tert*-butyl (1-imino-3-mercaptopropyl)carbamate was not achieved, and a polyether with amidine moieties can be prepared by post-polymerization modifications. Here, the polymer **61** can be functionalized with 3-mercaptopropionitrile *via* a thiol-ene reaction as described for polymethylvinylsiloxane.[234] The diblock copolymer containing nitrile groups could be transformed into an amidine by the treatment with ammonium sulfide followed by ammonia and zinc(II) chloride.

Another interesting functionality for gene delivery is ethylenediamine moiety due to a possible second cationic charge, and the different pK_s values of the protonated amino groups with approximately 7 and 10.[235] The thiol was synthesized analogous to **65** starting from 2-(*N*-(*tert*-butoxycarbonyl)methylamino)ethanol (Scheme 2.54). The amino groups were protected using di-*tert*-butyl dicarbonate to afford *N*,*N'*-bis(*tert*-butoxycarbonyl)-2-((2-aminoethyl)amino)ethanol (**74**) quantitatively, and the sulfur was introduced by mesy-

lation of the hydroxy moiety followed by substitution with potassium thioacetate. The low conversion of the mesylate into 2-(*N*-(*tert*-butoxycarbonyl)methylamino)ethyl thioacetate (**75**) can be improved as described for the synthesis of **64**. After characterization by NMR spectroscopy and mass spectrometry, **75** was converted into a mercaptan for the thiol-ene reaction.

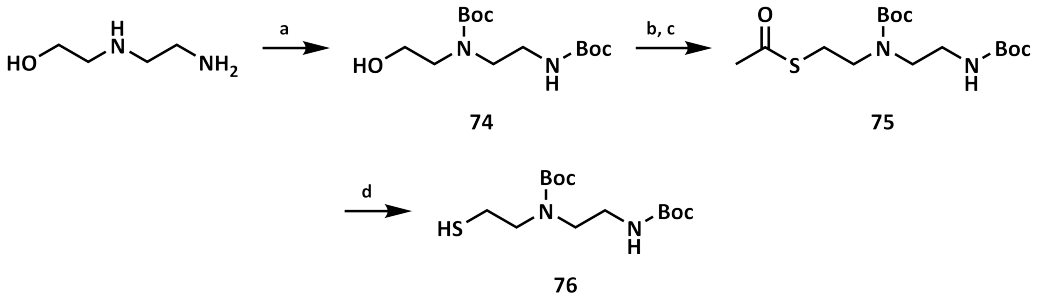

Scheme 2.54: Synthesis of *N,N'*-bis(*tert*-butoxycarbonyl)-2-((2-aminoethyl)amino)ethanethiol (**76**). Conditions: a) Boc_2O, NEt_3, THF, EtOH, 0 °C to RT, 24 h, >99%. b) MsCl, NEt_3, DCM, 0 °C to RT, 4 h, 79%. c) KSAc, DMF, 50 °C, 14 h, 27%. d) NaOMe, MeOH, RT, 1 h, >99%.[222, 236]

The thioacetate can be hydrolyzed under acidic conditions with cleavage of the *tert*-butoxycarbonyl groups or by saponification. Sodium methoxide was used for the preparation of *N,N'*-bis(*tert*-butoxycarbonyl)-2-((2-aminoethyl)amino)ethanethiol (**76**) to afford a mercaptan with low polarity similar to **61**, wherefore a high functionalization *via* a thiol-ene reaction is achievable without solubilization problems.

Nitrogen-containing aromatic heterocycles can also bind to polynucleotides as weaker bases, and to functionalize **61** to deliver genes, we selected an imidazole and a caffeine moiety for the side chain. Similar to **65** and **76**, 2-(imidazol-1-yl)ethanol was mesylated and substituted by potassium thioacetate to obtain 2-(imidazol-1-yl)ethyl thioacetate (**77**) as shown in Scheme 2.55. The reaction of the alcohol with mesyl chloride resulted in a moderate yield, which could be improved by using two equivalents of the acid chloride and quenching the reaction with aqueous sodium carbonate to cleave the mesyl group at the imidazole. Compared to **64** and **75**, the preparation of **77** reached a higher conversion in a shorter time by increasing the temperature by 10 °C. At -24 °C, **77** crystallized and was then characterized *via* X-ray analysis to confirm the structure as depicted in Figure 2.43. Furthermore, signals of the remaining *N,N*-dimethylformamide are visible in the ^{1}H NMR spectrum.

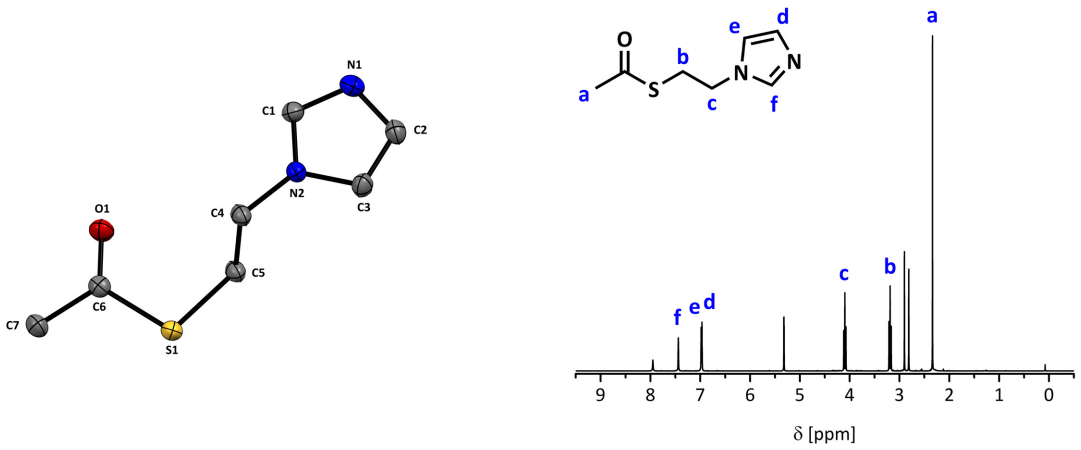

Figure 2.43: Molecular structure determined by X-ray analysis (left) and ^{1}H NMR spectrum in CD_2Cl_2 (right) of 2-(imidazol-1-yl)ethyl thioacetate (**77**).

The thiol was obtained by the treatment of **77** with sodium methoxide and distillation as a colorless liquid. The achieved moderate yield of **78** may be caused by the adjustment of a neutral pH with the acidic ion-exchange resin Dowex® 50WX8 and partially protonated **78**, which could not boil during the distillation.

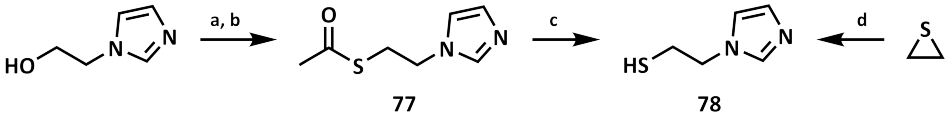

Scheme 2.55: Synthesis of 2-(imidazol-1-yl)ethanethiol (**78**). Conditions: a) MsCl, NEt_3, DCM, 0 °C to RT, 3 h, 64%. b) KSAc, DMF, 60 °C, 3 h, 57%. c) NaOMe, MeOH, RT, 2 h, 64%. d) HIm, EtPh, 115 °C, 24 h, 21%.[222, 237]

A direct synthesis of **78** is reported *via* the ring-opening of ethylene sulfide by imidazole.[237] Due to a possible polymerization, a solution of ethylene sulfide was added dropwise over 21 hours to an excess of imidazole dissolved in ethylbenzene at 115 °C. Besides the difficulty in preparing **78** at a larger scale under these diluted reaction conditions, a further disadvantage is the purification of the product resulting in a low yield containing 31 wt% imidazole after distillation (Figure 2.44).

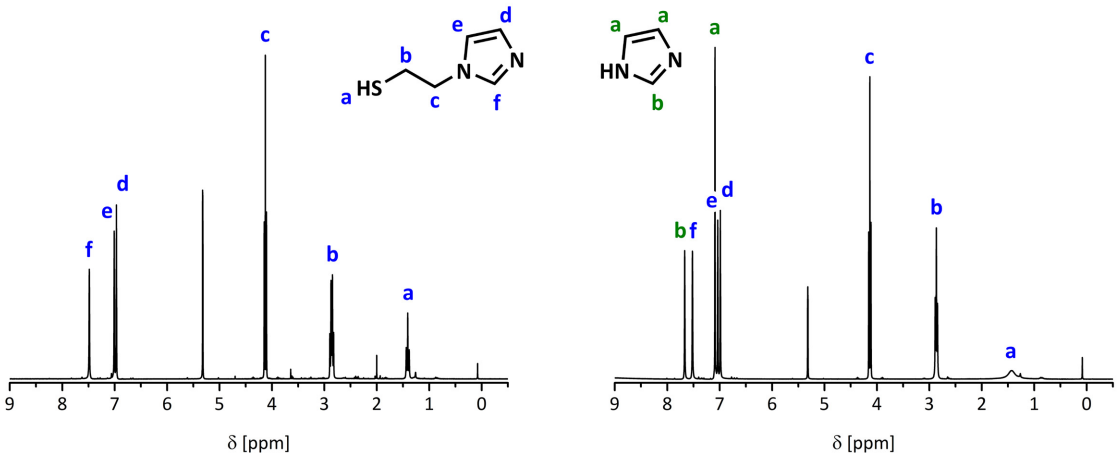

Figure 2.44: ^{1}H NMR spectra of **78** prepared from **77** (left) and ethylene sulfide (right) in CD_2Cl_2.

Varying the substitution at the imidazole ring from the 1 to the 4 or 5 position led to a proton at the nitrogen, which could result in a stronger interaction with nucleic acids by an additional hydrogen bond compared to **78**. For the conversion of the hydroxy group into a thiol, the heterocycle was protected with a *tert*-butoxycarbonyl moiety to prevent the formation of a 1-(methylsulfonyl)imidazole derivative (Scheme 2.56). The reaction of 2-(imidazol-4/5-yl)ethanol with di-*tert*-butyl dicarbonate afforded *N*-(*tert*-butyloxycarbonyl)-4-(2-hydroxyethyl)imidazole (**79**) in a moderate yield of 51%. In contrast, the analogous reaction of imidazole with the pyrocarbonate reached a high conversion of over 90% after 15 minutes.[238] Furthermore, the attachment of *tert*-butyloxycarbonyl groups to 2-(imidazol-4/5-yl)ethanol derivatives with one methylene moiety more or less between the imidazole ring and hydroxy group resulted in yields of 80% and higher.[239, 240] The following mesylation of **79** and substitution to *N*-(*tert*-butyloxycarbonyl)-4-(2-(acetylthio)ethyl)imidazole (**80**) succeeded with high conversions.

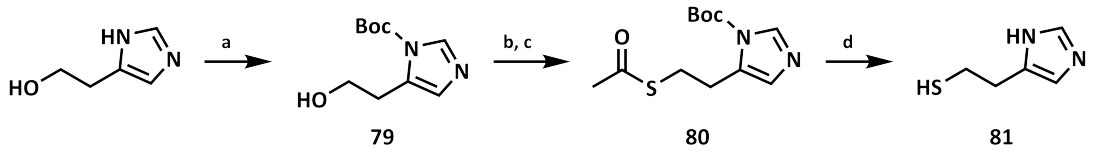

Scheme 2.56: Synthesis of 2-(imidazol-4/5-yl)ethanethiol (**81**). Conditions: a) Boc_2O, NEt_3, MeOH, RT, 19 h, 51% b) MsCl, NEt_3, DCM, 0 °C to RT, 4 h, >99%. c) KSAc, DMF, 60 °C, 16 h, 89%. d) NaOMe, MeOH, RT, 2 h, 90%.[222, 241]

The structure of **80** was identified by X-ray analysis and NMR spectroscopy (Figure 2.45). The thioester of **80** was hydrolyzed to achieve the thiol and functionalize the polymer **61**. Under the same conditions to cleave the acetyl group of **80**, the *tert*-butyloxycarbonyl moiety at the imidazole ring can be removed, and the reaction with sodium methoxide afforded 2-(imidazol-4/5-yl)ethanethiol (**81**) as a brown oil. A residue with approximately 15% acetyl functionality was determined from the ^{1}H NMR spectrum

of **81**, and the heterocycle was completely deprotected. For the synthesis of **79**, more than 1.5 equivalents of sodium methoxide can be used to react with both carbonyl groups. The product could be purified by distillation to yield a colorless compound.

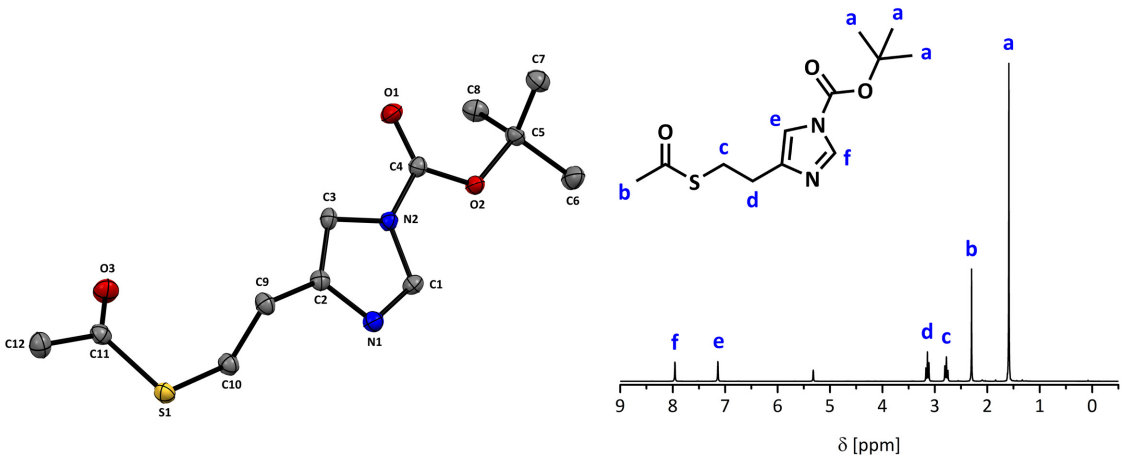

Figure 2.45: Molecular structure (left) and ^{1}H NMR spectrum in CD_2Cl_2 (right) of *N*-(*tert*-butyloxycarbonyl)-4-(2-(acetylthio)ethyl)imidazole (**80**).

Based on the binding of intercalation of methylxanthines like theophylline and caffeine into polynucleotides,, 2-(theophyllin-7-yl)ethanethiol (**83**) was prepared as a possible functionality to bind nucleic acids.[242, 243] To a suspension of 2-(theophyllin-7-yl)ethanol in dichloromethane, mesyl chloride was added, followed by triethylamine. After one hour, a clear solution was observed. The resulting mesylate was transformed into 2-(theophyllin-7-yl)ethyl thioacetate (**82**) using potassium thioacetate with a high yield (Scheme 2.57).

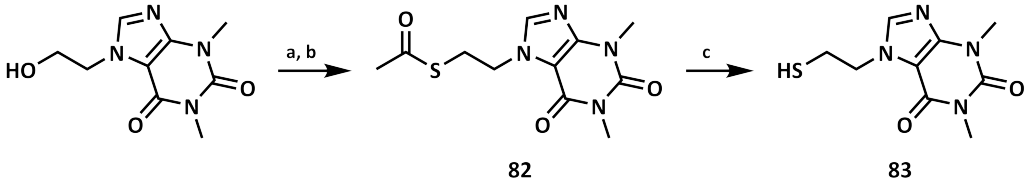

Scheme 2.57: Synthesis of 2-(theophyllin-7-yl)ethanethiol (**83**). Conditions: a) MsCl, NEt_3, DCM, 0 °C to RT, 4 h, >99%. b) KSAc, DMF, 60 °C, 3 h, 84%. c) NaOMe, MeOH, RT, 3 h, 92%.[222, 244]

To verify the structure of **82**, X-ray analysis, NMR spectroscopy, and mass spectrometry were used as characterization methods (Figure 2.46). The treatment of **82** with sodium methoxide afforded **83** as a beige solid with high conversions. To compare how the binding and delivery of nucleic acids depends on the functional groups, **61** was prepared on a large scale for the attachment of all mercaptans *via* a thiol-ene reaction.

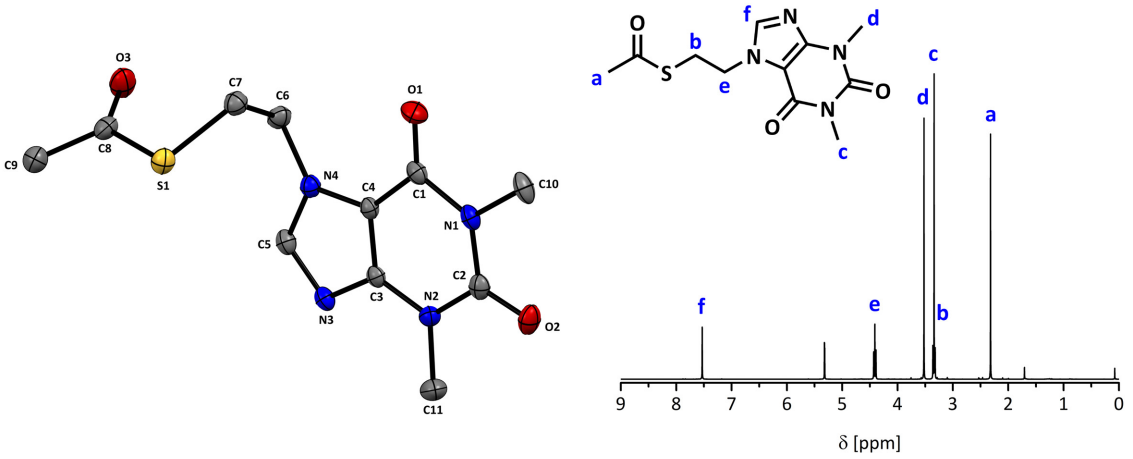

Figure 2.46: Molecular structure (left) and ^{1}H NMR spectrum in CD_2Cl_2 (right) of 2-(theophyllin-7-yl)ethyl thioacetate (**82**).

Based on the results of **62**, more than 30 repeating units of allyl glycidyl ether are necessary for an efficient binding of polynucleotides and higher cellular uptake of the polyplex micelles using modified **61** in comparison to PEI. The anionic ring-opening polymerization was carried out with 5 g poly(ethyleneoxide), and ethylbenzene was added to prevent broader distributions caused by high viscosities and poorer mixing. After purification *via* dialysis, a degree of polymerization of 37 was determined by NMR spectroscopy and a narrow polydispersity below 1.2 was measured by SEC analysis for the prepared polymer **61f**. Next, **61f** was radically functionalized by a thiol-ene reaction with the thiols under UV light irradiation (Scheme 2.58).

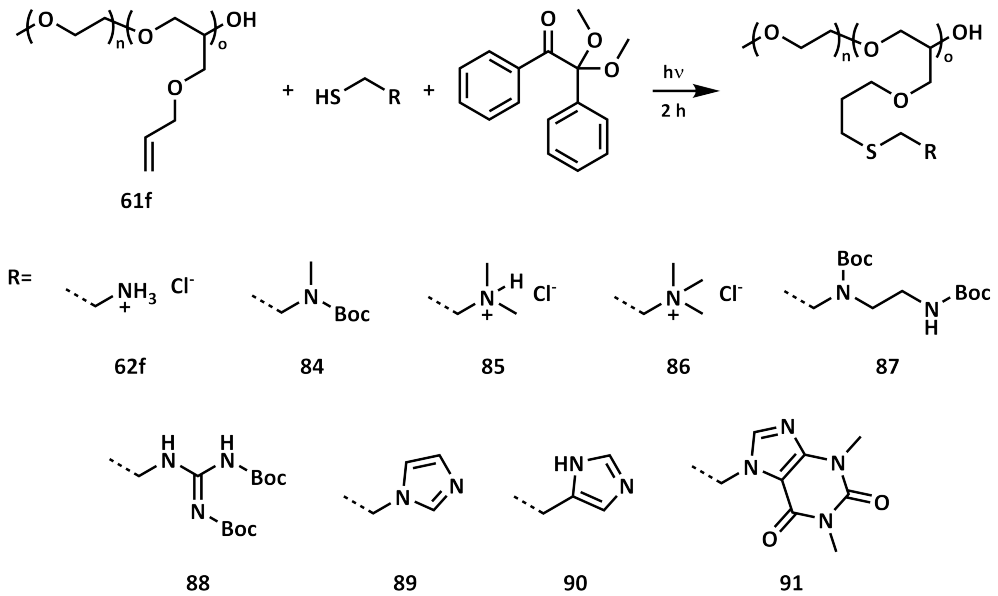

Scheme 2.58: Modification of **59f** with various mercaptans *via* a thiol-ene reaction.

Depending on the polarity and solubility of the mercaptans, a suitable solvent or solvent mixture was used for the modification of **61f**. The preparation of **84**, **87**, **88**, **89** and **90** occurred in tetrahydrofuran, and **91** in *N*,*N*-dimethylformamide. As before, the functionalization with cysteamine hydrochloride to achieve **62f** and the conversion of **61f** with

captamine hydrochloride to **85** was performed in a mixture of methanol and tetrahydrofuran. Due to the solubility of thioline chloride **63**, a mixture of *N*,*N*-dimethylformamide and methanol was applied for the thiol-ene reaction. Unexpectedly, the thiol-ene reaction using 2-(imidazol-4/5-yl)ethanethiol (**81**) did not succeed. In the ^{1}H NMR spectrum, the signals of the allyl groups are visible as for **59f**. A possible reason could be the deep brown color of **81**, which led to an inefficient initiation by UV light as well as residues of the thioacetate that may form a stabilized radical and prevent the addition to the carbon-carbon double bond. To prepare **90**, the mercaptan **81** could be purified *via* preparative high-performance liquid chromatography, or distillation is also possible to remove impurities and the brown color. Apart from the modification using **90**, high conversions over 99% of the allyl groups were determined by NMR spectroscopy for the thiol-ene reactions. In addition, the SEC analysis in *N*,*N*-dimethylacetamide showed narrow molecular weight distributions below 1.2 of the modified polymers with the exception of **88** (Table 2.13). Apart from **88** and **90**, a high degree of functionalization of over 99% was determined by NMR spectroscopy in combination with the SEC for the thiol-ene reaction of **61f** with the various thiols.

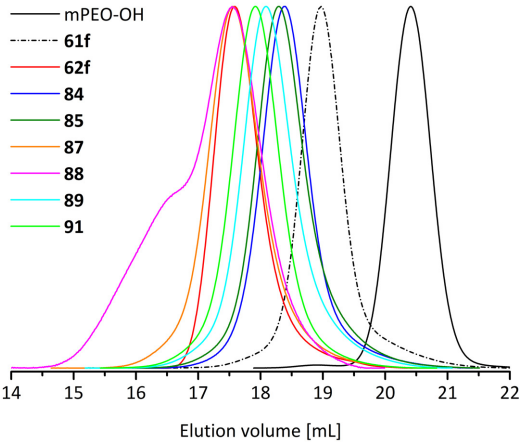

Figure 2.47: SEC elugrams in DMAc of **61f** and its modifications.

Table 2.13: SEC data in DMAc of **61f** and its modifications.

Polymer	$\overline{M}_n$ [a)]	$Đ$ [a)]
mPEO-OH	1,600 g·mol^{-1}	1.06
61f	3,700 g·mol^{-1}	1.12
62f	7,900 g·mol^{-1}	1.11
84	5,700 g·mol^{-1}	1.13
85	4,900 g·mol^{-1}	1.15
87	8,200 g·mol^{-1}	1.17
88	10,600 g·mol^{-1}	1.47
89	5,600 g·mol^{-1}	1.16
91	7,000 g·mol^{-1}	1.13

[a)] PEO calibration.

After a certain amount of *N*,*N'*-bis-(*tert*-butoxycarbonyl)-*N"*-2-mercaptoethylguanidine (**66**) is attached to the polymer, the bulky *tert*-butoxycarbonyl groups sterically hinder access to the remaining carbon-carbon double bonds. This lead to an inefficient radical transfer from the carbon to a thiol resulting in the formation of inter- and intramolecular cross-links of the allyl moieties. That explains the disappearance of the allyl signals in the ^{1}H NMR spectrum and the observed shoulder by SEC analysis depicted in Figure 2.47. Similarly to the synthesis of cysteamine hydrochloride into **66**, guanidine moieties at the polyether were introduced by a post-polymerization modification of **62f**. A variety of common chemicals can be used for a guanidinylation such as Goodman's reagent or a protected thiourea, and requires a deprotection of the functional group as a further reaction step. For a direct transformation of a primary amine into guanidine, the reagents are limited to

cyanamide, aminoiminomethanesulfonic acid, *S*-alkylisothiourea salts, and 1-amidinopyrazole salts. Here, cyanamide and 1-amidinopyrazole hydrochloride were selected for the reaction with **62f** as shown in Scheme 2.59

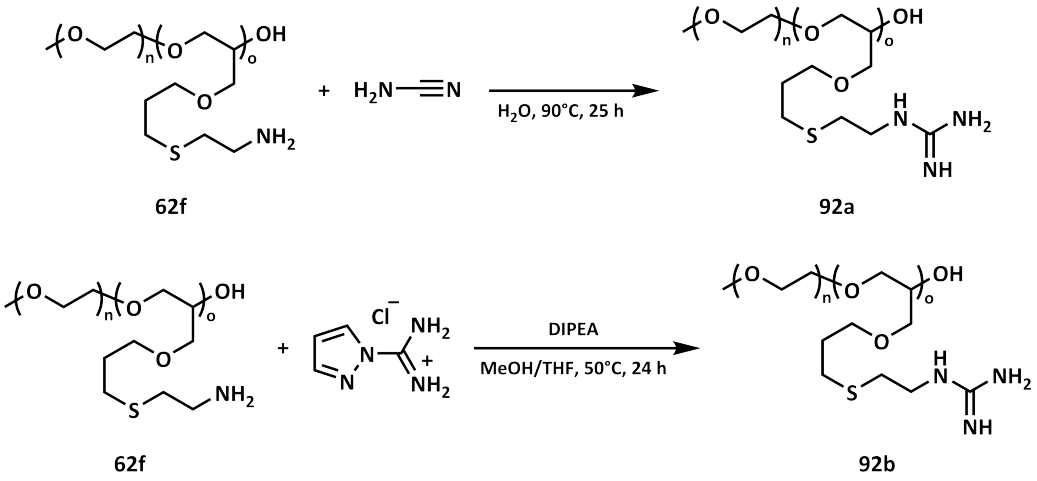

Scheme 2.59: Guanidinylation of **62f** *via* post-polymerization modification.

A functionalization of only 50% was determined by NMR spectroscopy for the preparation of **92a** using over a twofold excess of cyanamide. A higher conversion may be not attainable *via* this approach. Additionally, Mattheis *et al.* described the modification of poly(2-aminoethyl methacrylate) with maximal 60% transformation of the amino groups into guanidine moieties using 0.75 equivalents cyanamide or higher.[245] This method could be applied for a partial guanidinylation to achieve a mixture of both functionalities, which is reproducible. The treatment of **62f** with the more reactive 1-amidinopyrazole hydrochloride resulted in **92b** with 94% converted amino groups. A shift of the methylene protons next to the nitrogen from 3.1 to 3.4 ppm is visible in the ^{1}H NMR spectrum, and they were used to calculate the degree of modification (Figure 2.48). Furthermore, an additional signal was detected at 157 ppm for the imino carbon in the ^{13}C NMR spectrum, and higher molar masses than **62f** with narrow dispersities below 1.2 was observed by SEC analysis.

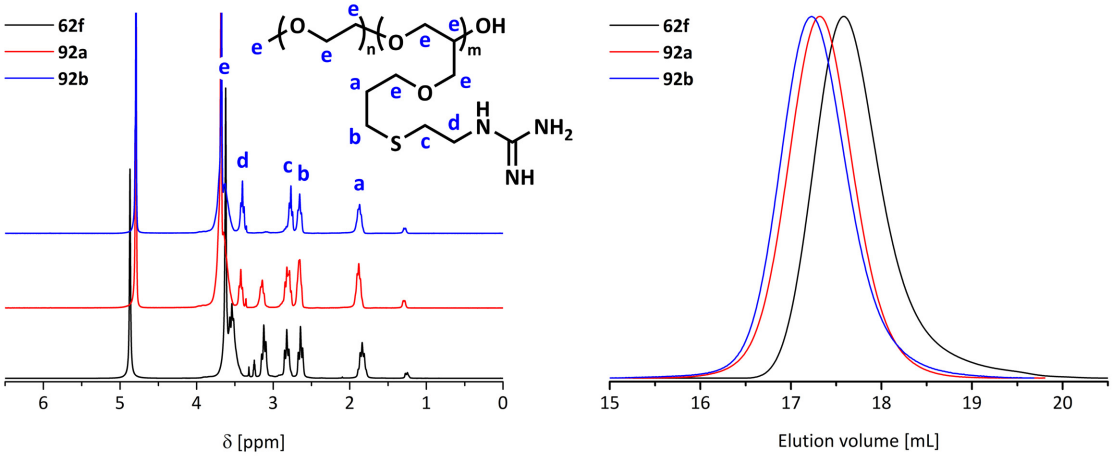

Figure 2.48: ^{1}H NMR spectra of **62f** in CD_3OD, **92a** and **92b** in D_2O (left) and the corresponding SEC elugrams in DMAc (right).

The diblock copolymers with a secondary amine and diamine groups were accessed by deprotection of the *tert*-butoxycarbonyl moieties of **84** and **87** under acidic conditions (Scheme 2.60). Trifluoroacetic acid was used as a strong acid with a non-nucleophilic anion to remove the protective groups and to avoid the cleavage of ether moieties along the polymer backbone as well as in the side chain.

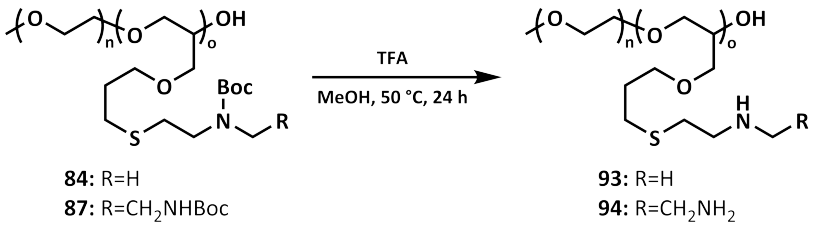

Scheme 2.60: Preparation of **93** and **94** by the deprotection of **84** and **87** with trifluoroacetic acid, respectively.

An incomplete decomposition of the carbamates between 69 and 76% was observed by the reaction of **84** with trifluoroacetic acid in methanol or under solvent-free conditions at room temperature overnight. For a higher degree of deprotection, the polymer solution in methanol with trifluoroacetic acid was heated to 50 °C. This resulted in the removal of the *tert*-butoxycarbonyl moiety to 94% for **93** and 98% in the case of **94**. A proton signal of the residual protecting group is visible at 1.5 ppm in the ^{1}H NMR spectrum of **93** as shown in Figure 2.49. Furthermore, shifts to higher molar masses were detected by SEC analysis due to the unprotonated amino groups, which can interact with the lithium chloride in the eluent. The coordination of lithium ions could increase the solvation shell and hydrodynamic volume. Additionally, **93** and **94** were dialyzed against brine to replace the counteranion with chloride to prevent any associated cytotoxicity, and then water to eliminate salts.

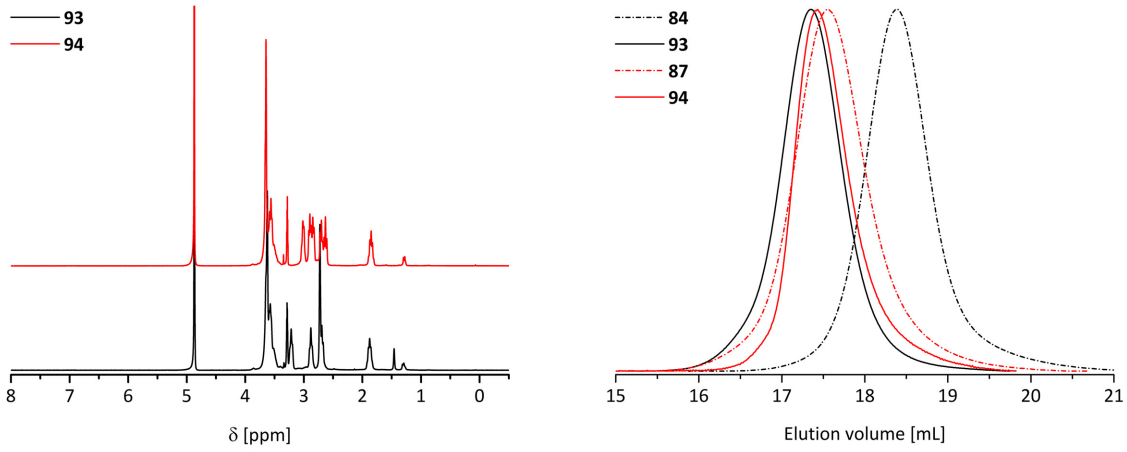

Figure 2.49: ^{1}H NMR spectra in CD_3OD (left) of **93** and **94**, and the SEC elugrams in DMAc (right) before and after deprotection.

Based on the complexation of nucleic acid in water, the polyelectrolyte segment of the polymer had to be hydrophilic for an efficient binding of the biomacromolecule. In the case of the pH-responsive polymer **89** containing imidazole moieties, the aggregation in

water was analyzed in the protonated and uncharged form. At a pH of 6, unimers of **89** were detected by dynamic light scattering with a hydrodynamic radius around 2 nm, and a turbid mixture with micelles in the range of 35 nm was observed at a higher pH of 7 (Figure 2.50). Additionally, the cryo-TEM images confirmed the spherical shape with core diameters between 9 and 14 nm, and a few cylindrical morphologies were also observed in two micrographs.

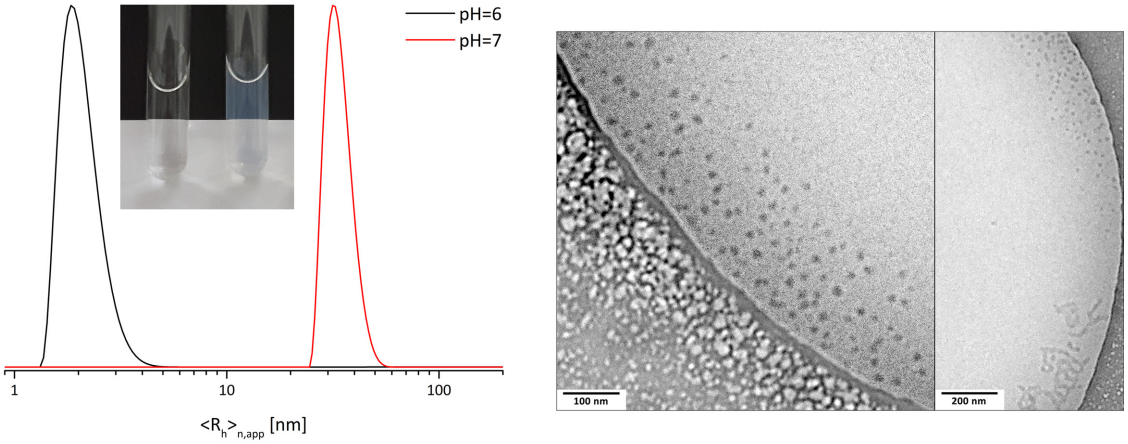

Figure 2.50: Number-weighted CONTIN plots of **89** (1 g·L^{-1}) in buffer solutions (left) and cryo-TEM images of **89** (1 g·L^{-1}) in water at a neutral pH (right).

The interaction of nucleic acids and imidazole moieties is enhanced at a pH below 6, caused by protonation of the heterocycle and ionic interactions with the negatively charged sugar-phosphate backbone. At a physiological pH of 7.4, **89** is largely uncharged, and was partially methylated to introduce permanent cationic moieties to improved the properties as a non-viral vector (Scheme 2.61). An incomplete alkylation was targeted to retain the pH responsivity for a buffering of the acidification in the endocytic pathway. That may lead to an increased osmotic pressure and better endosomal escape, as well as transfection of the polyplex micelles according to the proton sponge hypothesis.

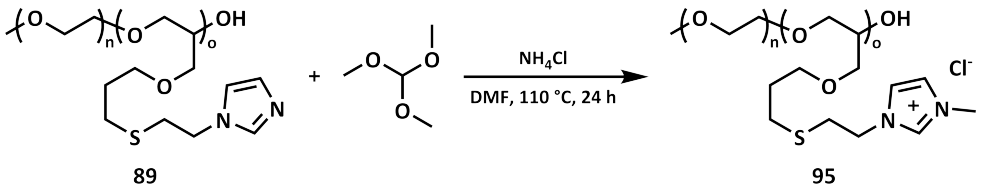

89 95

Scheme 2.61: Preparation of **95** by methylation of **89** with trimethyl orthoformate.

Trimethyl orthoformate was selected as a mild alkylating agent instead of methyl iodide, dimethyl sulfate or the Meerwein salt to avoid side reactions. The highly reactive reagents can methylate the thioether, and perhaps also the ether groups, which could subsequent react with nucleophiles to degrade the polymer or demethylation. A literature procedure was optimized for the post-polymerization modification using *N*,*N*-dimethylformamide as solvent and ammonium chloride as acid to obtain chloride as the counteranion of the polycation.[246] The degree of methylation was adjusted by the amount of added ammonium chloride, and **95a** and **95b** were prepared with different percentages of alkylation. From

NMR spectroscopy, the functionalization was determined to be 68% for **95a** and 84% for **95b** using the downfield shifted signals of the imidazolium moiety, introduced methyl group, and the methylene proton next to the heterocycle (Figure 2.51). Low dispersities of approximately 1.2 and slightly increased molecular weights were detected by SEC analysis in water. The minor changes in the SEC traces are the result of a similar hydrodynamic volume of **95a**, **95b**, and the protonated **89** under acidic pH, which has the same amount of cationic charges as the methylated polymers. A small shoulder at lower elution volume was observed after the modification, which currently can not be explained.

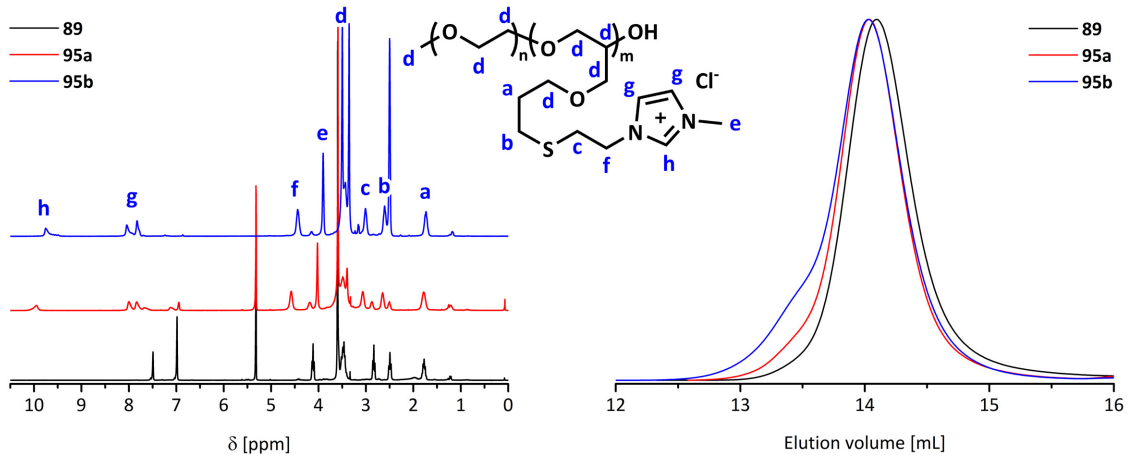

Figure 2.51: ^{1}H NMR spectra of **89** and **95a** in CD_2Cl_2 and **95b** in DMSO-d_6 (left) and the corresponding SEC elugrams in water (right).

Contrary to **89** functionalized with imidazole groups, the hydrophobic block with theophylline moieties of **91** does not dissolve in water at low pH values through protonation. The solubility can also not be improved by methylation. The use of xanthine derivatives with more hydrogen bond donors and no methyl groups at the pyrimidinedione scaffold could enhance the hydrophilicity. An increased solubility in water is reported for theobromine, theophylline and caffeine at higher temperatures than 50 °C.[247, 248] The polymer **91** may exhibit a lower critical solution temperature dependent on the pH value. An aqueous mixture of **91** was prepared by adding water to the polymer solution in DMSO. The formation of vesicles was detected by cryo-TEM measurements as depicted in Figure 2.52. Due to its solubility, **91** was not used for the binding and delivery of polynucleotides.

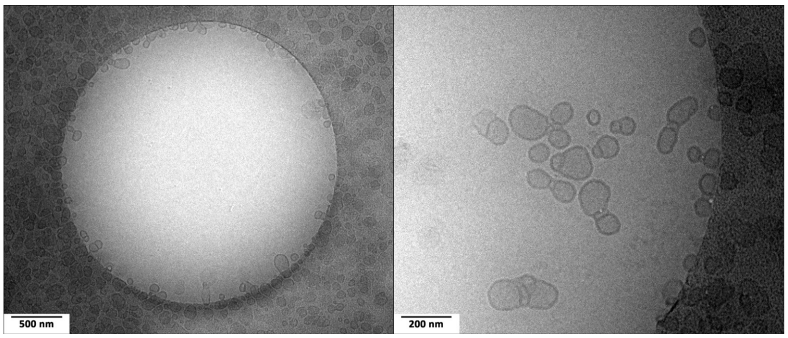

Figure 2.52: Cryo-TEM micrographs of **91** in water (1 g·L^{-1}) with 10% DMSO.

The hydrophilic block copolymers prepared by the modification of **61f** shown in Scheme 2.62 were used to compare how the different cationic moieties present impact the interaction of the polymer with pDNA, their cytotoxicty, uptake and transfection of the polyplex micelles. A. Landmann investigated the properties of the polycations with the nucleic acid using PEI as a reference.

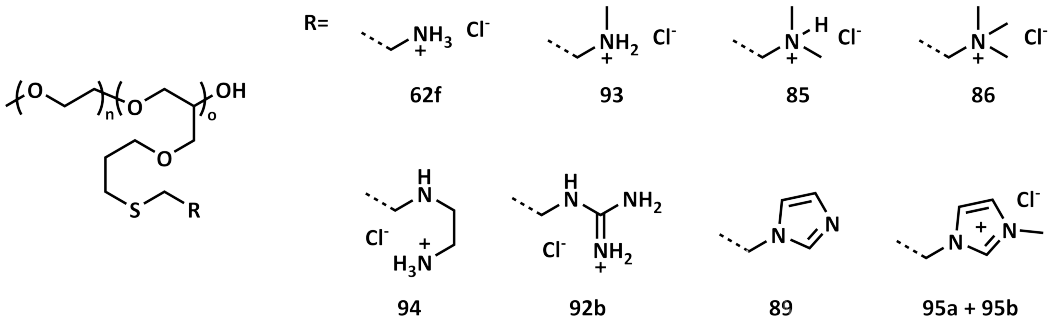

Scheme 2.62: Hydrophilic block copolymers for the characterization with pDNA as non-viral vectors.

To find the minimum quantity of polymer required to bind with most of the pDNA, an ethidium bromide displacement assay was conducted using fluorescence. The ratio of polymer to polynucleotide is given by N/P, where N is the amount of nitrogen from the polymer and P is the number of phosphorus or negative charges from the pDNA. A correction to the more appropriate charge ratio was done for the ethidium bromide displacement assay with N as the quantity of cationic moieties from the polyelectrolyte. The imidazole groups of **89**, **95a** and **95b**, as well as the guanidine functionality of **92b** counted as one N instead of two or three. No significant changes were observed for all polymers at higher than five N/P ratios, and a stronger interaction with pDNA was exhibited by **92b** and **94** (Figure 2.53). Also, the imidazole ring or methylimidazolium groups of **89**, **95a** and **95b** bind the polynucleotide stronger than the primary and secondary amines of **62f** and **93**, or the quaternary ammonium cations of **86**. The result was additionally examined by a gel retardation assay of the polyplex micelles in a buffer at a pH of 8, and **95b** with a higher degree of methylation shows a stronger interaction to the pDNA compared to **95a**. Furthermore, **89** is unable to bind with the nucleic acid independent of the N/P ratio at a pH beyond 7 where the polymer is uncharged.

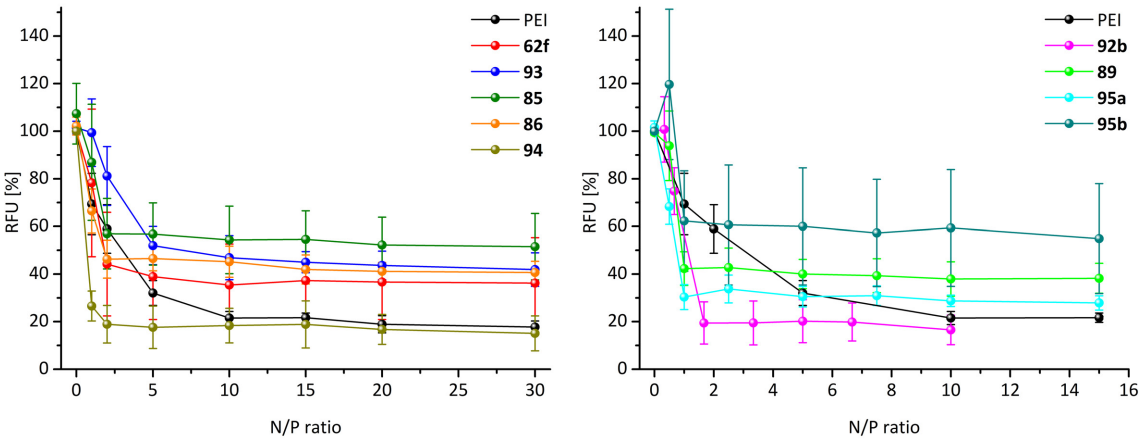

Figure 2.53: Ethidium bromide displacement assay of polyplex micelles with pDNA.

In the following characterizations the uncorrected N/P ratio of 15 with different charge ratios was used to prepare polyplex micelles with pDNA, which could limit the comparability. By dynamic light scattering, the hydrodynamic radii of the assembled polycations with the nucleic acid were measured at a concentration of $1\,\mathrm{g{\cdot}L^{-1}}$ in water under the assumption of spherical or globule shapes. Due to the excess of polymer, smaller aggregates and unimers of the polyelectrolytes were excluded from the number-weighted CONTIN plot to compare the sizes of the polyplex micelles. The complexation of pDNA with most of the polymers afforded a hydrodynamic radius between 30 and 70 nm, and lower radii were detected for **92b** and **94** (Figure 2.54). The smaller size results from a stronger interaction between the polymer and polynucleotide *via* hydrogen bonds of the guanidine and ethylenediamine group as observed by the ethidium bromide displacement assay. A decreased condensation of pDNA occurred with **89** as a consequence of the pH-dependent protonation of the imidazole rings, as well as the binding affinity to pDNA. This behavior is not anticipated for the polymer **85**, which contains tertiary amino groups. In comparison with the quaternary ammonium moiety, which can only interact *via* ionic bonds with the nucleic acid, the protonated tertiary amino group has the possibility to form a hydrogen bond. However, a better binding of the pDNA and a smaller hydrodynamic radius of the polyplex micelle was determined for **86** instead of **85**, which may be explained by the $\mathrm{p}K_\mathrm{b}$ value and the degree of protonation.

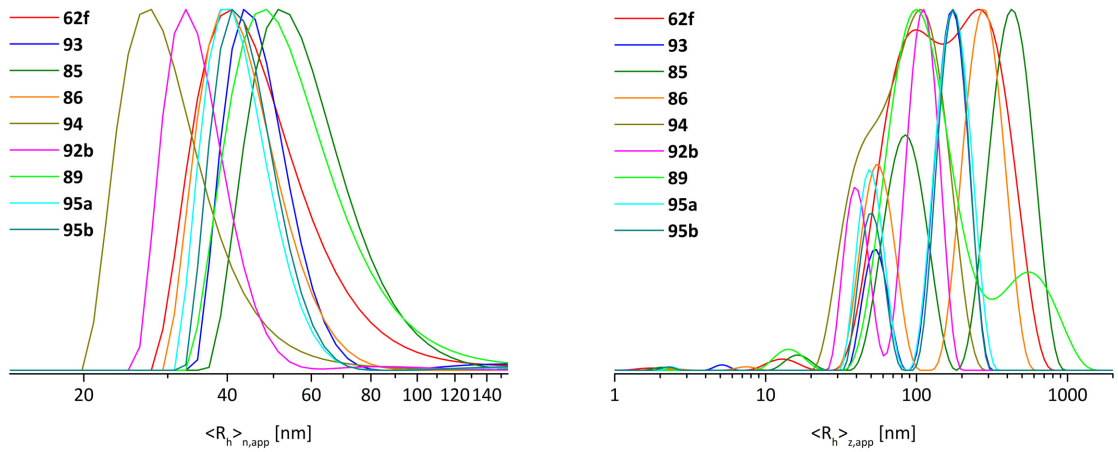

Figure 2.54: Number-weighted (left) and intensity-weighted CONTIN plots (right) of the polyplex micelles with pDNA ascertained by DLS.

Additionally, the stability of the polyplex micelles was examined by a heparin competition assay with ethidium bromide to detect the released pDNA *via* fluorescence (Figure 2.55). The formed polyplexes with the prepared polycations exhibit a higher stability than PEI, which mostly dissociated from the polynucleotide at a heparin concentration of 5 mg·mL^{-1}. However, a similar behavior was observed for the polymer **92b** with guanidine moieties and pDNA, but an increased stability of the polyplex micelle is assumed. Due to the uncorrected N/P ratio, a lower excess of **89**, **92b**, **95a** and **95b** was used to bind pDNA. Hence, there was a reduced amount of free polycations in solution, which formed interpolyelectrolyte complexes with heparin before acting as a competitor. Therefore, the heparin competition assay shows a higher instability of those polyplex micelles.

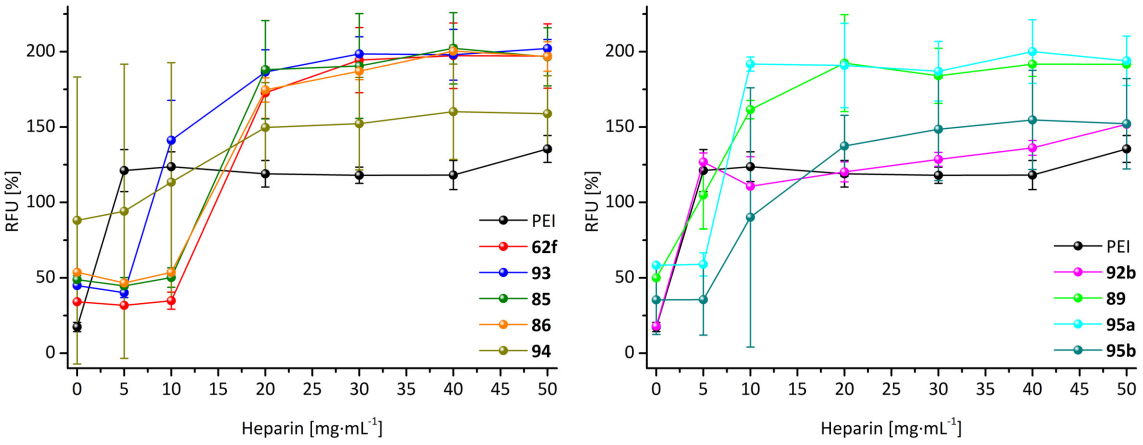

Figure 2.55: Heparin competition assay of polyplex micelles with pDNA.

An evaluation of the cytotoxicity occurred indirectly by a MTT assay measuring the metabolic activity of L929 cells, which decreases with the number of viable cells. For the cationic groups with one or less hydrogen bond donors, a significant reduction in cytotoxicity was observed, *e.g.* the tertiary amines of **85**, quaternary ammonium moieties of **86**, and the imidazole deivatives of **89**, **95a** and **95b** (Figure 2.56). The "softer" cations

with shielded charges by delocalization or a few alkyl groups could be less toxic, but contradict the result of **90b** with the resonance-stabilized guanidinium cation.

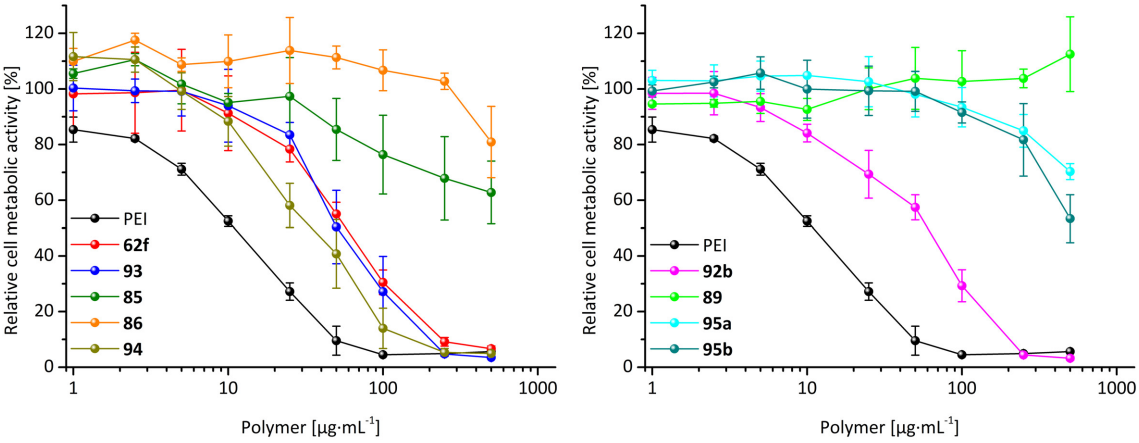

Figure 2.56: MTT assay of polyplex micelles with pDNA using L929 cells.

The cellular uptake and transfection efficiency of the polyplex micelles as non-viral vectors for gene delivery were investigated using L929 cells in Dulbecco's modified Eagle's medium with 10% fetal bovine serum. The block copolymer **89** functionalized with imidazole groups was not explored due to the poor binding of nucleic acids under physiological conditions. To quantify the uptake of the polynucleotide *via* fluorescence measurements after two and four hours in the cells, YOYO-1 labeled pDNA was used for the complexation with the polycations. In comparison to the polyplex with PEI, higher amounts of pDNA were detected in the cells with **62f** and **93** as non-viral vectors. The lowest uptake into the cells was observed for pDNA with the polymers **95a**, **95b** and **86**, which showed the lowest toxicity of all functionalized diblock copolymers. The size of the polyplex micelles appears to have no influence on the cellular uptake as the polyplex micelles with the smallest hydrodynamic radii, *e.g.* of **92b** and **94**, do not exhibit a higher fluorescence intensity in the cells compared to the larger ones. In addition, the large deviations of the measured values have to be considered, and the difference between the used polymers may not be so clear, with the exception of **93**. However, the cellular uptake of the polyplex micelles can be improved using targeting moieties attached at the poly(ethylene oxide). Therefore, low uptake behavior of polyplexes can be used to prevent the delivery of nucleic acids into undesired cells.

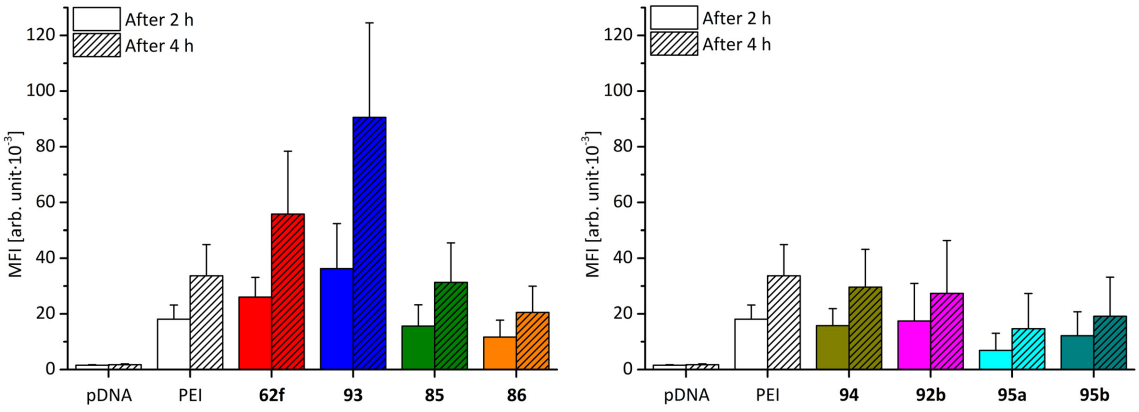

Figure 2.57: Uptake of polyplex micelles with YOYO-1 labeled pDNA in L929 cells.

After the delivery into the cells and endosomal escape, the polyplex micelles have to release the nucleic acid for gene expression, which was analyzed by the fluorescence of the produced green fluorescent protein after 48 hours. Apart from **62f** and **94**, the polyelectrolytes used for complexation of the green fluorescent protein expressing pDNA show a very poor transfection in comparison to PEI. The poor transfection of the polyplex micelle prepared with **93**, which have a good uptake, indicate a stay in the endosome or lysosome, and can be removed from the cell by exocytosis later on (Figure 2.58). In contrast to PEI, a moderate transfection was determined for the polyplex micelle with **62f**, and the best was obtained with **94**. A higher amount of transfected pDNA was also not detected for **95a** and **95b**, which can also buffer the acidification in the endosome besides **94** as assumed from the proton sponge hypothesis. Moreover, the efficiency of all polymers, including PEI, to deliver nucleic acids into cells was very low, and less than 5% of the cells exhibited the green fluorescent protein.

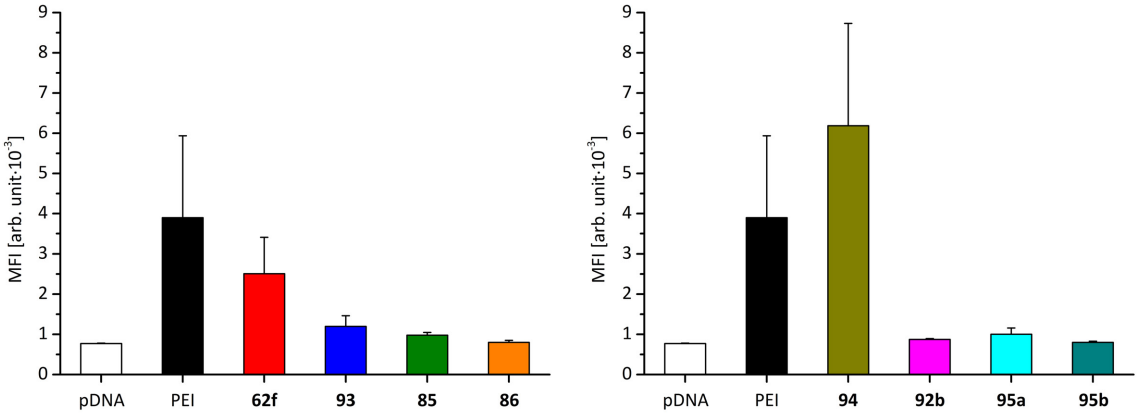

Figure 2.58: Transfection of polyplex micelles with green fluorescent protein expressing pDNA in L929 cells.

All in all, the most promising cationic group for use as a non-viral vector is the ethylenediamine moiety as observed for **94**, and the transfection efficiency can be enhanced by the attachment of targeting moieties to increase the uptake into the desired cells. A combina-

tion of polymers containing ethylenediamine moieties with a higher transfection of pDNA and other cationic groups could further improve the gene delivery. Therefore, the block copolymer **61f** can be modified with both the ethylenediamine moieties and amino groups or guanidine moieties. Based on the excess of thiols used to achieve a high conversion, partially different solubilities and diffusion rates, the reproducible modification of **61** *via* a thiol-ene reaction with two different mercaptans is challenging. Additionally, the amount of incorporated functionalities is difficult to calculate due to overlapping signals in the NMR spectra. Alternatively, a block copolymer with the mixed cationic groups can be prepared by a RAFT polymerization of acrylamides containing the desired moieties to bind the nucleic acids using a poly(ethylene oxide)-based macro chain transfer agent. This requires the synthesis of different acrylamides instead of mercaptans, and facilitates the adjustment of the ratio of different functional groups, and permits the second block to be analyzed more easily.

2.4 Amphiphilic Polyethers as Nanocarriers for Drug Delivery

The polyether-based polymer **61** can be extended by a hydrophobic poly(*tert*-butyl glycidyl ether) core segment to obtain an amphiphilic triblock terpolymer, which self-assemble into micelles in aqueous solution and can be used for drug delivery by encapsulation of hydrophobic molecules (Figure 2.59). First, Barthel *et al.* prepared and investigated a poly(ethylene oxide)-*block*-poly(allyl glycidyl ether)-*block*-poly(*tert*-butyl glycidyl ether) (**96**) system, as well as derivatives functionalized *via* a thiol-ene reaction using cysteamine, 3-mercaptopropionic acid, acetylcysteine, or β-D-thiogalactose in the middle block.[100, 213, 215] A further development of this system by increasing the hydrophobic segment was aimed to change the shape of the micelles from spheres into worm-like structures. A higher accumulation in the liver and spleen tissue was observed for worm-like micelles compared to spherical structures. Moreover, the attachment of targeting moieties at the polymer enhanced its uptake, due to the larger surface area and stronger receptor binding at the cell membrane.[249, 250]

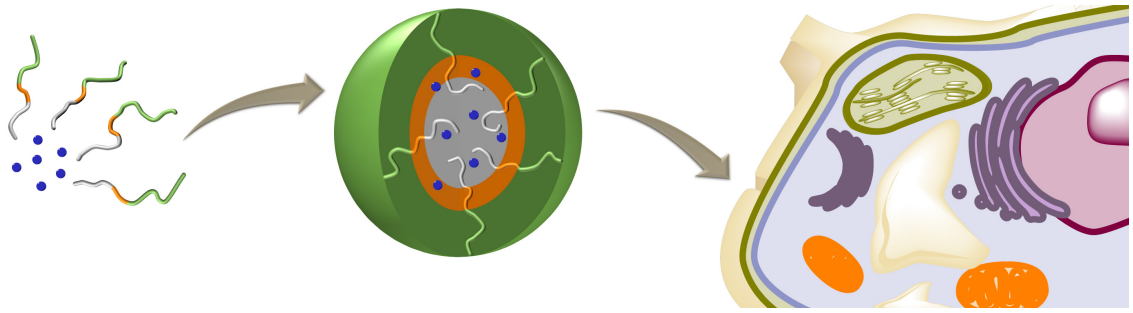

Figure 2.59: Self-assembly of an amphiphilic block copolymer with encapsulated guest molecules for drug delivery.

The triblock terpolymer **96** was synthesized by a sequential anionic ring-opening polymerization under solvent-free conditions using poly(ethylene oxide) as a macroinitiator as depicted in Scheme 2.63.[100] Briefly, α-methoxy-ω-hydroxy poly(ethylene oxide) was melted at 110 °C and deprotonated with sodium hydride to initiate the reaction with allyl glycidyl ether. To obtain the triblock terpolymer **96**, *tert*-butyl glycidyl ether was added 22 hours later and the polymerization was quenched with methanol after 24 hours. The polymer **96** was purified by drying under reduced pressure at 100 °C.

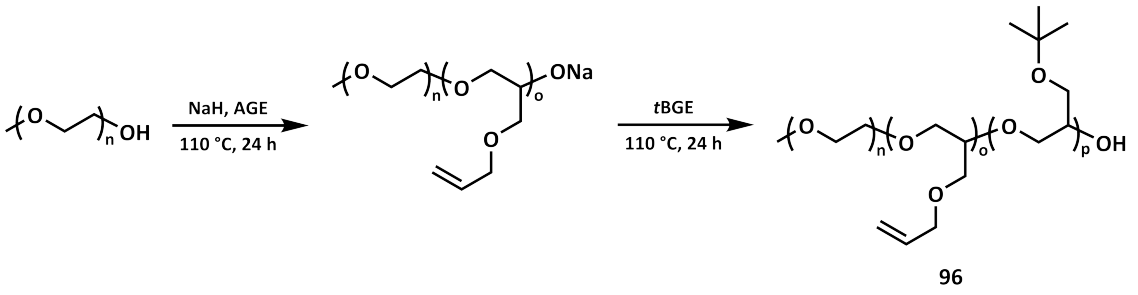

Scheme 2.63: Preparation of poly(ethylene oxide)-*block*-poly(allyl glycidyl ether)-*block*-poly(*tert*-butyl glycidyl ether) (**96**) *via* a sequential anionic ring-opening polymerization.

For worm-like structures in aqueous media, the third block of **96** was increased from a weight fraction of 26% up to 79% in eight approaches using the same macroinitiator with 42 repeating units. Also, similar equivalents of allyl glycidyl ether were added to afford a degree of polymerization between 11 and 15 for the middle block. From SEC measurements in chloroform, narrow molecular weight distributions and similar molar masses were observed for the intermediate diblock copolmers before adding the second monomer. However, higher dispersities of **96** were detected as the length of the hydrophobic block increased as a consequence of the rising viscosity (Table 2.14), and stronger magnetic stirring bars were used to counteract this problem. Moreover, an additional small peak at lower elution volumes is visible in the SEC traces of poly(ethylene oxide), the diblock copolymer intermediate and **96**, which are shown in Figure 2.60. This could be caused by the presence of α,ω-bis-hydroxy poly(ethylene oxide) as an impurity of the used α-methoxy-ω-hydroxy poly(ethylene oxide).[251, 252]

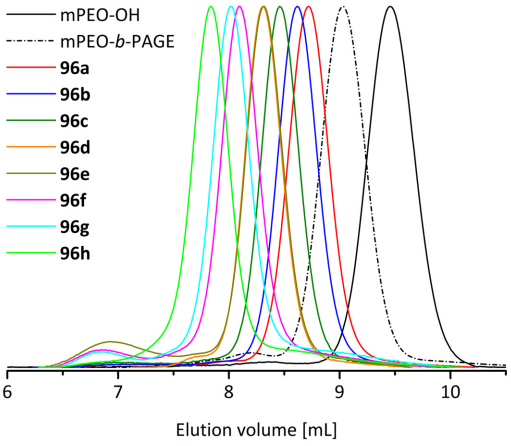

Figure 2.60: SEC elugrams in chloroform of **96** and its precursors.

Table 2.14: SEC data in chloroform of **96** and its precursors.

Polymer	$\overline{M}_n$ [a)]	$Đ$ [a)]
mPEO-OH	1,900 g·mol^{-}	1.04
mPEO-*b*-PAGE	2,600 g·mol^{-1}	1.08
96a	3,000 g·mol^{-}	1.09
96b	3,300 g·mol^{-1}	1.08
96c	3,800 g·mol^{-}	1.11
96d	4,200 g·mol^{-1}	1.04
96e	4,500 g·mol^{-}	1.34
96f	5,100 g·mol^{-1}	1.23
96g	5,200 g·mol^{-}	1.22
96h	6,200 g·mol^{-1}	1.15

[a)] PEO calibration.

The ratio of the allyl group to the *tert*-butyl moiety was determined by NMR spectroscopy. Based on this ratio and 42 repeating units of poly(ethylene oxide), the block lengths were calculated over the proton signals of the polyether backbone. Additionally, the average molar masses of **99** were measured and are given in Table 2.15.

Table 2.15: Calculated data of **96** based on ^{1}H NMR spectra.

Polymer	$\overline{M}_n$	DP[a)]
96a	4,400 g·mol^{-1}	9
96b	5,200 g·mol^{-1}	12
96c	6,100 g·mol^{-1}	23
96d	7,700 g·mol^{-1}	32
96e	8,200 g·mol^{-1}	39
96f	12,700 g·mol^{-1}	71
96g	14,800 g·mol^{-1}	86
96h	16,400 g·mol^{-1}	99

[a)] Determined for the P*t*BGE segment.

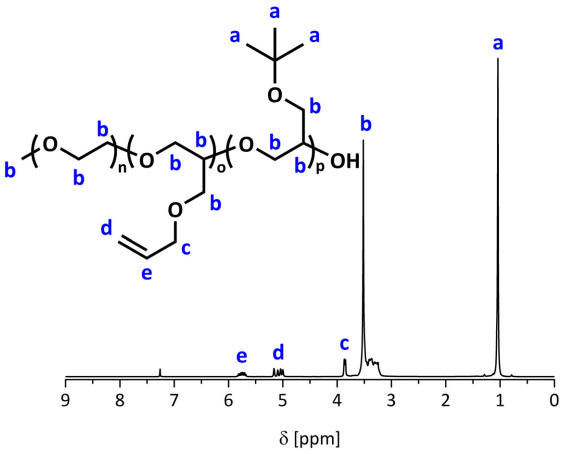

Figure 2.61: ^{1}H NMR spectrum of **96d** in $CDCl_3$.

Aqueous solutions of **96** were prepared by dissolving the polymer in tetrahydrofuran, adding water dropwise, and then evaporation of the organic solvent overnight. The concentrations of the mixtures were adjusted to 1 g·L^{-1} and the self-assembled structures investigated *via* dynamic light scattering and cryo-TEM. By increasing the hydrophobic segment weight fraction from 63 to 88% in poly(allyl glycidyl ether)-*block*-poly(*tert*-butyl glycidyl ether), the hydrodynamic radius increased from 6 nm for polymer **96a** to 32 nm for polymer **96h**. Larger aggregates are also visible in the intensity-weighted CONTIN plot, which scatters the light stronger than smaller objects (Figure 2.62). That results from the scattering cross section, which also depends on the radius of the particle and affects the intensity of scattered light according to $I \sim r^6$.[253]

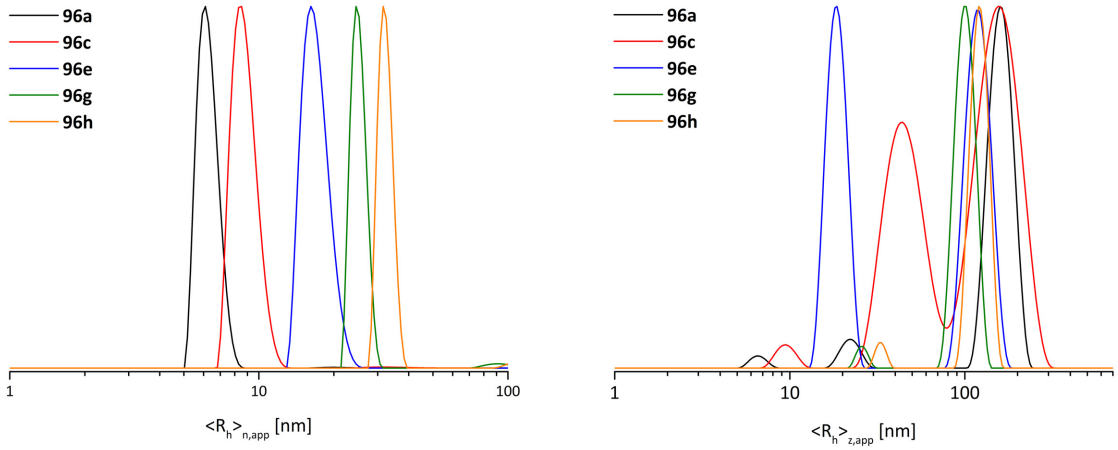

Figure 2.62: Number-weighted (left) and intensity-weighted CONTIN plots (right) of micelles of **96** in water (1 g·L^{-1}) as measured by DLS.

To confirm the spherical shape of the micelles formed by **96f**, **96g** and **96h** in water, the mixtures were subjected to cryo-TEM. A broad size distribution with core diameters of 30 up to 80 nm were visualized for **96h** as spheres (Figure 2.63). For **96f**, the polymer concentration in water was increased from 1.0 to 5.0 g·L^{-1}, and this resulted in the formation of polymersomes. Predominantly spherical micelles were detected at a concentration of

2.5 g·L^{-1} with a few smaller vesicles observed. The direct transition from a spherical shape into a vesicle can indicate that worm-like micelles are not achievable when poly(*tert*-butyl glycidyl ether) is incorporated as the hydrophobic block.

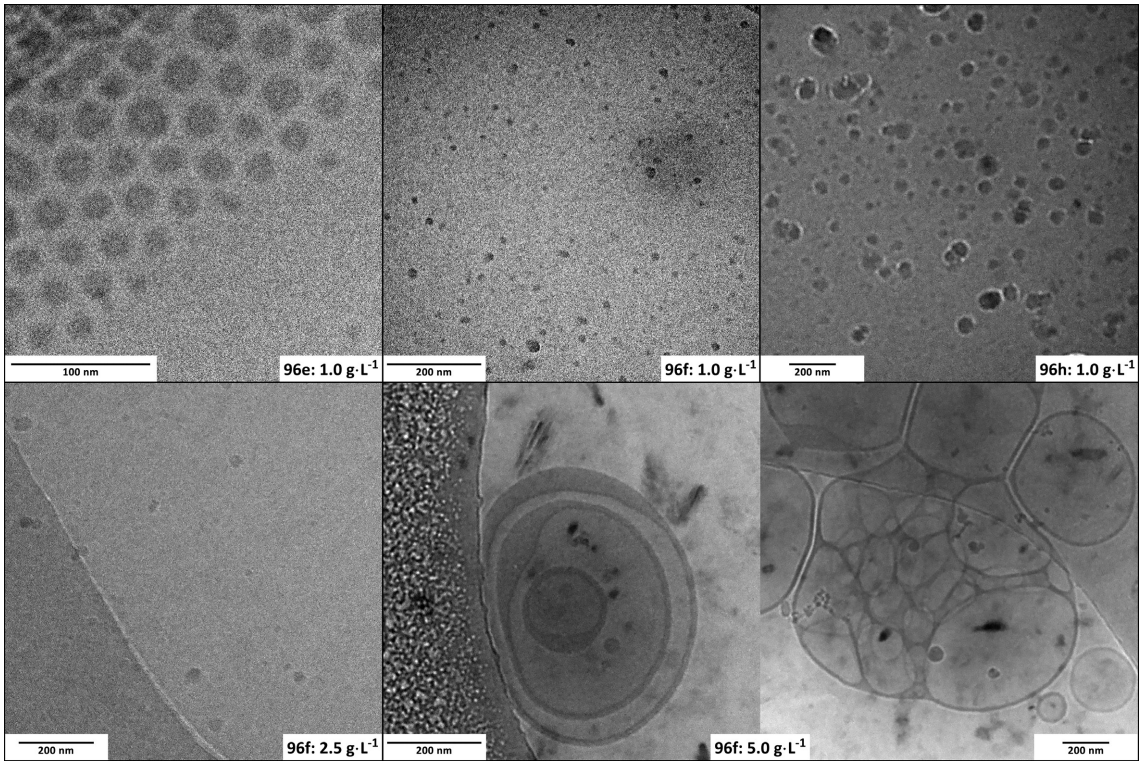

Figure 2.63: Cryo-TEM micrographs of **96e**, **96f** and **96h** with increasing hydrophobic segment in water.

However, **96** was modified *via* a thiol-ene reaction with 3-mercaptopropionic acid and cysteamine to introduce a pH-dependent anionic or cationic charge in the middle segment, which enhances the cellular uptake (Scheme 2.64).[215] The triblock terpolymers were functionalized with the carboxylic acid groups in tetrahydrofuran into **97** with high conversions over 99%, except for **96d** with a conversion of 92%, modified carbon-carbon double bonds. Furthermore, **96a**, **96e** and **96h** were selected for the attachment of cysteamine, and moderate to high degrees of functionalization were obtained for **98**, which decreased for higher block lengths of poly(*tert*-butyl glycidyl ether) from 92 to 56%. This resulted from the different solubilities of the high polar cysteamine in combination with acetic acid and the hydrophobic polymer segments. In contrast to the modification of **96** with amino moieties described in the literature, cysteamine was protonated with acetic acid to prevent radical side reactions of the primary amine.[215] Additionally, the ternary solvent mixture was changed to tetrahydrofuran and methanol, which resulted in an increased degree of functionalization from the reported 50% up to 92% for **96a**. The higher conversion can be explained by retardation in the radical thiol-ene reaction caused by the free electron pair of the amino groups, even at low concentrations of 5 mol%.[254] Herein, the use of acetic acid as an additive leads to a better solubility of cysteamine in tetrahydrofuran than cysteamine hydrochloride, and facilitates its modification.

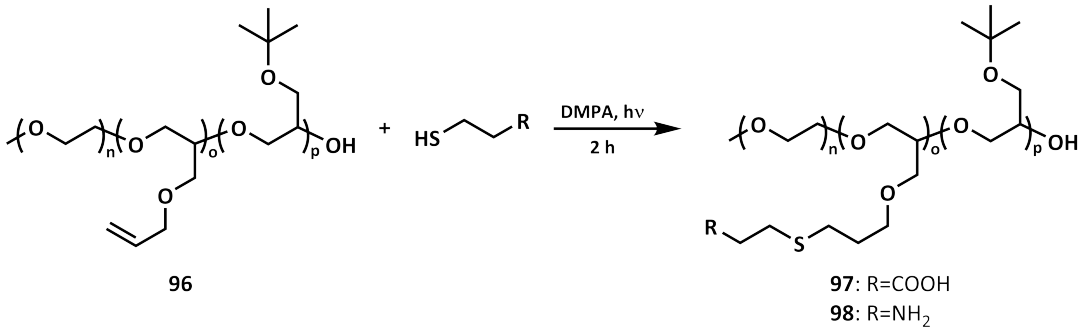

Scheme 2.64: Modification of poly(ethylene oxide)-*block*-poly(allyl glycidyl ether)-*block*-poly(*tert*-butyl glycidyl ether) (**96**) *via* a thiol-ene reaction.

The degree of functionalization was calculated from the ^{1}H NMR spectra, and SEC showed that the dispersities of **97** and **98** after modification of **96** were mostly narrow with values below 1.3 (Table 2.16). Moreover, micelles were prepared with the encapsulated dye Nile red as a model drug to observe the biodistribution of the carrier system *via* fluorescence in cooperation with the University Hospital. The size and ζ-potential of

Table 2.16: Characterization data of the modified poly(ethylene oxide)-*block*-poly(allyl glycidyl ether)-*block*-poly(*tert*-butyl glycidyl ether).

Polymer	Composition	$\overline{M}_n$	$Đ$	DoF[a)]
97a[b)]	PEO_{42}-*b*-$PAGE_{12,COOH}$-*b*-P*t*BGE_9	1,300 g·mol^{-1}	1.09	>99%
97c[b)]	PEO_{42}-*b*-$PAGE_{11,COOH}$-*b*-P*t*BGE_{23}	2,000 g·mol^{-1}	1.12	>99%
97e[b)]	PEO_{42}-*b*-$PAGE_{11,COOH}$-*b*-P*t*BGE_{39}	2,600 g·mol^{-1}	1.24	>99%
97h[b)]	PEO_{42}-*b*-$PAGE_{14,COOH}$-*b*-P*t*BGE_{99}	4,900 g·mol^{-1}	1.48	>99%
98a[c)]	PEO_{42}-*b*-$PAGE_{12,NH_2}$-*b*-P*t*BGE_9	2,200 g·mol^{-1}	1.12	92%
98e[c)]	PEO_{42}-*b*-$PAGE_{11,NH_2}$-*b*-P*t*BGE_{39}	3,300 g·mol^{-1}	1.11	75%
98h[c)]	PEO_{42}-*b*-$PAGE_{14,NH_2}$-*b*-P*t*BGE_{99}	6,100 g·mol^{-1}	1.18	56%

[a)] Determined by ^{1}H NMR, [b)] SEC (THF, PEO calibration), [c)] SEC (chloroform, PEO calibration).

the self-assembled structures in water were measured, and the results are shown in Figure 2.64. The hydrodynamic radii after modification of both products **97** and **98** were reduced from **96** according to dynamic light scattering measurements. The hydrophilic charged shell with electrostatic repulsion led to a lower aggregation number. An increase in the hydrophobic block length from 9 to 99 repeating units resulted in a nearly doubled radius of the functionalized triblock terpolymer micelles. As we predicted, the ζ-potential measurements *via* electrophoretic mobility of the polymer aggregates in water afforded a negative electrical potential for **97**, which is functionalized with carboxylic acid groups, and a positive potential for **98**, which is functionalized with amino moieties. However, the uncharged polymer **96** was also characterized by a negative potential, which is sometimes observed for uncharged polymers containing poly(ethylene oxide) self-assembled in water in the literature.[255–257]

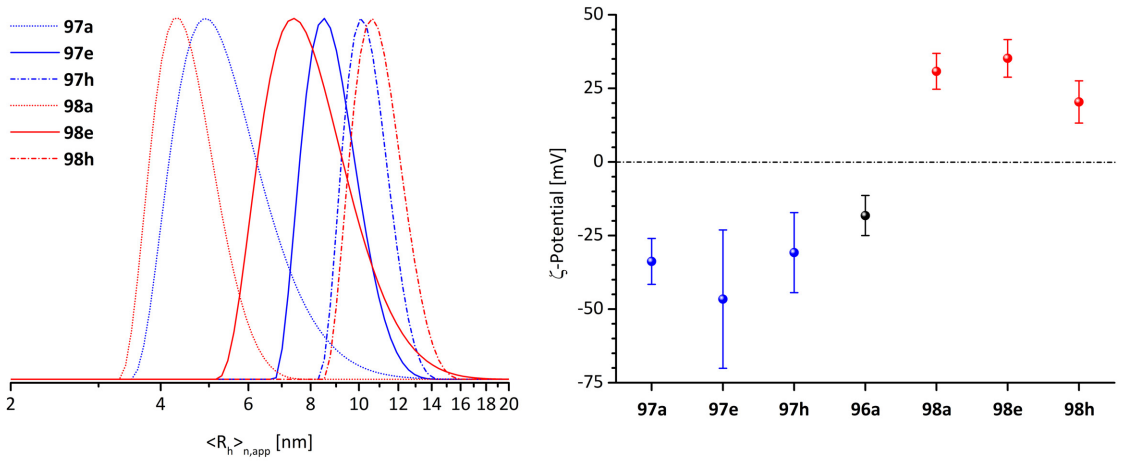

Figure 2.64: Number-weighted CONTIN plots (right) and ζ-potentials of **96** functionalized with carboxylic acids (blue) and amino groups (red) in water (right).

The polymers **97** and **98** that were prepared *via* a thiol-ene reaction of **96** with 3-mercaptopropionic acid and cysteamine can be investigated to explore the size-dependent uptake behavior and loading capacity at different pH values. Furthermore, the micelles of **98** with a cationic shell can be used as a delivery system for oligonucleotides like siRNA as a cargo. In the case of **97c**, S. Miwa and R. Takahashi explored the changes spherical micelles undergo with changes in pH, as well as encapsulation of the model drugs naphthalene, 1-naphthylamine and 1-naphthoic acid.[258, 259] An increase in the pH from 4 to 6 and 8 resulted in a decrease in aggregation number for the micelles due to electrostatic repulsion of the anionic charges in the shell, and a transition in the morphology from spheres into distorted spheroids. The naphthalene-based guest molecules also influence the morphology, changing the shape into polymersomes at a pH of 4. As before, the negative charge in the shell at higher pH values afforded a reduced loading capacity through a decreased aggregation number, and only spherical micelles were detected.

The self-assembly of amphiphilic polymers in selective solvents is driven by interfacial energy, and the smallest interface is reached through the formation of spheres.[260] When the hydrophobic segment of the polymer is more large and voluminous compared to the hydrophilic segment, the packing constraints disfavors spherical micelles and enables the formation of cylindrical or bilayer morphologies.[60] Due to the self-assembly in water of **96** into spheres and polymersomes with increasing poly(*tert*-butyl glycidyl ether) block length and concentrations, other hydrophobic monomers like benzyl glycidyl ether and lauryl glycidyl ether were used to achieve worm-like shapes. In contrast to the spherical shape of the *tert*-butyl groups with a possible high packing, the planar benzyl moieties along the polymer backbone are more bulky and can form π-interactions. Moreover, Raycraft *et al.* modified poly(ethylene oxide)-*block*–poly(β-6-heptenolactone) with 1-mercaptooctane by a thiol-ene reaction to 53% and observed worm-like micelles *via* TEM with 45 repeating units for both block segments.[261] Therefore, lauryl glycidyl ether (**100**) was synthesized as a hydrophobic block with a brush-like structure to obtain cylindrical morphologies at lower degrees of polymerization. Two simple synthetic approaches are commonly used to prepare glycidyl ethers by the conversion of alcohols with epichlorohydrin, and the oxidation of allyl

ethers by the Prileschajew reaction. The separation of lauryl alcohol and lauryl glycidyl ether by column chromatography and distillation is difficult, due to their similar polarity and boiling points as a consequence of the long unpolar alkyl chain. An impurity of lauryl alcohol in **100** will affect the anionic polymerization and a homopolymerization can occur as a side reaction. Herein, **100** was synthesized from lauryl bromide by substitution with allyl alcohol and oxidation as shown in Scheme 2.65 with an overall yield of 50%.

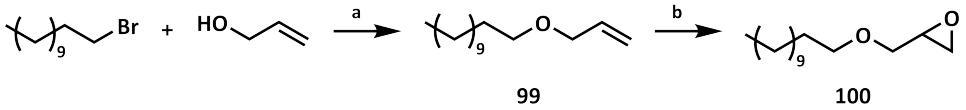

Scheme 2.65: Synthesis of lauryl glycidyl ether (**100**). Conditions: a) KOH, 60 °C, 4 h, 58%. b) *m*CPBA, DCM, 0 °C to RT, 40 h, 87%.[262, 263]

In the first step, allyl alcohol was deprotonated with potassium hydroxide to substitute lauryl bromide, and an additional equivalent was used as solvent. Lauryl allyl ether (**99**) was obtained in a moderate yield, and the purification by column chromatography also afforded unreacted lauryl bromide. To improve the conversion, a phase-transfer catalyst can be added and deprotonation with sodium hydride in solution could lead to higher yields. The oxidation of stearyl allyl ether to an epoxide in high yields using *meta*-chloroperoxybenzoic acid is described in the literature over a long reaction time, and similar conditions were used for the transformation of **99** into **100**.[263] The monomer was purified *via* vacuum distillation and the racemic mixture was analyzed by NMR spectroscopy (Figure 2.65).

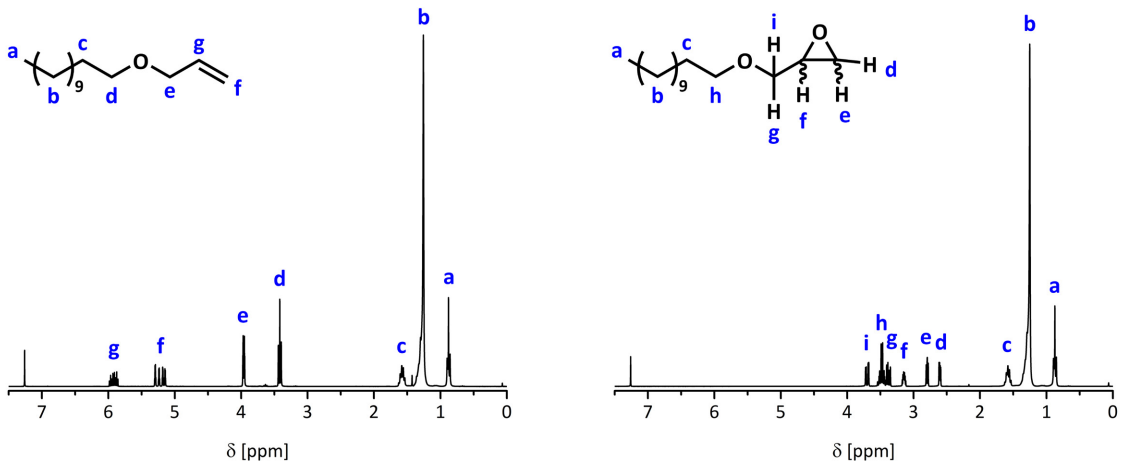

Figure 2.65: ^{1}H NMR spectra of lauryl allyl ether (**99**) (left) and lauryl glycidyl ether (**100**) (right) in $CDCl_3$.

Next, triblock terpolymers were prepared analogous to **96** by a solvent-free sequential anionic ring-opening polymerization at 110 °C using benzyl glycidyl ether and **100** instead of *tert*-butyl glycidyl ether. In the first approach, poly(ethylene oxide)-*block*-poly(allyl glycidyl ether)-*block*-poly(benzyl glycidyl ether) (**101a**) was synthesized by adding approximately 13 equivalents of benzyl glycidyl ether with a dispersity below 1.2. In a second attempt (**101b**), over 50 repeating units of the third block was targeted resulting in a broad molecular weight distribution (Figure 2.66). During the preparation of poly(ethylene

oxide)-*block*-poly(allyl glycidyl ether)-*block*-poly(lauryl glycidyl ether) (**102**), a transfer reaction occurred, and only 11 of the possible 25 units of lauryl glycidyl ether were added. The crude polymer **102** was purified *via* adsorption onto silica, flushing with isopropanol, and finally by desorption as described in the literature.[212]

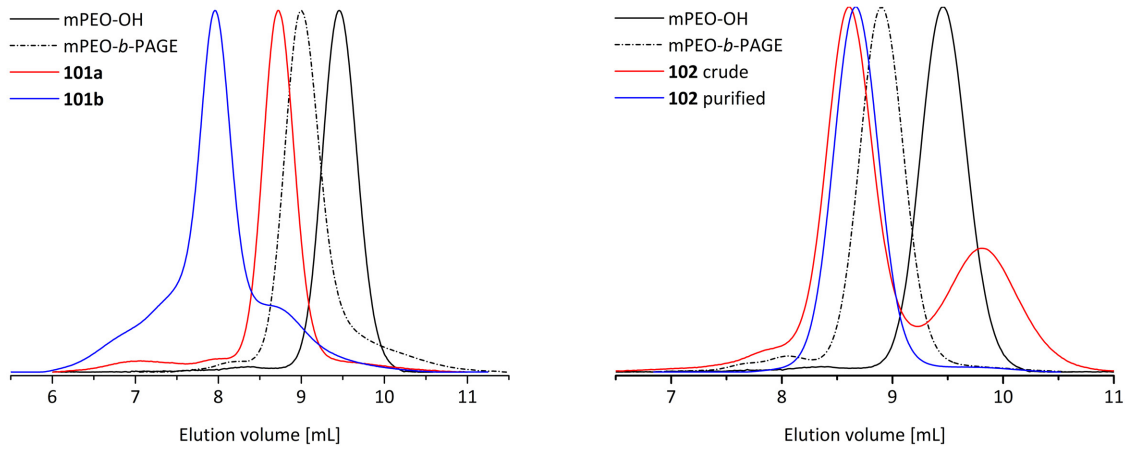

Figure 2.66: SEC elugrams in chloroform of **101a** and **101b** (left) and **102** (right) in comparison to the precursor polymers.

Chain transfer, a side reaction, resulted in both high and low molecular weight byproducts that are visible by SEC (Figure 2.66). The reduced propagation rate of benzyl glycidyl ether and **100** compared to *tert*-butyl glycidyl ether led to an increased probability of the chain transfer reaction by the alkoxide. The oxyanion acts as base and abstracts a proton from the α-position of the epoxide instead of a nucleophilic addition (Scheme 2.66). A new substituted allyloxide as an initiation species is formed, and this results in the formation of a homopolymer.

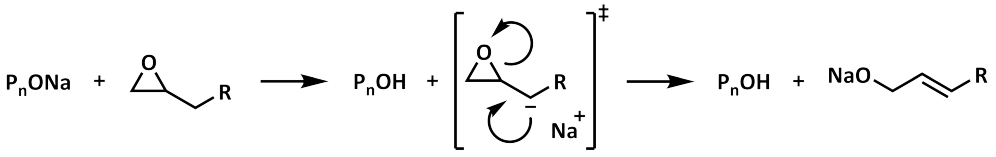

Scheme 2.66: Chain transfer reaction occurring in the anionic ring-opening polymerization of substituted epoxides.[264]

Crown ether can be used as an additive to reduce the aggregation of alkali metal cations and alkoxides of the polymer chain end, which lead to an increase in the reactivity of the anion and a significantly higher propagation rate to suppress the transfer reaction.[264, 265] For *N*,*N*-diethyl glycidyl amine, lauryl and cetyl glycidyl ethers, a solvent-free method with 18-crown-6has been reported, and a modified procedure was attempted.[266, 267] Herein, the polymerizations were carried out in ethylbenzene using potassium hydride to generate the alkoxide initiator of α-methoxy-ω-hydroxy poly(ethylene oxide) in a simpler way, and dibenzo-18-crown-6 was used to enhance the reactivity of the anion (Scheme 2.67). After quenching the reaction with methanol, the polymers were purified *via* dialysis against water and tetrahydrofuran to remove the crown ether, as well as the solvent and monomers with high boiling points.

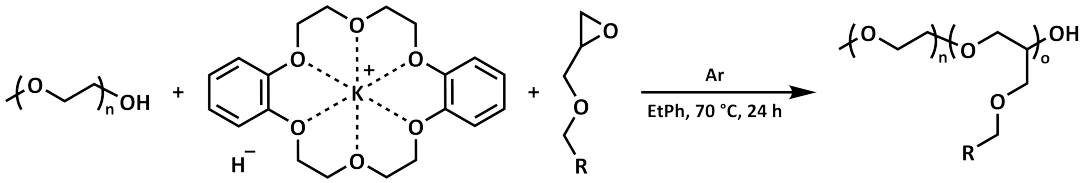

Scheme 2.67: Activated anionic ring-opening polymerization of glycidyl ethers with dibenzo-18-crown-6.

In first attempts, degrees of polymerization between 50 and 85 were targeted to confirm the chosen reaction conditions were suitable. The preparation of **61g**, poly(ethylene oxide)-*block*-poly(benzyl glycidyl ether) (**103a**), poly(ethylene oxide)-*block*-poly(lauryl glycidyl ether) (**104a**), and poly(ethylene oxide)-*block*-poly(allyl glycidyl ether-*co*-benzyl glycidyl ether) (**105**) with dibenzo-18-crown-6 as an additive afforded dispersities below 1.3 at high conversion. In comparison to the non-activated solvent-free anionic ring-opening polymerization of benzyl glycidyl ether and **100**, a chain transfer reaction was not observed in the SEC elugrams shown in Figure 2.67. In comparison to the literature, a nearly two-fold higher degree of polymerization was achieved for **100** with 54 repeating units.[267]

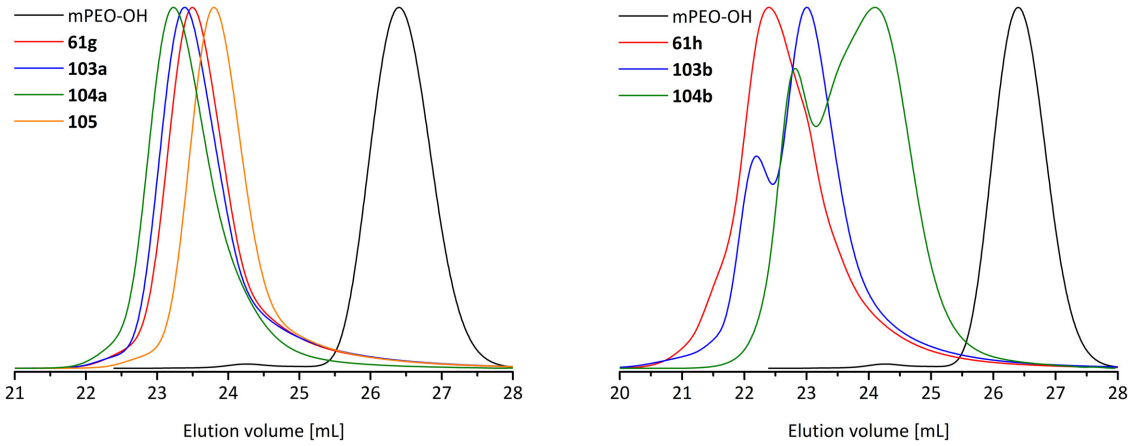

Figure 2.67: SEC elugrams in THF of copolymers **61**, **103**, **104**, **105** and their precursor prepared *via* an activated anionic ring-opening polymerization with less than 100 equivalents (left) and around 500 equivalents (right) of the glycidyl ether.

Next, the monomer to initiator ratio was raised from less than 100:1 up to 500:1 to afford **61h**, **103b** and **104b**. The formation of byproducts through chain transfer reactions were observed again by SEC analysis (Figure 2.67). Molar masses up to 15,000 g·mol^{-1} were achieved by the activated anionic ring-opening polymerization using a crown ether. However, it is not possible to prepare high molecular weight polyethers in a controlled manner *via* this approach. It may be possible to attain up to 150 repeating units upon further optimization without notable side reactions as the results in Table 2.17 indicate.

Table 2.17: SEC data in THF of poly(ethylene oxide)-*block*-poly(glycidyl ether).

Polymer	Composition	$\overline{M}_n$ [a)]	DP[a)]	$\overline{M}_n$ [b)]	$Đ$ [b)]
61g	PEO-*b*-PAGE	11,200 g·mol^{-1}	82	5,300 g·mol^{-1}	1.26
61h	PEO-*b*-PAGE	-	-	10,600 g·mol^{-1}	1.91
103a	PEO-*b*-PBnGE	14,400 g·mol^{-1}	76	5,400 g·mol^{-1}	1.28
103b	PEO-*b*-PBnGE	-	-	8,300 g·mol^{-1}	1.98
104a	PEO-*b*-PLGE	15,000 g·mol^{-1}	54	6,700 g·mol^{-1}	1.22
104b	PEO-*b*-PLGE	-	-	5,200 g·mol^{-1}	1.41
105	PEO-*b*-P(AGE-*co*-BnGE)	9,200 g·mol^{-1}	42:15	4,500 g·mol^{-1}	1.18

[a)] Determined by ^{1}H NMR, [b)] PEO calibration.

The self-assembled structure of the purified block copolymers **102**, **103a** and **104a** in water were analyzed by dynamic light scattering and cryo-TEM. Predominantly cylindrical morphologies and some vesicles were formed from the assembled diblock copolymer **103a** containing benzyl groups, and which were visualized by cryo-TEM (Figure 2.68). Hence, several hydrodynamic radii of 7-17 nm, 45-75 nm and 100-300 nm were detected by dynamic light scattering for the non-spherical micelles and larger aggregates. In contrast, **104a** that consists of long alkyl chains formed polymersomes and some coiled worm-like micelles in water with only large hydrodynamic radii between 220 and 380 nm according to dynamic light scattering. The triblock terpolymer **102**, with a lower polymerization degree of lauryl glycidyl ether than **104a**, and an additional hydrophobic poly(allyl glycidyl ether) segment of a similar length, formed several morphologies. In the cryo-TEM micrographs of **102**, rod and worm-like self-assembled structures are visible, in addition to a few small vesicles and spherical micelles. The cylindrical morphologies were further developed by J. K. Elter using monomers with branched chains and aromatic moieties like 2-ethylhexyl glycidyl ether, 2,3-bis(hexyloxy)propyl glycidyl ether, benzyl glycidyl ether and α-naphthylmethyl glycidyl ether.[268]

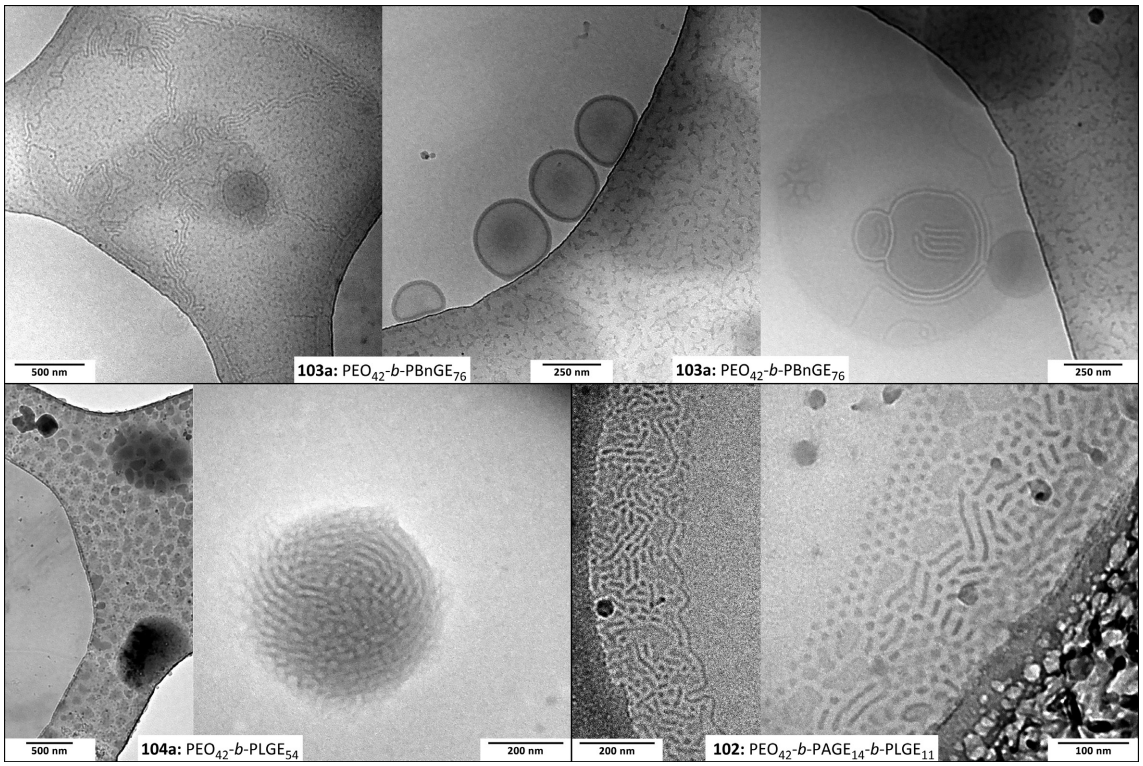

Figure 2.68: Cryo-TEM micrographs of **102** (bottom right), **103a** (upper row) and **104a** (bottom left) in water ($1\,g{\cdot}L^{-1}$).

Crosslinking the polymer micelles is advantageous for use in biomedical applications such as in drug delivery. Such micelles exhibit a higher stability against shear forces in the blood stream and dilution under physiological conditions due to the absence of a critical micelle concentration. Moreover, crosslinked polymeric micelles with encapsulated drugs exhibit an improved pharmacokinetic and biodistribution *in vivo* compared to conventional micelles without a crosslinked core.[269] A disulfide linkage is reversible and can be cleaved under reductive conditions in the intracellular environment, which could enhance the drug release and may lead to a better elimination of the polymer from the body.[270, 271] To cross-link the core of the micelles and to preserve the post-polymerization modification of a poly(allyl glycidyl ether) segment *via* a thiol-ene reaction similar to **96**, a monomer containing a protected thiol was synthesized for anionic polymerization in two steps as shown in Scheme 2.68.

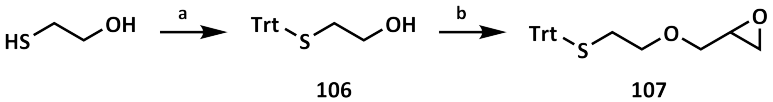

106 **107**

Scheme 2.68: Synthesis of 2-(tritylthio)ethyl glycidyl ether (**107**). Conditions: a) TrtCl, THF, 100 °C, 3 h, 95%. b) ECH, TBAB, KOH, THF, RT, 22 h, 78%.

As described in the literature, 2-mercaptoethanol was reacted with trityl chloride to obtain 2-(trityl)ethanol (**106**) in high yields.[272] Next, **106** was converted into a glycidyl ether with epichlorohydrin, potassium hydoxide and a phase transfer catalyst in tetrahydrofuran as reported for BINOL derivatives.[273] The alcohol was deprotonated and a nucleophilic ring-opening of epichlorohydrin occurred followed by an intramolecular ring-closing S_N2

reaction under elimination of chloride. After purification, **107** was characterized by NMR spectroscopy and the structure was confirmed by X-ray analysis. An additional carbon atom at the epoxide ring is visible in the molecular structure of **107** in Figure 2.69, caused by the racemic mixture. The carbon atom C23A in the molecular structure of **107** belongs to the *S*-enantiomer and C23 to the *R*-enantiomer.

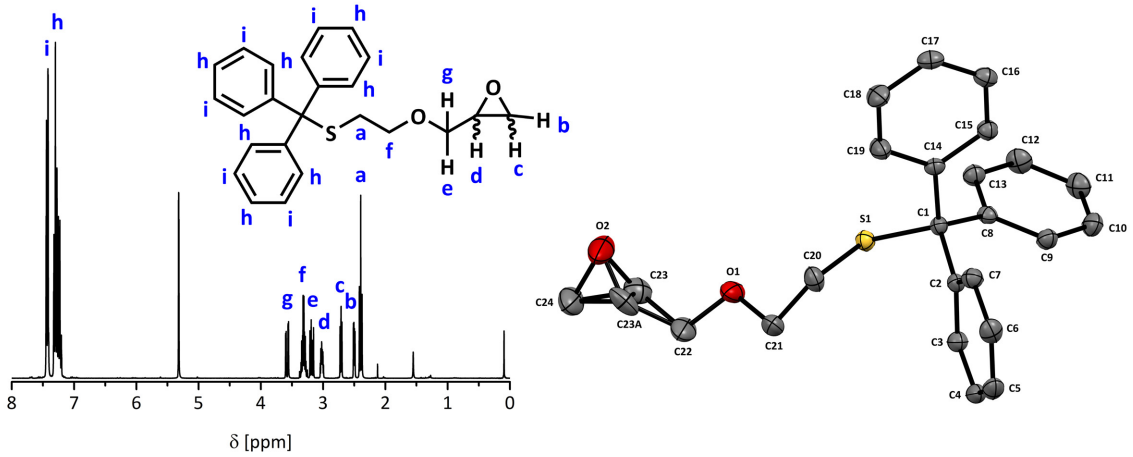

Figure 2.69: ^{1}H NMR spectrum of **107** in CD_2Cl_2 (left) and corresponding molecular structure determined by X-ray analysis (right).

The preparation of poly(ethylene oxide)-*block*-poly(2-(tritylthio)ethyl glycidyl ether) (**108**) *via* an activated anionic ring-opening polymerization with dibenzo-18-crown-6 and approximately 30 equivalents of **107** also resulted in side reactions. The formation of side products was supported by the broad molecular weight distribution observed by SEC analysis (Figure 2.70), and by the change in color of the reaction mixture from colorless to deep purple when the monomer solution was added. The steric hindrance of the trityl group may lead to chain transfer reactions, which could be suppressed by a copolymerization with *tert*-butyl glycidyl ether. A side reaction of the trityl moiety indicated by the purple color can be not excluded, and the polymerization of **107** requires further investigation. Seiwert *et al.* described the anionic copolymerization of 2-(methylthio)ethyl glycidyl ether with a low reactivity.[274] The use of a less bulky protecting group at the thiol could suppress undesired reactions, or a polymerization *via* monomer activated anionic polymerization using triisobutylaluminium can be attempted.

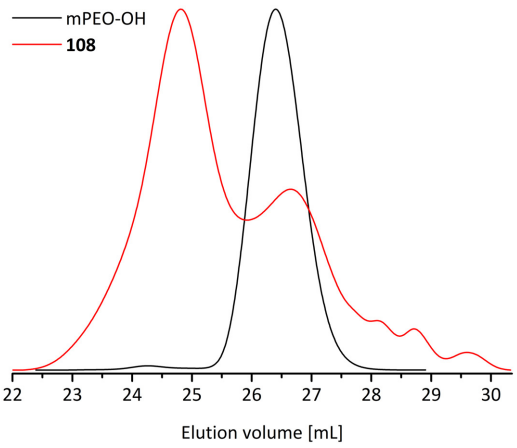

Figure 2.70: SEC elugrams in THF of **108** and its precursor.

Table 2.18: SEC data in THF of **108** and its precursor.

Polymer	$\overline{M}_n$ [a)]	$Đ$ [a)]
mPEO-OH	1,600 g·mol^{-1}	1.03
108	2,100 g·mol^{-1}	1.34

[a)] PEO calibration.

Now that we can successfully prepare polyethers under controlled conditions, the system based on **96** can be further developed for drug delivery by the attachment of targeting moieties for uptake into specific cell types. Additionally, the micelle core can be crosslinked by the incorporation of a functional monomer in the third block to hinder dissociation upon dilution after injection into the body, as well as to stabilize the worm-like morphology. Furthermore, the properties of the carrier such as toxicity, uptake, release of drugs and the elimination of the polymer from the body could be investigated.

3 Conclusion

Polyelectrolytes and polyampholytes are used in many applications as adsorptive materials or as stabilizers for catalysts, and are being developed for use in the biomedical field for drug delivery, biosensors, surface coatings, tissue engineering, and in membrane-based bioseparations.[275] In this thesis, different acrylate-based chargeable polymers with versatile usability and polyether-based block copolymers for drug and gene delivery were investigated.

The first part of this work aimed to prepare polyampholytes with a high charge density with the possibility to further functionalize them similarly to poly(dehydroalanine).[105] Herein, an imidazole moiety was selected as a cationic group that can be modified *via* alkylation, which may be used as a ligand in heterogenous catalysis or as a potential poly(ionic liquid). Yavari and Norouzi-Arasi reported the synthesis of ethyl 2-(imidazol-1-yl)acrylate (**1**) by a triphenylphosphine-mediated nucleophilic addition of imidazole to ethyl propiolate, which was optimized for a larger scale from 2 up to 148 mmol of the starting material.[115] The monomer **1** was free radically polymerized in various solvents. Protonation of the heterocycle resulted in lower molecular weights due to radical transfer to monomer reactions. After purification, the new material, poly(ethyl 2-(imidazol-1-yl)acrylate) (**3**), was converted into either a strong polycation or polyampholytes. The polycation (**4**) was accessed *via* methylation of the imidazole moieties, and the polyampholytes (**5**, **6**) were realized by hydrolyzing the ethyl ester, as well as in combination with alkylation of the imidazole groups (Scheme 3.1).

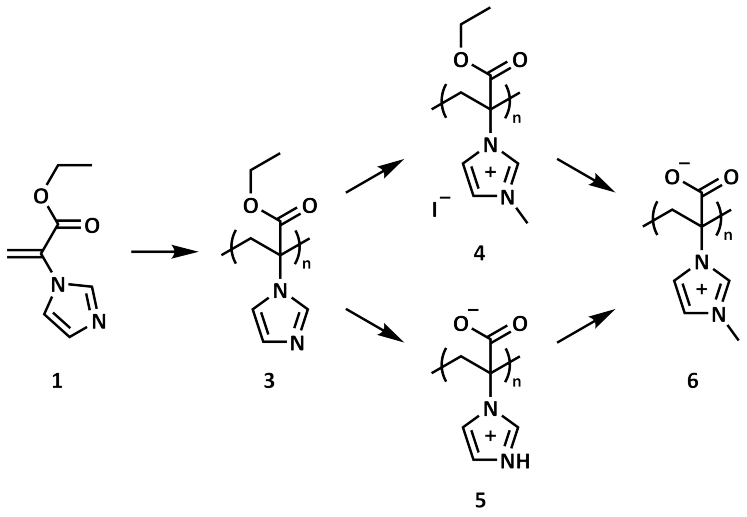

Scheme 3.1: Developed preparation method of poly(ethyl 2-(imidazol-1-yl)acrylate) (**3**) and its subsequent modification.

The two polycations prepared by alkylation of **3** using butyl bromide and benzyl bromide, as well as the polyampholyte poly(2-(3-methylimidazolium-1-yl)acrylate) (**6**), stabilize multi-walled carbon nanotube suspensions in water. Such dispersants of carbon nanotubes are used to prepare electrochemical sensors.[134] Furthermore, poly(2-(imidazolium-1-yl)acrylate) (**5**) was investigated as a pH-responsive coating for magnetic iron oxide nanoparticles by P. Biehl and M. von der Lühe for possible medical applications like drug delivery or hyperthermia.[137, 138]

For the use of **3** and its modifications in heterogeneous catalysis or drug delivery, the preparation of block copolymers containing **1** was attempted *via* RAFT polymerization. The controlled radical polymerization technique was optimized with different chain transfer agents and solvents, as well as by changing the reaction temperature. However, the RAFT polymerization of **1** did not proceed in a controlled manner, achieving high dispersities above 1.6. A kinetic investigation revealed that the monomer exhibited a retarded polymerization through slow reinitiation of the chain transfer agent.

To improve the properties of **3** for desired applications, monomer **1** was varied by altering the substitution position of the imidazole ring, as well as by exchanging the carboxylate ester for a phosphonate ester as shown in Scheme 3.2. The attachment of the imidazole moiety to the polymer backbone at the 2 or 4 positions permits functionalization by alkylation without losing the pH responsivity, and a second functionalization is further possible. Furthermore, an exchange of the carboxylate group by a phosphonate along the polymer results in a higher affinity to metal ions and an increased stability as a coating for metal oxide nanoparticles.

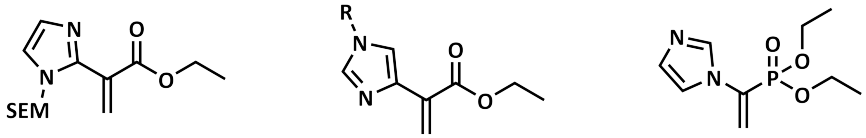

30 **41**: R=Trt **42**: R=SEM **46**

Scheme 3.2: Synthesized monomeric derivatives of ethyl 2-(imidazol-1-yl)acrylate (**1**) that display various benefits in terms of their application.

The monomer ethyl 2-(1-(2-(trimethylsilyl)ethoxy)methylimidazol-2-yl)acrylate (**30**) was synthesized in three steps *via* protection of imidazole, an acylation with acyl transfer, and followed by a Wittig reaction. Additionally, **30** was prepared by cyclization of ethyl 3-ethoxy-3-iminopropionate hydrochloride with aminoacetaldehyde diethyl acetal, protection of the heterocycle, and vinylation using paraformaldehyde. The monomer **30** was identified in the crude product of both synthetic approaches, but could not be isolated for polymerization. A possible reason may be the reactivity of the strong Micheal acceptor interacting with the silica during column chromatography or an autopolymerization. The other variation of **1** with the imidazole attached at position 4 was prepared with a trityl and 2-(trimethylsilyl)ethoxymethyl (SEM) protecting group starting from L-histidine. In contrast to the trityl group with an acidic deprotection, the SEM moiety can also be cleaved under mild conditions using fluoride salts. Selective removal of the

protecting group or hydrolysis of the ester moiety at functional polymers is challenging as the modifications of poly(methyl 2-((*tert*-butoxycarbonyl)amino)acrylate) showed.[276] Ethyl 2-(1-tritylimidazol-4-yl)acrylate (**41**) was synthesized in 5 steps with an overall yield of 6%, and ethyl 2-(1-(2-(trimethylsilyl)ethoxymethyl)imidazol-4-yl)acrylate (**42**) was obtained with a yield of 5% after 6 steps. Whilst the crystalline monomer **41** can be stored at -24 °C over months, **42** autopolymerizes after a few weeks. Both monomers were free radically polymerized achieving high molecular weights over 60,000 g·mol^{-1} according to SEC in *N*,*N*-dimethylacetamide against a PMMA calibration. Such polymers and their derivatives are of high interest in the area of coatings, surfactants, and the binding of metal ions.[98, 107–114] Our substantial progress in the synthesis of these functional monomers (**41** and **42**) has cleared the way for future studies to optimize and polymerize these interesting monomers successfully for use in heterogeneous catalysis.

The final derivative of **1** bearing a diethyl phosphonate group instead of an ethyl ester, diethyl 1-(imidazol-1-yl)vinylphosphonate (**46**), was synthesized in two steps with an overall yield of 11%. First, diethyl ethynylphosphonate (**45**) was prepared from trimethylsilylacetylene as well as ethynylmagnesium bromide with diethyl chlorophosphate similarly as described in the literature.[176, 177] In the second step, **45** was reacted with imidazole and triphenylphosphine, analogous to the synthesis of **1**, to afford the monomer **46**. Poly(diethyl 1-(imidazol-1-yl)vinylphosphonate) was prepared *via* free radical polymerization with an number average molar mass of 125,900 g·mol^{-1} and a broad dispersity of 6.7 according to SEC in chloroform against PMMA standards. Modification of this polymer by ester hydrolysis may be an interesting and ongoing project to obtain a polyampholyte as pH-responsive coating for magnetic iron oxide nanoparticles used in biomedical research. The polyampholyte with its metal affinity can further be applied in the field of water treatment.

For a simpler approach to prepare polyampholytes with a high charge density like **3** or poly(dehydroalanine) under controlled conditions, a modifiable system based on ethyl 2-(hydroxymethyl)acrylate (**48**) was developed using RAFT polymerization. The hydroxy group of the monomer or polymer can be activated and later substituted in a post-polymerization modification by several amines and azoles to obtain the precursor of the polyampholyte (Scheme 3.3).

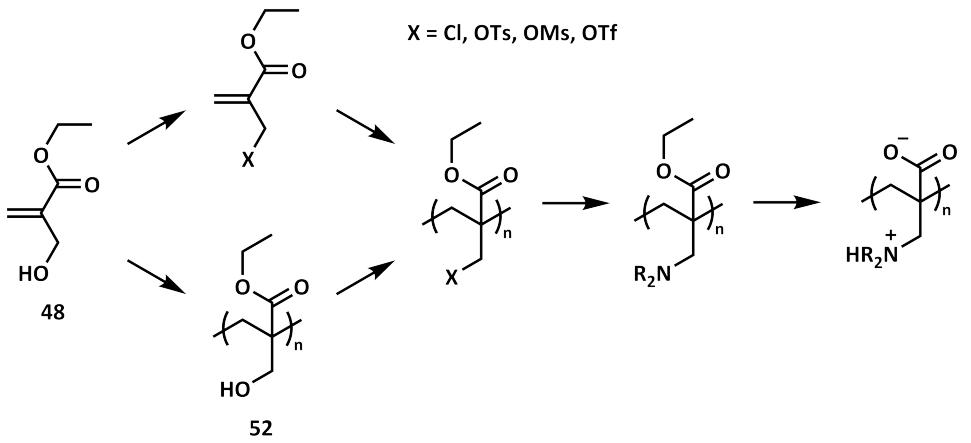

Scheme 3.3: Preparation and modification of an ethyl 2-(hydroxymethyl)acrylate-based system to obtain various polyampholytes.

The synthesis of **48** was achieved by the Morita-Baylis-Hillman reaction of ethyl acrylate and formaldehyde using triethylenediamine as described in the literature.[183] The hydroxy group of **48** was converted into a good leaving group by tosylation using tosyl chloride and chlorination with thionyl chloride. The radical polymerization of ethyl 2-(chloromethyl)acrylate led to radical transfer reactions and the RAFT polymerization of ethyl 2-((tosyloxy)methyl)acrylate resulted in the decomposition of the chain transfer agent as well as high dispersities. Therefore, **48** was polymerized *via* the RAFT technique to obtain homopolymers and diblock copolymers containing a hydrophilic poly(ethylene oxide) segment as well as a hydrophobic poly(*n*-butyl methacrylamide) block. The transformation of poly(ethyl 2-(hydroxymethyl)acrylate) (**52**) into a polyelectrolyte and polyampholyte was attempted by the activation of the hydroxy group using sulfonyl chlorides, followed by substitution with morpholine. From the reaction of **52** with tosyl chloride, only 45-56% of the primary alcohol moieties were effectively transformed due to steric hindrance, whilst the use of mesyl chloride afforded a degree of functionalization of 93%. However, the substitution of the mesylated polymer **52** with morpholine did not succeed, with a conversion of less then 15% of the mesyl groups into tertiary amines according to the ^{1}H NMR spectrum. For a higher degree of functionalization, **52** was reacted with triflyl chloride to obtain a better leaving group along the polymer with an increased nucleophilicity compared to the mesyl moiety. The modification of the triflated polymer with morpholine resulted in a higher degree of functionalization between 30 to 40%. Nevertheless, a further optimization of the polymer-analogous reactions is necessary to obtain a good alternative system to access polyampholytes.

Moreover, polyether-based block copolymers were developed for gene and drug delivery as depicted in Figure 3.1. The polymers were prepared *via* anionic ring-opening polymerization starting from poly(ethylene oxide) monomethyl ether.

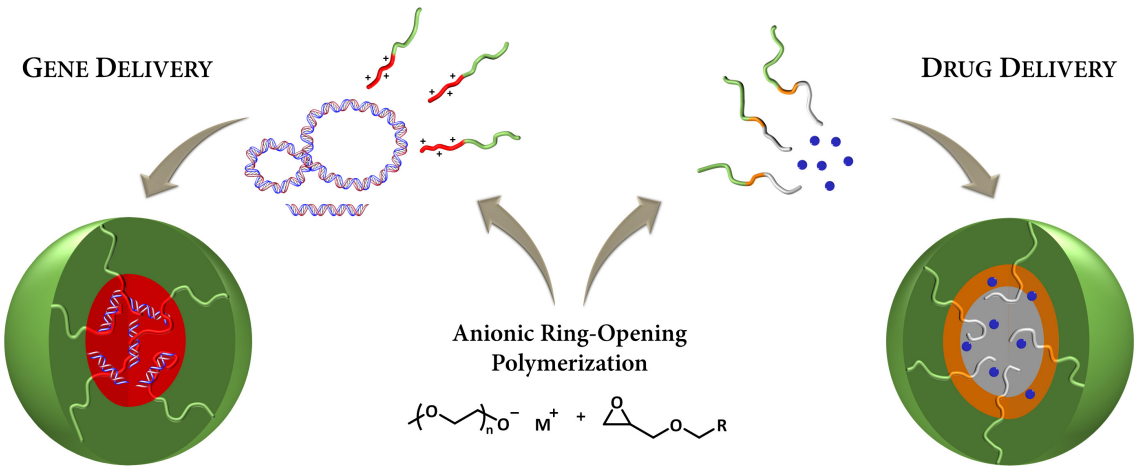

Figure 3.1: Preparation of polyether-based block copolymers and assembled structures for gene and drug delivery.

To deliver genes for the treatment of diseases, diblock copolymers were prepared containing a modifiable poly(allyl glycidyl ether) segment for the attachment of cationic moieties. Herein, poly(ethylene oxide)-*block*-poly(allyl glycidyl ether) (**61**) was prepared with an increasing number in repeating units of the second block of 15, 29, 45, 60, and 76. Cysteamine was used to introduce primary amino groups at the allyl moieties of **61** *via* a thiol-ene reaction. The resulting products were characterized by NMR spectroscopy and size exclusion chromatography. The formed polyplex micelles of pDNA and **61** modified with cysteamine exhibit a higher stability compared to linear poly(ethylene imine) (PEI) and which increases with an increase in the cationic block length. The higher amount of amino groups per polymer chain also led to an increased cytotoxicity. The polyplex micelles formed by pDNA and the prepared block copolymers containing an ionic segment with a degree of polymerization higher than 29 showed an improved uptake into cells in comparison to PEI. The type of cation also has an influence on the properties of the polyplex micelles and their gene delivery behavior. A variety of functional thiols were synthesized to modify **61** and to compare the impact of different nitrogen-based cations on the binding and transfection of nucleic acids. Theophylline, imidazole, guanidine, ethylenediamine, as well as primary, secondary, and tertiary amines were selected as positively chargeable groups. A quaternary ammonium ion was also explored. Besides the commercially available mercaptans, the thiols were generally synthesized by mesylation, substitution with potassium thioacetate and hydrolysis of the thioester starting from the corresponding alcohols. For the attachment of the different cationic moieties, the block copolymer **61** was prepared in a larger scale using dibenzo-18-crown-6 as activator and ethylbenzene as solvent. The modification of **61** with 37 repeating units of allyl glycidyl ether *via* a thiol-ene reaction using the mercaptans succeeded with a degree of functionalization over 99% according to the ^{1}H NMR spectra. One exception is the thiol containing a protected guanidine moiety, and the guanidinylation of **61** modified with primary amines was done using 1-amidinopyrazole. Furthermore, **61** modified with imidazole groups was partially methylated under mild conditions to introduce a permanent charge without loss

of basicity. After characterization of the polyelectrolytes shown in Scheme 3.4, the prepared polycations, as well as PEI as a reference, were used by A. Landmann and D. Hertz to form polyplex micelles with pDNA.

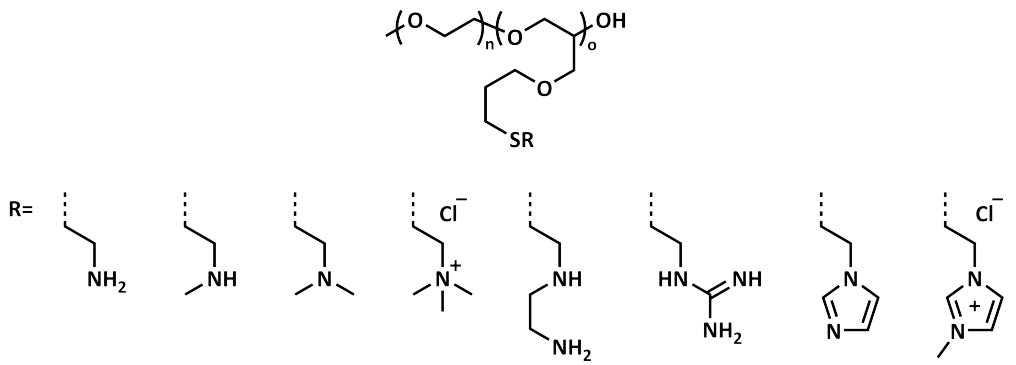

Scheme 3.4: Prepared and investigated polyelectrolytes containing various cationic groups as non-viral vectors for gene delivery.

The investigation of the polyplexes revealed that the ethylenediamine polymer pendent moiety displays the most promising properties to deliver pDNA. The block copolymers **61** modified with guanidine and ethylenediamine groups show a lower cytotoxicity compared to PEI and have the highest affinity to nucleic acid. However, the polyplex micelle of the polymer containing the ethylenediamine moiety exhibit the highest transfection rate of pDNA into cells, whilst the best cellular uptake was observed for the polyplex formed with the secondary amine-modified polymer.

A similar polyether to **61** with a third hydrophobic poly(*tert*-butyl glycidyl ether) block was prepared and modified *via* a thiol-ene reaction by M. Barthel *et al.* for drug delivery.[100, 215] The system was further developed and poly(ethylene oxide)-*block*-poly(allyl glycidyl ether)-*block*-poly(*tert*-butyl glycidyl ether) (**96**) was prepared by sequential anionic ring-opening polymerization. To achieve worm-like structured micelles for an improved cellular uptake, the poly(*tert*-butyl glycidyl ether) block of **96** was raised from 9 up to 99 repeating units. The self-assembled structures of **96** in water were analyzed by dynamic light scattering and cryo-TEM, but only spherical and vesicular morphologies were observed. Nevertheless, the allyl groups of the triblock terpolymers **96** were modified *via* a thiol-ene reaction with 3-mercaptopropionic acid and cysteamine to explore the size-dependent uptake behavior of the nanocarriers. Due to the non-cylindric structures of **96** in aqueous solution, the hydrophobic poly(*tert*-butyl glycidyl ether) segment was replaced by a block of benzyl and lauryl glycidyl ether. The benzyl glycidyl ether is commercially available, whilst lauryl glycidyl ether was synthesized in two steps starting with the etherification of allyl alcohol and lauryl bromide, and followed by the Prilezhaev reaction. Both monomers are less reactive and byproducts were formed during a conventional anionic ring-opening polymerization. Therefore, the polymerization with a more reactive propagating anion was investigated using dibenzo-18-crown-6 as activator to suppress the chain transfer reaction. Two diblock copolymers were prepared using this technique containing a poly(ethylene oxide) segment as well as a poly(benzyl glycidyl ether) or poly(lauryl glycidyl ether) block. These polymers with more than 50 hydrophobic

repeating units self-assembled in water to worm-like and partially vesicular morphologies. Moreover, 2-(tritylthio)ethyl glycidyl ether (**107**) as a cross-linker was synthesized starting from 2-mercaptoethanol by protection of the thiol and substitution with epichlorohydrin. Cross-linking the micellar core improves the pharmacokinetic and biodistribution *in vivo* of the nanocarrier compared to non-cross-linked micelles.[269] However, the activated anionic ring-opening polymerization of **107** resulted in chain transfer reactions and a pure polymer was not obtained. The project of polyethers for drug delivery as micelles with cylindrical morphologies and cross-linked cores was further developed as described in the publication of J. K. Elter *et al.*[268]

4 Zusammenfassung

Polyelektrolyte und Polyampholyte werden in vielen Bereichen eingesetzt wie in Materialien zur Adsorption, als Stabilisator für Katalysatoren, ebenso in biomedizinischen Anwendungen zum Transport von Wirkstoffen, in Biosensoren, als Beschichtungsmaterial, zur Gewebezüchtung oder in Membranen für Stofftrennungen.[275] Die vorliegende Arbeit untersucht verschiedene ionisierbare acrylatbasierende Polymere mit vielseitiger Verwendbarkeit und polyetherbasierende Blockcopolymere zum Transport von Wirkstoffen und Nukleinsäuren.

In der ersten Hälfte der Dissertation wurde die Herstellung von Polyampholyten mit hoher Ladungsdichte und der Möglichkeit zur Funktionalisierung analog zu Poly(dehydroalanin) angestrebt.[105] Dazu ist Imidazol als kationische Gruppe ausgewählt worden, welches durch eine Alkylierung modifizierbar ist. Das alkylierte Polymer könnte als Ligand in der heterogenen Katalyse oder als potentielle polyionische Flüssigkeit genutzt werden. Yavari und Norouzi-Arasi beschrieben die Synthese von 2-(Imidazol-1-yl)acrylsäureethylester (**1**) durch die triphenylphosphanvermittelte nukleophile Addition von Imidazol an Propiolsäureethylester. Diese wurde zur Herstellung im größeren Maßstab ausgehend von 2 auf 148 mmol der Edukte optimiert.[115] Das Monomer **1** wurde in verschiedenen Lösungsmitteln frei radikalisch polymerisiert. Eine Protonierung des Heterozyklus ergab dabei niedrigere Molmassen durch Radikaltransferreaktionen zum Monomer. Nach der Reinigung wurde das neue Material Poly(2-(imidazol-1-yl)acrylsäureethylester) (**3**) entweder zu einem starken Polykation oder zu einem Polyampholyt umgesetzt. Das Polykation (**4**) ist durch die Methylierung des Imidazolringes erhalten worden und die Polyampholyten (**5**, **6**) wurden mittels Hydrolyse des Esters sowie in Kombination mit der Methylierung der Imidazolgruppen hergestellt (Schema 4.1).

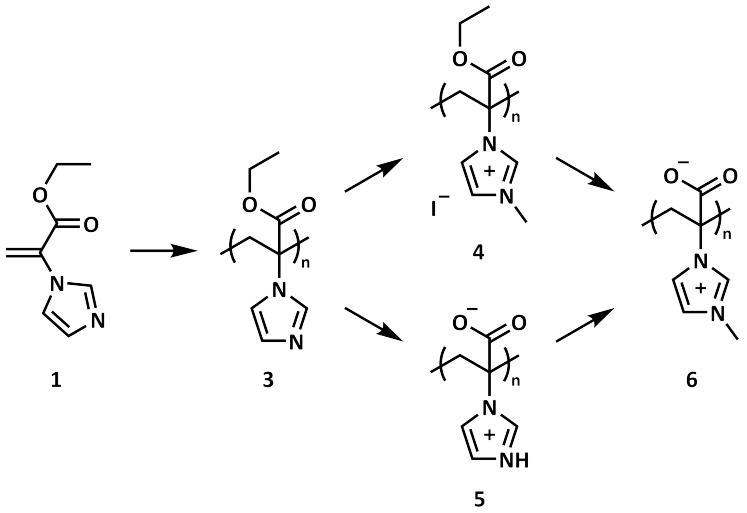

Schema 4.1: Entwickelte Herstellungsmethode von Poly(2-(imidazol-1-yl)acrylsäureethylester) (**3**) und dessen Modifikationen.

Zwei Polykationen, hergestellt durch die Alkylierung von **3** mit Butylbromid und Benzylbromid, und auch der Polyampholyt Poly(2-(3-methylimidazolium-1-yl)acrylat) (**6**) stabilisierten die Suspensionen von Kohlenstoffnanoröhren in Wasser. Solche Dispersionen von Kohlenstoffnanoröhren werden genutzt, um elektrochemische Sensoren herzustellen.[134] Weiterhin wurde Poly(2-(imidazol-1-yl)acrylsäure) (**5**) als pH-responsive Beschichtung von magnetischen Eisenoxidnanopartikeln von P. Biehl und M. von der Lühe für mögliche Anwendungen wie Wirkstofftransport oder Hyperthermie untersucht.[137, 138]

Um das Polymer **3** und dessen Modifikationen für die heterogene Katalyse oder zum Wirkstofftransport zu verwenden, wurde die Herstellung von Blockcopolymeren mit einem Segment des Monomers **1** mittels RAFT-Polymerisation untersucht. Durch Variation der RAFT-Agentien, Lösungsmittel und Reaktionstemperatur ist versucht worden, die kontrollierte radikalische Polymerisation zu optimieren. Jedoch gelang die RAFT-Polymerisation von **1** nicht unter kontrollierten Bedingungen und hohe Polydispersitäten über 1,6 wurden erhalten. Eine kinetische Untersuchung zeigte, dass das Monomer eine Verzögerung in der Polymerisation durch eine langsame Reinitiierung des Kettentransferreagenzes verursacht.

Um die Eigenschaften des Polymers **3** für die gewünschten Verwendung zu verbessern, wurde das Monomer **1** in der Substitutionsposition des Imidazolrings variiert und auch der Carbonsäureester durch einen Phosphonsäureester ersetzt (Schema 4.2). Die Verknüpfung des Imidazolringes an das Polymerrückgrad über die 2- oder 4-Position ermöglicht eine Funktionalisierung durch Alkylierung ohne Verlust der pH-Responsivität sowie eine zweite Funktionalisierung. Der Austausch der Carboxylgruppe durch eine Phosphonatgruppe am Polymer hingegen führt zu einer höheren Affinität zu Metallionen und erhöht dessen Stabilität bei Beschichtung von magnetischen Eisenoxidnanopartikeln.

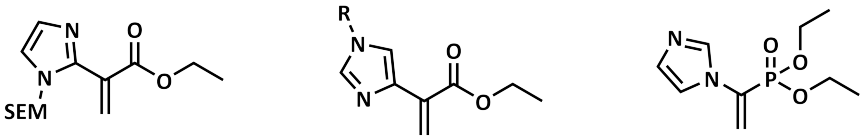

30 **41**: R=Trt **46**
42: R=SEM

Schema 4.2: Synthetisierte Monomerderivate von 2-(Imidazol-1-yl)acrylsäureethylester (**1**), die verschiedene Vorteile im Bezug ihrer Anwendung aufweisen.

Das Monomer 2-(1-(2-(Trimethylsilyl)ethoxy)methylimidazol-2-yl)acrylsäureethylester (**30**) wurde in drei Stufen synthetisiert, angefangen mit der Einführung einer Schutzgruppe am Imidazol, Acylierung mit Acyltransfer und einer Wittig-Reaktion zum Schluss. Zusätzlich wurde **30** über die Zyklisierung von 3-Ethoxy-3-iminopropionsäureethylester mit 2,2-Diethoxyethylamin, Einführung einer Schutzgruppe am Heterozyklus und Olefinierung mit Paraformaldehyd synthetisiert. Das Monomer **30** konnte in den Rohprodukten beider Synthesevarianten identifiziert, aber für eine Polymerisation nicht isoliert werden. Möglicherweise kann die hohe Reaktivität des Michael-Akzeptors ursächlich sein, was eine stärkere Wechselwirkung mit dem Silikagel während der Säulenchromatographie oder einer Autopolymerisation ermöglicht. Die Variante von **1** mit der Substitution des Imidazols an der 4-Position wurde mit einer Trityl- und einer 2-(Trimethylsilyl)ethoxy)methylgruppe (SEM) hergestellt, ausgehend von L-Histidin. Im Gegensatz zu der Tritylgruppe mit saurer Entschützung kann die SEM-Gruppe auch unter milden Bedingungen mit Fluoridionen entfernt werden. Eine selektive beziehungsweise orthogonale Spaltung der Schutzgruppen oder Esterhydrolyse an funktionellen Polymeren kann eine Herausforderung darstellen, wie Modifikationen an Poly(2-((*tert*-butoxycarbonyl)amino)acrylsäuremethylester) gezeigt haben.[276] Das Monomer 2-(1-tritylimidazol-4-yl)acrylsäureethylester (**41**) wurde mit einer Ausbeute von 6% in 5 Stufen synthetisiert und 2-(1-(2-(Trimethylsilyl)ethoxy)methylimidazol-4-yl)acrylsäureethylester (**42**) mit einer Ausbeute von 5% in 6 Stufen. Während das kristalline Monomer **41** bei -24 °C über Monate gelagert werden kann, ist bei dem Monomer **42** eine Autopolymerisation bereits nach einigen Wochen möglich. Beide Monomere wurden frei radikalisch polymerisiert und Molmassen über 60.000 $g \cdot mol^{-1}$ laut Größenausschlusschromatographie (SEC) in *N*,*N*-Dimethylacetamid mit PMMA-Kalibration sind erreicht worden. Solche Polymere und ihre Derivate sind für Forschungen auf den Gebieten der Oberflächenbeschichtung, grenzflächenaktive Substanzen und metallionenbindende Materialien sehr interessant.[98, 107–114] Dies könnte auch zu künftigen Forschungen an den kontrolliert polymerisierten Monomeren **41** und **42** zur Verwendung als Materialien für heterogenen Katalyse anregen.

Das Derivat von **1** mit dem Phosphonsäureester anstatt des Carbonsäureesters, 1-(Imidazol-1-yl)vinylphosphonsäurediethylester (**46**), wurde mit einer Ausbeute von 11% in zwei Stufen synthetisiert. Zunächst ist Ethinylphosphonsäurediethylester (**43**) ausgehend von Trimethylsilylacetylen und Ethinylmagnesiumbromid analog zur Literatur hergestellt worden.[176, 177] Im zweiten Reaktionsschritt wurde **43** mit Imidazol und Triphenylphosphan in gleicher Weise wie bei der Synthese von **1** umgesetzt, um das Monomer **44** zu erhalten. Poly(1-(imidazol-1-yl)vinylphosphonsäurediethylester) ist danach mittels frei

radikalischer Polymerisation mit einer Molmasse von 125.900 g·mol^{-1} und einer Polydispersität von 6.7 gemäß der SEC-Messung in Chloroform mit PMMA-Kalibration hergestellt worden. Eine Modifizierung des Polymers durch Hydrolyse der Estergruppen könnte ein weiterführendes Projekt sein, um den Polyampholyt als pH-responsive Beschichtungen von magnetischen Eisenoxidnanopartikeln für biomedizinische Anwendungen zu erforschen. Darüber hinaus kann der Polyampholyt mit Metallionenaffinität auch auf dem Gebiet der Wasseraufbereitung verwendet werden.

Zur einfacheren Herstellung von Polyampholyten mit hoher Ladungsdichte wie **3** oder Poly(dehydroalanin) mit kontrollierten Polymerisationsmethoden wurde ein modifizierbares System basierend auf 2-(Hydroxymethyl)acrylsäureethylester (**46**) unter der Verwendung der RAFT-Polymerisation entwickelt. Die Hydroxygruppe des Monomers oder der Wiederholungseinheit des Polymers kann aktiviert und danach in einer polymeranalogen Reaktion mit verschiedenen Aminen und Azolen substituiert werden, um die Vorstufe des Polyampholyten zu erhalten (Schema 4.3).

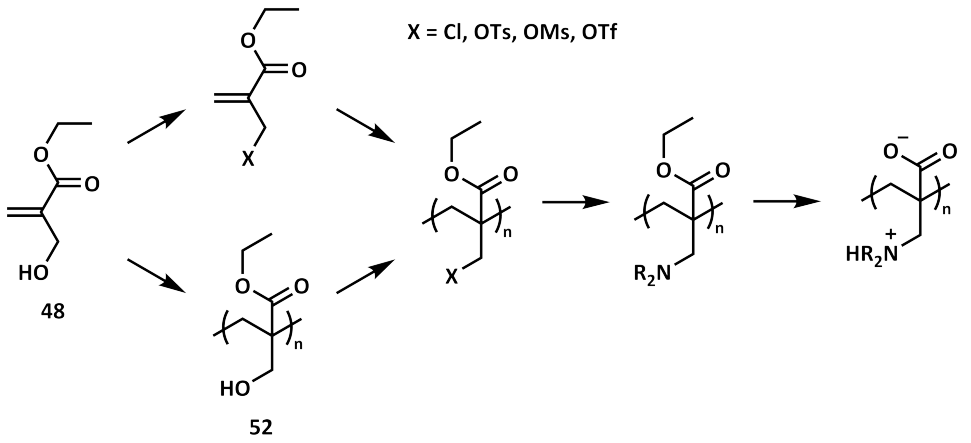

Schema 4.3: Herstellung und Modifizierung des 2-(Hydroxymethyl)acrylsäureethylesterbasierenden Systems zur Herstellung verschiedener Polyampholyte.

Die Synthese von **46** erfolgte durch die Morita-Baylis-Hillman Reaktion von Acrylsäureethylester mit Formaldehyd und Triethylendiamin nach der Literaturvorschrift.[183] Die Hydroxygruppe von **46** wurde durch Tosylierung mit *para*-Toluolsulfonsäurechlorid und Chlorierung mit Thionylchlorid in eine Abgangsgruppe transformiert. Während bei der radikalischen Polymerisation von 2-(Chlormethyl)acrylsäureethylester Radikaltransferreaktionen stattfanden, führte die RAFT-Polymerisation von 2-((Tosyloxy)methyl)acrylsäureethylester zur Zersetzung des Kettentransferreagenzes und einer hohen Molmassenverteilung. Deshalb wurde **46** mit der RAFT-Methode polymerisiert, um Homopolymere und Blockcopolymere mit einem hydrophilen Poly(ethylenoxid) Segment als auch einem hydrophoben Block aus Poly(methacrylsäure-*n*-butylester) zu erhalten. Die Transformation von Poly(2-(hydroxymethyl)acrylsäureethylester) (**50**) in Polyelektrolyte und Polyampholyte wurde mit der Aktivierung der Hydroxygruppe durch Sulfonsäurechloride und anschließender Substitution mit Morpholin versucht. Bei der Reaktion von **50** mit Tosylchlorid konnten nur 45-56% der primären Hydroxygruppen durch die sterische Hinderung umgesetzt, während eine Mesylierung einen Funktionalisierungsgrad von 93% ergab. Jedoch war

die Substitution des mesylierten Polymers **50** mit Morhpolin nicht erfolgreich und weniger als 15% der Mesylgruppen reagierten zu tertiäre Aminen basierend auf dem ^{1}H NMR-Spektrum. Zur Erhöhung des Funktionalisierungsgrades bei der Substitution wurde **50** mit Triflylchlorid umgesetzt, um eine reaktivere Abgangsgruppe mit erhöhter Nukleophilie gegenüber der Mesylgruppe am Polymer zu erhalten. Die Modifizierung des triflierten Polymers mit Morpholin ergab einen höheren Funktionalisierungsgrad von 30-40%. Dennoch ist eine weitere Optimierung der polymeranalogen Reaktion notwendig, damit das System eine gute Alternative zur Herstellung von Polyampholyten darstellt.

Darüber hinaus wurden polyetherbasierende Blockcopolymere für den Transport von Nukleinsäuren und Wirkstoffen entwickelt, wie es die Abbildung 4.1 zeigt. Die Polymere wurden mittels anionischer Ringöffnungspolymerisation ausgehend von α-Methoxy-ω-hydroxy-poly(ethylenoxid) hergestellt.

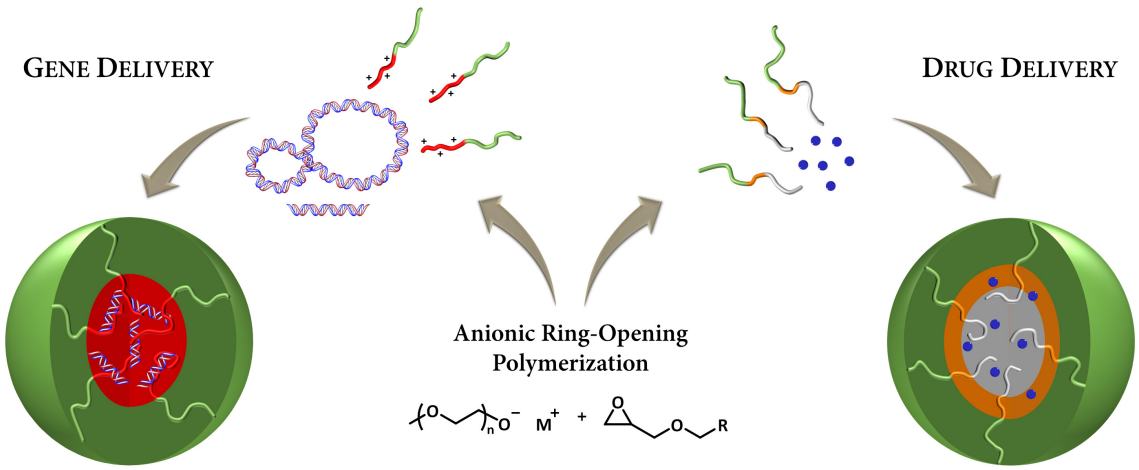

Abbildung 4.1: Herstellung von polyetherbasierende Blockcopolymeren und deren Mizellbildung für den Transport von Nukleinsäuren und Wirkstoffen.

Für den Transport und die Transfektion von Nukleinsäuren zur Behandlung von Krankheiten wurden Diblockcopolymere mit dem modifizierbaren Poly(allylglycidylether)-Segment zur Einführung von kationischen Gruppen verwendet. Dazu ist Poly(ethylenoxid)-*block*-poly(allylglycidylether) (**59**) mit zunehmender Länge des zweiten Blocks von 15, 29, 45, 60 und 76 Wiederholungseinheiten hergestellt worden. Cysteamin wurde verwendet, um primäre Amine an den Allylgruppen der Polymere **59** durch die Thiol-En-Reaktion einzuführen. Die Produkte sind anschließend mittels NMR-Spektroskopie und SEC charakterisiert worden. Die gebildeten Polyplexmizellen aus Plasmid und der mit Cysteamin-modifizierten Polymere **59** zeigten gegenüber dem linearen Poly(ethylenimin) (PEI) eine höhere Stabilität, welche sich mit steigendem kationischem Block erhöht. Eine größere Anzahl an Aminogruppen pro Polymerkette führt allerdings auch zu einem Anstieg der Zytotoxizität. Die gebildeten Polyplexmizellen aus Plasmid und den hergestellten Blockcopolymeren mit einem kationischen Segment, das einen höheren Polymerisationsgrad als 29 besitzt, zeigten im Vergleich mit PEI eine stark verbesserte Aufnahme in die Zellen. Die Art des Kations hat ebenfalls einen Einfluss auf die Eigenschaften der Polyplexmizellen und deren Transport von Nukleinsäuren. Eine Vielfalt an funktionellen Thiolen wurde syn-

thetisiert, um das Polymer **59** zu modifizieren und die Auswirkungen der unterschiedlichen stickstoffbasierenden Kationen auf die Bindung und Transfektion von Plasmid zu vergleichen. Hierbei wurden als positiv ionisierbare Gruppen Theophyllin, Imidazol, Guanidin, Ethylendiamin sowie auch primäre, sekundäre und tertiäre Amine ausgewählt. Auch ein quartäres Ammoniumion konnte untersucht werden. Neben den kommerziell erhältlichen Merkaptanen wurden die Thiole generell aus den entsprechenden Alkoholen durch Mesylierung, Substitution mit Kaliumthioacetat und Hydrolyse des Thioesters synthetisiert. Für die Modifizierung des Polymers mit den unterschiedlichen kationischen Gruppen ist das Blockcopolymer **59** im größeren Maßstab mit Dibenzo-18-krone-6 als Aktivator in Ethylbenzol als Lösungsmittel hergestellt worden. Die Modifizierung von **59**, das 37 Wiederholungseinheiten von Allylglycidylether hat, mit den Merkaptanen erfolgte durch die Thiol-En-Reaktion. Basierend auf den ^{1}H NMR-Spektren gelang die polymeranaloge Reaktion mit hohen Funktionalisierungsgraden über 99%. Eine Ausnahme ist das Thiol mit der geschützten Guanidingruppe und eine Guanidinylierung des mit primären Aminogruppen modifizierten Polymers **59** wurde unter Verwendung von 1-Amidinopyrazol durchgeführt. Weiterhin ist **59** modifiziert mit Imidazolgruppen unter milden Bedingungen nur teilweise methyliert worden, um eine permanente kationische Ladung ohne Verlust der Basizität zu erhalten. Nach der Charakterisierung der Polyelektrolyte, abgebildet im Schema 4.4, wurden die Polykationen und PEI als Referenz zur Bildung von Polyplexmizellen mit Plasmid verwendet.

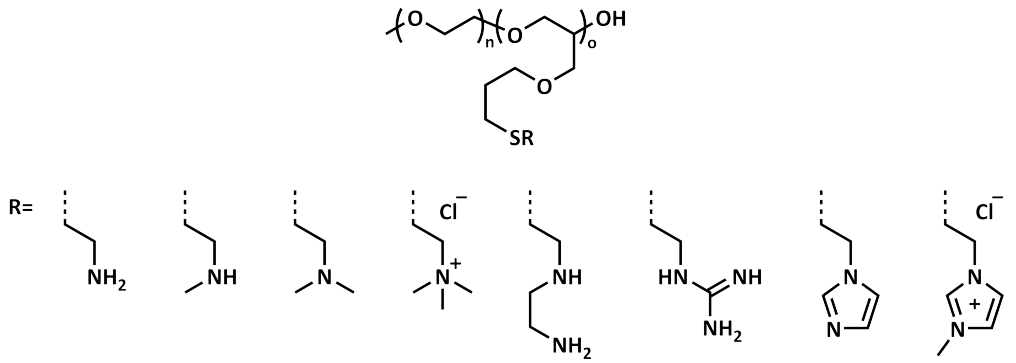

Schema 4.4: Hergestellte und untersuchte Polyelektrolyte als nicht-virale Vektoren für den Transport von Nukleinsäuren.

Die Untersuchung der Polyplexe ergab, dass das Polymer mit den Ethylendiamingruppen die vielversprechendsten Eigenschaften für den Transport von Plasmid besitzt. Die mit Guanidingruppen und Ethylendiamingruppen modifizierten Blockcopolymere zeigten eine geringere Zytotoxizität als PEI und eine höhere Affinität zu den Nukleinsäuren. Jedoch hatte das Plasmid des Polyplexes mit dem Polymer, welches Ethylendiamingruppen enthielt, eine höhere Transfektion in Zellen, während der Polyplex des Polymers mit der Modifizierung von sekundären Aminenen die beste Aufnahme zeigte.

Ein ähnlicher Polyether zu **59** mit einem dritten hydrophoben Poly(*tert*-butylglycidylether)-Segment wurde von M. Barthel *et al.* zum Transport von Wirkstoffen hergestellt und mittels Thiol-En-Reaktion modifiziert.[100, 215] Das Polymersystem wurde weiterentwickelt und Poly(ethylenoxid)-*block*-poly(allylglycidylether)-*block*-poly(*tert*-butylglycidylether)

(**94**) ist durch eine sequenzielle anionische Ringöffnungspolymerisation der Glycidylether gewonnen. Um wurmartige Mizellen mit einer verbesserten Zellaufnahme zu erhalten, wurde der Poly(*tert*-butylglycidylether)-Block von **94** schrittweise von 9 auf 99 Wiederholungseinheiten erhöht. Die in Wasser gebildeten Mizellen sind mit dynamischer Lichtstreuung und Kryotransmissionselektronenmikroskopie analysiert worden, es wurden aber nur sphärische und vesikuläre Morphologien detektiert. Dennoch sind die Allylgruppen des Triblockterpolymers durch die Thiol-En-Reaktion mit 3-Mercaptopropionsäure und Cysteamin modifiziert worden, um das Aufnahmeverhalten in Zellen in Abhängigkeit der Größe des Nanotransporters zu erforschen. Aufgrund der nicht zylindrischen Morphologie der Polymere **94** in Wasser wurde das hydrophobe Poly(*tert*-butylglycidylether)-Segment durch einen Block aus Benzylglycidylether und Laurylglycidylether ersetzt. Während der Benzylglycidylether kommerziell erhältlich ist, wurde der Laurylglycidylether in zwei Stufen synthetisiert, ausgehend von einer Ethersynthese mit Laurylbromid und Allylalkohol, gefolgt von einer Prileschajew-Reaktion. Beide Monomere sind wenig reaktiv, und Nebenprodukte bilden sich bei der konventionellen anionischen Ringöffnungspolymerisation. Deshalb wurde die Polymerisation mit einem reaktiveren Anion am Kettenende mit Dibenzo-18-krone-6 als Aktivator untersucht, um die Kettentransferreaktion zu unterdrücken. Zwei Diblockcopolymere sind mit dieser Methode hergestellt worden, welche aus einem Poly(ethylenoxid)-Segment und entweder einem Poly(benzylglycidylether)-Block oder Poly(laurylglycidylether)-Block bestehen. Diese beiden Polymere mit mehr als 50 Wiederholungseinheiten des hydrophoben Segments bilden in Wasser wurmartige Mizellen und zum Teil vesikuläre Strukturen. Desweiteren wurde 2-(Tritylthio)ethylglycidylether (**105**) als Quervernetzer ausgehend von 2-Mercaptoethanol durch den Schutz des Thiols und Substitution mit Epichlorhydrin synthetisiert. Ein quervernetzter Mizellkern verbessert die Pharmakokinetik und Verteilung des Nanotransporters *in vivo* im Vergleich zu nicht vernetzten Mizellen.[269] Allerdings traten auch bei der aktivierten anionischen Ringöffnungspolymerisation von **105** Kettentransferreaktionen auf und ohne Nebenprodukte wurde das Polymer nicht erhalten. Das Projekt, Polyethern als zylindrische Mizellen mit einem quervernetzten Kern zum Wirkstofftransport zu benutzen, von J. K. Elter *et al.* weiterentwickelt und publiziert.[268]

5 Experimental Section

5.1 Materials

All chemicals were obtained from *Sigma-Aldrich*, *Acros Organics*, *Tokyo Chemical Industry Co., Ltd.*, *ABCR GmbH*, *Alfa Aesar*, *Carbolution Chemicals GmbH*, *Fluorochem Ltd.*, *BLD Pharmatech Ltd.*, *Carl Roth GmbH & Co. KG*, *Grüssing GmbH*, *VWR International*, *Merck KGaA*, *AppliChem GmbH*, *Th.Geyer GmbH & Co. KG*, *Boron Molecular Pty Limited*, *Strem Chemicals Inc.* or *Rapp Polymere GmbH* and used without further purification unless otherwise stated. All deuterated solvents were obtained from *Deutero GmbH*.

Azobisisobutyronitrile was recrystallized from cold methanol, dried under vacuum and stored at -24 °C. α-Methoxy-ω-amino poly(ethylene oxide) (2,000 g·mol^{-1}) was dried *via* azeotropic distillation from dry toluene under reduced pressure.

α-Methoxy-ω-hydroxy poly(ethylene oxide) (2,000 g·mol^{-1}) was purified by precipitation in diethyl ether, azeotropic distillation from dry toluene under reduced pressure and drying at 110 °C under vacuum. The white crystals were stored under an argon atmosphere. Allyl glycidyl ether, benzyl glycidyl ether, *tert*-butyl glycidyl ether and lauryl glycidyl ether were dried over calcium hydride under an argon atmosphere overnight, distilled under reduced pressure and stored at -30 °C before use. For anionic polymerizations and purification of potassium hydride cyclohexane, ethylbenzene, and tetrahydrofuran were refluxed over sodium with benzophenone under an argon atmosphere before being distilled. Potassium hydride was purified under an argon atmosphere by decantation of paraffin and washing the solid several times with dry cyclohexane. The white powder was dried under vacuum and stored under an argon atmosphere.

Dowex® 50WX8 ion-exchange resin (100-200 mesh) was treated analogously to the literature[222] before use. Therefore, 100 g Dowex® 50WX8 was stirred in 0.5 L of acetone for 5 minutes, filtered and washed with acetone (0.8 L), methanol (0.5 L), 6 M hydrochloric acid (0.5 L) and water (1.0 L). The ion-exchange resin was dried under vacuum and stored.

5.2 Instruments and Methods

Nuclear magnetic resonance spectroscopy

^{1}H NMR and proton decoupled ^{13}C NMR spectra were recorded either on an Avance I spectrometer (250 MHz) equipped with a broadband observe probe, a Fourier spectrometer (300 MHz) equipped with a dual ^{1}H/^{13}C probe, an Avance I spectrometer (300 MHz) equipped with a dual ^{1}H/^{13}C probe, or an Avance III spectrometer (400 MHz) equipped with a broadband fluorine observe probe from the *Bruker Corporation*. Chemical shifts are given in parts per million and referenced to the residual signal of the deuterated solvent.[277, 278] To enhance the resolution of the ^{1}H NMR spectra the FID was extended to the doubled amount of data points by zero filling, multiplied by a sine bell apodization function and a Fourier transform performed.

Proton decoupled ^{19}F NMR and ^{31}P NMR spectra were recorded on an Avance III spectrometer (400 MHz) equipped with a broadband fluorine observe probe operating at a fluorine frequency of 377 MHz and phosphorus frequency of 162 MHz from the *Bruker Corporation*.

Proton decoupled ^{13}C solid-state magic angle spinning NMR spectra were acquired utilizing cross polarization with a contact time of 2 ms and a spinning frequency of 15 kHz. All data were collected on an Avance III HD spectrometer (400 MHz) from the *Bruker Corporation* equipped with a 4 mm dual channel probe. The sample temperature was set to 300 K. The carbon chemical shifts were referenced externally, setting the high-frequency (methylene) signal of adamantane to 38.5 ppm.[279]

Mass spectrometry

Electron ionization mass spectra were performed on a SSQ 710 single quadrupole mass spectrometer from *Finnigan MAT*. The sample was inserted into the instrument using a direct evaporation probe equipped with a rhenium wire. The sample was heated and ionized by electron ionization with an energy of 70 eV. The mass-to-charge ratio was monitored between 20 and 500.

Ultra high performance liquid chromatography coupled with high resolution mass spectrometry was carried out using an UltiMate 3000 UHPLC system from *Thermo Fisher Scientific Inc.* equipped with a column compartment TCC-3200, an HPG-3400 RS binary pump, a WPS-3000 autosampler set to 10 °C, a 25 μL injection syringe and a 100 μL sample loop. A gradient of solution A and B (Table 5.1) were used as eluent at a flow rate of 0.4 mL·min^{-1} on an Accucore^{TM} C18 LC column (2.6 μ, 100 × 2.1 mm) from *Thermo Fisher Scientific Inc.* at 25 °C. Mass spectra were recorded with a Q exactive plus orbitrap mass spectrometer from *Thermo Fisher Scientific Inc.* coupled to a heated electrospray source. The column flow was switched at 0.5 min from waste to the mass spectrometer, and back again at 11.5 min to the waste to prevent source contamination. For monitoring, a full scan mode was selected with the following parameters. Polarity: positive, scan range from 100 to 1500 mass-to-charge ratio, resolution of 280,000, AGC target of $3{\cdot}10^{6}$ and maximum IT of 200 ms. General settings: sheath gas flow rate of 60, auxiliary gas flow

rate of 20, sweep gas flow rate of 5, spray voltage of 3.0 kV, capillary temperature of 360 °C, S-lens RF level of 50, auxiliary gas heater temperature of 400 °C, and an aquisition time frame of 0.5-11.5 min.

Table 5.1: Eluent mixtures of solution A and B used for UHPLC.

Time	0.0 min	0.2 min	8.0 min	11.0 min	11.1 min	12.0 min
Solution A[a)]	100%	100%	0%	0%	100%	100%
Solution B[b)]	0%	0%	100%	100%	0%	0%

[a)] Water with 2% acetonitrile and 0.1% formic acid, [b)] Acetonitrile with 0.1% formic acid.

Elemental analysis

The elemental composition was determined with an Euro EA - CHNS Elemental Analyser from the *HEKAtech GmbH*. The halogen content was determined by Schöniger oxidation using a TitroLine *alpha plus* from *SI Analytic GmbH*.

X-ray crystallography

The intensity data was collected on a *Nonius* Kappa CCD diffractometer using graphite-monochromated Mo-Kα radiation. The data was corrected for Lorentz and polarization effects, absorption was taken into account on a semi-empirical basis using multiple-scans.[280–282] The structure was solved by direct methods (SHELX[283]) and refined by full-matrix least squares techniques against Fo^2 (SHELXL-97[283]). All hydrogen atoms were located by difference Fourier synthesis and refined isotropically. Mercury[284] was used for structure representations.

Size exclusion chromatography

SEC in water was performed on a *Jasco* system equipped with a PU-980 pump and a RI-930 refractive index detector. Water with 0.3% trifluoroacetic acid and 0.1 M sodium chloride was applied as eluent at a flow rate of 1 mL·min^{-1} on a PSS SUPREMA-MAX 300 Å column (10 μm particle size) and the column oven was set to 30 °C. The system was calibrated with poly(2-vinylpyridine) standards (1,300-81,900 g·mol^{-1}) from *Polymer Source, Inc.*

SEC in *N*,*N*-dimethylacetamide was performed on an *Agilent 1200* system equipped with a G1310A pump, a G1362A refractive index detector, and both a PSS GRAM 30 Å and a PSS GRAM 1,000 Å column (10 μm particle size) in series. *N*,*N*-Dimethylacetamide with 2.1 g·L^{-1} of lithium chloride was applied as eluent at a flow rate of 1 mL·min^{-1} and the column oven was set to 40 °C. The system was calibrated with poly(methyl methacrylate) standards (505-981,000 g·mol^{-1}) and poly(ethylene oxide) standards (440-969,700 g·mol^{-1}) from *PSS Polymer Standards Service GmbH*.

SEC in tetrahydrofuran was performed on an *Agilent 1260 Infinity* system equipped with a G1310B pump, a G1315D refractive index detector, and three PSS SDV 100 Å, PSS SDV 1,000 Å and PSS SDV 100,000 Å columns (5 μm particle size) in series. Tetrahydrofuran was applied as eluent at a flow rate of 1 mL·min^{-1} and the column oven was set to 40 °C. The

system was calibrated with poly(methyl methacrylate) standards (400-2,200,000 g·mol^{-1}) and poly(ethylene oxide) standards (238-969,000 g·mol^{-1}) from *PSS Polymer Standards Service GmbH*.

SEC in chloroform was performed on a *Shimadzu* system equipped with a SCL-10A system controller, a LC-10AD pump, and a RID-10A refractive index detector. A solvent mixture of chloroform, triethylamine, and isopropyl alcohol (94/4/2) was applied as eluent at a flow rate of 1 mL·min^{-1} on a PSS SDV linear S column (5 μm particle size) and the column oven was set to 40 °C. The system was calibrated with poly(ethylene oxide) standards (440-44,700 g·mol^{-1}) from *PSS Polymer Standards Service GmbH*.

Dynamic light scattering

DLS was performed on a CGS-3 compact goniometer system from *ALV-Laser Vertriebsgesellschaft mbH* equipped with a LSE-5004 correlator and a He–Ne laser 1145/P from the *JDS Uniphase Corporation* operating at an excitation wavelength of 633 nm. The samples were measured at a scattering angle of 90° in a toluene bath connected to an Eco silver thermostat from *LAUDA Dr. R. Wobser GmbH & Co. KG* set to 25 °C. The CONTIN algorithm was applied to analyze the obtained correlation functions. The apparent hydrodynamic radii were calculated according to the Stokes–Einstein equation using ALV-correlator software version 3.0. All CONTIN plots are number-weighted.

Cryogenic transmission electron microscopy

Cryo-TEM was performed at an acceleration voltage of 200 kV on a Tecnai G^2 20 cryo-transmission electron microscope from *FEI Company* equipped with a 4k × 4k Eagle HS CCD and a 1k × 1k Olympus MegaView camera. QUANTIFOIL® R 3.5/1 on 400 mesh copper grids from *Quantifoil Micro Tools GmbH* were cleaned using an argon plasma treatment for 120 s before 8.5 μL of the samples were blotted using a Vitrobot Mark IV from the *FEI Company*. The samples were plunge-frozen in liquid ethane and stored under nitrogen before being transferred to the microscope utilizing a Gatan transfer stage.

Thermogravimetric analysis

TGA was performed on a TGA 8000^{TM} Thermogravimetric Analyzer from *PerkinElmer, Inc.* under a nitrogen atmosphere at a heating rate of 10 K·min^{-1} from 30 to 800 °C.

Zeta potential

Zeta potential measurements were performed on a Zetasizer Nano ZS from *Malvern Instruments GmbH* using the M3-PALS technique with a 633 nm laser beam at a detection angle of 135°.

Glovebox

Anionic ring-opening polymerizations of glycidyl ethers were carried out in an UNIlab Pro SP Workstation from *M. Braun Inertgas-Systeme GmbH* equipped with a MB-TFT70 touch panel, an integrated freezer set to -30 °C, a gas purifier, a solvent filter and a particle filter under an argon atmosphere. Reaction mixtures were heated in a copper bath.

Lyophilisation

Aqueous solutions of polymers were freeze-dried on an Alpha 1-2 LDplus device from *Martin Christ Gefriertrocknungsanlagen GmbH* at 37 mbar with an ice condenser temperature of -58 °C.

Solvent purification system

Dry acetonitrile, dichloromethane, tetrahydrofuran and toluene were obtained using a PureSolv-EN^{TM} solvent purification system from *Innovative Technology, Inc.* under an argon atmosphere using activated aluminia as a drying agent. Dry cyclohexane, diethyl ether, *N*,*N*-dimethylformamide, ethanol and methanol were obtained using an SPS-800 solvent purification system from *M. Braun Inertgas-Systeme GmbH* under a nitrogen atmosphere using activated aluminia as a drying agent.

Ultrapure water

A MicroPure UV water system equipped with a UV photo-oxidation at 185/254 nm from *TKA Wasseraufbereitungssysteme GmbH* was used to obtain ultrapure water with a conductivity less than 0.07 μS·cm^{-1}.

UV irradiation

Reactions carried out under ultraviolet light were performed in a UVACUBE 100 from *Dr. Hönle AG* that houses a mercury lamp (100 W) under stirring.

Centrifugation

Precipitated polymers were collected by centrifugation using a Heraeus Megafuge 8 Centrifuge from *Thermo Fisher Scientific Inc.* at 8,000 rpm for 5 minutes.

Dialysis

Spectra/Por® 6 standard regenerated cellulose dialysis tubing with a nominal molecular weight cut-off of 1 kDa from *Spectrum Laboratories, Inc.* were used to purify polymers. The membranes were stirred for 30 minutes in ultrapure water to remove sodium azide and then loaded with the crude polymer solution.

Thin layer chromatography

Aluminium sheets coated with silica gel 60 F254 (*Merck KGaA*) were used for thin layer chromatography. The detection was carried out using ultraviolet light (254 or 365 nm) or by staining with an aqueous potassium permanganate solution (0.1 M) and subsequent heating.

Column chromatography

The purification of crude products by column chromatography was performed using silica gel 60 (particle size of 40-63 μm) from *Macherey-Nagel GmbH & Co. KG* as the stationary phase. Before using dichloromethane, methanol, or tetrahydrofuran as eluents, the stabilizer and impurities were removed by distillation.

Preparation of micellar solutions

To a solution of amphiphilic polymer (40-25 $g \cdot L^{-1}$) in tetrahydrofuran, in combination with a dye if required, double the volume of ultrapure water was added dropwise and stirred overnight in open vessels. The desired polymer concentration was adjusted with ultrapure water and the mixture was filtered using a Nylon syringe filter with a pore size of 1 μm.

Preparation of polyplex micelles and their investigation

The preparation of polyplex micelles and their investigation by ethidium bromide displacement assay, heparin competition assay, 3-(4,5-dimethylthiazol-2-yl)-2,5-diphenyltetrazolium bromide assay, as well as uptake and transfection were performed by D. Hertz and A. Landmann according to a procedure described in the literature.[285]

5.3 Synthesis of Ethyl 2-(imidazol-1-yl)acrylate (1)

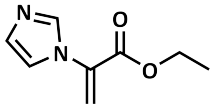

Ethyl 2-(imidazol-1-yl)acrylate was prepared by a modified literature procedure.[115]
To a solution of imidazole (10.093 g, 148.25 mmol) in dichloromethane (350 mL), ethyl propiolate (15.0 mL, 148.01 mmol, 1.00 eq.) was added at -15 °C and cooled to -30 °C. A solution of triphenylphosphine (38.701 g, 147.55 mmol, 1.00 eq.) in dichloromethane (80 mL) was added dropwise and the reaction mixture was allowed to warm to room temperature overnight. After 20 hours, the mixture was concentrated under reduced pressure and purified by column chromatography (DCM, followed by EA) to afford 18.706 g ethyl 2-(imidazol-1-yl)acrylate (75%) as a yellow oil, which crystallized at -24 °C.

TLC: R_f = 0.25-0.00 (DCM), 0.58-0.32 (EA).

^{1}H NMR (400 MHz, CD_2Cl_2, 25 °C): δ = 1.34 (t, 3 H, J = 7.1 Hz), 4.32 (q, 2 H, J = 7.1 Hz), 5.83 (d, 1 H, J = 1.1 Hz), 6.26 (d, 1 H, J = 1.1 Hz), 7.04 (dd, 1 H, J = 1.4, 0.9 Hz), 7.15 (t, 1 H, J = 1.4 Hz), 7.70 (dd, 1 H, J = 1.3, 1.0 Hz) ppm.

^{13}C NMR (101 MHz, CD_2Cl_2, 25 °C): δ = 14.4, 62.8, 119.2, 120.0, 135.0, 137.6, 162.7 ppm.

Ethyl 2-(imidazol-1-yl)acrylate was prepared using a reduced amount of triphenylphosphine and additives by a modified literature procedure.[115, 116]
To a solution of imidazole (0.5 M) in dichloromethane, ethyl propiolate (1.0 eq.), sodium acetate (0.5 eq.) and acetic acid (0.5 eq.) were added at 0 °C. A solution of triphenylphosphine in dichloromethane (1.0 M) was added dropwise and the reaction mixture was allowed to warm to room temperature overnight. After 22 hours, the mixture was concentrated under reduced pressure and purified by column chromatography (DCM, followed by EA) to afford ethyl 2-(imidazol-1-yl)acrylate as a yellow oil.

Table 5.2: Synthesis of ethyl 2-(imidazol-1-yl)acrylate under varied conditions.

Entry	Imidazole	Triphenylphosphine	Yield
1[a)]	0.512 g	0.187 g (0.09 eq.)	0.548 g (44%)
2	0.512 g	0.196 g (0.10 eq.)	0.796 g (64%)
3	0.509 g	0.379 g (0.19 eq.)	1.041 g (83%)
4[b)]	5.018 g	4.863 g (0.25 eq.)	3.683 g (30%)

[a)] Reaction without acetic acid and sodium acetate, [b)] Reaction cooled to -20 °C.

5.4 Synthesis of Ethyl 3-(imidazol-1-yl)acrylate (2)

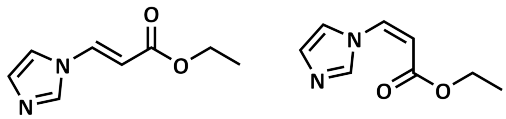

To a solution of imidazole (0.500 g, 7.34 mmol) in chloroform (72 mL), ethyl propiolate (0.95 mL, 9.37 mmol, 1.30 eq.) was added and allowed to react for 72 hours at room temperature. The reaction mixture was concentrated under reduced pressure and was purified by column chromatography (EA) to afford 0.940 g ethyl (*E*/*Z*)-3-(imidazol-1-yl)acrylate (77%, *E*/*Z* ratio of 0.6:1.0) as an orange oil and 0.197 g ethyl (*E*)-3-(imidazol-1-yl)acrylate (16%) as orange crystals.

TLC: R_f = 0.53-0.39 (EA).

^{1}H NMR (300 MHz, CD_2Cl_2, 25 °C):
Ethyl (*E*)-3-(imidazol-1-yl)acrylate: $\delta = 1.31$ (t, 3 H, $J = 7.1$ Hz), 4.22 (q, 2 H, $J = 7.1$ Hz), 6.06 (d, 1 H,$J = 14.2$ Hz), 7.12 (m, 1 H), 7.26 (t, 1 H, $J = 1.4$ Hz), 7.75 (m, 1 H), 7.90 (d, 1 H, $J = 14.2$ Hz) ppm.
Ethyl (*Z*)-3-(imidazol-1-yl)acrylate: $\delta = 1.29$ (t, 3 H, $J = 7.1$ Hz), 4.22 (q, 2 H, $J = 7.1$ Hz), 5.51 (d, 1 H, $J = 10.7$ Hz), 6.93 (d, 1 H, $J = 10.7$ Hz), 7.04 (m, 1 H), 7.82 (t, 1 H, $J = 1.5$ Hz), 8.05 (m, 1 H) ppm.

^{13}C NMR (75 MHz, CD_2Cl_2, 25 °C):
Ethyl (*E*)-3-(imidazol-1-yl)acrylate: δ = 14.6, 61.4, 107.4, 116.8, 132.1, 136.9, 138.5, 166.4 ppm.
Ethyl (*Z*)-3-(imidazol-1-yl)acrylate: δ = 14.5, 61.3, 106.5, 121.2, 130.5, 133.0, 140.3, 165.0 ppm.

5.5 Preparation of Poly(ethyl 2-(imidazol-1-yl)acrylate) (3)

5.5.1 Free Radical Polymerization

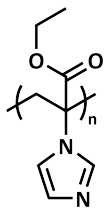

A solution of ethyl 2-(imidazol-1-yl)acrylate (1.8 M), azobisisobutyronitrile (0.5 mol%), and additive in solvent was deoxygenated by three freeze-pump-thaw cycles and heated to 65 °C for 48 hours. The polymerization was terminated by cooling in liquid nitrogen, and the mixture precipitated in ethyl acetate (45 mL) to afford the polymer as a pale beige solid.

Table 5.3: Polymerization of ethyl 2-(imidazol-1-yl)acrylate in the presence of various additives and the corresponding yield.

Entry	Monomer	Initiator	Solvent	Additive	Yield
1	0.502 g	1.9 mg	Benzene	-	0.199 g (40%)
2	0.499 g	2.2 mg	Anisole	-	0.218 g (44%)
3	0.506 g	2.0 mg	THF	-	0.213 g (42%)
4	0.501 g	2.1 mg	MeCN	-	0.148 g (29%)
5	0.495 g	2.5 mg	DMF	-	0.173 g (35%)
6	0.506 g	2.3 mg	DMSO	-	0.252 g (50%)
7	0.503 g	2.5 mg	HOAc	-	0.262 g (40%[a)])
8	0.502 g	2.4 mg	HFIP	HOAc (5 eq.)	0.170 g (26%[a)])
9	0.518 g	2.6 mg	*i*PrOH	HOAc (5 eq.)	0.291 g (43%[a)])
10	0.505 g	2.2 mg	TFE	HOAc (5 eq.)	0.132 g (20%[a)])
11	0.521 g	2.4 mg	EGME	HOAc (5 eq.)	0.546 g (80%[a)])
12	0.510 g	2.1 mg	DMF	HOAc (5 eq.)	0.264 g (40%[a)])
13	0.506 g	2.5 mg	DMSO	HOAc (5 eq.)	0.151 g (23%[a)])
14	0.504 g	2.6 mg	Water	HOAc (5 eq.)	0.501 g (52%[a)])
15	0.497 g	2.5 mg	DMF	37% $HCl_{aq.}$ (1.1 eq.)	0.602 g (99%)
16	0.501 g	2.3 mg	DMSO	37% $HCl_{aq.}$ (1.1 eq.)	0.607 g (99%)
17	0.502 g	2.3 mg	Water	37% $HCl_{aq.}$ (1.1 eq.)	0.525 g (86%)

[a)] Calculation based on 85% protonation of the polymer with HOAc.

Table 5.4: SEC data of poly(ethyl 2-(imidazol-1-yl)acrylate) in the presence of various additives and the corresponding yield.

Entry	Solvent	Additive	$\overline{M}_n$ [a)]	$Đ$ [a)]	$\overline{M}_n$ [b)]	$Đ$ [b)]
1	Benzene	-	13,400 g·mol^{-1}	1.59	29,400 g·mol^{-1}	1.51
2	Anisole	-	11,500 g·mol^{-1}	1.65	23,800 g·mol^{-1}	1.53
3	THF	-	8,700 g·mol^{-1}	1.49	16,500 g·mol^{-1}	1.56
4	MeCN	-	8,600 g·mol^{-1}	1.48	17,000 g·mol^{-1}	1.42
5	DMF	-	10,000 g·mol^{-1}	1.54	20,600 g·mol^{-1}	1.45
6	DMSO	-	13,300 g·mol^{-1}	1.45	30,200 g·mol^{-1}	1.45
7	HOAc	-	1,500 g·mol^{-1}	1.34	-	-
8	HFIP	HOAc	1,400 g·mol^{-1}	1.43	-	-
9	*i*PrOH	HOAc	1,500 g·mol^{-1}	1.43	-	-
10	TFE	HOAc	1,400 g·mol^{-1}	1.47	-	-
11	EGME	HOAc	1,200 g·mol^{-1}	1.37	-	-
12	DMF	HOAc	2,700 g·mol^{-1}	1.39	-	-
13	DMSO	HOAc	2,700 g·mol^{-1}	1.53	-	-
14	Water	HOAc	1,200 g·mol^{-1}	1.32	-	-
15	DMF	HCl	2,100 g·mol^{-1}	1.37	-	-
16	DMSO	HCl	1,000 g·mol^{-1}	1.52	-	-
17	Water	HCl	400 g·mol^{-1}	1.44	-	-

[a)] SEC (Water, P2VP calibration), [b)] SEC (DMAc, PMMA calibration).

Poly(ethyl 2-(imidazol-1-yl)acrylate) was further prepared under the following optimized conditions:
A solution of ethyl 2-(imidazol-1-yl)acrylate (5.005 g, 30.12 mmol), and azobisisobutyronitrile (0.038 g, 0.23 mmol, 0.8 mol%) in dimethyl sulfoxide (12 mL) was deoxygenated by flushing with argon for 15 minutes and heated to 70 °C for 22 hours. The mixture was cooled to room temperature, diluted with dichloromethane (12 mL) and precipitated in a mixture of ethyl acetate and methyl *tert*-butyl ether (1:1, 300 mL) to afford 3.329 g poly(ethyl 2-(imidazol-1-yl)acrylate) as a pale beige solid.

^{1}H NMR (400 MHz, DMSO-d_6, 60 °C): δ = 0.63-1.51 (3 H), 1.52-3.12 (2 H), 3.50-4.59 (2 H), 6.26-8.45 (3 H) ppm.

^{13}C ssMAS: δ = 5.7-12.4, 28.7-53.9, 53.9-78.8, 109.2-140.9, 158.9-172.4 ppm.

SEC (Water, P2VP calibration): $\overline{M}_n$ = 8,200 g·mol^{-1}, $Đ$ = 1.80.

SEC (DMAc, PMMA calibration): $\overline{M}_n$ = 20,500 g·mol^{-1}, $Đ$ = 1.60.

5.5.2 RAFT Polymerization

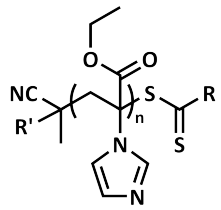

A solution of ethyl 2-(imidazol-1-yl)acrylate (5.0 M), chain transfer agent (1.0 mol%), and azobisisobutyronitrile (0.3 mol%) in solvent was deoxygenated by flushing with argon for 10 minutes and heated to 70 °C for 24 hours. The mixture was cooled to room temperature and precipitated in ethyl acetate (45 mL) to afford poly(ethyl 2-(imidazol-1-yl)acrylate) as a solid.

Table 5.5: RAFT polymerization of ethyl 2-(imidazol-1-yl)acrylate.

Entry	Monomer	Chain Transfer Agent	Initiator	Solvent	Yield
1	0.509 g	8.9 mg CPADB	1.5 mg	DMF	0.096 g (19%)
2	0.507 g	9.3 mg CPATTC	1.3 mg	DMF	0.212 g (42%)
3	0.504 g	8.6 mg CPzCD	1.4 mg	DMF	0.168 g (33%)
4	0.508 g	8.8 mg CPzCD	1.5 mg	DMSO	0.293 g (58%)
5	0.509 g	8.6 mg CPzCD	1.3 mg	Anisole	0.210 g (41%)

Table 5.6: SEC data from the RAFT polymerizations of ethyl 2-(imidazol-1-yl)acrylate.

Entry	Chain Transfer Agent	Solvent	$\overline{M}_n$ [a)]	$Đ$ [a)]	$\overline{M}_n$ [b)]	$Đ$ [b)]
1	CPADB	DMF	2,700 g·mol^{-1}	1.86	500 g·mol^{-1}	5.82
2	CPATTC	DMF	4,600 g·mol^{-1}	2.03	7,900 g·mol^{-1}	2.21
3	CPzCD	DMF	6,200 g·mol^{-1}	1.68	6,600 g·mol^{-1}	2.24
4	CPzCD	DMSO	6,300 g·mol^{-1}	1.62	4,100 g·mol^{-1}	2.83
5	CPzCD	Anisole	11,100 g·mol^{-1}	1.61	10,500 g·mol^{-1}	1.79

[a)] SEC (Water, P2VP calibration), [b)] SEC (DMAc, PMMA calibration).

Kinetic study of the RAFT polymerization of ethyl 2-(imidazol-1-yl)acrylate:
A solution of ethyl 2-(imidazol-1-yl)acrylate (5.0 M), trioxane, 2-cyanobutan-2-yl 4-chloro-3,5-dimethylpyrazole-1-carbodithioate (1.0 mol%) and azobisisobutyronitrile (0.3 mol%) in 1.2 mL anisole was deoxygenated by flushing with argon for 10 minutes and heated. To monitor the polymerization by ^{1}H NMR and SEC (DMAc), samples at 0.5, 1, 2, 3, 5, 8, 12, 16 and 24 hours were taken. The polymerization was terminated by cooling in liquid nitrogen before the mixture was precipitated in ethyl acetate (45 mL) to afford poly(ethyl 2-(imidazol-1-yl)acrylate) as a beige solid.

Table 5.7: Polymerization of ethyl 2-(imidazol-1-yl)acrylate *via* RAFT.

Entry	Monomer	Chain Transfer Agent	Initiator	Trioxane	Temperature	Time
6	1.003 g	17.4 mg CPzCD	2.5 mg	23.0 mg	70 °C	24 h
7	1.003 g	17.2 mg CPzCD	2.3 mg	31.5 mg	85 °C	5 h

5.6 Preparation of Poly(ethylene oxide)-*block*-poly(ethyl 2-(imidazol-1-yl)acrylate)

5.6.1 4-((4-Chloro-3,5-dimethylpyrazole-1-carbonothioyl)thio)-4-cyanovaleric acid (12)

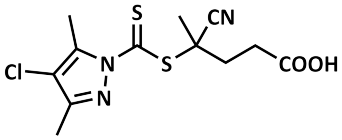

4-((4-Chloro-3,5-dimethylpyrazole-1-carbonothioyl)thio)-4-cyanovaleric acid was prepared according to a literature procedure.[286]
A suspension of bis(4-chloro-3,5-dimethypyrazolesulfanylthiocarbonyl)disulfide (5.123 g, 12.45 mmol) and 4,4'-azobis(4-cyanovaleric acid) (7.193 g, 25.66 mmol, 2.06 eq.) in 1,4-dioxane (40 mL) was deoxygenated by flushing with argon for 30 minutes and heated to 75 °C for 21 hours. The solution was concentrated under reduced pressure and purified by column chromatography (DCM:MeOH, 20:1) to afford 6.598 g 4-((4-chloro-3,5-dimethylpyrazole-1-carbonothioyl)thio)-4-cyanovaleric acid (80%) as a yellow solid.

TLC: R_f = 0.56-0.35 (DCM:MeOH, 20:1).

^{1}H NMR (300 MHz, $CDCl_3$, 25 °C): δ = 1.90 (s, 3 H), 2.28 (s, 3 H), 2.35-2.63 (m, 2 H), 2.63-2.83 (m, 2 H), 2.70 (s, 3 H), 9.12 (br s, 1 H) ppm.

^{13}C NMR (75 MHz, $CDCl_3$, 25 °C): δ = 11.7, 15.4, 24.6, 29.7, 33.2, 44.8, 117.5, 119.1, 141.0, 149.6, 177.3, 193.5 ppm.

5.6.2 *N*-Succinimidyl 4-((4-chloro-3,5-dimethylpyrazole-1-carbonothioyl)thio)-4-cyanovalerate (13)

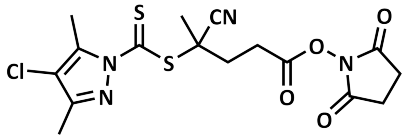

N-Succinimidyl 4-((4-chloro-3,5-dimethylpyrazole-1-carbonothioyl)thio)-4-cyanovalerate was prepared by a modified literature procedure.[189]
To a solution of 4-((4-chloro-3,5-dimethylpyrazole-1-carbonothioyl)thio)-4-cyanovaleric acid (6.475 g, 19.51 mmol) and *N*-hydroxysuccinimide (1.744 g, 15.15 mmol, 0.78 eq.) in dry dichloromethane (30 mL) under an argon atmosphere, dicyclohexylcarbodiimide (3.146 g, 15.25 mmol, 0.78 eq.) was added. The reaction mixture was stirred for 16 hours at room temperature, before being filtered and concentrated under reduced pressure. The crude product was purified by column chromatography (CH:EA, 1:1) to afford 3.118 g *N*-succinimidyl
4-((4-chloro-3,5-dimethylpyrazole-1-carbonothioyl)thio)-4-cyanovalerate (48%) as a yellow solid.

TLC: R_f = 0.50-0.34 (CH:EA, 1:1).

^{1}H NMR (300 MHz, $CDCl_3$, 25 °C): δ = 1.91 (s, 3 H), 2.29 (s, 3 H), 2.46-2.61 (m, 2 H), 2.62-2.76 (m, 2 H), 2.70 (s, 3 H), 2.84 (s, 4 H), 2.92-3.03 (m, 2 H) ppm.

^{13}C NMR (75 MHz, $CDCl_3$, 25 °C): δ = 11.6, 15.2, 24.5, 25.6, 26.9, 32.6, 44.4, 117.4, 118.7, 140.9, 149.6, 167.1, 168.8, 193.1 ppm.

UHPLC/HRMS:
t_R = 6.7 min, m/z = 879.0612 $[M_2+Na]^+$, 451.0257 $[M+Na]^+$, 429.0439 $[M+H]^+$
calculated: m/z = 879.0657 ($C_{32}H_{34}Cl_2N_8O_8S_4Na^+$), 451.0272 ($C_{16}H_{17}ClN_4O_4S_2Na^+$), 429.0453 ($C_{17}H_{17}ClN_4O_4S_2^+$).

5.6.3 *N*-(Poly(ethylene oxide)) 4-((4-chloro-3,5-dimethylpyrazole-1-carbonothioyl)thio)-4-cyanovaleramide (14)

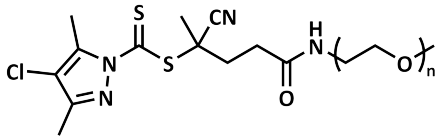

N-(Poly(ethylene oxide)) 4-((4-chloro-3,5-dimethylpyrazole-1-carbonothioyl)thio)-4-cyanovaleramide was prepared by a modified literature procedure.[189]

To a solution of *N*-succinimidyl 4-((4-chloro-3,5-dimethylpyrazole-1-carbonothioyl)thio)-4-cyanovalerate (1.321 g, 3.08 mmol, 1.24 eq.) in dry dichloromethane (20 mL) under an argon atmosphere, a solution of α-methoxy-ω-amino poly(ethylene oxide) (5.011 g, 2.49 mmol) in dry dichloromethane (7 mL) was added and the mixture stirred for 22 hours at room temperature. The reaction mixture was precipitated in diethyl ether (700 mL) to afford 5.334 g *N*-(poly(ethylene oxide)) 4-((4-chloro-3,5-dimethylpyrazole-1-carbonothioyl)thio)-4-cyanovaleramide (92%) as a bright yellow solid.

^{1}H NMR (300 MHz, $CDCl_3$, 25 °C): δ = 1.18 (s, 3 H), 2.26 (s, 3 H), 2.33-2.63 (m, 4 H), 2.67 (s, 3 H), 3.35 (s, 3 H), 3.32-3.94 (183 H) 6.39 (s, 1 H) ppm.

^{13}C NMR (75 MHz, $CDCl_3$, 25 °C): δ = 11.6, 15.3, 24.6, 31.7, 34.2, 39.5, 45.2, 59.1, 69.6-72.3, 117.3, 119.4, 140.8, 149.4, 170.5, 194.0 ppm.

SEC (DMAc, PEO calibration): $\overline{M}_n$ = 1,900 g·mol^{-1}, $Đ$ = 1.10.

5.6.4 Synthesis of Poly(ethylene oxide)-*block*-poly(ethyl 2-(imidazol-1-yl)acrylate)

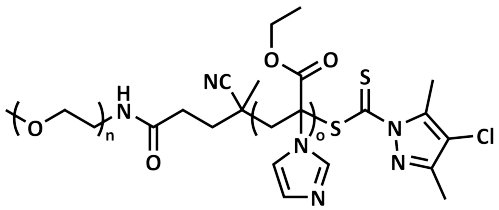

A solution of ethyl 2-(imidazol-1-yl)acrylate (1.013 g, 6.10 mmol), *N*-(poly(ethylene oxide)) 4-((4-chloro-3,5-dimethylpyrazole-1-carbonothioyl)thio)-4-cyanovaleramide (0.133 g, 58.2 μmol) and azobisisobutyronitrile (0.9 mg, 5.5 μmol) in anisole (1.2 mL) was deoxygenated by flushing with argon for 10 minutes and heated to 70 °C. The polymerization was monitored by SEC (DMAc) and cooled to room temperature after 23 hours.

5.7 Preparation of Poly(ethyl 2-(3-methylimidazolium-1-yl iodide)acrylate) (4)

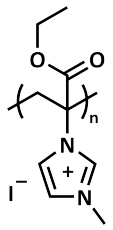

Poly(ethyl 2-(3-methylimidazolium-1-yl iodide)acrylate) was prepared by a modified literature procedure.[287]
A solution of poly(ethyl 2-(imidazol-1-yl)acrylate) (0.300 g) in methanol (5 mL) was deoxygenated by flushing with argon for 5 minutes before methyl iodide (0.6 mL, 9.00 mmol, 5 eq. per repeating unit) was added. The mixture was stirred for 48 hours at room temperature and precipitated in ethyl acetate (175 mL) to afford 0.456 g poly(ethyl 2-(3-methylimidazolium-1-yl iodide)acrylate) (82%) as a yellow solid.

^{1}H NMR (400 MHz, D_2O, 60 °C): δ = 2.47-3.52 (2 H), 6.58-7.42 (2 H), 7.67-8.47 (1 H) ppm.

^{13}C ssMAS: δ = 21.5-54.2, 55.2-80.0, 53.9-78.8, 106.2-143.1, 152.5-184.9 ppm.

SEC (Water, P2VP calibration): $\overline{M}_n$ = 6,600 g·mol^{-1}, $Đ$ = 1.37.

5.8 Preparation of Poly(2-(imidazolium-1-yl)acrylate) (5)

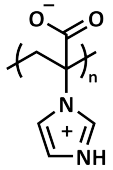

Poly(2-(imidazol-1-yl)acrylic acid was prepared by a modified literature procedure.[102]
To a solution of poly(ethyl 2-(imidazol-1-yl)acrylate) (0.102 g) in methanol (2 mL), a solution of lithium hydroxide monohydrate (0.162 g, 3.87 mol, 6 eq. per repeating unit) in water (2 mL) was added. The mixture was heated to 65 °C for 48 hours, dialyzed against water, and freeze-dried to afford 0.076 g poly(2-(imidazolium-1-yl)acrylate) (90%) as a white solid.

^{1}H NMR (400 MHz, D_2O, 60 °C): δ = 1.14-2.11 (3 H), 3.16-4.77 (7 H), 7.01-10.19 (3 H) ppm.

^{13}C ssMAS: δ = 4.4-15.7, 26.0-54.8, 54.8-69.2, 108.4-141.3, 154.9-172.9 ppm.

SEC (Water, P2VP calibration): $\overline{M}_n$ = 6,600 g·mol^{-1}, $Đ$ = 1.37.

5.9 Preparation of Poly(2-(3-methylimidazolium-1-yl)acrylate) (6)

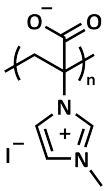

Poly(2-(3-methylimidazolium-1-yl)acrylate was prepared from poly(ethyl 2-(3-methylimidazolium-1-yl iodide)acrylate) by a modified literature procedure.[102]
To a solution of poly(ethyl 2-(3-methylimidazolium-1-yl iodide)acrylate) (0.251 g) in methanol (2.5 mL), a solution of lithium hydroxide monohydrate (0.179 g, 4.26 mol, 5 eq. per repeating unit) in water (2.5 mL) was added. The mixture was heated to 65 °C for 48 hours, dialyzed against water, and freeze-dried to afford 0.142 g poly(2-(3-methylimidazolium-1-yl)acrylate) (quantitative) as a yellowish solid.

^{1}H NMR (400 MHz, D_2O, 60 °C): δ = 2.27-3.69 (2 H), 3.70-4.42 (3 H), 6.66-9.68 (3 H) ppm.

^{13}C ssMAS: δ = 25.1-35.6, 35.6-72.9, 106.7-144.6, 157.1-178.2 ppm.

SEC (Water, P2VP calibration): $\overline{M}_n$ = 4,800 g·mol^{-1}, $Đ$ = 1.57.

Poly(2-(3-methylimidazolium-1-yl)acrylate was prepared from poly(2-(imidazolium-1-yl)acrylate) by a modified literature procedure.[287]
A solution of poly(2-(imidazolium-1-yl)acrylate) (0.098 g) in methanol (2 mL) and water (2 mL) was deoxygenated by flushing with argon for 5 minutes. Methyl iodide (0.25 mL, 4.00 mol, 5.5 eq. per repeating unit) was then added. The mixture was heated to 65 °C for 24 hours, before being dialyzed against water, a water:methanol mixture (1:1), and finally water. The resulting solution was freeze-dried to afford 0.083 g poly(2-(3-methylimidazolium-1-yl)acrylate) (42%) as a white solid.

SEC (Water, P2VP calibration): $\overline{M}_n$ = 6,800 g·mol^{-1}, $Đ$ = 1.45.

5.10 Synthesis of Ethyl 2-(imidazol-2-yl)acrylate

5.10.1 1-(2-(Trimethylsilyl)ethoxy)methylimidazole (15)

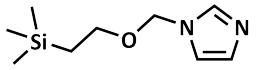

1-(2-(Trimethylsilyl)ethoxy)methylimidazole was prepared by a modified literature procedure.[288]

To a solution of imidazole (5.005 g, 73.52 mmol) in dry tetrahydrofuran (100 mL) under an argon atmosphere, sodium hydride (60% in mineral oil, 3.567 g, 89.19 mmol, 1.21 eq.) was added in portion at 0 °C, and warmed to room temperature after 15 minutes. The suspension was stirred for one hour, and cooled to 0 °C before 2-(trimethylsilyl)ethoxymethyl chloride (15.5 mL, 87.58 mmol, 1.19 eq.) was added dropwise. The reaction mixture was warmed to room temperature after 15 minutes and stirred for further 21 hours. The reaction was quenched by the addition of a saturated aqueous ammonium chloride solution (50 mL) and water (50 ml). The organic phase was separated and the aqueous phase was extracted with ethyl acetate (3× 50 mL). The combined organic phase was dried over anhydrous magnesium sulfate, filtered and concentrated under reduced pressure. The crude product was purified by column chromatography (EA:MeOH, 20:1) to afford 11.431 g 1-(2-(trimethylsilyl)ethoxy)methylimidazole (78%) as a yellowish liquid.

TLC: R_f = 0.61-0.32 (EA:MeOH, 20:1, visualized with $KMnO_4$ stain).

^{1}H NMR (300 MHz, CD_2Cl_2, 25 °C): δ = -0.02 (s, 9 H), 0.89 (m , 2 H), 3.48 (m , 2 H), 5.26 (s, 2 H), 7.02 (t, 1 H, J = 1.1 Hz), 7.05 (t, 1 H, J = 1.3 Hz) 7.55 (t, 1 H, J = 1.0 Hz) ppm.

^{13}C NMR (75 MHz, CD_2Cl_2, 25 °C): δ = -1.3, 18.2, 66.8, 76.4, 119.5, 130.2, 137.9 ppm.

5.10.2 Ethyl 2-(1-(2-(trimethylsilyl)ethoxy)methylimidazol-2-yl)-2-oxoacetate (16)

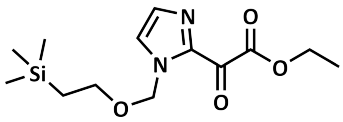

Ethyl 2-(1-(2-(trimethylsilyl)ethoxy)methylimidazol-2-yl)-2-oxoacetate was prepared according to a literature procedure.[157]

To a solution of *N*-(2-(trimethylsilyl)ethoxy)methylimidazole (4.490 g, 22.64 mmol) in dry dichloromethane (150 mL) under an argon atmosphere, ethyl chlorooxoacetate (2.5 mL, 22.34 mmol, 0.99 eq.) was added dropwise at -20 °C. After 20 minutes, dry Hünig's base (4.0 mL, 22.96 mmol, 1.01 eq.) was added at -11 °C to the solution before the solution was slowly warmed to room temperature. The reaction mixture was stirred for a further 15 hours and washed with water (3× 100 mL). The organic phase was dried over anhydrous magnesium sulfate, filtered and concentrated under reduced pressure. The crude product was purified by column chromatography (CH:EA, 1:1) to afford 6.812 g ethyl 2-(1-(methoxymethylimidazol-2-yl)-2-oxoacetate (93%) as a yellow oil.

TLC: R_f = 0.68-0.60 (CH:EA, 1:1).

^{1}H NMR (300 MHz, $CDCl_3$, 25 °C): δ = -0.02 (s, 9), 0.93 (m, 2 H), 1.41 (t, 3 H, J = 7.1 Hz), 3.59 (m, 2 H), 4.46 (q, 2 H, J = 7.1 Hz), 5.78 (s, 2 H,), 7.36 (d, 1 H, J = 1.0 Hz) 7.42 (d, 1 H, J = 1.0 Hz) ppm.

^{13}C NMR (75 MHz, CD_2Cl_2, 25 °C): δ = -1.3, 14.2, 18.0, 62.7, 67.5, 126.4, 132.5, 140.0, 163.6, 177.7 ppm.

EI-MS: m/z = 465 $[M_2\text{-SEM}]^{\cdot+}$, 299 $[M+H]^+$, 269 $[M\text{-Et}]^{\cdot+}$, 225 $[M\text{-COOEt}]^{\cdot+}$, 225 $[M\text{-SiMe}_3]^{\cdot+}$, 197 $[M\text{-C}_2H_4SiMe_3]^{\cdot+}$, 197 $[M\text{-COCOOEt}]^{\cdot+}$, 182 $[M\text{-OC}_2H_3SiMe_3]^+$, 167 $[M\text{-SEM}]^{\cdot+}$.

5.10.3 2-Methyl-1-(methoxymethyl)imidazole (18a)

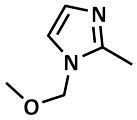

2-Methyl-1-(methoxymethyl)imidazole was prepared by a modified literature procedure.[288]

To a solution of 2-methylimidazole (10.037 g, 122.24 mmol) in dry tetrahydrofuran (125 mL) under an argon atmosphere, sodium hydride (60% in mineral oil, 4.896 g, 122.41 mmol, 1.00 eq.) was added in portion at 0 °C. After 1.5 hours, chloromethyl methyl ether (9.3 mL, 122.44 mmol, 1.00 eq.) was added dropwise at -15 °C, stirred for 30 minutes and warmed to room temperature. After 23 hours, the reaction was quenched with saturated aqueous ammonium chloride solution (24 mL), and water (24 mL) was added. The organic phase was separated, the aqueous phase was diluted with water (100 mL) and extracted with dichloromethane (3× 200 mL). The combined organic phase was dried over anhydrous magnesium sulfate, filtered and concentrated under reduced pressure. The crude product was purified by distillation (51 °C, $1.1\cdot10^{-2}$ mbar) to afford 12.145 g 2-methyl-1-(methoxymethyl)imidazole (79%) as a colorless viscous liquid.

^{1}H NMR (300 MHz, CD_2Cl_2, 25 °C): δ = 2.37 (s, 3 H), 3.25 (s, 3 H), 5.14 (s, 2 H), 6.84 (d, 1 H, J = 1.4 Hz), 6.93 (d, 1 H, J = 1.4 Hz) ppm.

5.10.4 Ethyl 2-(1-(methoxymethyl)imidazol-2-yl)acetate (19a)

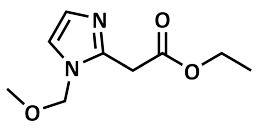

Ethyl 2-(1-(methoxymethyl)imidazol-2-yl)acetate was prepared according to a literature procedure.[158]

To a solution of 2-methyl-1-(methoxymethyl)imidazole (1.526 g, 12.10 mmol) and dry Hünig's base (4.2 mL, 24.11 mmol, 1.99 eq.) in dry acetonitrile (12 mL) under an argon at-

mosphere, ethyl chloroformate (2.3 mL, 24.16 mmol, 2.00 eq.) was added dropwise at 0 °C. The reaction mixture was slowly warmed to room temperature and concentrated under reduced pressure after 19 hours. To the residue, water (50 mL) was added and extracted with dichloromethane (50 mL). The pH value of the aqueous phase was adjusted to 10 with potassium carbonate and extracted with dichloromethane (4× 50 mL). The combined organic phase was dried over anhydrous magnesium sulfate, filtered and concentrated under reduced pressure. The crude product was purified by column chromatography (EA:MeOH, 10:1) to afford 2.146 g of a 1.0:1.4 mixture of ethyl 2-(1-(methoxymethyl)imidazol-2-yl)acetate (30%) and diethyl 2-(1-(methoxymethyl)imidazol-2-yl)malonate as a yellow oil.

TLC: $R_f = 0$. (EA:MeOH, 10:1).

^{1}H NMR (300 MHz, CD_2Cl_2, 25 °C): δ = 1.24 (t, 3 H, J = 7.1 Hz), 3.23 (s, 3 H), 3.82 (s, 2 H), 4.14 (q, 2 H, J = 7.1 Hz), 5.20 (s, 2 H), 6.92 (d, 1 H, J = 1.4 Hz), 7.00 (d, 1 H, J = 1.4 Hz) ppm.

5.10.5 2-Methyl-1-benzylimidazole (18b)

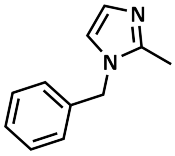

To a solution of 2-methylimidazole (6.052 g, 73.71 mmol) in dry tetrahydrofuran (100 mL) under an argon atmosphere, sodium hydride (60% in mineral oil, 3.230 g, 80.76 mmol, 1.10 eq.) was added in portion at 0 °C. After 15 minutes, the mixture was warmed to room temperature, stirred for 45 minutes, and benzyl chloride (9.3 mL, 80.82 mmol, 1.10 eq.) was added dropwise at 0 °C. After 15 minutes, the suspension was warmed to room temperature, and stirred for 18 hours. The reaction was quenched by the addition of a saturated aqueous ammonium chloride solution (5 mL) before being diluted with water (250 mL). The mixture was extracted with dichloromethane (300 mL), the aqueous phase diluted with water (200 mL) and extracted with dichloromethane (150 mL). The combined organic phase was washed with water (300 mL), brine (300 mL), dried over anhydrous magnesium sulfate, filtered and concentrated under reduced pressure. The crude product was purified by column chromatography (THF:NEt_3, 20:1) and distillation (86 °C, $2 \cdot 10^{-3}$ mbar) to afford 10.903 g 2-methyl-1-benzylimidazole (86%) as a colorless liquid.

TLC: R_f = 0.68-0.53 (THF:NEt_3, 20:1).

^{1}H NMR (300 MHz, CD_2Cl_2, 25 °C): δ = 2.29 (s, 3 H), 5.05 (s, 2 H), 6.87 (m, 1 H), 7.08 (m, 1 H), 7.25-7.39 (m, 5 H) ppm.

5.10.6 Ethyl 2-(1-benzylimidazol-2-yl)acetate (19b)

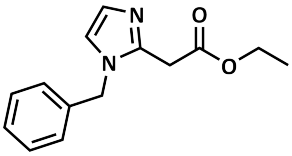

Ethyl 2-(1-benzylimidazol-2-yl)acetate was prepared according to a literature procedure.[158]
To a solution of 2-methyl-1-benzylimidazole (10.678 g, 62.00 mmol) and triethylamine (17.3 mL, 123.97 mmol, 2.00 eq.) in dry acetonitrile (75 mL) under an argon atmosphere, ethyl chloroformate (11.8 mL, 123.96 mmol, 2.00 eq.) was added dropwise at 0 °C. After 3 hours, the suspension was warmed to room temperature, stirred for 2 hours, and then filtered. The filtrate was concentrated under reduced pressure and stirred for one hour in water (200 mL). The mixture was extracted with diethyl ether (3× 125 mL) and ethyl acetate (1× 150 mL, 1× 50 mL). The combined organic phase was dried over anhydrous magnesium sulfate, filtered and concentrated under reduced pressure. The crude product was purified by column chromatography (EA) to afford 1.913 g ethyl 2-(1-benzylimidazol-2-yl)acetate (13%) as a yellow oil and 0.863 g diethyl 2-(1-benzylimidazol-2-yl)malonate.

TLC: R_f = 0.30-0.17 (EA).

^{1}H NMR (300 MHz, CD_2Cl_2, 25 °C): δ = 1.21 (t, 3 H, J = 7.1 Hz), 3.71 (s, 2 H), 4.09 (q, 2 H, J = 7.1 Hz), 5.11 (s, 2 H), 6.89 (d , 1 H, J = 1.3 Hz), 6.95 (d , 1 H, J = 1.3 Hz), 7.06-7.17 (m, 2 H), 7.25-7.41 (m, 3 H) ppm.

5.10.7 Ethyl 2-(imidazol-2-yl)acetate (24)

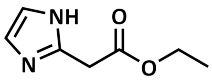

Ethyl 2-(imidazol-2-yl)acetate was prepared according to a literature procedure.[159]
To a solution of ethyl 3-ethoxy-3-iminopropionate hydrochloride (11.183 g, 57.16 mmol) in dry ethanol (225 mL) under an argon atmosphere, aminoacetaldehyde diethyl acetal (8.3 mL, 56.74 mmol, 0.99 eq.) was added and the mixture was heated to 100 °C for 5 hours. The solution was cooled to room temperature, hydrogen chloride (4.0 M in 1,4-dioxane, 56 mL, 224.00 mmol, 3.92 eq.) was added and heated to 100 °C. After 12.5 hours, the reaction mixture was cooled to room temperature and 8.845 g sodium carbonate and water (25 mL) were added. The suspension was dried over anhydrous magnesium sulfate, filtered and concentrated under reduced pressure. The crude product was purified by column chromatography (EA:NEt_3, 20:1) to afford 4.426 g ethyl 2-(imidazol-2-yl)acetate (50%) as a pink solid and 1.332 g ethyl 2-(1-(diethoxymethylimidazol-2-yl)acetate.

TLC: R_f = 0.46-0.33 (EA:NEt_3, 20:1, visualized with $KMnO_4$ stain).

^{1}H NMR (300 MHz, CD_2Cl_2, 25 °C): δ = 1.24 (t, 3 H, J = 7.1 Hz), 3.82 (s, 2 H), 4.15 (q, 2 H, J = 7.1 Hz), 7.00 (d , 2 H, J = 0.2 Hz), 9.58 (br s, 1 H) ppm.

^{13}C NMR (75 MHz, CD_2Cl_2, 25 °C): δ = 14.4, 34.7, 61.9, 122.5, 141.5, 170.5 ppm.

5.10.8 Ethyl 2-(1-(2-(trimethylsilyl)ethoxy)methylimidazol-2-yl)acetate (29)

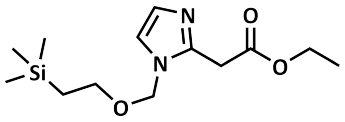

Ethyl 2-(imidazol-2-yl)acetate was prepared according to a literature procedure.[288]
To a solution of ethyl 2-(imidazol-2-yl)acetate (4.387 g, 28.45 mmol) in dry tetrahydrofuran (56 mL) under an argon atmosphere, sodium hydride (60% in mineral oil, 1.465 g, 36.62 mmol, 1.29 eq.) was added in portion at 0 °C, stirred for 15 minutes, and warmed to room temperature. After one hour to the mixture 2-(trimethylsilyl)ethoxymethylchloride (6.0 mL, 33.90 mmol, 1.19 eq.) was added dropwise at 0 °C, stirred for 30 minutes and warmed to room temperature. After 17 hours, the reaction was quenched by the addition of saturated aqueous ammonium chloride solution (20 mL) and water (20 mL). The organic phase was separated and the aqueous phase was extracted with dichloromethane (3× 100 mL). The combined organic phase was dried over anhydrous magnesium sulfate, filtered and concentrated under reduced pressure. The crude product was purified by column chromatography (EA:MeOH, 20:1) to afford 6.054 g ethyl 2-(1-(2-(trimethylsilyl)ethoxy)methylimidazol-2-yl)acetate (75%) as a bright orange oil.

TLC: R_f = 0.74-0.50 (EA:MeOH, 20:1, visualized with $KMnO_4$ stain).

^{1}H NMR (300 MHz, $CDCl_3$, 25 °C): δ = -0.03 (s, 9 H), 0.88 (m, 2 H), 1.25 (t, 3 H, J = 7.1 Hz), 3.46 (m, 2 H), 3.92 (s, 2 H), 4.17 (q, 2 H, J = 7.1 Hz), 5.28 (s, 2 H), 6.98 (d , 1 H, J = 1.5 Hz), 7.00 (d , 1 H, J = 1.5 Hz) ppm.

^{13}C NMR (75 MHz, $CDCl_3$, 25 °C): δ = -1.3, 14.3, 17.8, 33.6, 61.6, 66.6, 75.9, 120.8, 127.2, 141.7, 168.9 ppm.

5.10.9 Ethyl 2-(1-(2-(trimethylsilyl)ethoxy)methylimidazol-2-yl)acrylate (30)

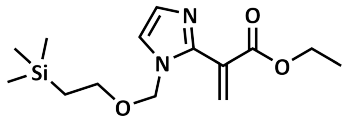

Ethyl 2-(1-(2-(trimethylsilyl)ethoxy)methylimidazol-2-yl)acrylate was prepared *via* a Wittig reaction by a modified literature procedure.[289]
To a suspension of methyltriphenylphosphonium bromide (6.002 g 16.80 mmol, 1.00 eq.) in dry tetrahydrofuran (16.5 mL) under an argon atmosphere, potassium bis(trimethylsilyl)amide solution (1.0 M in tetrahydrofuran, 16.8 mL, 16.80 mmol, 1.00 eq.) was added dropwise at -77 °C. The suspension was warmed to room temperature, stirred for 1.5 hours, and a solution of ethyl 2-(1-(methoxymethylimidazol-2-yl)-2-oxoacetate (5.015 g, 16.80 mmol) in dry tetrahydrofuran (16.5 mL) was added dropwise at -77 °C. After 15 minutes, the mixture was warmed to room temperature and stirred for 3.5 hours. The reaction was quenched by the addition of 0.1 M hydrochloric acid (20 mL) and saturated aqueous sodium bicarbonate solution (75 mL). The mixture was extracted with dichloromethane (1× 100 mL, 3× 50 mL), the combined organic phase was dried over anhydrous magnesium sulfate, filtered and concentrated under reduced pressure. The crude product was purified by column chromatography (CH:EA, 1:4) to afford 77.3 mg impure ethyl 2-(1-(2-(trimethylsilyl)ethoxy)methylimidazol-2-yl)acrylate as a yellowish oil.

TLC: R_f = 0.51-0.44 (CH:EA, 1:4, visualized with $KMnO_4$ stain).

Ethyl 2-(1-(2-(trimethylsilyl)ethoxy)methylimidazol-2-yl)acrylate was prepared by a modified literature procedure.[290]
A suspension of potassium carbonate (1.464 g, 10.59 mmol, 2.52 eq.), paraformaldehyde (0.320 g, 10.64 mmol, 2.53 eq.), tetra-*n*-butylammonium bromide (0.069 g, 0.21 mmol, 0.05 eq.) and ethyl 2-(1-(2-(trimethylsilyl)ethoxy)methylimidazol-2-yl)acetate (1.195 g, 4.20 mmol) in dry acetonitrile (8.5 mL) was heated to 60 °C for 16 hours. The reaction mixture was cooled to room temperature, filtered and concentrated under reduced pressure. The residue was diluted with water (50 mL) and extracted with ethyl acetate (3× 50 mL). The combined organic phase was dried over anhydrous magnesium sulfate, filtered and concentrated under reduced pressure. The crude product was purified by column chromatography (CH:EA, 1:4) to afford 54.7 mg impure ethyl 2-(1-(2-(trimethylsilyl)ethoxy)methylimidazol-2-yl)acrylate as a yellow oil.

TLC: R_f = 0.59-0.48 (CH:EA, 1:4, visualized with $KMnO_4$ stain).

5.11 Synthesis of Ethyl 2-(imidazol-4-yl)acrylate (31)

5.11.1 Ethyl but-3-enoate

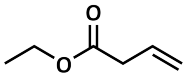

Ethyl but-3-enoate was prepared according to a literature procedure.[165]
To a solution of dry ethanol (42 mL, 719.13 mmol, 1.66 eq.) and triethylamine (67.0 mL, 480.69 mmol, 1.11 eq.) in dry diethyl ether (500 mL) under an argon atmosphere, crotonoyl chloride (90%, 46.0 mL, 432.21 mmol) was added at 0 °C. The reaction mixture was slowly warmed to room temperature and quenched by the addition of saturated aqueous sodium bicarbonate solution (25 mL) after 12 hours. The organic phase was washed with water (200 mL) and the aqueous phase was extracted with diethyl ether (2× 150 mL). The combined organic phase was dried over anhydrous magnesium sulfate, filtered and concentrated under reduced pressure. The crude product was purified by distillation (47 °C, 44 mbar) to afford 37.971 g ethyl but-3-enoate (77%) as a colorless liquid.

^{1}H NMR (400 MHz, $CDCl_3$, 25 °C): δ = 1.27 (t, 3 H, J = 7.1 Hz), 3.09 (dt, 2 H, J = 6.9, 1.5 Hz), 4.15 (q, 2 H, J = 7.2 Hz), 5.15 (m, 1 H), 5.18 (m, 1 H), 5.93 (m, 1 H) ppm.

^{13}C NMR (101 MHz, $CDCl_3$, 25 °C): δ = 14.3, 39.4, 60.8, 118.6, 130.5, 171.7 ppm.

5.11.2 Ethyl 2-(oxiran-2-yl)acetate (32)

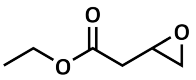

Ethyl 2-(oxiran-2-yl)acetate was prepared according to a literature procedure.[166]
To a solution of ethyl but-3-enoate (30.031 g, 263.10 mmol) in dry dichloromethane (500 mL) under an argon atmosphere, *meta*-chloroperoxybenzoic acid (≤77%, 80.970 g, 361.30 mmol, 1.37 eq.) was added in portion at 0 °C. The reaction mixture was slowly warmed to room temperature and filtered after 20 hours. The filtrate was washed with saturated aqueous sodium carbonate solution (2× 400 mL) and water (400 mL), dried over anhydrous magnesium sulfate, filtered and concentrated under reduced pressure. The crude product was purified by distillation (52 °C, 4 mbar) to afford 25.081 g ethyl 2-(oxiran-2-yl)acetate (73%) as a colorless liquid.

^{1}H NMR (300 MHz, $CDCl_3$, 25 °C): δ = 1.27 (t, 3 H, J = 7.2 Hz), 2.55 (m, 3 H), 2.84 (t, 1 H, J = 4.4 Hz), 3.28 (m, 1 H), 4.18 (q, 2 H, J = 7.1 Hz) ppm.

^{13}C NMR (75 MHz, $CDCl_3$, 25 °C): δ = 14.3, 38.2, 46.9, 48.2, 61.0, 170.5 ppm.

5.11.3 Ethyl 4-bromo-3-hydroxybutanoate (33)

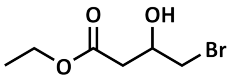

Ethyl 4-bromo-3-hydroxybutanoate was prepared by a modified literature procedure.[291] To a solution of ethyl 2-(oxiran-2-yl)acetate (5.962 g, 45.81 mmol) in dry tetrahydrofuran (500 mL) under an argon atmosphere, lithium bromide (6.364 g, 73.29 mmol, 1.60 eq.) was added at 0 °C followed by acetic acid (8.0 mL, 139.75 mmol, 3.05 eq.). The reaction mixture was stirred for 2.5 hours and warmed to room temperature. After 18.5 hours, the solution was concentrated under reduced pressure and the residue was dissolved in ethyl acetate (250 mL). The organic phase was washed with saturated aqueous sodium bicarbonate solution (125 mL) and water (125 mL), dried over anhydrous magnesium sulfate, filtered and concentrated under reduced pressure. The crude product was purified by column chromatography (CH:EA, 2:1) to afford 8.883 g ethyl 4-bromo-3-hydroxybutanoate (92%) as a pale yellowish liquid.

TLC: R_f = 0.58-0.39 (CH:EA, 2:1, visualized with $KMnO_4$ stain).

^{1}H NMR (300 MHz, $CDCl_3$, 25 °C): δ = 1.28 (t, 3 H, J = 7.2 Hz), 2.64 (m, 2 H), 3.15 (br s, 1 H), 3.49 (m, 2 H), 4.18 (q, 2 H, J = 7.1 Hz), 4.23 (m, 1 H) ppm.

^{13}C NMR (75 MHz, $CDCl_3$, 25 °C): δ = 14.3, 37.4, 39.4, 61.2, 67.7, 171.9 ppm.

EI-MS: m/z = 211 $[M+H]^+$, 193 $[M\text{-}OH]^{\cdot+}$, 165 $[M\text{-}OEt]^{\cdot+}$, 131 $[M\text{-}Br]^{\cdot+}$, 123 $[M\text{-}CH_2COOEt]^{\cdot+}$, 117 $[M\text{-}CH_2Br]^{\cdot+}$, 93 $[CH_2Br]^{\cdot+}$

5.11.4 Ethyl 4-bromo-3-oxobutanoate (34)

Ethyl 4-bromo-3-oxoybutanoate was prepared by a modified literature procedure.[292] To a solution of ethyl 4-bromo-3-hydroxybutanoate (1.510 g, 7.16 mmol) in dry dichloromethane (70 mL) under an argon atmosphere, Dess-Martin periodinane (4.521 g, 10.13 mmol, 1.42 eq.) was added at 0 °C. After 30 minutes, the reaction mixture was warmed to room temperature and stirred for 23.5 hours. The organic phase was washed with saturated aqueous sodium bicarbonate solution (75 mL) and a saturated aqueous sodium sulfite solution (75 mL), dried over anhydrous magnesium sulfate, filtered and concentrated under reduced pressure. The crude product was purified by column chromatography (CH:EA, 3:1) to afford 0.689 g ethyl 4-bromo-3-oxobutanoate (46%) as an orange liquid.

TLC: R_f = 0.57-0.53 (CH:EA, 3:1).

^{1}H NMR (300 MHz, $CDCl_3$, 25 °C):
Ethyl 4-bromo-3-oxobutanoate δ = 1.29 (t, 3 H, J = 7.1 Hz), 3.70 (s, 2 H), 4.05 (s, 2 H), 4.21 (q, 2 H, J = 7.1 Hz) ppm.
Ethyl (*Z*)-4-bromo-3-hydroxybut-2-enoate: δ = 1.30 (t, 3 H, J = 7.2 Hz), 3.85 (s, 2 H), 4.22 (q, 2 H, J = 7.1 Hz), 5.28 (s, 1 H), 12.00 (s, 1 H) ppm.

^{13}C NMR (75 MHz, $CDCl_3$, 25 °C):
Ethyl 4-bromo-3-oxobutanoate: δ = 14.2, 34.0, 46.2, 61.9, 166.7, 194.7 ppm.
Ethyl (*Z*)-4-bromo-3-hydroxybut-2-enoate: δ = 14.3, 28.8, 60.8, 92.0, 170.6, 172.2 ppm.

5.11.5 2-(Imidazol-5/4-yl)acetonitrile (35)

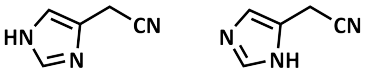

2-(Imidazol-5/4-yl)acetonitrile was prepared by a modified literature procedure.[169, 170] To a solution of L-histidine hydrochloride monohydrate (55.199 g, 263.32 mmol) in water (600 mL), a solution of sodium hypochlorite pentahydrate (90.554 g, 550.44 mmol, 2.09 eq.) in water (100 mL) was added dropwise at -5 to -10 °C. After one hour, the reaction mixture was slowly warmed to room temperature and stirred for further 22 hours. The solution pH was adjusted to 10 with solid sodium hydroxide, concentrated under reduced pressure and freeze-dried. A soxhlet extraction with ethyl acetate of the residue afforded 19.064 g 2-(imidazol-5/4-yl)acetonitrile (68%) as an ochre solid.

^{1}H NMR (300 MHz, DMSO-d_6, 25 °C): δ = 3.83 (d, 2 H, J = 0.9 Hz), 7.05 (q, 1 H, J = 1.2, 0.9 Hz), 7.64 (d, 1 H, J = 1.2 Hz), 12.14 (br s, 1 H) ppm.

^{13}C NMR (75 MHz, DMSO-d_6, 25 °C): δ = 16.4, 114.7, 119.0, 129.6, 135.8 ppm.

5.11.6 2-(Imidazol-4-yl)acetic acid hydrochloride (36)

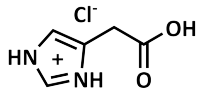

2-(Imidazol-4-yl)acetic acid hydrochloride was prepared by a modified literature procedure.[169]
A solution of 2-(imidazol-5/4-yl)acetonitrile (19.020 g, 177.56 mmol) in 6.0 M hydrochloric acid (290 mL) was heated to 110 °C for 5 hours and concentrated under reduced pressure. The residue was dried and recrystallized from methanol (350 mL) at -25 °C to afford 18.094 g 2-(imidazol-4-yl)acetic acid hydrochloride (63%) as a pale beige solid.

^{1}H NMR (300 MHz, MeOD-d_4, 25 °C): δ = 3.87 (d, 2 H, J = 0.9 Hz), 7.47 (m, 1 H), 8.88 (d, 1 H, J = 1.5 Hz) ppm.

^{13}C NMR (75 MHz, MeOD-d_4, 25 °C): δ = 30.6, 118.7, 128.8, 135.1, 171.8 ppm.

5.11.7 Ethyl 2-(1-tritylimidazol-4-yl)acetate (38)

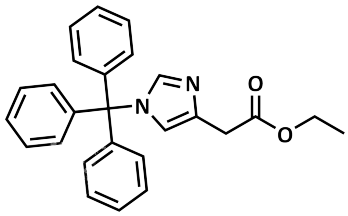

Ethyl 2-(1-tritylimidazol-4-yl)acetate was prepared by a modified literature procedure.[169] To a suspension of 2-(imidazol-4-yl)acetic acid hydrochloride (14.345 g, 88.24 mmol) in dry ethanol (270 mL) under an argon atmosphere, acetyl chloride (20.0 mL, 280.27 mmol, 3.18 eq.) was added dropwise at 0 °C. After one hour, the reaction mixture was warmed to room temperature, stirred for further 4 hours and concentrated under reduced pressure. The crude ethyl 2-(imidazol-4/5-yl)acetate was dried in vacuum and suspended in dry *N*,*N*-dimethylformamide (180 mL). Under vigorous stirring, triethylamine (31.0 mL, 222.41 mmol, 2.52 eq.) was added, followed by trityl chloride (20.815 g, 74.66 mmol, 0.85 eq.), and stirred for 19.5 hours. The mixture was diluted with ethyl acetate (500 mL) and washed with saturated aqueous sodium bicarbonate solution (400 mL), water (200 mL) and brine (250 mL). The organic phase was dried over anhydrous magnesium sulfate, filtered and concentrated under reduced pressure. The crude product was purified by column chromatography (CH:EA, 1:1) to afford 14.471 g ethyl 2-(1-tritylimidazol-4-yl)acetate (49%) as a pale yellowish solid.

TLC: R_f = 0.54-0.37 (CH:EA, 1:1).

^{1}H NMR (300 MHz, CD_2Cl_2, 25 °C): δ = 1.22 (t, 3 H, J = 7.1 Hz), 3.56 (d, 2 H, J = 0.8 Hz), 4.12 (q, 2 H, J = 7.1 Hz), 6.78 (d, 1 H, J = 1.3 Hz), 7.18 (m, 6 H), 7.35 (m, 9 H), 7.37 (d, 1 H, J = 1.4 Hz) ppm.

^{13}C NMR (75 MHz, CD_2Cl_2, 25 °C): δ = 14.3, 34.8, 60.8, 75.4, 119.8, 128.1, 129.9, 134.1, 138.5, 142.5, 171.3 ppm.

5.11.8 Ethyl 2-(1-tritylimidazol-4-yl)acrylate (41)

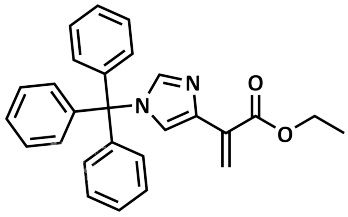

Ethyl 2-(1-tritylimidazol-4-yl)acrylate was prepared by a modified literature procedure.[290]

A suspension of ethyl 2-(1-tritylimidazol-4-yl)acetate (14.451 g, 36.45 mmol), potassium carbonate (15.128 g, 109.46 mmol, 3 eq.), paraformaldehyde (3.349 g, 111.54 mmol, 3.06 eq.)

and tetra-*n*-butylammonium bromide (0.602 g, 1.87 mmol, 0.05 eq.) in dry toluene (75 mL) was stirred for 22.5 hours at 50 °C. To the mixture, water (200 mL) was added and extracted with dichloromethane (1× 200 mL, 2× 100 mL). The combined organic phase was dried over anhydrous magnesium sulfate, filtered and concentrated under reduced pressure. The crude product was purified by column chromatography (CH:EA, 1:1) to afford 5.639 g ethyl 2-(1-tritylimidazol-4-yl)acrylate (38%) as a yellowish solid.

TLC: R_f = 0.70-0.57 (CH:EA, 1:1).

^{1}H NMR (300 MHz, CD_2Cl_2, 25 °C): δ = 1.22 (t, 3 H, J = 7.1 Hz), 4.17 (q, 2 H, J = 7.1 Hz), 6.17 (d, 1 H, J = 2.0 Hz), 6.51 (d, 1 H, J = 2.0 Hz), 7.20 (m, 6 H), 7.35 (m, 10 H), 7.40 (d, 1 H, J = 1.4 Hz) ppm.

^{13}C NMR (75 MHz, CD_2Cl_2, 25 °C): δ = 14.5, 61.3, 75.9, 121.9, 122.7, 128.6, 130.3, 134.0, 136.1, 139.2, 143.1, 166.5 ppm.

EI-MS: m/z = 408 $[M]^{\cdot+}$, 379 $[M\text{-}Et]^{\cdot+}$, 243 $[Trt]^{\cdot+}$, 165 $[M\text{-}Trt]^{\cdot+}$.

5.11.9 Ethyl 2-(imidazol-4/5-yl)acetate (37)

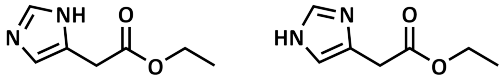

Ethyl 2-(imidazol-4/5-yl)acetate was prepared by a modified literature procedure.[169] To a suspension of 2-(imidazol-4-yl)acetic acid hydrochloride (6.025 g, 37.06 mmol) in dry ethanol (130 mL) under an argon atmosphere, acetyl chloride (10.5 mL, 147.14 mmol, 3.97 eq.) was added dropwise at -15 °C. The reaction mixture was slowly warmed to room temperature over 4 hours and stirred for further 20 hours. A saturated aqueous sodium carbonate solution (50 mL) was added and the pH value was adjusted to 9 with solid sodium carbonate. The mixture was concentrated under reduced pressure, suspended in saturated aqueous sodium bicarbonate solution (100 mL) and extracted with ethyl acetate (4× 125 mL). The combined organic phase was dried over anhydrous magnesium sulfate, filtered and concentrated under reduced pressure. The crude product was purified by short column chromatography (THF:NEt_3, 20:1) to afford 4.262 g ethyl 2-(imidazol-4/5-yl)acetate (75%) as a yellow oil.

TLC: R_f = 0.71-0.55 (THF:NEt_3, 20:1, visualized with $KMnO_4$ stain).

^{1}H NMR (300 MHz, CD_2Cl_2, 25 °C): δ = 1.23 (t, 3 H, J = 7.1 Hz), 3.64 (d, 2 H, J = 0.9 Hz), 4.13 (q, 2 H, J = 7.1 Hz), 6.96 (q, 1 H, J = 1.2, 0.9 Hz), 7.58 (d, 1 H, J = 1.2 Hz), 10.2 (br s, 1 H) ppm.

^{13}C NMR (75 MHz, CD_2Cl_2, 25 °C): δ = 14.5, 33.7, 61.4, 118.0, 131.5, 135.5, 171.7 ppm.

Ethyl 2-(imidazol-4/5-yl)acetate was prepared by a modified literature procedure.[168] A solution of ethyl 4-bromo-3-oxobutanoate (1.009 g, 4.83 mmol) in formamide (4.0 mL, 100.35 mmol, 20.79 eq.) was deoxygenated by flushing with argon for 10 minutes and

heated to 120 °C. After 2 hours, the reaction mixture was heated to 160 °C for 12 hours, and then concentrated under reduced pressure. No product was observed in the residue.

Ethyl 2-(imidazol-4/5-yl)acetate was prepared according to literature procedure.[293]
A suspension of ethyl 4-bromo-3-oxobutanoate (0.254 g, 1.21 mmol), formamidine hydrochloride (0.202 g, 2.50 mmol, 2.06 eq.) and potassium carbonate (0.665 g, 4.81 mmol, 3.96 eq.) in dry *N*,*N*-dimethylformamide (2.4 mL) under an argon atmosphere was heated to 100 °C for 15 hours. The reaction mixture was cooled to room temperature and concentrated under reduced pressure. No product was observed in the residue.

5.11.10 Ethyl 2-(1-(2-(trimethylsilyl)ethoxymethyl)imidazol-4/5-yl)acetate (40/39)

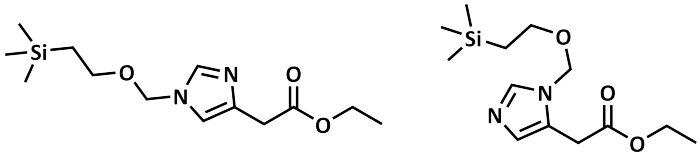

Ethyl 2-(1-(2-(trimethylsilyl)ethoxymethyl)imidazol-4/5-yl)acetate was prepared by a modified literature procedure.[174]
To a solution of ethyl 2-(imidazol-4/5-yl)acetate (7.461 g, 48.40 mmol) in dry tetrahydrofuran (98 mL) under an argon atmosphere, sodium hydride (60% in mineral oil, 2.446 g, 61.16 mmol, 1.26 eq.) was added in portion at 0 °C. After 15 minutes, the reaction mixture was warmed to room temperature and stirred for one hour. The suspension was cooled to 0 °C and 2-(trimethylsilyl)ethoxymethyl chloride (10.4 mL, 58.76 mmol, 1.21 eq.) was added. After 15 minutes, the mixture was warmed to room temperature and stirred for further 17 hours. The reaction was quenched by the addition of saturated aqueous ammonium chloride solution (45 mL) and water (90 mL). The organic phase was separated and the aqueous phase was extracted with dichloromethane (3× 150 mL). The combined organic phase was dried over anhydrous magnesium sulfate, filtered and concentrated under reduced pressure. The crude product was purified by column chromatography (EA:MeOH, 20:1) to afford 9.385 g ethyl 2-(1-(2-(trimethylsilyl)ethoxymethyl)imidazol-4/5-yl)acetate (68%, 4:5 regioisomers ratio of 1.0:0.5) as a yellow oil.

TLC: R_f = 0.76-0.50 (EA:MeOH, 20:1).

^{1}H NMR (300 MHz, CD_2Cl_2, 25 °C):
Ethyl 2-(1-(2-(trimethylsilyl)ethoxymethyl)imidazol-4-yl)acetate: δ = -0.02 (s, 9 H), 0.90 (m, 2 H), 1.24 (t, 3 H, J = 7.1 Hz), 3.49 (m, 2 H), 3.58 (d, 2 H, J = 0.9 Hz), 4.13 (q, 2 H, J = 7.1 Hz), 5.21 (s, 2 H), 6.98 (dt, 1 H, J = 1.4, 0.9 Hz), 7.47 (d, 1 H, J = 1.4 Hz) ppm.
Ethyl 2-(1-(2-(trimethylsilyl)ethoxymethyl)imidazol-5-yl)acetate: δ = -0.02 (s, 9 H), 0.88 (m, 2 H), 1.25 (t, 3 H, J = 7.1 Hz), 3.43 (m, 2 H), 3.69 (d, 2 H, J = 0.8 Hz), 4.14 (q, 2 H, J = 7.1 Hz), 5.26 (s, 2 H), 6.90 (dt, 1 H, J = 1.1, 0.8 Hz), 7.48 (d, 1 H, J = 1.1 Hz) ppm.

^{13}C NMR (75 MHz, CD_2Cl_2, 25 °C):
Ethyl 2-(1-(2-(trimethylsilyl)ethoxymethyl)imidazol-4-yl)acetate: δ = -1.26, 14.6, 18.2, 35.0, 61.2, 66.9, 76.5, 117.4, 136.4, 137.3, 171.6 ppm.
Ethyl 2-(1-(2-(trimethylsilyl)ethoxymethyl)imidazol-5-yl)acetate: δ = -1.28, 14.5, 18.1, 30.4, 61.7, 66.4, 75.1, 125.1, 130.1, 138.8, 170.3 ppm.

5.11.11 Ethyl 2-(1-(2-(trimethylsilyl)ethoxymethyl)imidazol-4-yl)acetate (40)

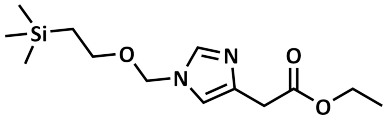

Ethyl 2-(1-(2-(trimethylsilyl)ethoxymethyl)imidazol-4-yl)acetate was prepared by a modified literature procedure.[173, 294]
To a solution of ethyl 2-(1-(2-(trimethylsilyl)ethoxymethyl)imidazol-4/5-yl)acetate (9.371 g, 32.95 mmol) in dry tetrahydrofuran (66 mL) under an argon atmosphere, 2-(trimethylsilyl)ethoxymethyl chloride (0.58 mL, 3.28 mmol, 0.10 eq.) was added. The reaction mixture was heated to 70 °C for 72 hours and concentrated under reduced pressure. The crude product was purified by column chromatography (EA:MeOH, 20:1) to afford 7.897 g ethyl 2-(1-(2-(trimethylsilyl)ethoxymethyl)imidazol-4-yl)acetate (84%) as a yellow oil.

TLC: R_f = 0.58-0.50 (EA:MeOH, 20:1).

^{1}H NMR (300 MHz, $CDCl_3$, 25 °C): δ = -0.03 (s, 9 H), 0.89 (m, 2 H), 1.26 (t, 3 H, J = 7.1 Hz), 3.48 (m, 2 H), 3.67 (d, 2 H, J = 0.9 Hz), 4.15 (q, 2 H, J = 7.1 Hz), 5.24 (s, 2 H), 7.03 (dt, 1 H, J = 1.4, 0.9 Hz), 7.68 (d, 1 H, J = 1.4 Hz) ppm.

^{13}C NMR (75 MHz, $CDCl_3$, 25 °C): δ = -1.26, 14.6, 18.2, 35.0, 61.2, 66.9, 76.5, 117.4, 136.4, 137.3, 171.6 ppm.

5.11.12 Ethyl 2-(1-(2-(trimethylsilyl)ethoxymethyl)imidazol-4-yl)acrylate (42)

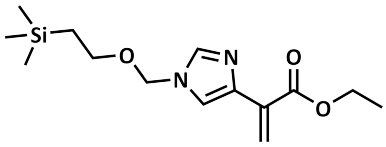

Ethyl 2-(1-(2-(trimethylsilyl)ethoxymethyl)imidazol-4-yl)acrylate was prepared by a modified literature procedure.[290]
To a solution of ethyl 2-(1-(2-(trimethylsilyl)ethoxymethyl)imidazol-4-yl)acetate (7.586 g, 26.67 mmol) in dry acetonitrile (54 mL) under an argon atmosphere, paraformaldehyde (2.378 g, 79.18 mmol, 2.97 eq.), tetra-*n*-butylammonium bromide (0.429 g, 1.33 mmol, 0.05 eq.) and potassium carbonate (10.932 g, 79.10 mmol, 2.97 eq.) was added. The reaction mixture was heated to 60 °C and stirred for 16 hours. The suspension was filtered

and concentrated under reduced pressure. To the residue, water (100 mL) was added, and then extracted with ethyl acetate (1× 100 mL, 3× 50 mL). The combined organic phase was dried over anhydrous magnesium sulfate, filtered and concentrated under reduced pressure. The crude product was purified by column chromatography (EA:MeOH, 100:1) to afford 2.045 g ethyl 2-(1-(2-(trimethylsilyl)ethoxymethyl)imidazol-4-yl)acrylate (26%) as a yellowish oil.

TLC: R_f = 0.87-0.74 (EA:MeOH, 100:1).

^{1}H NMR (300 MHz, $CDCl_3$, 25 °C): δ = -0.02 (s, 9 H), 0.91 (m, 2 H), 1.36 (t, 3 H, J = 7.1 Hz), 3.52 (m, 2 H), 4.30 (q, 2 H, J = 7.1 Hz), 5.31 (s, 2 H), 6.34 (d, 1 H, J = 1.3 Hz), 6.69 (d, 1 H, J = 1.3 Hz), 7.62 (d, 1 H, J = 1.4 Hz), 7.85 (s, 1 H) ppm.

^{13}C NMR (75 MHz, $CDCl_3$, 25 °C): δ = -1.28, 14.4, 17.9, 61.1, 66.9, 76.6, 116.8, 119.1, 124.2, 132.2, 136.9, 165.9 ppm.

EI-MS: m/z = 491 $[M_2\text{-}C_2H_4SiMe_3]^{\cdot+}$, 296 $[M]^{\cdot+}$, 223 $[M\text{-}SiMe_3]^{\cdot+}$, 223 $[M\text{-}COOEt]^{\cdot+}$, 195 $[M\text{-}C_2H_4SiMe_3]^{\cdot+}$, 180 $[M\text{-}C_3H_7SiMe_3]^{\cdot+}$, 166 $[M\text{-}C_4H_9SiMe_3]^{\cdot+}$.

5.12 Preparation of Poly(ethyl 2-(imidazol-4-yl)acetate)

5.12.1 Poly(ethyl 2-(1-tritylimidazol-4-yl)acetate) (43)

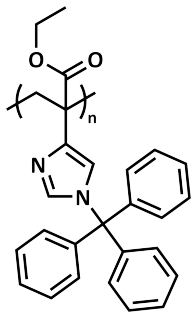

To a solution of ethyl 2-(1-tritylimidazol-4-yl)acetate) (4.324 g, 10.58 mmol) in anisole (4.3 mL), azobisisobutyronitrile (11.4 mg, 69.4 μmol) was added. The reaction mixture was deoxygenated by flushing with argon for 15 minutes and heated to 70 °C. After 24 hours, the mixture was cooled to room temperature and the polymer was purified by dialysis against tetrahydrofuran.

SEC (DMAc, PMMA calibration): $\overline{M}_n$ = 157,900 g·mol^{-1}, $Đ$ = 1.25.

5.12.2 Poly(ethyl 2-(1-(2-(trimethylsilyl)ethoxymethyl)imidazol-4-yl)acetate) (44)

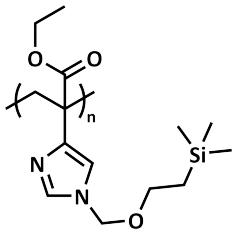

A solution of ethyl 2-(1-(2-(trimethylsilyl)ethoxymethyl)imidazol-4-yl)acetate) (1.954 g, 6.59 mmol) and azobisisobutyronitrile (7.3 mg, 44.5 μmol) in *N*,*N*-dimethylformamide (2.7 mL) was deoxygenated by flushing with argon for 10 minutes and heated to 70 °C for 25 hours. The polymer was purified by dialysis against methanol.

^{1}H NMR (400 MHz, CD_2Cl_2, 25 °C): δ = -0.42-0.32 (9 H), 0.56-1.45 (5 H), 1.51-2.99 (2 H), 3.00-4.47 (4 H), 4.81-6.11 (2 H), 6.26-9.04 (2 H) ppm.

^{13}C NMR (101 MHz, CD_2Cl_2, 25 °C): δ = -1.0, 13.9, 18.3, 49.0, 60.2, 66.8, 76.2, 119.8, 134.8, 140.0, 172.9 ppm.

SEC (DMAc, PMMA calibration): $\overline{M}_n$ = 67,600 g·mol^{-1}, $Đ$ = 1.68.

5.13 Synthesis of Diethyl 1-(imidazol-1-yl)vinylphosphonate

5.13.1 Diethyl ethynylphosphonate (45)

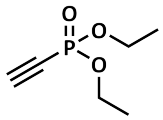

Diethyl ethynylphosphate was prepared by a modified literature procedure.[176]
To a solution of trimethylsilylacetylene (21.5 mL, 152.72 mmol) in dry diethyl ether (500 mL) under an argon atmosphere, ethylmagnesium bromide (3.0 M in diethyl ether, 56.0 mL, 168.00 mmol, 1.10 eq.) at -10 °C was added dropwise. After 15 minutes, the mixture was warmed to room temperature and stirred for 2.5 hours. The solution was cooled to -10 °C and diethyl chlorophosphate (22.5 mL, 155.70 mmol, 1.02 eq.) was added dropwise. After 30 minutes, the mixture was warmed to room temperature and stirred for further 3.5 hours. The reaction was quenched by the addition of a saturated aqueous ammonium chloride solution (20 mL), dried over anhydrous magnesium sulfate, filtered and concentrated under reduced pressure. The crude material was dissolved in dichloromethane (500 mL) and tetrabutylammonium fluoride trihydrate (52.392 g, 166.05 mmol, 1.09 eq.) was added at 0 °C. After 15 minutes, the reaction mixture was warmed to room temperature and stirred for 1.5 hours. The organic phase was washed with water (2× 400 mL), dried over anhydrous

magnesium sulfate, filtered and concentrated under reduced pressure. The crude product was purified by column chromatography (EA) to afford 6.157 g diethyl ethynylphosphonate (25%) as a colorless oil.

Diethyl ethynylphosphate was furthermore prepared by another literature procedure.[177] To diethyl chlorophosphate (8.5 mL, 58.62 mmol, 1.01 eq.) under an argon atmosphere, ethynylmagnesium bromide (0.5 M in tetrahydrofuran, 116.0 mL, 58.00 mmol) was added dropwise over one hour at -15 °C. After 15 minutes, the mixture was warmed to room temperature and stirred for 2.3 hours. The reaction was quenched with saturated aqueous sodium bicarbonate solution (20 mL) and concentrated under reduced pressure. The residue was dissolved in dichloromethane (15 mL), dried over anhydrous magnesium sulfate, filtered and concentrated under reduced pressure. The crude product was purified by column chromatography (EA) to afford 2.071 g diethyl ethynylphosphonate (22%) as a yellowish viscous liquid.

TLC: R_f = 0.74-0.64 (EA, visualized with $KMnO_4$ stain).

^{1}H NMR (400 MHz, $CDCl_3$, 25 °C): δ = 1.37 (dt, 6 H, J = 7.1, 0.8 Hz), 2.90 (d, 1 H, J = 13.2 Hz), 4.17 (m, 4 H) ppm.

^{13}C NMR (101 MHz, $CDCl_3$, 25 °C): δ = 16.2 (d, J = 7.0 Hz), 63.6 (d, J = 5.6 Hz), 74.5 (d, J = 288.9 Hz), 87.8 (d, J = 50.7 Hz) ppm.

^{31}P NMR (162 MHz, $CDCl_3$, 25 °C): δ = -8.38 ppm.

5.13.2 Diethyl 1-(imidazol-1-yl)vinylphosphonate (46)

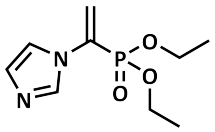

Diethyl 1-(imidazol-1-yl)vinylphosphonate was prepared by a modified literature procedure.[115]
To a solution of diethyl ethynylphosphonate (5.964 g, 36.78 mmol) in dry dichloromethane (75 mL) under an argon atmosphere, imidazole (2.516 g, 36.96 mmol, 1.00 eq.) was added at -20 °C. A solution of triphenylphosphine (9.629 g, 36.71 mmol, 0.99 eq.) in dry dichloromethane (15 mL) was added dropwise, and the reaction mixture was allowed to warm to room temperature overnight. After 24 hours, the mixture was concentrated under reduced pressure and purified by column chromatography (THF:NEt_3, 100:1) and a second column chromatography (EA:NEt_3, 20:1) to afford 4.072 g diethyl 1-(imidazol-1-yl)vinylphosphonate (48%) as a pale yellowish oil.

TLC: R_f = 0.55-0.35 (THF:NEt_3, 100:1), 0.43-0.31 (EA:NEt_3, 20:1).

^{1}H NMR (300 MHz, CD_2Cl_2, 25 °C): δ = 1.30 (dt, 6 H, J = 7.1, 0.5 Hz), 4.14 (m, 4 H), 5.97 (dd, 1 H, J = 24.7, 1.1 Hz), 6.06 (dd, 1 H, J = 3.2, 1.1 Hz), 7.05 (m, 1 H), 7.25 (m, 1 H), 7.79 (m, 1 H) ppm.

^{13}C NMR (75 MHz, CD_2Cl_2, 25 °C): δ = 16.6 (d, J = 6.0 Hz), 63.8 (d, J = 6.0 Hz), 118.8 (d, J = 3.0 Hz), 121.9 (d, J = 15.9 Hz), 130.3, 134.0, 136.7, 136.9 (d, J = 2.3 Hz) ppm.

^{31}P NMR (162 MHz, CD_2Cl_2, 25 °C): δ = 12.27 ppm.

EI-MS: 230 $[M]^{\cdot+}$, 215 $[M\text{-}Me]^{\cdot+}$, 201$[M\text{-}Et]^{\cdot+}$.

5.14 Preparation of Poly(diethyl 1-(imidazol-1-yl)vinylphosphonate) (47)

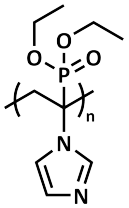

A mixture of diethyl 1-(imidazol-1-yl)vinylphosphonate (3.521 g, 15.29 mmol) and azobisisobutyronitrile (16.6 mg, 0.1 mmol) was deoxygenated by flushing with argon for 15 minutes and heated to 70 °C. After 24 hours, the mixture was cooled to room temperature and the polymer was purified by dialysis against methanol to afford 0.256 g poly(diethyl 1-(imidazol-1-yl)vinylphosphonate) as a yellow solid.

^{1}H NMR (400 MHz, CD_2Cl_2, 25 °C): δ = 0.19-1.88, 1.90-3.27, 3.37-5.08, 6.48-11.17 ppm.

^{13}C NMR (101 MHz, CD_2Cl_2, 25 °C): δ = 11.6-20.1, 42.0-48.2, 58.9-69.2, 116.8-131.9, 134.9-143.6 ppm.

^{31}P NMR (162 MHz, CD_2Cl_2, 25 °C): δ = 5.64-38.87 ppm.

SEC (Chloroform, PMMA calibration): $\overline{M}_n$ = 125,900 g·mol^{-1}, $Đ$ = 6.74.

5.15 Synthesis of Ethyl 2-(hydroxymethyl)acrylate (48)

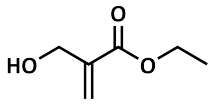

Ethyl 2-(hydroxymethyl)acrylate was prepared according to a literature procedure.[183] To a solution of ethyl acrylate (82.0 mL, 751.88 mmol), triethylenediamine (5.041 g, 44.93 mmol, 0.06 eq.) in acetonitrile (90 mL), and a formaldehyde solution (37% in water, 85.0 mL, 1.142 mol, 1.52 eq.) was added and heated to 50 °C for 59 hours. The solution was cooled to room temperature and 6.0 M hydrochloric acid (4 mL) was added. The mixture was diluted with water (200 mL) and extracted with diethyl ether (1× 300 mL, 2× 150 mL). The combined organic phase was washed with brine (200 mL), dried over anhydrous magnesium sulfate, filtered and concentrated under reduced pressure. The crude product was purified by column chromatography (CH:EA, 2:1) to afford 63 g ethyl 2-(hydroxymethyl)acrylate (64%), which was furthermore distilled (53 °C, 0.7 mbar) to afford 43.363 g ethyl 2-(hydroxymethyl)acrylate (44%) as a colorless liquid.

TLC: R_f = 0.45-0.36 (CH:EA, 2:1).

^{1}H NMR (300 MHz, $CDCl_3$, 25 °C): δ = 1.31 (t, 3 H, J = 7.2 Hz), 2.39 (s, 1 H), 4.24 (q, 2 H, J = 7.2 Hz), 4.32 (dd, 2 H, J = 1.4, 0.8 Hz), 5.82 (q, 1 H, J = 1.4), 6.52 (dt, 1 H, J = 1.4, 0.8 Hz) ppm.

^{13}C NMR (75 MHz, $CDCl_3$, 25 °C): δ = 14.3, 61.0, 62.7, 125.7, 139.7, 166.5 ppm.

5.16 Synthesis of Ethyl 2-(chloromethyl)acrylate (49)

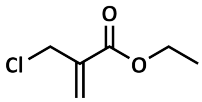

Ethyl 2-(chloromethyl)acrylate was prepared according to a literature procedure.[295] To ethyl 2-(hydroxymethyl)acrylate (14.0 mL, 114.89 mmol) under an argon atmosphere, thionyl chloride (12.5 mL, 172.33 mmol, 1.50 eq.) was added dropwise at 0 °C. After 1.5 hours, the reaction mixture was warmed to room temperature and stirred for 18 hours. The solution was diluted with n-heptane (75 mL) and concentrated under reduced pressure. The crude product was purified by column chromatography (CH:EA, 5:1) and distillation (48 °C, 5 mbar) to afford 10.127 g ethyl 2-(chloromethyl)acrylate (59%) as a colorless liquid.

TLC: R_f = 0.74-0.62 (CH:EA, 5:1, visualized with $KMnO_4$ stain).

^{1}H NMR (300 MHz, $CDCl_3$, 25 °C): δ = 1.30 (t, 3 H, J = 7.1 Hz), 4.23 (q, 2 H, J = 7.1 Hz), 4.29 (dt, 2 H, J = 1.2, 0.3 Hz), 5.96 (m, 1 H), 6.35 (m, 1 H) ppm.

^{13}C NMR (75 MHz, $CDCl_3$, 25 °C): δ = 14.5, 43.3, 61.8, 128.8, 137.9, 165.4 ppm.

5.17 Preparation of Poly(ethyl 2-(chloromethyl)acrylate) (50)

5.17.1 Free Radical Polymerization

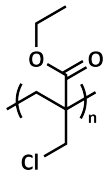

Poly(ethyl 2-(chloromethyl)acrylate) was prepared by a modified literature procedure.[182, 296]

A solution of ethyl 2-(chloromethyl)acrylate and azobisisobutyronitrile (1.0 mol%) in solvent was degassed by three freeze-pump-thaw cycles and heated to 65 °C. The polymerization was terminated by cooling in liquid nitrogen and the mixture was precipitated in methanol (45 mL) to afford the polymer as a white solid.

^{1}H NMR (300 MHz, CD_2Cl_2, 25 °C): δ = 1.12-1.10 (3 H), 1.80-3.00 (2 H), 3.60-4.28 (4 H) ppm.

Elemental Analysis: C = 49.6%, H = 6.1%, Cl = 23.8%
calculated: C = 48.5%, H = 6.1%, Cl = 23.9%

Table 5.8: Free radical polymerization of ethyl 2-(chloromethyl)acrylate.

Entry	Monomer	Initiator	Solvent	Time	Yield
1	0.762 g	8.0 mg	-	60 h	0.596 g (78%)
2	0.503 g	4.7 mg	220 μL Benzene	41 h	0.162 g (32%)
3	0.507 g	5.2 mg	220 μL Anisole	69 h	0.133 g (22%)

Table 5.9: SEC data of free radically polymerized poly(ethyl 2-(chloromethyl)acrylate).

Entry	Solvent	$\overline{M}_n$ [a)]	$Đ$ [a)]
1	-	14,100 g·mol^{-1}	1.67
2	Benzene	6,600 g·mol^{-1}	1.73
3	Anisole	3,300 g·mol^{-1}	1.38

[a)] SEC (THF, PMMA calibration).

5.17.2 RAFT Polymerization

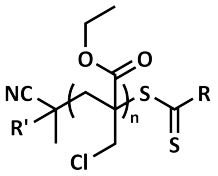

A solution of ethyl 2-(chloromethyl)acrylate, chain transfer agent (1.0 mol%) and azobisisobutyronitrile (0.3 mol%) in solvent was degassed by three freeze-pump-thaw cycles and heated to 65 °C. The polymerization was terminated by cooling in liquid nitrogen and the mixture was precipitated in methanol (45 mL) to afford the polymer as a solid.

Table 5.10: RAFT polymerization of ethyl 2-(chloromethyl)acrylate.

Entry	Monomer	Chain Transfer Agent	Initiator	Solvent	Yield
1[a)]	0.504 g	9.4 mg CPzCD	1.4 mg	-	0.067 g (13%)
2[b)]	0.516 g	9.6 mg CPzCD	1.7 mg	220 μL Benzene	0.037 g (7%)

[a)] Polymerized for 64 h, [b)] Polymerized for 50 h.

Table 5.11: SEC data from the RAFT polymerizations of ethyl 2-(chloromethyl)acrylate.

Entry	Solvent	Chain Transfer Agent	$\overline{M}_n$ [a)]	$Đ$ [a)]
1	-	CPzCD	6,500 g·mol^{-1}	1.53
2	Benzene	CPzCD	1,800 g·mol^{-1}	2.06

[a)] SEC (THF, PMMA calibration).

5.18 Synthesis of Ethyl 2-((tosyloxy)methyl)acrylate (51)

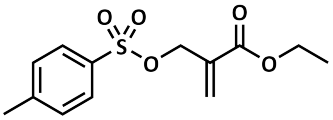

Ethyl 2-((tosyloxy)methyl)acrylate was prepared by a modified literature procedure.[185] To a solution of ethyl 2-(hydroxymethyl)acrylate (2.4 mL, 19.70 mmol) and tosyl chloride (4.651 g, 24.40 mmol, 1.24 eq.) in dry dichloromethane (200 mL) under an argon atmosphere, sodium hydride (60% in mineral oil, 0.943 g, 23.57 mmol, 1.20 eq.) was added in portion at 0 °C. The reaction mixture was warmed to room temperature and stirred for 25 hours. The reaction was quenched with saturated aqueous sodium bicarbonate solution (20 mL) and diluted with water (100 mL). The organic phase was separated and the aqueous phase extracted with dichloromethane (50 mL). The combined organic phase was washed with water (100 mL), and brine (100 mL), dried over anhydrous magnesium sulfate, filtered and concentrated under reduced pressure. The crude product was purified by column chromatography (DCM) to afford 3.553 g ethyl 2-((tosyloxy)methyl)acrylate (63%) as a colorless oil.

TLC: R_f = 0.69-0.54 (DCM).

^{1}H NMR (300 MHz, CD_2Cl_2, 25 °C): δ = 1.24 (t, 3 H, J = 7.1 Hz), 2.45 (s, 3 H), 4.15 (q, 2 H, J = 7.1 Hz), 4.71 (dd, 2 H, J = 1.5, 0.9 Hz), 5.96 (dt, 1 H, J = 1.5, 0.9 Hz), 6.34 (q, 1 H, J = 0.9), 7.38 (m, 2 H), 7.79 (m, 2 H) ppm.

^{13}C NMR (75 MHz, CD_2Cl_2, 25 °C): δ = 14.4, 22.0, 61.7, 68.5, 128.5, 129.2, 130.5, 133.4, 134.5, 145.8, 164.8 ppm.

5.19 Preparation of Poly(ethyl 2-((tosyloxy)methyl)acrylate)

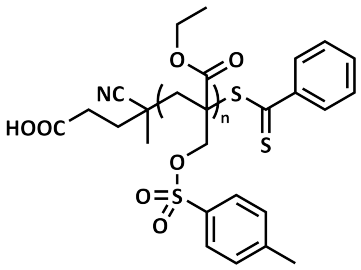

A solution of ethyl 2-((tosyloxy)methyl)acrylate, trioxane, 4-cyanovaleric acid dithiobenzoate and 2,2'-azobis(4-methoxy-2,4-dimethylvaleronitrile) in dry tetrahydrofuran (0.7 mL) was degassed by three freeze-pump-thaw cycles and heated to 40 °C for 12 hours. To monitor the polymerization by ^{1}H NMR and SEC (DMAc), samples at 0.5, 1, 2, 3, 5, 8 and 12 hours were taken. The polymerization was terminated by cooling in liquid nitrogen and the mixture precipitated in methanol (45 mL) to afford poly(ethyl 2-((tosyloxy)methyl)acrylate) as a white solid.

^{1}H NMR (300 MHz, CD_2Cl_2, 25 °C): δ = 1.10 (3 H), 1.53-2.26 (m, 2 H), 2.41 (3 H), 3.50-4.65 (m, 4 H), 7.37 (2 H), 7.79 (2 H) ppm.

Table 5.12: RAFT polymerization of ethyl 2-((tosyloxy)methyl)acrylate.

Entry	Monomer	Chain Transfer Agent	Initiator	Trioxane
1	1.211 g	12.0 mg (1.0 mol%)	4.2 mg (0.3 mol%)	68.3 mg
2	0.988 g	9.8 mg (1.0 mol%)	1.0 mg (0.1 mol%)	67.2 mg

5.20 Preparation of Poly(ethyl 2-(hydroxymethyl)acrylate) (52)

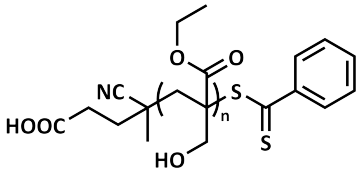

Ethyl 2-(hydroxymethyl)acrylate was polymerized by a modified literature procedure.[188] A solution of ethyl 2-(hydroxymethyl)acrylate (5.0 M), 4-cyanovaleric acid dithiobenzoate (1.0 mol%), 2,2'-azobis(4-methoxy-2,4-dimethylvaleronitrile) (0.1 mol%) and trioxane in dry tetrahydrofuran was deoxygenated by flushing with argon for 30 minutes at -15 °C before being heated to 40 °C. The polymerization was terminated by cooling in liquid nitrogen and the mixture precipitated in diethyl ether to afford the polymer as a pink solid.

^{1}H NMR (300 MHz, Acetone-d_6, 25 °C): δ = 0.98-1.59 (3 H), 1.59-2.38 (2 H), 3.25-4.95 (5 H), 7.35-8.09 ppm.

^{13}C NMR (75 MHz, Acetone-d_6, 25 °C): δ = 13.5-14.6, 41.2-45.3, 49.9-52.6, 60.0-65.6, 173.2-178.3 ppm.

Table 5.13: RAFT polymerization of ethyl 2-(hydroxymethyl)acrylate.

Polymer	Monomer	Chain Transfer Agent	Initiator	Trioxane	Yield
52a[a)]	5.002 g	0.107 g	11.7 mg	-	3.545 g (71%)
52b[b)]	14.913 g	0.325 g	35.0 mg	1.208 g	11.415 g (77%)
52c[c)]	14.916 g	0.324 g	35.3 mg	1.211 g	7.759 g (52%)

Polymerized for [a)] 18 h, [b)] 13 h, [c)] 15 h.

Table 5.14: SEC data from the RAFT polymerization of ethyl 2-(hydroxymethyl)acrylate.

Polymer	Conversion[a)]	$\overline{M}_n$[a)]	DP[a)]	$\overline{M}_n$[b)]	$Đ$[b)]
52a	-	-	-	18,300 g·mol^{-1}	1.13
52b	78%	11,100 g·mol^{-1}	83	20,700 g·mol^{-1}	1.11
52c	50%	7,100 g·mol^{-1}	53	16,700 g·mol^{-1}	1.11

[a)] Determined by ^{1}H NMR, [b)] SEC (DMAc, PMMA calibration).

Kinetic study of the RAFT polymerization of ethyl 2-(hydroxymethyl)acrylate.
A solution of ethyl 2-(hydroxymethyl)acrylate (2.990 g, 22.98 mmol), 4-cyanovaleric acid dithiobenzoate (0.067 g, 0.24 mmol), 2,2'-azobis(4-methoxy-2,4-dimethylvaleronitrile) (0.022 g, 0.07 mmol) and trioxane (0.309 g, 3.43 mmol) in dry tetrahydrofuran (4.6 mL) was degassed by three freeze-pump-thaw cycles and heated to 40 °C for 18 hours. To monitor the polymerization by ^{1}H NMR and SEC (DMAc), samples at 0.5, 1, 2, 3, 5, 8, 12 and 18 hours were taken. The polymerization was terminated by cooling in liquid nitrogen and the mixture precipitated in cyclohexane (45 mL) to afford 1.365 g poly(ethyl 2-(hydroxymethyl)acrylate) as a pink solid.

5.21 Preparation of Poly(ethylene oxide)-*block*-poly(ethyl 2-(hydroxymethyl)acrylate)

5.21.1 *N*-Succinimidyl 4-((phenylcarbonothioyl)thio)-4-cyanovalerate

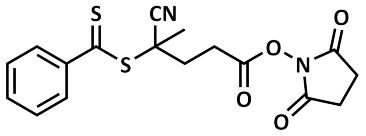

N-Succinimidyl 4-((phenylcarbonothioyl)thio)-4-cyanovalerate was prepared according to a literature procedure.[189]
To a solution of 4-cyanovaleric acid dithiobenzoate (2.214 g, 7.92 mmol) and *N*-hydroxysuccinimide (0.919 g, 7.99 mmol, 1.01 eq.) in dry dichloromethane (15 mL) under an argon atmosphere, *N*,*N'*-dicyclohexylcarbodiimide (1.661 g, 8.55 mmol, 1.08 eq.) was added. The reaction mixture was stirred for 23.5 hours at room temperature, filtered and concentrated under reduced pressure. The residue was purified by column chromatography (CH:EA, 1:1) to afford 1.867 g *N*-succinimidyl 4-((phenylcarbonothioyl)thio)-4-cyanovalerate (63%) as a pink solid.

TLC: R_f = 0.53-0.43 (CH:EA, 1:1).

^{1}H NMR (300 MHz, CD_2Cl_2, 25 °C): δ = 1.95 (s, 3 H), 2.50-2.80 (m, 2 H), 2.82 (s, 2 H), 2.99 (m, 2 H), 7.43 (m, 2 H), 7.59 (m, 1 H), 7.94 (m, 2) ppm.

5.21.2 *N*-(Poly(ethylene oxide)) 4-((phenylcarbonothioyl)thio)-4-cyanovaleramide (53)

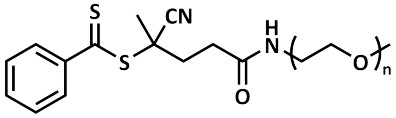

N-(Poly(ethylene oxide)) 4-((phenylcarbonothioyl)thio)-4-cyanovaleramide was prepared according to a literature procedure.[189]
To a solution of *N*-succinimidyl 4-((phenylcarbonothioyl)thio)-4-cyanovalerate (1.155 g, 3.07 mmol, 1.23 eq.) in dry dichloromethane (22 mL) under an argon atmosphere, a solution of α-methoxy-ω-amino poly(ethylene oxide) (5.005 g, 2.49 mmol) in dry dichloromethane (6 mL) was added and stirred for 22 hours at room temperature. The reaction mixture was precipitated in diethyl ether (500 mL) to afford 5.013 g *N*-(poly(ethylene oxide)) 4-((phenylcarbonothioyl)thio)-4-cyanovaleramide (89%) as a pink solid.

^{1}H NMR (300 MHz, CD_2Cl_2, 25 °C): δ = 1.92 (s, 3 H), 2.34-2.68 (m, 4 H), 3.32 (s, 3 H), 3.38-3.90 (183 H) 6.37 (s, 1 H), 7.41 (t, 2 H, J = 7.8 Hz), 7.58 (t, 1 H, J = 7.1 Hz), 7.91 (d, 2 H, J = 7.3 Hz) ppm.

SEC (DMAc, PEO calibration): $\overline{M}_n$ = 2,000 g·mol^{-1}, $Đ$ = 1.07.

5.21.3 Poly(ethylene oxide)-*block*-poly(ethyl 2-(hydroxymethyl)acrylate) (54)

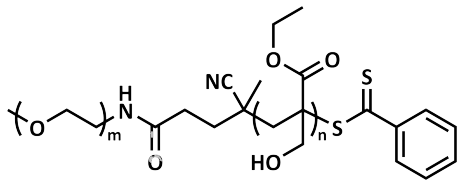

A solution of ethyl 2-(hydroxymethyl)acrylate (5.046 g, 38.77 mmol), *N*-(poly(ethylene oxide)) 4-((phenylcarbonothioyl)thio)-4-cyanovaleramide (1.101 g, 0.48 mmol), 2,2'-azo-bis(4-methoxy-2,4-dimethylvaleronitrile) (16.0 mg, 0.05 mmol) and trioxane (0.356 g, 3.96 mmol) in dry tetrahydrofuran (7.7 mL) was deoxygenated by flushing with argon for 15 minutes at -15 °C before being heated to 40 °C for 14 hours. The polymerization was terminated by cooling in liquid nitrogen and the mixture was poured into cyclohexane (350 mL). The polymer was dissolved in acetone and precipitated in *n*-pentane (2× 350 mL) to afford 4.645 g poly(ethylene oxide)-*block*-poly(ethyl 2-(hydroxymethyl)acrylate) (76%) as a pink solid.

^{1}H NMR (300 MHz, Acetone-d_6, 25 °C): δ = 0.95-1.55, 1.59-2.29, 3.30-3.4.94, 7.16-7.32, 7.38-7.52, 7.54-7.67, 7.81-7.97 ppm.

Table 5.15: SEC data of poly(ethylene oxide)-*block*-poly(ethyl 2-(hydroxymethyl)acrylate).

Polymer	Conversion[a)]	$\overline{M}_n$[a)]	DP[a)]	$\overline{M}_n$[b)]	$Đ$[b)]
54	82%	11,300 g·mol^{-1}	69	20,600 g·mol^{-1}	1.10

[a)] Determined by ^{1}H NMR, [b)] SEC (DMAc, PMMA calibration).

5.22 Preparation of Poly(ethyl 2-(hydroxymethyl)acrylate)-*block*-poly(*n*-butyl methacrylamide)

5.22.1 *n*-Butyl methacrylamide (55)

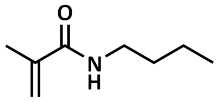

N-Butyl methacrylamide was prepared according to a literature procedure.[190]
To a solution of methacryloyl chloride (9.5 mL, 98.15 mmol) and hydroquinone (0.082 g, 0.75 mmol, 0.01 eq.) in dry dichloromethane (120 mL) under an argon atmosphere, *n*-butylamine (11.5 mL, 116.35 mmol, 1.19 eq.) and dry Hünig's base (23.5 mL, 134.91 mmol, 1.37 eq.) were added at -20 °C. After 30 minutes, the reaction mixture was warmed to room temperature, stirred for 3.5 hours and washed with water (2× 100 mL). The organic phase was dried over anhydrous magnesium sulfate, filtered and concentrated under reduced pressure. The crude product was purified by distillation (60 °C, $5{\cdot}10^{-3}$ mbar) to afford 11.400 g *n*-butyl methacrylamide (81%) as a colorless liquid.

^{1}H NMR (300 MHz, $CDCl_3$, 25 °C): δ = 0.92 (t, 3 H, J = 7.2 Hz), 1.28-1.43 (m, 2 H), 1.45-1.58 (m, 2 H), 1.95 (dd, 3 H, J = 1.6, 1.0 Hz), 3.30 (td, 2 H ,J = 7.2, 5.7 Hz), 5.25 (m, 1 H), 5.65 (p, 1 H, J = 1.0 Hz), 5.82 (br s, 1 H) ppm.

^{13}C NMR (75 MHz, $CDCl_3$, 25 °C): δ = 13.9, 18.9, 20.2, 31.8, 39.5, 119.2, 140.4, 168.6 ppm.

5.22.2 Poly(ethyl 2-(hydroxymethyl)acrylate)-*block*-poly(*n*-butyl methacrylamide) (56)

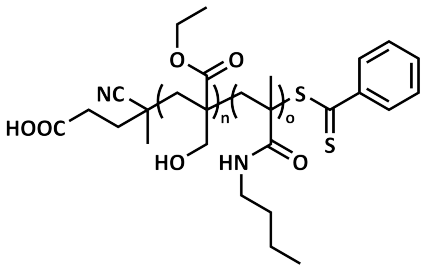

A solution of *n*-butyl methacrylamide (5.007 g, 35.46 mmol), poly(ethyl 2-(hydroxymethyl)acrylate) (3.695 g, 0.33 mmol), 2,2'-azobis(4-methoxy-2,4-dimethylvaleronitrile) (10.7 mg, 0.03 mmol) and trioxane (0.364 g, 4.04 mmol) in dry tetrahydrofuran (7.5 mL) was deoxygenated by flushing with argon for 20 minutes at -15 °C, and heated to 40 °C for 12 hours. The polymerization was terminated by cooling in liquid nitrogen and the mixture was poured into cyclohexane (900 mL). The polymer was dissolved in dichloromethane and precipitated in diethyl ether (2× 900 mL) to afford 5.188 g poly(ethyl 2-(hydroxymethyl)acrylate)-*block*-poly(*n*-butyl methacrylamide) (60%) as a purple solid.

^{1}H NMR (300 MHz, CD_2Cl_2, 25 °C): δ = 0.15-2.25, 2.63-4.99, 5.70-6.53, 7.27-8.24 ppm.

^{13}C NMR (75 MHz, CD_2Cl_2, 25 °C): δ = 12.9-15.8, 19.8-21.9, 29.6-32.6, 39.4-47.9, 49.5-52.4, 59.7-64.6, 173.5-181.5 ppm.

Table 5.16: SEC data of poly(ethyl 2-(hydroxymethyl)acrylate)-*block*-poly(*n*-butyl methacrylamide).

Polymer	Conversion[a)]	$\overline{M}_n$[a)]	DP[a)]	$\overline{M}_n$[b)]	$Đ$[b)]
56	37%	17,100 g·mol^{-1}	42	26,400 g·mol^{-1}	1.17

[a)] Determined by ^{1}H NMR, [b)] SEC (DMAc, PMMA calibration).

5.23 Modification of Poly(ethyl 2-(hydroxymethyl)acrylate)

5.23.1 Tosylation of Poly(ethyl 2-(hydroxymethyl)acrylate) (57)

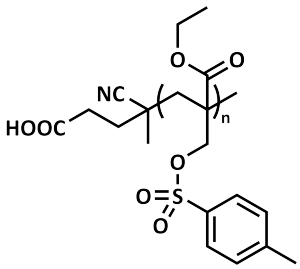

Poly(ethyl 2-(hydroxymethyl)acrylate) was tosylated by a modified literature procedure.[193]

To a solution of poly(ethyl 2-(hydroxymethyl)acrylate) (0.207 g, 0.02 mmol) in dry dichloromethane (3 mL) and dry pyridine (2 mL) under an argon atmosphere, a suspension of tosyl chloride (0.863 g, 4.52 mmol, 2.85 eq. per repeating unit) in dry dichloromethane (1 mL) was added at 0 °C. The reaction mixture was warmed to room temperature and stirred for 48 hours. The solution was diluted with dichloromethane (30 mL) and washed with a saturated aqueous ammonium chloride solution (100 mL), a saturated aqueous sodium carbonate solution (100 mL), and brine (100 mL). The organic phase was dried over anhydrous magnesium sulfate, filtered and concentrated under reduced pressure. The polymer was precipitated in methanol (45 mL) to afford 0.182 g poly(ethyl 2-((tosyloxy)methyl)acrylate) (40%) as a beige solid.

^{1}H NMR (300 MHz, $CDCl_3$, 25 °C): δ = 0.53-2.93, 3.10-5.14, 7.11-8.31 ppm.

SEC (THF, PMMA calibration): $\overline{M}_n$ = 13,800 g·mol^{-1}, $Đ$ = 1.32.

Elemental Analysis: C = 55.2%, H = 6.0%, N = 0.4%, S = 6.2%
calculated: C = 54.9%, H = 5.7%, N = 0.1%, S = 11.3%

5.23.2 Mesylation of Poly(ethyl 2-(hydroxymethyl)acrylate) (58)

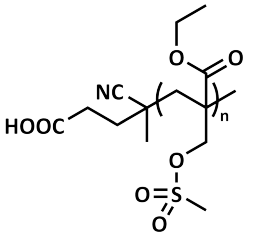

Poly(ethyl 2-(hydroxymethyl)acrylate) was mesylated by a modified literature procedure.[193]
To a solution of poly(ethyl 2-(hydroxymethyl)acrylate) (1.011 g, 0.14 mmol) in dry dichloromethane (10 mL) and dry pyridine (3.4 mL) under an argon atmosphere, mesyl chloride (2.9 mL, 37.47 mmol, 5 eq. per repeating unit) was added dropwise at -15 °C. The reaction mixture was warmed to room temperature and stirred for 24 hours. The polymer was precipitated in methanol (2× 220 mL) and diethyl ether (2× 220 mL) to afford 1.531 g poly(ethyl 2-((mesyloxy)methyl)acrylate) (96%) as a white solid.

^{1}H NMR (300 MHz, CD_2Cl_2, 25 °C): δ = 1.20-1.44 (3 H), 1.79-2.46 (2 H), 3.03-3.34 (3 H), 3.94-4.80 (4 H) ppm.

SEC (THF, PMMA calibration): $\overline{M}_n$ = 10,400 g·mol^{-1}, $Đ$ = 1.22.

Elemental Analysis: C = 41.3%, H = 5.9%, N < 0.3%, S = 15.0%, Cl = 0.4%
calculated: C = 40.8%, H = 5.8%, N = 0.1%, S = 15.6%, Cl = 0.0%

5.23.3 Poly(ethyl 2-(morpholinomethyl)acrylate) (59)

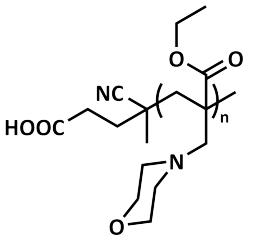

A solution of poly(ethyl 2-((mesyloxy)methyl)acrylate) (0.203 g), triethylamine (0.7 mL, 5.02 mmol, 6.36 eq. per repeating unit) and morpholine (0.4 mL, 4.16 mmol, 5.27 eq. per repeating unit) in dry 1,4-dioxane (2.4 mL) was heated to 110 °C for 48 hours. The polymer was purified by dialysis against a mixture of tetrahydrofuran and methanol (1:1) to afford 0.135 g polymer (69%) as a white solid.

Poly(ethyl 2-(morpholinomethyl)acrylate) was prepared *via* triflation.
To a solution of poly(ethyl 2-(hydroxymethyl)acrylate) (0.199 g) and triethylamine (1.2 mL, 8.25 mmol, 5.39 eq. per repeating unit) in dry dichloromethane (2 mL) under an argon atmosphere, trifluoromethanesulfonyl chloride (0.8 mL, 7.56 mmol, 4.94 eq. per repeating unit) were added at 0 °C. After 20 minutes, the reaction mixture was warmed to room temperature and stirred for 15 hours. The polymer was precipitated in a mixture of methanol and water (8:1, 45 mL), dried and dissolved in dry tetrahydrofuran (2 mL)

under an argon atmosphere. To the solution, morpholine (0.5 mL, 5.78 mmol, 8.50 eq. per repeating unit) was added and heated to 70 °C for 20 hours. The polymer was purified by dialysis against water to afford 0.117 g polymer (38%) as a white solid.

^{1}H NMR (300 MHz, CD_2Cl_2, 25 °C): δ = ppm.

SEC (DMAc, PMMA calibration): $\overline{M}_n$ = 14,500 g·mol^{-1}, $Đ$ = 1.16.

Elemental Analysis: C = 50.7%, H = 6.6%, N = 2.7%, S = 0.6%
calculated: C = 60.3%, H = 8.6%, N = 7.0%, S = 0.0%

5.24 Synthesis of Thiols

5.24.1 2-(*N*-(*tert*-Butoxycarbonyl)methylamino)ethanol

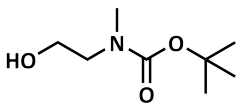

2-*N*-(*tert*-Butoxycarbonyl)methylamino)ethanol was prepared according to a literature procedure.[222]
To a solution of di-*tert*-butyl dicarbonate (49.744 g, 227.92 mmol, 0.96 eq.) in dry dichloromethane (500 mL) under an argon atmosphere, *N*-methylethanolamine (19.0 mL, 237.02 mmol) was added at 0 °C followed by triethylamine (42.0 mL, 301.33 mmol, 1.27 eq.). After 30 minutes, the mixture was warmed to room temperature and stirred for 22 hours. The reaction was quenched by the addition of 1.0 M hydrochloric acid (300 mL) at 0 °C and diluted with dichloromethane (250 mL). The organic phase was washed with 1.0 M hydrochloric acid (300 mL), a saturated aqueous sodium bicarbonate solution (300 mL), and brine (300 mL), dried over anhydrous magnesium sulfate, filtered and concentrated under reduced pressure. The crude product was dried under vacuum to afford 37.507 g 2-*N*-(*tert*-butoxycarbonyl)methylamino)ethanol (94%) as a colorless oil.

^{1}H NMR (250 MHz, $CDCl_3$, 25 °C): δ = 1.44 (s, 9 H), 2.52 (s, 1 H), 2.90 (s, 3 H), 3.37 (t, 2 H, J = 5.4 Hz), 3.72 (t, 2 H, J =5.4 Hz) ppm.

^{13}C NMR (63 MHz, $CDCl_3$, 25 °C): δ = 28.5, 35.6, 51.6, 61.6, 80.1 ppm.

5.24.2 2-(*N*-(*tert*-Butoxycarbonyl)methylamino)ethyl thioacetate (64)

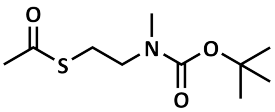

2-(*N*-(*tert*-Butoxycarbonyl)methylamino)ethyl thioacetate was prepared according to a literature procedure.[222]
To a solution of 2-(*N*-(*tert*-butoxycarbonyl)methylamino)ethanol (37.505 g, 214.04 mmol) and triethylamine (40.0 mL, 286.98 mmol, 1.34 eq.) in dry dichloromethane (450 mL) under an argon atmosphere, mesyl chloride (20.0 mL, 258.42 mmol, 1.21 eq.) was added dropwise

at 0 °C. After 15 minutes, the mixture was warmed to room temperature and stirred for 4 hours. The reaction was quenched by the addition of 1.0 M hydrochloric acid (350 mL) at 0 °C and diluted with dichloromethane (150 mL). The organic phase was washed with water (300 mL) and a saturated aqueous sodium bicarbonate solution (300 mL), dried over anhydrous magnesium sulfate, filtered and concentrated under reduced pressure. The resulting 36.9 g crude 2-*N*-(*tert*-butoxycarbonyl)methylamino)ethyl mesylate and potassium thioacetate (25.299 g, 218.91 mmol, 1.50 eq.) were dissolved in dry *N*,*N*-dimethylformamide (300 mL) under an argon atmhosphere and stirred for one hour at room temperature. The reaction mixture was heated to 50 °C for 14 hours and concentrated under reduced pressure. The residue was diluted with water (400 mL) and extracted with diethyl ether (1× 500 mL, 2× 200 mL). The combined organic phase was washed with water (2× 250 mL), dried over anhydrous magnesium sulfate, filtered and concentrated under reduced pressure. The crude product was purified by column chromatography (CH:EA, 4:1) to afford 13.584 g 2-(*N*-(*tert*-butoxycarbonyl)methylamino)ethyl thioacetate (27%) as a yellow oil.

TLC: R_f = 0.50-0.39 (CH:EA, 4:1).

^{1}H NMR (300 MHz, $CDCl_3$, 25 °C): δ = 1.45 (s, 9 H), 2.33 (s, 3 H), 2.88 (s, 3 H), 2.99 (t, 2 H, J = 7.1 Hz), 3.34 (t, 2 H, J = 7.1 Hz) ppm.

^{13}C NMR (75 MHz, $CDCl_3$, 25 °C): δ = 27.3, 28.5, 30.8, 34.9, 48.4, 79.8, 155.6, 195.5 ppm.

5.24.3 2-(*N*-(*tert*-Butoxycarbonyl)methylamino)ethanethiol (65)

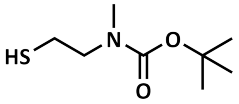

2-(*N*-(*tert*-Butoxycarbonyl)methylamino)ethanethiol was prepared according to a literature procedure.[222]

To a solution of 2-(*N*-(*tert*-butoxycarbonyl)methylamino)ethyl thioacetate (2.009 g, 8.61 mmol) in dry methanol (17 mL) under an argon atmosphere, sodium methoxide (5.4 M in methanol, 2.4 mL, 12.96 mmol, 1.50 eq.) was added dropwise. After stirring for one hour, the reaction mixture was neutralized with Dowex® 50WX8, filtered and concentrated under reduced pressure. The crude product was purified by filtering through a short pad of silica (EA) to afford 1.527 g 2-(*N*-(*tert*-butoxycarbonyl)methylamino)ethanethiol (93%) as a yellow oil.

^{1}H NMR (300 MHz, $CDCl_3$, 25 °C): δ = 1.31 (t, 1 H, J = 8.4 Hz), 1.46 (s, 9 H), 2.65 (m, 2 H), 2.89 (s, 3 H), 3.37 (t, 2 H, J = 7.3 Hz) ppm.

5.24.4 Thiocholine chloride (63)

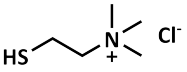

Thiocholine chloride was prepared according to a literature procedure.[222]
A solution of acetylthiocholine chloride (2.661 g, 13.46 mmol) in 6.0 M hydrochloric acid (25 mL) under an argon atmosphere was heated to 85 °C for one hour. The reaction mixture was concentrated under reduced pressure and dried under vacuum to afford 2.476 g thiocholine chloride (quantitative) as a white solid.

^{1}H NMR (300 MHz, D_2O, 25 °C): δ = 2.89 (m, 2 H), 3.09 (t, 9 H, J = 0.6 Hz), 3.49 (m, 2 H) ppm.

5.24.5 *N,N'*-Bis(*tert*-butoxycarbonyl)-2-((2-aminoethyl)amino)ethanol (74)

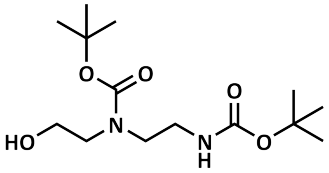

N,N'-Bis(*tert*-butoxycarbonyl)-2-((2-aminoethyl)amino)ethanol was prepared by a modified literature procedure.[236]
To a solution of di-*tert*-butyl dicarbonate (69.607 g, 318.93 mmol, 2.22 eq.) in dry ethanol (150 mL) and dry tetrahydrofuran (150 mL) under an argon atmosphere, 2-(2-aminoethylamino)ethanol (14.5 mL, 143.39 mmol) followed by triethylamine (60.0 mL, 430.46 mmol, 3.00 eq.) was added at 0 °C. After 30 minutes, the reaction mixture was warmed to room temperature and stirred for 24 hours. To the solution, 1.0 M hydrochloric acid (250 mL) was added and extracted with methyl *tert*-butyl ether (600 mL). The organic phase was washed with 1.0 M hydrochloric acid (250 mL), a saturated aqueous sodium bicarbonate solution (250 mL), and brine (250 mL), dried over anhydrous magnesium sulfate, filtered and concentrated under reduced pressure. The crude product was dried under vacuum to afford 46.954 g *N,N'*-bis(*tert*-butoxycarbonyl)-2-((2-aminoethyl)amino)ethanol (quantitative) as a colorless oil.

^{1}H NMR (300 MHz, $CDCl_3$, 25 °C): δ = 1.40 (s, 9 H), 1.43 (s, 9 H), 3.06 (br s, 1 H), 3.28 (m, 2 H), 3.34 (m, 4 H), 3.69 (m, 2 H), 4.99 (br s, 1 H) ppm.

^{13}C NMR (63 MHz, $CDCl_3$, 25 °C): δ = 28.5, 40.0, 48.6, 51.4, 62.0, 79.6, 80.4 156.8 ppm.

5.24.6 *N,N'*-Bis(*tert*-butoxycarbonyl)-2-((2-aminoethyl)amino)ethyl thioacetate (75)

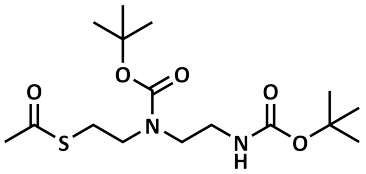

N,N'-Bis(*tert*-butoxycarbonyl)-2-((2-aminoethyl)amino)ethyl thioacetate was prepared by a modified literature procedure.[222]

To a solution of *N,N'*-bis(*tert*-butoxycarbonyl)-2-((2-aminoethyl)amino)ethanol (46.934 g, 143.39 mmol) and triethylamine (26.0 mL, 186.53 mmol, 1.3 eq.) in dry dichloromethane (300 mL) under an argon atmosphere, mesyl chloride (13.5 mL, 174.43 mmol, 1.22 eq.) was added at 0 °C. After 15 minutes the reaction mixture was warmed to room temperature and stirred for 4 hours. The reaction was quenched by the addition of 1.0 M hydrochloric acid (250 mL) at 0 °C and diluted with dichloromethane (100 mL). The organic phase was washed with water (250 mL) and a saturated aqueous sodium bicarbonate solution (250 mL), dried over anhydrous magnesium sulfate, filtered and concentrated under reduced pressure. The resulting 46.6 g crude *N,N'*-bis(*tert*-butoxycarbonyl)-2-((2-aminoethyl)amino)ethyl mesylate and potassium thioacetate (21.144 g, 187.76 mmol, 1.54 eq.) were dissolved in dry *N,N*-dimethylformamide (200 mL) under an argon atmosphere and stirred for a half hour at room temperature. The reaction mixture was heated to 50 °C for 14 hours and concentrated under reduced pressure. The residue was diluted with water (400 mL) and extracted with diethyl ether (1× 500 mL, 2× 200 mL). The combined organic phase was washed with water (2× 250 mL), dried over anhydrous magnesium sulfate, filtered and concentrated under reduced pressure. The crude product was purified by column chromatography (CH:EA, 3:1) to afford 11.708 g *N,N'*-bis(*tert*-butoxycarbonyl)-2-((2-aminoethyl)amino)ethyl thioacetate (21%) as a yellow oil, which crystallized.

TLC: R_f = 0.45-0.33 (CH:EA, 3:1).

^{1}H NMR (400 MHz, $CDCl_3$, 25 °C): δ = 1.42 (s, 9 H), 1.47 (s, 9 H), 2.33 (s, 3 H), 3.01 (m, 2 H), 3.26 (t, 2 H, J = 6.3 Hz), 3.34 (m, 4 H), 4.75 (br s, 1 H), 4.92 (br s, 1 H) ppm.

^{13}C NMR (101 MHz, $CDCl_3$, 25 °C): δ = 28.5, 30.8, 39.9, 47.1, 47.5, 79.4, 80.5, 156.1, 195.3 ppm.

UHPLC/HRMS: t_R = 6.4 min, m/z = 747.3620 $[M_2+Na]^+$, 385.1756 $[M+Na]^+$, 363.1938 $[M+H]^+$
calculated: m/z = 747.3643 ($C_{32}H_{60}N_4O_{10}S_2Na^+$), 385.1768 ($C_{16}H_{30}N_2O_5SNa^+$), 363.1948 ($C_{16}H_{31}N_2O_5S^+$).

5.24.7 *N,N'*-Bis(*tert*-butoxycarbonyl)-2-((2-aminoethyl)amino)ethanethiol (76)

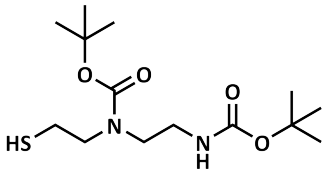

N,N'-is(*tert*-butoxycarbonyl)-2-((2-aminoethyl)amino)ethanethiol was prepared by a modified literature procedure.[222]

To a solution of *N,N'*-bis(*tert*-butoxycarbonyl)-2-((2-aminoethyl)amino)ethyl thioacetate (3.020 g, 8.33 mmol) in dry methanol (16.5 mL) under an argon atmosphere, sodium methoxide (5.4 M in methanol, 2.3 mL, 12.42 mmol, 1.49 eq.) was added dropwise. After stirring for one hour, the reaction mixture was neutralized with Dowex® 50WX8, filtered and concentrated under reduced pressure. The crude product was purified by filtering through a short pad of silica (EA) to afford 2.746 g *N,N'*-bis(*tert*-butoxycarbonyl)-2-((2-aminoethyl)amino)ethanethiol (quantitative) as a yellow oil.

^{1}H NMR (300 MHz, $CDCl_3$, 25 °C): $\delta = 1.30$ (t, 1 H, $J = 6.4$ Hz), 1.42 (s, 9 H), 1.45 (s, 9 H), 2.65 (q, 2 H, $J = 7.7$ Hz), 3.24 (m, 2 H), 3.33 (m, 4 H), 4.79 (br s, 1 H), 4.95 (br s, 1 H) ppm.

5.24.8 3-((4-Methoxybenzyl)oxy)propionitrile (67a)

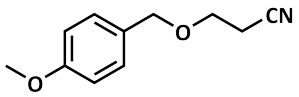

3-((4-Methoxybenzyl)oxy)propionitrile was prepared according to a literature procedure.[227]

To a mixture of anise alcohol (11.855 g, 85.80 mmol, 0.91 eq.) and aqueous sodium hydroxide (16.4 M, 5.3 mL, 86.26 mmol, 0.91 eq.), acrylonitrile (6.2 mL, 94.64 mmol) was added dropwise at 0 °C. After 15 minutes, the reaction mixture was warmed to room temperature and stirred for 7 hours. After quenching the reaction by the addition of 1.0 M hydrochloric acid at 0 °C, the mixture was neutralized with a saturated aqueous sodium bicarbonate solution and extracted with ethyl acetate (1× 100 mL, 2× 50 mL). The combined organic phase was dried over anhydrous magnesium sulfate, filtered and concentrated under reduced pressure. The crude product was purified by column chromatography (CH:EA, 2:1) to afford 15.625 g
3-((4-methoxybenzyl)oxy)propionitrile (95%) as a pale yellowish liquid.

TLC: R_f = 0.54-0.38 (CH:EA, 2:1).

^{1}H NMR (300 MHz, CD_2Cl_2, 25 °C): $\delta = 2.59$ (t, 2 H, $J = 6.3$ Hz), 3.64 (t, 2 H, $J = 6.3$ Hz), 3.80 (s, 3 H), 4.49 (s, 2 H), 6.89 (m, 2 H), 7.28 (m, 2 H) ppm.

^{13}C NMR (75 MHz, CD_2Cl_2, 25 °C): δ = 19.4, 55.7, 65.0, 73.3, 114.3, 118.6, 129.9, 130.1, 160.0 ppm.

5.24.9 3-((4-Methoxybenzyl)oxy)propanethioamide (68a)

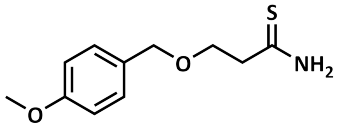

3-((4-Methoxybenzyl)oxy)propanethioamide was prepared according to literature procedure.[228]

To a solution of 3-((4-methoxybenzyl)oxy)propionitrile (6.666 g, 34.86 mmol) in dry pyridine (34.5 mL) and triethylamine (4.8 mL) under an argon atmosphere, ammonium sulfide (40-44% in water, 12.5 mL, 77.05 mmol, 2.21 eq.) was added. The reaction mixture was heated to 60 °C for 23 hours and concentrated under reduced pressure. The residue was diluted with 125 mL dichloromethane and washed with 0.2 M hydrochloric acid (150 mL) and water (2× 100 mL). The organic phase was dried over anhydrous magnesium sulfate, filtered and concentrated under reduced pressure. The crude product was purified by column chromatography (CH:EA, 1:1) to afford 6.245 g 3-((4-methoxybenzyl)oxy)propanethioamide (80%) as a yellow oil.

TLC: R_f = 0.55-0.38 (CH:EA, 1:1).

^{1}H NMR (400 MHz, CD_2Cl_2, 25 °C): δ = 2.94 (t, 2 H, J = 5.6 Hz), 3.75 (t, 2 H, J = 5.6 Hz), 3.79 (s, 3 H), 4.46 (s, 2 H), 6.88 (m, 2 H), 7.25 (m, 2 H), 7.63 (br s, 1 H), 7.85 (br s, 1 H) ppm.

^{13}C NMR (101 MHz, CD_2Cl_2, 25 °C): δ = 45.9, 55.8, 68.5, 73.5, 114.3, 130.0, 130.3, 160.0, 208.8 ppm.

5.24.10 *tert*-Butyl (3-((4-methoxybenzyl)oxy)propanethioyl)carbamate (69a)

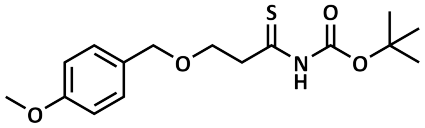

tert-Butyl (3-((4-methoxybenzyl)oxy)propanethioyl)carbamate was prepared by a modified literature procedure.[225, 226]

To a solution of 3-((4-methoxybenzyl)oxy)propanethioamide (4.498 g, 19.96 mmol) in dry tetrahydrofuran (250 mL) under an argon atmosphere, sodium hydride (60% in mineral oil, 1.778 g, 44.45 mmol, 2.23 eq.) was added in portion at -20 °C. After one hour, the reaction mixture was warmed to room temperature and stirred for a further hour. To the solution, di-*tert*-butyl dicarbonate (4.827 g, 22.12 mmol, 1.11 eq.) was added at -20 °C and warmed to room temperature after 15 minutes. The reaction was quenched by the addition of saturated aqueous sodium bicarbonate solution (50 mL) after 3.5 hours and concentrated under reduced pressure. The residue was diluted with water (300 mL) and extracted with ethyl acetate (1× 200 mL, 2× 100 mL). The combined organic phase was dried over

anhydrous magnesium sulfate, filtered and concentrated under reduced pressure. The crude product was purified by column chromatography (CH:EA, 5:1) to afford 5.159 g *tert*-butyl (3-((4-methoxybenzyl)oxy)propanethioyl)carbamate (79%) as a yellow oil.

TLC: R_f = 0.51-0.42 (CH:EA, 5:1).

^{1}H NMR (300 MHz, CD_2Cl_2, 25 °C): δ = 1.49 (s, 9 H), 3.39 (t, 2 H, J = 6.3 Hz), 3.79 (s, 3 H), 3.82 (t, 2 H, J = 6.3 Hz), 4.46 (s, 2 H), 6.87 (m, 2 H), 7.26 (m, 2 H), 9.34 (br s, 1 H) ppm.

^{13}C NMR (75 MHz, CD_2Cl_2, 25 °C): δ = 28.2, 55.7, 68.8, 73.2, 83.6, 114.2, 129.9, 130.8, 149.2, 159.8 ppm.

5.24.11 *tert*-Butyl (1-imino-3-((4-methoxybenzyl)oxy)propyl)carbamate (70a)

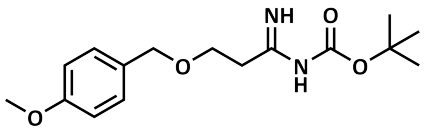

tert-Butyl (1-imino-3-((4-methoxybenzyl)oxy)propyl)carbamate was prepared by a modified literature procedure.[225, 229]
To a suspension of *tert*-butyl (3-((4-methoxybenzyl)oxy)propanethioyl)carbamate (4.496 g, 13.81 mmol) and zinc chloride (2.034 g, 14.93 mmol, 1.08 eq.) under an argon atmosphere, an ammonia solution (7.0 M in methanol, 10.0 mL, 70 mmol, 5.07 eq.) was added at 0 °C. After 15 minutes, the reaction mixture was warmed to room temperature and stirred for further 24 hours. The suspension was diluted with ethyl acetate (100 mL), filtered trough kieselguhr and washed with 0.02 M hydrochloric acid (250 mL) and water (200 mL). The organic phase was dried over anhydrous magnesium sulfate, filtered and concentrated under reduced pressure to afford 3.886 g *tert*-butyl (1-imino-3-((4-methoxybenzyl)oxy)propyl)carbamate (91%) as a yellow oil.

^{1}H NMR (300 MHz, CD_2Cl_2, 25 °C): δ = 1.45 (s, 9 H), 2.50 (t, 2 H, J = 5.7 Hz), 3.70 (t, 2 H, J = 5.7 Hz), 3.79 (s, 3 H), 4.46 (s, 2 H), 6.88 (m, 2 H), 7.25 (m, 2 H), 9.04 (br s, 1 H) ppm.

^{13}C NMR (75 MHz, CD_2Cl_2, 25 °C): δ = 28.4, 38.1, 55.7, 67.4, 73.4, 114.3, 130.0, 130.4, 160.0 ppm.

UHPLC/HRMS: t_R = 3.7 min, m/z = 639.3357 $[M_2+Na]^+$, 309.1805 $[M+H]^+$
calculated: m/z = 639.3364 ($C_{32}H_{48}N_4O_8Na^+$), 309.1809 ($C_{16}H_{25}N_2O_4^+$).

5.24.12 3-(*tert*-Butyldimethylsilyloxy)propionitrile (67b)

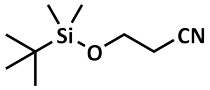

3-(*tert*-Butyldimethylsilyloxy)propionitrile was prepared by a modified literature procedure.[232]

To a solution of *tert*-butyldimethylsilyl chloride (25.3619 g, 168.27 mmol, 1.10 eq.) in dry tetrahydrofuran (130 mL) under an argon atmosphere, 3-hydroxypropionitrile (10.5 mL, 153.63 mmol) and imidazole (14.745 g, 216.58 mmol, 1.41 eq.) were added at 0 °C. After 15 minutes, the reaction mixture was warmed to room temperature, stirred for 4 hours and concentrated under reduced pressure. The residue was diluted with water (200 mL) and extracted with dichloromethane (2× 150 mL). The combined organic phase was washed with water (2× 150 mL), dried over anhydrous magnesium sulfate, filtered and concentrated under reduced pressure. The crude product was purified by distillation (50 °C, 0.7 mbar) to afford 25.835 g 3-(*tert*-butyldimethylsilyloxy)propionitrile (91%) as a colorless liquid.

^{1}H NMR (300 MHz, $CDCl_3$, 25 °C): δ = 0.09 (s, 6 H), 0.90 (s, 9 H), 2.53 (t, 2 H, J = 6.3 Hz), 3.83 (t, 2 H, J = 6.3 Hz) ppm.

^{13}C NMR (75 MHz, $CDCl_3$, 25 °C): δ = -5.3, 18.3, 21.9, 25.9, 58.6, 118.2 ppm.

5.24.13 3-((*tert*-Butyldimethylsilyl)oxy)propanethioamide (68b)

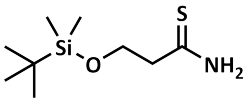

3-((*tert*-Butyldimethylsilyl)oxy)propanethioamide was prepared by a modified literature procedure.[233]

Into a solution of 3-(*tert*-butyldimethylsilyloxy)propionitrile (15.017 g, 81.02 mmol) in pyridine (90 mL) and triethylamine (20 mL), hydrogen sulfide (generated with sodium sulfide hydrate and 6.0 M hydrochloric acid) was bubbled for 1.5 hours and heated to 60 °C. After 15 hours, the solution was concentrated under reduced pressure, diluted with water (200 mL) and extracted with dichloromethane (2× 150 mL). The combined organic phase was washed with water (200 mL), dried over anhydrous magnesium sulfate, filtered and concentrated under reduced pressure. The crude product was purified by column chromatography (CH:EA, 3:1) to afford 12.646 g 3-((*tert*-butyldimethylsilyl)oxy)propanethioamide (71%) as pale yellowish crystals.

TLC: R_f = 0.77-0.64 (CH:EA, 3:1).

^{1}H NMR (300 MHz, $CDCl_3$, 25 °C): δ = 0.07 (s, 6 H), 0.87 (s, 9 H), 2.90 (t, 2 H, J = 5.4 Hz), 3.90 (t, 2 H, J = 5.3 Hz), 7.90 (br s, 1 H), 8.15 (br s, 1 H) ppm.
^{13}C NMR (75 MHz, $CDCl_3$, 25 °C): δ = -5.4, 18.2, 25.9, 47.9, 61.4, 208.8 ppm.

5.24.14 *tert*-Butyl (3-((*tert*-butyldimethylsilyl)oxy)propanethioyl)carbamate (69b)

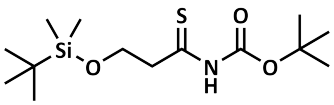

tert-Butyl (3-((*tert*-butyldimethylsilyl)oxy)propanethioyl)carbamate was prepared by a modified literature procedure.[225, 226]

To a solution of 3-((*tert*-butyldimethylsilyl)oxy)propanethioamide (12.527 g, 57.09 mmol) in dry tetrahydrofuran (600 mL) under an argon atmosphere, sodium hydride (60% in mineral oil, 4.908 g, 122.72 mmol, 2.15 eq.) was added in portion at -30 °C. After one hour, the reaction mixture was warmed to room temperature and stirred for a further hour. To the solution, di-*tert*-butyl dicarbonate (14.3775 g, 65.86 mmol, 1.15 eq.) was added at -30 °C and warmed to room temperature after 15 minutes. The reaction was quenched by the addition of saturated aqueous sodium bicarbonate solution (100 mL) after 3 hours and concentrated under reduced pressure. The residue was diluted with water (500 mL) and extracted with ethyl acetate (1× 200 mL, 3× 100 mL). The combined organic phase was dried over anhydrous magnesium sulfate, filtered and concentrated under reduced pressure. The crude product was purified by column chromatography (CH:EA, 5:1) to afford 18.945 g *tert*-butyl (3-((*tert*-butyldimethylsilyl)oxy)propanethioyl)carbamate (quantitative) as a yellowish oily liquid.

TLC: R_f = 0.77-0.71 (CH:EA, 5:1).

^{1}H NMR (300 MHz, $CDCl_3$, 25 °C): δ = 0.08 (s, 6 H), 0.90 (s, 9 H), 1.50 (s, 9 H), 3.20 (m, 2 H), 3.94 (t, 2 H, J = 5.9 Hz), 9.70 (br s, 1 H) ppm.

^{13}C NMR (75 MHz, $CDCl_3$, 25 °C): δ = -5.4, -3.4, 18.3, 25.8, 26.0, 27.6, 28.1, 61.9, 83.2 ppm.

5.24.15 *tert*-Butyl (3-((*tert*-butyldimethylsilyl)oxy)-1-iminopropyl)carbamate (70b)

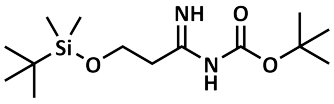

tert-Butyl (3-((*tert*-butyldimethylsilyl)oxy)-1-iminopropyl)carbamate was prepared by a modified literature procedure.[225, 229]

To a suspension of zinc chloride (5.174 g, 37.96 mmol, 1.02 eq.) in an ammonia solution (7.0 M in methanol, 30 mL, 210 mmol, 5.62 eq.) under an argon atmosphere, a solution of *tert*-butyl (3-((*tert*-butyldimethylsilyl)oxy)propanethioyl)carbamate (11.934 g, 37.35 mmol) in dry methanol (30 mL) was added at 0 °C. The reaction mixture was stirred for 1.5 hours, diluted with water (500 mL) and extracted with ethyl acetate (1× 200 mL, 2× 100 mL). The combined organic phase was dried over anhydrous magnesium sulfate,

filtered and concentrated under reduced pressure to afford 10.448 g *tert*-butyl (3-((*tert*-butyldimethylsilyl)oxy)-1-iminopropyl)carbamate (92%) as yellow crystals.

^{1}H NMR (300 MHz, $CDCl_3$, 25 °C): δ = 0.06 (s, 6 H), 0.87 (s, 9 H) 1.47 (s, 9 H), 2.51 (t, 2 H, J = 5.4 Hz), 3.88 (t, 2 H, J = 5.4 Hz), 7.72 (br s, 1 H) ppm.

^{13}C NMR (75 MHz, $CDCl_3$, 25 °C): δ = -5.5, 18.2, 25.9, 28.2, 39.6, 60.5, 79.7, 162.7, 172.2 ppm.

UHPLC/HRMS: t_R = 4.8 min, m/z = 303.2093 $[M+H]^+$
calculated: m/z = 303.2098 ($C_{14}H_{31}N_2O_3Si^+$).

5.24.16 *tert*-Butyl (3-hydroxy-1-iminopropyl)carbamate (71)

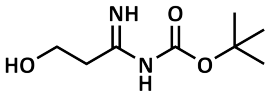

tert-Butyl (3-hydroxy-1-iminopropyl)carbamate was prepared by a modified literature procedure.[297, 298]
To a solution of *tert*-butyl (1-imino-3-((4-methoxybenzyl)oxy)propyl)carbamate (0.090 g, 0.29 mmol) in dichloromethane (2.6 mL), a saturated aqueous sodium bicarbonate solution (0.3 mL) and 2,3-dichloro-5,6-dicyano-1,4-benzoquinone (0.080 g, 0.35 mmol, 1.21 eq.) were added at 0 °C. After 30 minutes, the reaction mixture was warmed to room temperature and stirred for 1.5 hours. To the dispersion, water (25 mL) was added and extracted with dichloromethane (3× 25 mL). The combined organic phase was dried over anhydrous magnesium sulfate, filtered and concentrated under reduced pressure to afford the educt only.

TLC: R_f = 0.65-0.50 (EA:MeOH, 10:1).

^{1}H NMR (300 MHz, CD_2Cl_2, 25 °C): δ = 1.45 (s, 9 H), 2.54 (t, 2 H, J = 5.7 Hz), 3.71 (t, 2 H, J = 5.7 Hz), 3.79 (s, 3 H), 4.46 (s, 2 H), 6.88 (m, 2 H), 7.25 (m, 2 H), 7.93 (br s, 1 H) ppm.

tert-Butyl (3-hydroxy-1-iminopropyl)carbamate was prepared according to literature procedure.[299]
To a solution of *tert*-butyl (1-imino-3-((4-methoxybenzyl)oxy)propyl)carbamate (0.100 g, 0.33 mmol) in acetonitrile (4.0 mL), a ceric ammonium nitrate solution (1.0 M in water, 1.3 mL, 1.34 mmol, 4.11 eq.) was added at 0 °C. The reaction mixture was warmed to room temperature and stirred for 46 hours. The solution was diluted with water (50 mL) and extracted with ethyl acetate (1× 50 mL, 2× 25 mL). The combined organic phase was dried over anhydrous magnesium sulfate, filtered and concentrated under reduced pressure to afford 4-methoxybenzaldehyde and no product.

^{1}H NMR (300 MHz, CD_2Cl_2, 25 °C): δ = 3.90 (s, 3 H), 7.04 (d, 2 H, J = 8.3 Hz), 7.88 (d, 2 H, J = 8.3 Hz), 9.83 (s, 1 H) ppm.

To a solution of *tert*-butyl (3-((*tert*-butyldimethylsilyl)oxy)-1-iminopropyl)carbamate (10.293 g, 34.03 mmol) in dichloromethane (165 mL), tetra-*n*-butylammonium fluoride trihydrate (10.488 g, 33.24 mmol, 0.98 eq.) was added. After 3 hours, the reaction mixture was concentrated under reduced pressure and purified by a short column chromatography (EA:MeOH, 10:1) to afford 5.9178 g *tert*-butyl (3-hydroxy-1-iminopropyl)carbamate (92%) as a pale yellowish solid.

TLC: R_f = 0.48-0.29 (EA:MeOH, 10:1).

^{1}H NMR (300 MHz, CD_3CN, 25 °C): δ = 1.43 (s, 9 H), 2.41 (t, 2 H, J = 5.7 Hz), 3.72 (t, 2 H, J = 5.7 Hz), 5.87 (br s, 3 H) ppm.

^{13}C NMR (75 MHz, CD_3CN, 25 °C): δ = 28.3, 39.2, 59.7, 79.7, 163.4, 173.0 ppm.

EI-MS: m/z = 189 $[M+H]^+$, 158 $[M\text{-}CH_2OH]^{\cdot+}$, 132 $[M+H\text{-}t\text{Bu}]^+$, 115 $[M\text{-}Ot\text{Bu}]^{\cdot+}$, 57 $[t\text{Bu}]^{\cdot+}$.

5.24.17 3-((*tert*-Butoxycarbonyl)amino)-3-iminopropyl thioacatate (72)

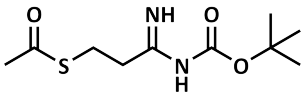

To a solution of *tert*-butyl (3-hydroxy-1-iminopropyl)carbamate (0.212 g, 1.13 mmol) and triethylamine (0.45 mL, 3.23 mmol, 2.86 eq.) in dry *N*,*N*-dimethylformamide (3.2 mL) under an argon atmosphere, mesyl chloride (0.09 mL, 1.16 mmol, 1.03 eq.) was added at 0 °C. After one hour, the reaction mixture was warmed to room temperature, stirred for a further hour and thioacetic acid (0.15 mL, 2.13 mmol, 1.89 eq.) was added. The suspension was stirred for one hour and heated to 60 °C for 16 hours. The reaction was quenched by the addition of a saturated aqueous sodium bicarbonate solution (3.2 mL), diluted with water (50 mL) and extracted with diethyl ether (3× 25 mL). The combined organic phase was dried over anhydrous magnesium sulfate, filtered and concentrated under reduced pressure and purified by column chromatography (CH:EA, 2:1) to afford 0.105 g 3-((*tert*-butoxycarbonyl)amino)-3-oxopropyl thioacetate (38%) as a yellow oil.

TLC: R_f = 0.55-0.43 (CH:EA, 2:1).

^{1}H NMR (300 MHz, $CDCl_3$, 25 °C): δ = 1.44 (s, 9 H), 2.27 (s, 3 H), 3.01 (m, 2 H), 3.09 (m, 2 H), 7.81 (s, 1 H) ppm.

^{13}C NMR (75 MHz, $CDCl_3$, 25 °C): δ = 23.4, 28.0, 30.5, 36.5, 82.7, 150.6, 173.1, 195.8 ppm.

UHPLC/HRMS: t_R = 4.9 min, m/z = 517.1635 $[M_2{-}Na]^+$, 270.0763 $[M+Na]^+$
calculated: m/z = 517.1649 ($C_{20}H_{34}N_2O_8S_2Na^+$), 270.0770 ($C_{10}H_{17}NO_4SNa^+$).

To a solution of *tert*-butyl (3-hydroxy-1-iminopropyl)carbamate (0.209 g, 1.11 mmol) in dry *N*,*N*-dimethylformamide (3.2 mL) under an argon atmosphere, triethylamine (0.55 mL, 3.95 mmol, 3.55 eq.) and mesyl chloride (0.09 mL, 1.16 mmol, 1.05 eq.) were added at 0 °C.

After one hour, the reaction mixture was warmed to room temperature, stirred for a further hour and thioacetic acid (0.12 µL, 1.63 mmol, 1.47 eq.) was added at 0 °C. The suspension was stirred for two hours at room temperature and heated to 60 °C for 12.5 hours. The reaction was quenched by the addition of a saturated aqueous sodium bicarbonate solution (5 mL), diluted with water (50 mL) and extracted with diethyl ether (3× 25 mL). The combined organic phase was dried over anhydrous magnesium sulfate, filtered and concentrated under reduced pressure and purified by column chromatography (CH:EA, 1:2) to afford 0.031 g 3-((*tert*-butoxycarbonyl)amino)-3-iminopropyl thioacatate (11%) as a yellow oil.

TLC: R_f = 0.51-0.39 (CH:EA, 1:2).

^{1}H NMR (300 MHz, CD_2Cl_2, 25 °C): δ = 1.46 (s, 9 H), 2.32 (s, 3 H), 2.49 (t, 2 H, J = 7.3 Hz), 3.13 (t, 2 H, J = 7.3 Hz), 7.61 (s, 1 H), 9.04 (br s, 1 H) ppm.

UHPLC/HRMS: t_R = 3.2 min, m/z = 247.1105 $[M+H]^+$
calculated: m/z = 247.1111 ($C_{10}H_{19}N_2O_3S^+$).

5.24.18 *N,N'*-Bis-(*tert*-butoxycarbonyl)-*N''*-2-mercaptoethylguanidine (66)

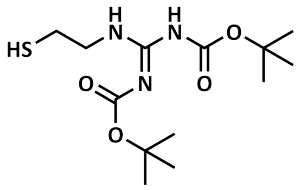

N,N'-Bis-(*tert*-butoxycarbonyl)-*N''*-2-mercaptoethylguanidine was prepared by a modified literature procedure.[223]
To a suspension of cysteamine hydrochloride (3.046 g, 26.81 mmol) and triethylamine (11.0 mL, 78.92 mmol, 2.94 eq.) in dry *N,N*-dimethylformamide (110 mL) under an argon atmosphere, *N,N'*-bis-*tert*-butoxycarbonylthiourea (7.309 g, 26.45 mmol, 0.99 eq.) was added. The reaction mixture was stirred for 22 hours, concentrated under reduced pressure and purified by filtering through a short pad of silica (CH:EA, 1:1) to afford 8.026 g *N,N'*-bis-(*tert*-butoxycarbonyl)-*N''*-2-mercaptoethylguanidine (94%) as a white solid.

TLC: R_f = 0.53-0.39 (CH:EA, 1:1).

^{1}H NMR (300 MHz, $CDCl_3$, 25 °C): δ = 1.42 (t, 1 H, J = 8.6 Hz), 1.49 (s, 9 H), 2.71 (dt, 2 H, J = 8.6, 6.5 Hz), 3.62 (q, 2 H, J = 6.3 Hz), 8.67 (s, 1 H), 11.48 (s, 1 H) ppm.

^{13}C NMR (75 MHz, $CDCl_3$, 25 °C): δ = 24.3, 28.2, 28.4, 43.8, 79.6, 83.4, 153.3, 156.3, 163.5 ppm.

5.24.19 2-(Imidazol-1-yl)ethyl thioacetate (77)

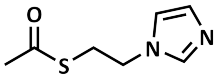

2-(Imidazol-1-yl)ethyl thioacetate was prepared by a modified literature procedure.[222, 244]

To a solution of 2-(imidazol-1-yl)ethanol (15.035 g, 134.08 mmol) in dry dichloromethane (250 mL) under an argon atmosphere, mesyl chloride (13.0 mL, 167.97 mmol, 1.25 eq.) was added dropwise at 0 °C followed by triethylamine (35.0 mL, 251,10 mmol, 1.87 eq.). After 30 minutes, the reaction mixture was warmed to room temperature and stirred for 3 hours. The solution was washed with a saturated aqueous sodium bicarbonate solution (150 mL) and the aqueous phase was extracted with dichloromethane (2× 100 mL). The combined organic phase was dried over anhydrous magnesium sulfate, filtered and concentrated under reduced pressure. The resulting 16.4 g crude 2-(imidazol-1-yl)ethyl mesylate and potassium thioacetate (14.8153 g, 129.73 mmol, 1.50 eq.) were dissolved in dry *N*,*N*-dimethylformamide (200 mL) under an argon atmosphere and heated to 60 °C for 3 hours. The mixture was diluted with a saturated aqueous sodium bicarbonate solution (100 mL) and water (50 mL) and extracted with dichloromethane (1× 200 mL, 2× 100 mL). The combined organic phase was dried over anhydrous magnesium sulfate, filtered and concentrated under reduced pressure. The crude product was purified by column chromatography (THF) to afford 8.369 g 2-(imidazol-1-yl)ethyl thioacetate (37%) as an orange oily liquid, which crystallized at -24 °C.

TLC: R_f = 0.73-0.46 (THF).

^{1}H NMR (300 MHz, CD_2Cl_2, 25 °C): δ = 2.34 (s, 3 H), 3.19 (t, 2 H, J = 6.8 Hz), 4.10 (t, 2 H, J = 6.8 Hz), 6.97 (t, 1 H, J = 1.3 Hz), 6.99 (t, 1 H, J = 1.1 Hz), 7.45 (m, 1 H) ppm.

^{13}C NMR (75 MHz, CD_2Cl_2, 25 °C): δ = 30.7, 31.0, 46.7, 119.4, 129.9, 137.7, 195.1 ppm.

EI-MS: m/z = 170 $[M]^{\cdot+}$, 128 $[M+H\text{-}Ac]^+$, 95 $[M\text{-}SAc]^{\cdot+}$.

5.24.20 2-(Imidazol-1-yl)ethanethiol (78)

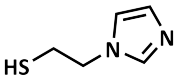

2-(Imidazol-1-yl)ethanethiol was prepared by a modified literature procedure.[222, 237]

To a solution of 2-(imidazol-1-yl)ethyl thioacetate (5.031 g, 29.55 mmol) in dry methanol (58 mL) under an argon atmosphere, sodium methoxide (5.4 M in methanol, 7.0 mL, 37.80 mmol, 1.28 eq.) was added dropwise. After stirring for 2 hours, the reaction mixture was neutralized with Dowex® 50WX8, filtered and concentrated under reduced pressure. The crude product was purified by distillation (78 °C, $2.8 \cdot 10^{-2}$ mbar) to afford 2.416 g 2-(imidazol-1-yl)ethanethiol (64%) as a colorless liquid.

^{1}H NMR (300 MHz, CD_2Cl_2, 25 °C): δ = 1.42 (t, 1 H, J = 8.0 Hz), 2.86 (q, 2 H, J = 6.9 Hz), 4.12 (t, 2 H, J = 6.6 Hz), 6.97 (t, 1 H, J = 1.3 Hz), 7.01 (t, 1 H, J = 1.1 Hz), 7.48 (t, 1 H, J = 1.2 Hz) ppm.

^{13}C NMR (75 MHz, CD_2Cl_2, 25 °C): δ = 26.4, 50.4, 119.2, 129.9, 137.8 ppm.

2-(Imidazol-1-yl)ethanethiol was prepared by according to a literature procedure.[237]
A solution of imidazole (9.572 g, 140.6 mmol) in dry ethylbenzene (140 mL) under an argon atmosphere was heated to 115 °C, and a solution of ethylene sulfide (2.636 g, 43.85 mmol, 0.31 eq.) in dry ethylbenzene (42 mL) was added dropwise over 21 hours. After 3 hours, the reaction mixture was concentrated under reduced pressure, suspended in dry diethyl ether (50 mL) and cooled to 4 °C for 24 hours. The solid was filtered, washed with dry diethyl ether (20 mL), and the combined organic phase was concentrated under reduced pressure. The crude product was purified by distillation (71 °C, $4{\cdot}10^{-2}$ mbar) to afford 1.706 g 2-(imidazol-1-yl)ethanethiol (21%) as a colorless liquid containing 31 wt% imidazole.

^{1}H NMR (300 MHz, CD_2Cl_2, 25 °C): δ = 1.43 (br s, 1 H), 2.87 (t, 2 H, J = 6.6 Hz), 4.14 (t, 2 H, J = 6.6 Hz), 6.99 (t, 1 H, J = 1.4 Hz), 7.04 (t, 1 H, J = 1.1 Hz), 7.52 (t, 1 H, J = 1.2 Hz) ppm.

5.24.21 *N*-(*tert*-Butyloxycarbonyl)-4-(2-hydroxyethyl)imidazole (79)

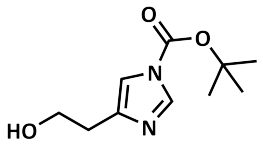

N-(*tert*-Butyloxycarbonyl)-4-(2-hydroxyethyl)imidazole was prepared by a modified literature procedure.[241]
To a solution of 4-(2-hydroxyethyl)imidazole (10.045 g, 89.59 mmol) and di-*tert*-butyl dicarbonate (26.313 g, 120.57 mmol, 1.35 eq.) in methanol (35 mL), triethylamine (18.5 mL, 132.73 mmol, 1.48 eq.) was added dropwise. The reaction mixture was stirred for 19 hours and concentrated under reduced pressure. The crude product was purified by column chromatography (EA:MeOH, 20:1) to afford 9.646 g *N*-(*tert*-butyloxycarbonyl)-4-(2-hydroxyethyl)imidazole (51%) as a yellow oil, which crystallized.

TLC: R_f = 0.46-0.35 (EA:MeOH, 20:1).

^{1}H NMR (300 MHz, CD_2Cl_2, 25 °C): δ = 1.59 (s, 9 H), 2.37 (m, 2 H), 3.82 (t, 2 H, J = 6.0 Hz), 7.16 (m, 1 H), 7.98 (d, 1 H, J = 1.3 Hz) ppm.

^{13}C NMR (75 MHz, CD_2Cl_2, 25 °C): δ = 28.1, 31.3, 62.2, 85.9, 114.1, 137.1, 142.0, 147.6 ppm.

5.24.22 *N*-(*tert*-Butyloxycarbonyl)-4-(2-(acetylthio)ethyl)imidazole (80)

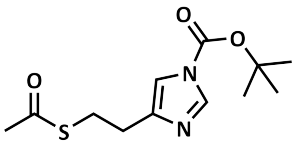

N-(*tert*-Butyloxycarbonyl)-4-(2-(acetylthio)ethyl)imidazole was prepared by a modified literature procedure.[222, 241]

To a solution of *N*-(*tert*-butyloxycarbonyl)-4-(2-hydroxyethyl)imidazole (9.598 g, 45.22 mmol) and triethylamine (7.6 mL, 54.53 mmol, 1.21 eq.) in dry dichloromethane (90 mL) under an argon atmosphere, mesyl chloride (3.9 mL, 49.75 mmol, 1.10 eq.) was added dropwise at 0 °C. After one hour, the mixture was warmed to room temperature and stirred for 3 hours. The reaction was quenched by the addition of saturated aqueous sodium bicarbonate solution (20 mL) and the organic phase was washed with water (50 mL). The aqueous phase was extracted with dichloromethane (3× 50 mL), the combined organic phase was dried over anhydrous magnesium sulfate, filtered and concentrated under reduced pressure. The resulting 13.9 g crude *N*-(*tert*-butyloxycarbonyl)-4-(2-((mesyl)oxy)ethyl)imidazole and potassium thioacetate (7.879 g, 68.99 mmol, 1.53 eq.) were dissolved in dry *N*,*N*-dimethylformamide (100 mL) under an argon atmhosphere and heated to 60 °C for 16 hours. The mixture was diluted with a saturated aqueous sodium bicarbonate solution (60 mL) and water (60 mL) and extracted with ethyl acetate (1× 120 mL, 6× 75 mL). The combined organic phase was dried over anhydrous magnesium sulfate, filtered and concentrated under reduced pressure. The crude product was purified by column chromatography (CH:EA, 1:1) to afford 10.892 g *N*-(*tert*-butyloxycarbonyl)-4-(2-(acetylthio)ethyl)imidazole (89%) as a reddish oily liquid, which crystallized.

TLC: R_f = 0.63-0.49 (CH:EA, 1:1).

^{1}H NMR (250 MHz, CD_2Cl_2, 25 °C): δ = 1.59 (s, 9 H), 2.30 (s, 3 H), 2.78 (t, 2 H, J = 7.3), 3.14 (t, 2 H, J = 7.3 Hz), 7.14 (m, 1 H), 7.96 (d, 1 H, J = 1.3 Hz) ppm.

^{13}C NMR (63 MHz, CD_2Cl_2, 25 °C): δ = 28.2, 28.8, 31.0, 85.8, 114.0, 137.2, 142.2, 147.6, 195.9 ppm.

EI-MS: m/z = 271 $[M+H]^+$, 227 $[M\text{-}Ac]^{\cdot+}$, 215 $[M+H_2\text{-}t\text{Bu}]^+$, 195 $[M\text{-}SAc]^{\cdot+}$, 171 $[M+H\text{-}t\text{Bu-}Ac]^+$, 155 $[M+H\text{-}O t\text{Bu-}Ac]^+$, 139 $[M+H\text{-}t\text{Bu-}SAc]^+$, 127 $[M+H\text{-Boc-}Ac]^+$.

5.24.23 2-(Imidazol-4/5-yl)ethanethiol (81)

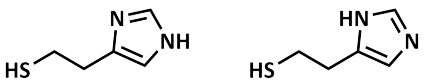

2-(Imidazol-4/5-yl)ethanethiol was prepared by a modified literature procedure.[222]

To a solution of *N*-(*tert*-butyloxycarbonyl)-4-(2-(acetylthio)ethyl)imidazole (1.536 g, 5.68 mmol) in dry methanol (11 mL) under an argon atmosphere, sodium methoxide (5.4 M in methanol, 1.5 mL, 8.10 mmol, 1.43 eq.) was added dropwise. After stirring for 1.5 hours,

the reaction mixture was neutralized with Dowex® 50WX8, filtered and concentrated under reduced pressure to afford 0.657 g 2-(imidazol-4/5-yl)ethanethiol (90%) as brown oil.

^{1}H NMR (300 MHz, CD_2Cl_2, 25 °C): δ = 1.44 (t, 1 H, J = 3.5 Hz), 2.86 (m, 4 H), 6.87 (m, 1 H), 7.38 (br s, 1 H), 7.58 (d, 1 H, J = 1.2 Hz) ppm.

5.24.24 2-(Theophyllin-7-yl)ethyl thioacetate (82)

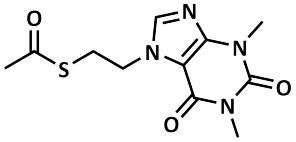

2-(Theophyllin-7-yl)ethyl thioacetate was prepared by a modified literature procedure.[222, 244]

To a suspension of 7-(2-hydroxyethyl)theophylline (17.461 g, 77.88 mmol) in dry dichloromethane (150 mL) under an argon atmosphere, mesyl chloride (7.5 mL, 96.91 mmol, 1.24 eq.) was added dropwise at -20 °C followed by triethylamine (20.5 mL, 147.08 mmol, 1.89 eq.). After 30 minutes, the reaction mixture was warmed to room temperature and stirred for 3 hours. The reaction was quenched by the addition of a saturated aqueous sodium bicarbonate solution (10 mL), dried over anhydrous magnesium sulfate, filtered and concentrated under reduced pressure. The resulting 37.3 g crude 2-(theophyllin-7-yl)ethyl mesylate was dissolved in dry *N*,*N*-dimethylformamide (160 mL) under an argon atmosphere, potassium thioacetate (13.874 g, 121.48 mmol, 1.56 eq.) was added and heated to 60 °C for 3 hours. The reaction mixture was concentrated under reduced pressure, diluted with water (150 mL) and extracted with ethyl acetate (1× 300 mL, 3× 150 mL). The combined organic phase was dried over anhydrous magnesium sulfate, filtered and concentrated under reduced pressure. The crude product was purified by column chromatography (EA) to afford 18.373 g 2-(theophyllin-7-yl)ethyl thioacetate (84%) as a pale ochre solid.

TLC: R_f = 0.57-0.45 (EA).

^{1}H NMR (300 MHz, CD_2Cl_2, 25 °C): δ = 2.32 (s, 3 H), 3.34 (s, 3 H), 3.34 (t, 2 H, J = 6.3 Hz), 3.52 (s, 3 H), 4.41 (t, 2 H, J = 6.3 Hz), 7.53 (s, 1 H) ppm.

^{13}C NMR (75 MHz, CD_2Cl_2, 25 °C): δ = 28.2, 30.1, 30.4, 31.0, 46.9, 107.2, 142.1, 149.7, 152.1, 155.6, 195.3 ppm.

EI-MS: m/z = 282 $[M]^{\cdot+}$, 239 $[M\text{-}Ac]^+$, 207 $[M\text{-}SAc]^+$, 193 $[M\text{-}CH_2SAc]^{\cdot+}$, 180 $[M\text{-}C_2H_3SAc]^{\cdot+}$, 154 $[M\text{-}C_3H_3NO_2Ac]^{\cdot+}$.

5.24.25 2-(Theophyllin-7-yl)ethanethiol (83)

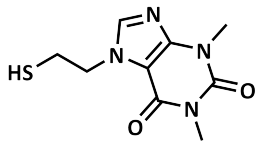

2-(Theophyllin-7-yl)ethanethiol was prepared by a modified literature procedure.[222] To a suspension of 2-(theophyllin-7-yl)ethyl thioacetate (2.775 g, 9.83 mmol) in dry methanol (30 mL) under an argon atmosphere, sodium methoxide (5.4 M in methanol, 2.8 mL, 15.12 mmol, 1.54 eq.) was added dropwise. After stirring for 3 hours, the reaction mixture was neutralized with Dowex® 50WX8, filtered and concentrated under reduced pressure to afford 2.177 g 2-(theophyllin-7-yl)ethanethiol (92%) as a beige solid.

^{1}H NMR (300 MHz, CD_2Cl_2, 25 °C): δ = 1.36 (t, 1 H, J = 8.9 Hz), 3.00 (dt, 2 H, J = 8.9, 6.3 Hz), 3.34 (s, 3 H), 3.54 (s, 3 H), 4.41 (t, 2 H, J = 6.3 Hz), 7.62 (s, 1 H) ppm.

^{13}C NMR (75 MHz, CD_2Cl_2, 25 °C): δ = 25.9, 28.3, 30.1, 50.6, 142.3, 149.9, 152.2, 155.7 ppm.

5.25 Synthesis of Lauryl glycidyl ether

5.25.1 Lauryl allyl ether (99)

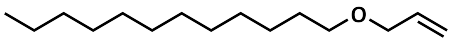

Lauryl allyl ether was prepared according to a literature procedure.[262] A suspension of potassium hydroxide powder (3.389 g, 204.06 mmol, 1.02 eq.) in allyl alcohol (28.0 mL, 411.71 mmol, 2.06 eq.) under an argon atmosphere was stirred for 2 hours before lauryl bromide (48.0 mL, 199.91 mmol) was added. The reaction mixture was heated to 60 °C for 4 hours, diluted with diethyl ether (150 mL), filtered and concentrated under reduced pressure. The crude product was purified by column chromatography (CH, followed by Et_2O) to afford 26.075 g lauryl allyl ether (58%) as a yellowish liquid and 19.249 g lauryl bromide.

TLC: R_f = 0.34-0.20 (CH), 0.99-0.91 (Et_2O, visualized with $KMnO_4$ stain).

^{1}H NMR (300 MHz, $CDCl_3$, 25 °C): δ = 0.87 (t, 3 H, J = 6.7 Hz), 1.12-1.40 (m, 18 H), 1.49-1.69 (m, 2 H), 3.42 (t, 2 H, J = 6.7 Hz), 3.96 (dt, 2 H, J = 5.6, 1.4 Hz), 5.22 (ddt, 1 H, J = 10.4, 1.8, 1.3 Hz), 5.27 (dq, 1 H, J = 17.2, 1.7 Hz), 5.92 (ddt, 1 H, J = 10.3, 17.2, 5.6 Hz) ppm.

^{13}C NMR (75 MHz, $CDCl_3$, 25 °C): δ = 14.3, 22.9, 26.4, 29.5, 29.7-29.9, 32.1, 70.1, 72.0, 116.8, 135.3 ppm.

5.25.2 Lauryl glycidyl ether (100)

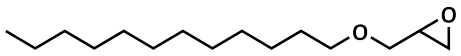

Lauryl glycidyl ether was prepared by a modified literature procedure.[263]
To a solution of lauryl allyl ether (26.045 g, 115.04 mmol) in dichloromethane (155 mL), *meta*-chloroperoxybenzoic acid (≤77%, 36.997 g, 165.08 mmol, 1.44 eq.) was added in portion at 0 °C. The reaction mixture was warmed to room temperature and stirred for 40 hours. The suspension was diluted with dichloromethane (150 mL) and washed a with 1.0 M aqueous sodium hydroxide solution (200 mL) and water (200 mL). The organic phase was dried over anhydrous magnesium sulfate, filtered and concentrated under reduced pressure. The crude product was purified by distillation (93 °C, $1 \cdot 10^{-3}$ mbar) to afford 24.228 g lauryl glycidyl ether (87%) as a colorless liquid, which crystallized at 4 °C.

^{1}H NMR (300 MHz, $CDCl_3$, 25 °C): δ = 0.87 (t, 3 H, J = 6.7 Hz), 1.13-1.43 (m, 18 H), 1.58 (dt, 2 H, J = 13.8, 6.9 Hz), 2.61 (dd, 1 H, J = 5.1, 2.7 Hz), 2.80 (dd, 1 H, J = 5.0, 4.1 Hz), 3.15 (dddd, 1 H, J = 5.8, 4.1, 3.1, 2.7 Hz), 3.38 (dd, 1 H, J = 11.5, 5.8 Hz), 3.47 (m, 2 H), 3.70 (ddd, 1 H, J = 11.5, 3.1, 0.3 Hz) ppm.

^{13}C NMR (75 MHz, $CDCl_3$, 25 °C): δ = 14.3, 22.8, 26.2, 29.5, 29.6, 29.7-29.9, 32.1, 44.5, 51.1, 71.6, 71.9 ppm.

5.26 Synthesis of 2-(Tritylthio)ethyl glycidyl ether

5.26.1 2-(Tritylthio)ethanol (106)

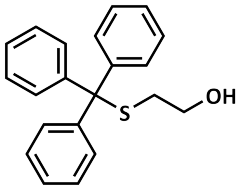

2-(Tritylthio)ethanol was prepared according to a literature procedure.[272]
To a solution of trityl chloride (7.985 g, 28.64 mmol, 1.00 eq.) in dry tetrahydrofuran (18 mL) under an argon atmosphere, 2-mercaptoethanol (2.0 mL, 28.52 mmol) was added and heated to 100 °C for 3 hours. The mixture was concentrated under reduced pressure and the residue was washed with a mixture of cyclohexane:ethyl acetate (2:1, 2× 60 mL) and *n*-pentane (2× 25 mL). The washing solutions were combined and further product crystallized. The solid was dried under vacuum to afford 8.645 g 2-(tritylthio)ethanol (95%) as white crystals.

^{1}H NMR (250 MHz, CD_2Cl_2, 25 °C): δ = 1.66 (s, 1 H), 2.44 (t, 2 H, J = 6.3 Hz), 3.37 (t, 2 H, J = 6.3 Hz), 7.15-7.7.36 (m, 9 H), 7.39-7.53 (m, 6 H) ppm.

^{13}C NMR (63 MHz, CD_2Cl_2, 25 °C): δ = 35.7, 61.3, 67.1, 127.3, 128.5, 130.1, 145.4 ppm.

5.26.2 2-(Tritylthio)ethyl glycidyl ether (107)

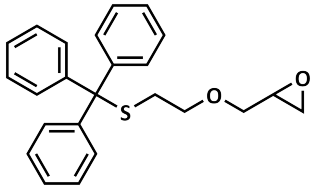

2-(Tritylthio)ethyl glycidyl ether was prepared by a modified literature procedure.[273] To a solution of 2-(tritylthio)ethanol (13.585 g, 42.39 mmol) in tetrahydrofuran (210 mL), potassium hydroxide powder (10.233 g, 182.39 mmol, 4.30 eq.) and tetra-*n*-butylammonium bromide (1.398 g, 4.34 mmol, 0.10 eq.) were added. The suspension was stirred for 1.5 hours before epichlorohydrin (6.7 mL, 85.45 mmol, 2.02 eq.) was added. After 20.5 hours, the reaction mixture was concentrated under reduced pressure, diluted with ethyl acetate (250 mL) and washed with a mixture of brine and water (1:1, 2× 200 mL) and water (200 mL). The organic phase was dried over anhydrous magnesium sulfate, filtered and concentrated under reduced pressure. The crude product was purified by column chromatography (CH:EA, 5:1) to afford 12.391 g 2-(tritylthio)ethyl glycidyl ether (78%) as white crystals.

TLC: R_f = 0.49-0.39 (CH:EA, 5:1).

^{1}H NMR (300 MHz, CD_2Cl_2, 25 °C): δ = 2.40 (t, 2 H, J = 6.7 Hz), 2.50 (dd, 1 H, J = 5.1, 2.7 Hz), 2.71 (dd, 1 H, J = 5.1, 4.1 Hz), 3.02 (m, 1 H), 3.18 (dd, 1 H, J = 11.5, 6.1 Hz), 3.32 (m, 2 H), 3.58 (dd, 1 H, J = 11.5, 2.8 Hz), 7.19-7.35 (m, 9 H), 7.38-7.48 (m, 6 H) ppm.

^{13}C NMR (75 MHz, CD_2Cl_2, 25 °C): δ = 32.3, 44.5, 51.1, 67.1, 70.2, 72.2, 127.2, 128.4, 130.1, 145.4 ppm.

5.27 Preparation of Poly(ethylene oxide)-*block*-poly(allyl glycidyl ether) (61)

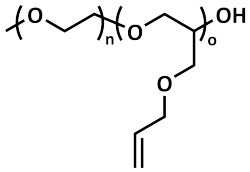

Poly(ethylen oxide)-*block*-poly(allyl glycidyl ether) was prepared by a modified literature procedure.[100]

To a melt of α-methoxy-ω-hydroxy poly(ethylene oxide) at 110 °C, a spatula tip of sodium hydride (95%, approx. 1.2 eq.) was added. After 2 hours, allyl glycidyl ether was added and stirred for 24 hours. The polymerization was quenched with methanol (0.5 mL) and the polymer was dried under vacuum at 100 °C to afford poly(ethylene oxide)-*block*-poly(allyl glycidyl ether) (≥97%).

^{1}H NMR (250 MHz, $CDCl_3$, 25 °C): δ = 3.25-3.83, 3.86-4.09, 5.05-5.37, 5.74-6.02 ppm.

^{13}C NMR (63 MHz, $CDCl_3$, 25 °C): δ = 69.3-71.1, 72.0-72.7, 78.4-79.3, 116.5-117.6, 134.4-135.8 ppm.

Table 5.17: Preparation of poly(ethylene oxide)-*block*-poly(allyl glycidyl ether).

Polymer	Poly(ethylene oxide)	Allyl glycidyl ether	Yield
61a	0.493 g (0.26 mmol)	0.5 mL (4.21 mmol, 16.09 eq.)	0.963 g
61b	0.531 g (0.28 mmol)	1.0 mL (8.43 mmol, 29.88 eq.)	1.372 g
61c	0.527 g (0.28 mmol)	1.5 mL (12.64 mmol, 45.15 eq.)	1.967 g
61d	0.508 g (0.27 mmol)	2.1 mL (17.70 mmol, 65.58 eq.)	2.483 g
61e	0.504 g (0.27 mmol)	2.5 mL (21.07 mmol, 78.69 eq.)	2.835 g

Table 5.18: SEC data of poly(ethylene oxide)-*block*-poly(allyl glycidyl ether).

Polymer	$\overline{M}_n$ [a)]	DP[a)]	$\overline{M}_n$ [b)]	$Đ$ [b)]
61a	3,500 g·mol^{-1}	15	2,600 g·mol^{-1}	1.15
61b	5,200 g·mol^{-1}	29	3,400 g·mol^{-1}	1.06
61c	7,000 g·mol^{-1}	45	4,000 g·mol^{-1}	1.07
61d	8,700 g·mol^{-1}	60	4,500 g·mol^{-1}	1.25
61e	10,600 g·mol^{-1}	76	5,000 g·mol^{-1}	1.24

[a)] Determined by ^{1}H NMR, [b)] SEC (chloroform, PEO calibration).

5.28 Anionic Polymerization of Glycidyl Ethers in Solution

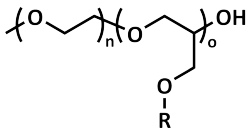

Poly(ethylene oxide)-*block*-poly(glycidyl ether) were prepared by a modified literature procedure.[266]

To a stirred mixture of dibenzo-18-crown-6 (1.5 eq.) and a spatula tip of potassium hydride (approx. 1.2 eq.) in dry ethylbenzene under an argon atmosphere, α-methoxy-ω-hydroxy poly(ethylene oxide) was added and heated to 70 °C. After 2 hours, a glycidyl ether was added and stirred overnight. The polymerization was quenched with dry methanol and cooled to room temperature. The polymer was purified by dialysis against a mixture of water and tetrahydrofuran (1:1) and tetrahydrofuran to afford poly(ethylene oxide)-*block*-poly(glycidyl ether).

^{1}H NMR (300 MHz, 25 °C):

Poly(ethylene oxide)-*block*-poly(allyl glycidyl ether) ($CDCl_3$): δ = 3.17-3.85, 3.90-4.14, 5.06-5.38, 5.75-6.06 ppm.

Poly(ethylene oxide)-*block*-poly(benzyl glycidyl ether) (CD_2Cl_2): δ = 3.27-3.83, 4.33-4.54, 7.11-7.42 ppm.

Poly(ethylene oxide)-*block*-poly(allyl glycidyl ether-*co*-benzyl glycidyl ether) (Acetone-d_6): δ = 3.18-3.90, 3.91-4.10, 4.42-4.68, 5.03-5.38, 5.72, 6.01, 7.14-7.59 ppm.

Poly(ethylene oxide)-*block*-poly(lauryl glycidyl ether) ($CDCl_3$): δ = 0.76-0.98, 1.14-1.38, 1.46-1.65, 3.16-3.75 ppm.

Table 5.19: Preparation of poly(ethylene oxide)-*block*-poly(glycidyl ether).

Polymer	PEO	DB18C6	Solvent	Glycidyl ether	Time	Yield
61f[a)]	5.004 g	1.346 g	26.5 mL	AGE (12.5 mL, 39.63 eq.)	27 h	10.897 g
61g	0.149 g	0.055 g	1.3 mL	AGE (0.7 mL, 74.5 eq.)	20 h	0.777 g
61h	0.150 g	0.051 g	10.0 mL	AGE (4.8 mL, 507.6 eq.)	27 h	-
103a	0.150 g	0.057 g	1.3 mL	BnGE (0.9 mL, 74.1 eq.)	20 h	0.868 g
103b	0.149 g	0.051 g	10.0 mL	BnGE (6.1 mL, 505.4 eq.)	27 h	-
105	0.149 g	0.047 g	1.5 mL	AGE (0.5 mL, 50.0 eq.) BnGE (0.2 mL, 14.9 eq.)	22 h	0.696 g
104a	0.147 g	0.052 g	1.3 mL	LGE (1.1 mL, 51.1 eq.)	20 h	0.997 g
104b	0.149 g	0.050 g	10.0 mL	LGE (11.0 mL, 504.5 eq.)	24 h	-
108[b)]	0.159 g	0.050 g	2.3 mL	TTEGE (0.931 g, 29.3 eq.)	20 h	-

[a)] Dialyzed against dichloromethane, [b)] TTEGE were added dissolved in 1.5 mL ethylbenzene.

Table 5.20: SEC data of poly(ethylene oxide)-*block*-poly(glycidyl ether).

Polymer	Glycidyl ether	$\overline{M}_n$ [a)]	DP[a)]	$\overline{M}_n$ [b)]	$Đ$[b)]
61f	AGE	6,100 g·mol^{-1}	37	5,800 g·mol^{-1}	1.19
61g	AGE	11,200 g·mol^{-1}	82	5,300 g·mol^{-1}	1.26
61h	AGE	-	-	10,600 g·mol^{-1}	1.91
103a	BnGE	14,400 g·mol^{-1}	76	5,400 g·mol^{-1}	1.28
103b	BnGE	-	-	8,300 g·mol^{-1}	1.98
105	AGE:BnGE	9,200 g·mol^{-1}	42:15	4,500 g·mol^{-1}	1.18
104a	LGE	15,000 g·mol^{-1}	54	6,700 g·mol^{-1}	1.22
104b	LGE	-	-	5,200 g·mol^{-1}	1.41
108	TTEGE	-	-	2,100 g·mol^{-1}	1.34

[a)] Determined by ^{1}H NMR, [b)] SEC (THF, PEO calibration).

5.29 Preparation of Poly(ethylene oxide)-*block*-poly(3-((2-aminoethyl)thio)propyl glycidyl ether) (62)

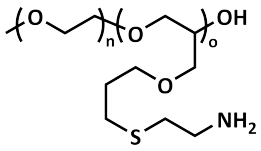

A solution of poly(ethylene oxide)-*block*-poly(allyl glycidyl ether), cysteamine hydrochloride (3.0 eq. per double bond) and 2,2-dimethoxy-2-phenylacetophenone (0.3 eq. per double bond) in a mixture of tetrahydrofuran and methanol (1:2) was deoxygenated by flushing with argon for 10 minutes. The reaction mixture was irradiated with UV light for 2 hours and the polymer was purified by dialysis against tetrahydrofuran, a mixture of tetrahydrofuran and water (1:1), and finally water. The aqueous polymer solution was freeze-dried to afford poly(ethylene oxide)-*block*-poly(3-((2-aminoethyl)thio)propyl glycidyl ether) as a yellowish solid.

^{1}H NMR (250 MHz, MeOD-d_4, 25 °C): δ = 1.65-2.00, 2.45-2.73, 2.74-2.97, 2.98-3.21, 3.29-3.99 ppm.

^{13}C NMR (63 MHz, MeOD-d_4, 25 °C): δ = 29.0-29.3, 29.5-29.8, 30.5-30.9,40.0-40.4, 70.7-70.9, 71.2-71.5, 71.7-72.0, 79.8-80.3 ppm.

Table 5.21: Preparation of poly(ethylene oxide)-*block*-poly(3-((2-aminoethyl)thio)propyl glycidyl ether).

Polymer	**61** (PEO-*block*-PAGE)	Thiol	DMPA	Solvent	Yield
62a	0.200 g **61a** (PEO_{42}-*b*-$PAGE_{15}$)	0.501 g	0.088 g	3.0 mL	0.218 g
62b	0.199 g **61b** (PEO_{42}-*b*-$PAGE_{29}$)	0.352 g	0.062 g	3.0 mL	0.188 g
62f	1.012 g **61f** (PEO_{42}-*b*-$PAGE_{37}$)	3.560 g	0.479 g	6.0 mL	1.466 g
62c	0.202 g **61c** (PEO_{42}-*b*-$PAGE_{45}$)	0.386 g	0.074 g	3.0 mL	0.236 g
62d	0.204 g **61d** (PEO_{42}-*b*-$PAGE_{60}$)	0.669 g	0.096 g	4.5 mL	0.242 g
62e	0.208 g **61e** (PEO_{42}-*b*-$PAGE_{76}$)	0.657 g	0.096 g	4.5 mL	0.260 g

Table 5.22: SEC data of poly(ethylene oxide)-*block*-poly(3-((2-aminoethyl)thio)propyl glycidyl ether).

Polymer	$\overline{M}_n$ [a)]	DoF[a)]	$\overline{M}_n$ [b)]	$Đ$ [b)]	$\overline{M}_n$ [c)]	$Đ$ [c)]
62a	4,700 g·mol^{-1}	>99%	-	-	4,600 g·mol^{-1}	1.31
62b	7,400 g·mol^{-1}	>99%	-	-	6,800 g·mol^{-1}	1.45
62f	9,000 g·mol^{-1}	>99%	7,900 g·mol^{-1}	1.11	6,400 g·mol^{-1}	1.13
62c	10,500 g·mol^{-1}	>99%	-	-	8,700 g·mol^{-1}	1.87
62d	13,400 g·mol^{-1}	>99%	-	-	8,700 g·mol^{-1}	1.24
62e	16,400 g·mol^{-1}	>99%	-	-	10,200 g·mol^{-1}	1.34

[a)] Determined by ^{1}H NMR, [b)] SEC (DMAc, PEO calibration), [c)] SEC (water, P2VP calibration).

5.30 Modification of Poly(ethylene oxide)-*block*-poly(allyl glycidyl ether)

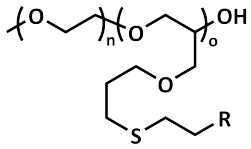

A solution of poly(ethylene oxide)$_{42}$-*block*-poly(allyl glycidyl ether)$_{37}$ (**61f**), thiol (3.0 eq. per double bond) and 2,2-dimethoxy-2-phenylacetophenone (0.3 eq. per double bond) in solvent was deoxygenated by flushing with argon for 10 minutes. The reaction mixture was irradiated with UV light for 2 hours, and the polymer was purified by dialysis against tetrahydrofuran.

^{1}H NMR (300 MHz, 25 °C):
84 ($CDCl_3$): δ = 1.39-1.56, 1.76-1.91, 2.52-2.67, 2.81-2.95, 3.27-3.41, 3.41-3.69 ppm.
85 (MeOD-d_4): δ = 1.81-1.99, 2.59-2.81, 2.83-3.10, 3.33-3.46, 3.46-3.95 ppm.
86 (MeOD-d_4): δ = 1.82-2.10, 2.65-2.89, 2.89-3.10, 3.10-3.29, 3.43-3.83 ppm.
87 ($CDCl_3$): δ = 1.32-1.64, 1.75-1.94, 2.43-2.74, 3.10-3.69, 4.75-5.34 ppm.
88 ($CDCl_3$): δ = 1.40-1.67, 1.76-1.99, 2.45-3.15, 3.25-3.83, 8.43-8.87, 11.31-11.62 ppm.

89 (CD_2Cl_2): δ = 1.68-1.88, 2.40-2.57, 2.77-2.93, 3.31-3.75, 4.03-4.22, 6.94-7.10, 7.48-7.65 ppm.
91 (CD_2Cl_2): δ = 1.65-1.98, 2.40-2.69, 2.83-3.05, 3.21-3.36, 3.36-3.76, 4.25-4.60, 7.55-7.87 ppm.
^{13}C NMR (75 MHz, 25 °C):
84($CDCl_3$): δ = 28.1-29.2, 29.4-30.6, 34.4-35.3, 48.3-50.1, 69.3-71.9, 78.5-79.2, 79.4-80.1, 155.3-156.0 ppm.
85 (MeOD-d_4): δ = 26.6-26.8, 29.2-29.4, 30.6-30.9, 43.4-43.7, 57.7-58.1, 70.5-70.9, 71.4-71.7, 71.9-72.3, 80.0-80.3 ppm.
86 (MeOD-d_4): δ = 24.8-25.6, 29.5-30.2, 30.5-31.2, 53.4-54.4, 66.5-67.3, 70.4-72.5, 79.7-80.7 ppm.
87 ($CDCl_3$): δ = 27.5-29.3, 29.3-30.8, 38.8-40.4, 46.3-48.8, 69.2-71.8, 78.2-79.6, 79.8-80.7, 154.9-157.2 ppm.

88 ($CDCl_3$): δ = 28.0-28.3, 28.3-28.7, 29.6-29.9, 31.1-31.2, 40.0-40.2, 69.8-70.1, 70.6-70.8, 79.2-79.6, 83.0-83.4, 153.0-153.3, 156.0-156.4, 163.5-163.7 ppm.
89 (CD_2Cl_2): δ = 25.9-26.3, 29.0-29.7, 30.0-30.8, 33.3-34.1, 47.1-48.0, 68.1-68.5, 69.5-72.1, 79.0-79.8, 118.9-119.8, 129.5-130.3, 137.4-138.3 ppm.
91 (CD_2Cl_2): δ = 18.7-19.1, 27.8-28.5, 28.7-29.6, 29.8-30.9, 31.8-32.3, 32.7-33.5, 40.1-40.7, 46.8-48.1, 69.5-72.2, 76.7-77.2, 78.6-80.0, 106.7-107.4, 141.6-142.6, 149.3-150.0, 151.7-152.4, 155.3-155.9 ppm.

Table 5.23: Thiol-ene reaction of poly(ethylene oxide)-*block*-poly(allyl glycidyl ether).

Polymer	**61f**	Thiol[a)]	DMPA	Solvent	Yield
84	0.251 g	0.946 g **65**	0.125 g	2.5 mL THF	0.524 g
85[b)]	0.505 g	2.213 g CA	0.244 g	4.0 mL MeOH:THF (3:1)	0.731 g
86[b)]	0.352 g	1.002 g **63**	0.166 g	3.3 mL DMF:MeOH (3:1)	0.400 g
87	0.399 g	2.377 g **76**	0.192 g	3.0 mL THF	0.956 g
88	0.520 g	3.100 g **66**	0.248 g	5.0 mL THF	1.773 g
89	0.716 g	1.845 g **78**	0.341 g	5.0 mL THF	1.367 g
90	0.212 g	0.645 g **81**	0.103 g	2.0 mL THF	0.277 g
91[c)]	0.352 g	1.627 g **83**	0.168 g	3.5 mL DMF	0.705 g

[a)] Depicted in Scheme 5.1, [b)] Dialyzed against methanol, methanol:water 1:1, and finally water, [c)] Dialyzed against dichloromethane.

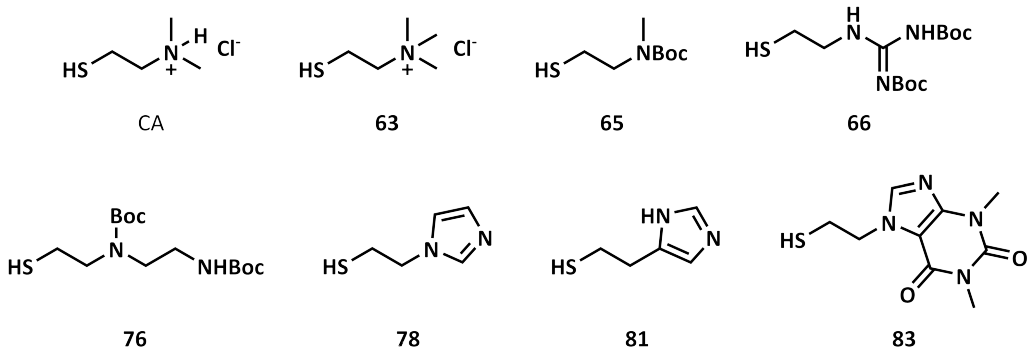

Scheme 5.1: Thiols for modification of poly(ethylene oxide)-*block*-poly(allyl glycidyl ether).

Table 5.24: SEC data of modified poly(ethylene oxide)-*block*-poly(allyl glycidyl ether).

Polymer	Thiol	$\overline{M}_n$[a)]	DoF[a)]	$\overline{M}_n$[b)]	$Đ$[b)]	$\overline{M}_n$[c)]	$Đ$[c)]
84	**65**	13,100 g·mol^{-1}	>99%	5,700 g·mol^{-1}	1.13	-	-
85	CA	9,900 g·mol^{-1}	>99%	4,900 g·mol^{-1}	1.15	6,200 g·mol^{-1}	1.14
86	**63**	11,800 g·mol^{-1}	>99%	-	-	6,500 g·mol^{-1}	1.09
87	**76**	14,100 g·mol^{-1}	>99%	8,200 g·mol^{-1}	1.17	-	-
88	**66**	-	-	10,600 g·mol^{-1}	1.47	-	-
89	**78**	10,800 g·mol^{-1}	>99%	5,600 g·mol^{-1}	1.16	5,900 g·mol^{-1}	1.14
90	**81**	-	-	-	-	-	-
91	**83**	14,900 g·mol^{-1}	>99%	7,000 g·mol^{-1}	1.13	-	-

[a)] Determined by ^{1}H NMR, [b)] SEC (DMAc, PEO calibration), [c)] SEC (water, P2VP calibration).

5.31 Preparation of Poly(ethylene oxide)-*block*-poly(3-((2-(*N*-guanidyl)ethyl)thio)propyl glycidyl ether) (92)

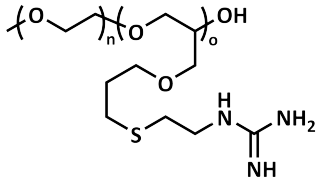

Poly(ethylene oxide)-*block*-poly(3-((2-aminoethyl)thio)propyl glycidyl ether) was guanidinylated with cyanamide according to a literature procedure.[245]
A solution of poly(ethylene oxide)-*block*-poly(3-((2-aminoethyl)thio)propyl glycidyl ether) (0.101 g) and cyanamide (0.048 g, 1.15 mmol, 2.74 eq.) in water (1.0 mL) was deoxygenated by flushing with argon for 5 minutes and heated to 90 °C for 25 hours. The polymer was purified by dialysis against water and the aqueous polymer solution was freeze-dried to afford 0.105 g guanidinylated polymer with a degree of functionalization of approximately 50%.

^{1}H NMR (300 MHz, D_2O, 25 °C): δ = 1.77-2.03, 2.54-2.73, 2.73-2.97, 3.02-3.28, 3.38-3.51, 3.51-4.08 ppm.

^{13}C NMR (75 MHz, D_2O, 25 °C): δ = 27.3-27.5, 27.7-27.9, 28.6-28.7, 28.7-28.9, 30.1-30.3, 38.4-38.8, 40.5-40.9, 58.0-58.1, 68.6-70.2, 77.9-78.6, 156.8-156.9 ppm.

SEC (DMAc, PMMA calibration): $\overline{M}_n$ = 10,700 g·mol^{-1}, $Đ$ = 1.09.

SEC (Water, P2VP calibration): $\overline{M}_n$ = 6,000 g·mol^{-1}, $Đ$ = 1.13.

Poly(ethylene oxide)-*block*-poly(3-((2-aminoethyl)thio)propyl glycidyl ether) was guanidinylated with 1-amidinopyrazole hydrochloride according to a literature procedure.[300]
To a solution of poly(ethylene oxide)-*block*-poly(3-((2-aminoethyl)thio)propyl glycidyl ether) (0.100 g) and 1-amidinopyrazole hydrochloride (0.311 g, 2.12 mmol, 5.11 eq.) in dry tetrahydrofuran (0.5 mL) and dry methanol (1.0 mL) under an argon atmosphere, dry Hünig's base (0.6 mL, 3.16 mmol, 7.61 eq.) was added. The reaction mixture was heated to 50 °C for 24 hours and the polymer was purified by dialysis against water. The aqueous polymer solution was freeze-dried to afford 0.103 g guanidinylated polymer with a degree of functionalization of 94%.

^{1}H NMR (300 MHz, D_2O, 25 °C): δ = 1.78-2.04, 2.57-2.72, 2.72-2.94, 3.29-3.49, 3.49-4.04 ppm.

^{13}C NMR (75 MHz, D_2O, 25 °C): δ = 27.4-28.3, 28.4-29.4, 29.9-30.8, 40.4-41.5, 68.5-71.3, 77.8-78.8, 157.1-157.6 ppm.

SEC (DMAc, PMMA calibration): $\overline{M}_n$ = 11,000 g·mol^{-1}, $Đ$ = 1.11.

SEC (Water, P2VP calibration): $\overline{M}_n$ = 5,900 g·mol^{-1}, $Đ$ = 1.19.

5.32 Cleavage of *N*-*tert*-Butyloxycarbonyl Groups at Polyethers

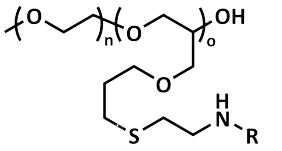

93: R=Me
94: R=$C_2H_4NH_2$

A solution of modified poly(ethylene oxide)-*block*-poly(allyl glycidyl ether) (**84** or **87**) in methanol and trifluoroacetic acid was heated to 50 °C. The polymer was purified by dialysis against a mixture of brine and water (1:1) and water before the aqueous polymer solution was freeze-dried.

^{1}H NMR (300 MHz, MeOD-d_4, 25 °C):
Poly(ethylene oxide)-*block*-poly(3-((2-(methylamino)ethyl)thio)propyl glycidyl ether) (**93**): δ = 1.39-1.55, 1.77-2.10, 2.55-2.79, 2.80-3.00, 3.12-3.26, 3.26-3.38, 3.44-3.82 ppm.
Poly(ethylene oxide)-*block*-poly(3-((2-((2-aminoethyl)amino)ethyl)thio)propyl glycidyl ether) (**94**): δ = 1.17-1.40, 1.71-2.07, 2.51-2.76, 2.80-2.96, 2.96-3.20, 3.22-3.38, 3.38-3.84 ppm.

^{13}C NMR (75 MHz, MeOD-d_4, 25 °C):
Poly(ethylene oxide)-*block*-poly(3-((2-(methylamino)ethyl)thio)propyl glycidyl ether) (**93**): δ = 28.0-28.7, 28.8-29.7, 30.1-31.2, 33.4-34.3, 70.2-72.7, 79.5-80.6 ppm.
Poly(ethylene oxide)-*block*-poly(3-((2-((2-aminoethyl)amino)ethyl)thio)propyl glycidyl ether) (**94**): δ = 19.1-19.6, 28.9-30.0, 30.6-31.5, 31.8-32.7, 39.8-40.9, 46.8-47.7, 69.7-73.5, 79.2-81.2 ppm.

Table 5.25: Cleavage of *N*-*tert*-butyloxycarbonyl groups at polyethers.

Polymer	Educt	Solvent	Time	Yield
93	0.104 g **84**	2.0 mL MeOH:TFA (1:1)	24 h	0.081 g
94	0.351 g **87**	7.0 mL MeOH:TFA (3:4)	48 h	0.191 g

Table 5.26: SEC data of polyethers after deprotection of *N*-*tert*-butyloxycarbonyl groups.

Polymer	$\overline{M}_n$ [a)]	DoF[a)]	$\overline{M}_n$ [b)]	$Đ$ [b)]	$\overline{M}_n$ [c)]	$Đ$ [c)]
93	9,700 g·mol^{-1}	95%	9,400 g·mol^{-1}	1.13	6,900 g·mol^{-1}	1.13
94	10,600 g·mol^{-1}	98%	8,900 g·mol^{-1}	1.11	8,000 g·mol^{-1}	1.20

[a)] Determined by ^{1}H NMR, [b)] SEC (DMAc, PEO calibration), [c)] SEC (water, P2VP calibration).

5.33 Methylation of Poly(ethylene oxide)-*block*-poly(3-((2-(imidazol-1-yl)ethyl)thio)propyl glycidyl ether) (95)

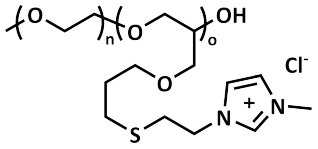

Poly(ethylene oxide)-*block*-poly(3-((2-(imidazol-1-yl)ethyl)thio)propyl glycidyl ether) was methylated by a modified literature procedure.[246]
To a suspension of poly(ethylene oxide)-*block*-poly(3-((2-(imidazol-1-yl)ethyl)thio)propyl glycidyl ether) (**89**) and ammonium chloride in dry *N*,*N*-dimethylformamide under an argon atmosphere, trimethyl orthoformate was added and heated to 110 °C for 24 hours. The polymer was purified by dialysis against methanol.

^{1}H NMR (300 MHz, DMSO-d_6, 25 °C): δ = 1.59-1.91, 2.54-2.76, 2.90-3.13, 3.13-3.20, 3.26-3.78, 3.82-4.06, 4.06-4.25, 4.29-4.62, 6.80-6.92, 7.12-7.32, 7.62-8.23, 9.40-9.93 ppm.

^{13}C NMR (75 MHz, DMSO-d_6, 25 °C): δ = 27.0-27.7, 29.0-29.6, 30.3-31.0, 35.6-36.1, 47.7-48.4, 68.6-70.8, 77.6-78.4, 122.2-122.8, 123.0-123.9, 136.9-137.4 ppm.

Table 5.27: Methylation of poly(ethylene oxide)-*block*-poly(3-((2-(imidazol-1-yl)ethyl)thio)propyl glycidyl ether).

Polymer	**89**	Trimethyl orthoformate	Ammonium chloride	Solvent	Yield
95a	0.110 g	0.15 mL (3.60 eq.)	0.014 g (0.68 eq.)	0.15 mL	0.091 g
95b	0.309 g	0.50 mL (4.35 eq.)	0.052 g (0.93 eq.)	0.50 mL	0.273 g

Table 5.28: SEC data of methylated poly(ethylene oxide)-*block*-poly(3-((2-(imidazol-1-yl)ethyl)thio)propyl glycidyl ether).

Polymer	$\overline{M}_n$ [a)]	DoF[a)]	$\overline{M}_n$ [b)]	$Đ$ [b)]
95a	12,200 g·mol^{-1}	68%	6,300 g·mol^{-1}	1.18
95b	12,300 g·mol^{-1}	84%	6,800 g·mol^{-1}	1.20

[a)] Determined by ^{1}H NMR, [b)] SEC (Water, P2VP calibration).

5.34 Preparation of Poly(ethylene oxide)-*block*-poly(allyl glycidyl ether)-*block*-poly(glycidyl ether)

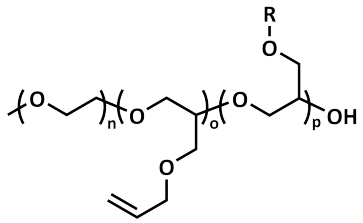

Poly(ethylene oxide)-*block*-poly(allyl glycidyl ether)-*block*-poly(glycidyl ether) was prepared by a modified literature procedure.[100]
To a melt of α-methoxy-ω-hydroxy poly(ethylene oxide) at 110 °C, a spatula tip of sodium hydride (95%, approx. 1.2 eq.) was added. After 2 hours, allyl glycidyl ether was added, stirred for 22 hours and another glycidyl ether was added. The polymerization was quenched after 24 hours with methanol (0.5 mL) and the polymer was dried under vacuum at 100 °C to afford poly(ethylene oxide)-*block*-poly(allyl glycidyl ether)-*block*-poly(glycidyl ether).

^{1}H NMR (250 MHz, $CDCl_3$, 25 °C):
Poly(ethylene oxide)-*block*-poly(allyl glycidyl ether)-*block*-poly(*tert*-butyl glycidyl ether): δ = 0.98-1.23, 3.16-3.87, 3.88-4.13, 5.05-5.38, 5.74-6.03 ppm.
Poly(ethylene oxide)-*block*-poly(allyl glycidyl ether)-*block*-poly(benzyl glycidyl ether): δ = 3.01-3.85, 3.87-4.18, 4.30-4.64, 5.02-5.41, 5.73-6.05 ppm.
Poly(ethylene oxide)-*block*-poly(allyl glycidyl ether)-*block*-poly(lauryl glycidyl ether): δ = 0.67-0.94, 0.95-1.38, 1.39-1.71, 3.06-3.84, 3.84-4.15, 5.03-5.42, 5.74-6.10 ppm.

^{13}C NMR (63 MHz, $CDCl_3$, 25 °C):
Poly(ethylene oxide)-*block*-poly(allyl glycidyl ether)-*block*-poly(*tert*-butyl glycidyl ether): δ = 27.3-28.4, 61.3-64.1, 69.5-71.6, 72.1-72.7, 78.5-80.1, 116.3-117.3, 134.7-135.6 ppm.
Poly(ethylene oxide)-*block*-poly(allyl glycidyl ether)-*block*-poly(benzyl glycidyl ether): δ = 69.1-71.5, 72.2-72.7, 73.1-73.8, 77.3-77.4, 78.5-79.3, 116.6-117.3, 126.9-128.1 ppm.
Poly(ethylene oxide)-*block*-poly(allyl glycidyl ether)-*block*-poly(lauryl glycidyl ether): δ = 13.7-14.8, 22.4-23.4, 25.8-26.8, 28.6-30.6, 31.6-32.5, 69.3-72.7, 78.3-79.5, 116.3-117.3, 134.5-135.7 ppm.

Table 5.29: Preparation of poly(ethylene oxide)-*block*-poly(allyl glycidyl ether)-*block*-poly(glycidyl ether).

Polymer	PEO	Allyl glycidyl ether	Glycidyl ether	Yield
96a	3.018 g	2.7 mL (13.93 eq.)	2.6 mL *t*BGE (11.20 eq.)	7.444 g
96b	2.000 g	2.0 mL (15.47 eq.)	2.0 mL *t*BGE (12.93 eq.)	4.499 g
96c	2.024 g	1.7 mL (12.93 eq.)	3.6 mL *t*BGE (23.58 eq.)	6.996 g
96d	0.306 g	0.3 mL (14.00 eq.)	0.8 mL *t*BGE (33.80 eq.)	1.321 g
96e	0.338 g	0.3 mL (14.08 eq.)	1.1 mL *t*BGE (41.19 eq.)	1.536 g
96f	0.303 g	0.3 mL (15.18 eq.)	1.6 mL *t*BGE (70.89 eq.)	1.984 g
96g	0.303 g	0.3 mL (15.18 eq.)	1.9 mL *t*BGE (84.89 eq.)	2.299 g
96h	0.305 g	0.3 mL (14.04 eq.)	2.3 mL *t*BGE (99.11 eq.)	2.547 g
101a	0.245 g	0.3 mL (16.19 eq.)	0.3 mL BnGE (12.60 eq.)	0.710 g
101b	0.329 g	0.3 mL (14.47 eq.)	1.4 mL BnGE (52.53 eq.)	2.100 g
102[a)]	0.109 g	0.1 mL (14.55 eq.)	0.4 mL LGE (25.57 eq.)	0.115 g

[a)] Purified by filtrating through a short pad of silica (CH:*i*PrOH, 1:1, followed by *i*PrOH), the polymer was desorbed from silica with a mixture of MeOH and THF (2:1) and concentrated under reduced pressure.[212]

Table 5.30: SEC data of intermediate poly(ethylene oxide)-*block*-poly(allyl glycidyl ether).

Polymer	$\overline{M}_n$ [a)]	DP[a)]	$\overline{M}_n$ [b)]	$Đ$[b)]
96a	3,300 g·mol^{-1}	12	2,600 g·mol^{-1}	1.08
96b	3,600 g·mol^{-1}	15	2,700 g·mol^{-1}	1.08
96c	3,100 g·mol^{-1}	11	2,700 g·mol^{-1}	1.10
96d	3,400 g·mol^{-1}	14	2,700 g·mol^{-1}	1.08
96e	3,200 g·mol^{-1}	11	2,800 g·mol^{-1}	1.06
96f	3,500 g·mol^{-1}	14	2,600 g·mol^{-1}	1.12
96g	3,500 g·mol^{-1}	14	2,400 g·mol^{-1}	1.15
96h	3,500 g·mol^{-1}	14	2,600 g·mol^{-1}	1.10
10a	3,600 g·mol^{-1}	15	2,300 g·mol^{-1}	1.13
101b	-	-	2,500 g·mol^{-1}	1.13
102	3,400 g·mol^{-1}	14	2,600 g·mol^{-1}	1.13

[a)] Determined by ^{1}H NMR, [b)] SEC (chloroform, PEO calibration).

Table 5.31: SEC data of poly(ethylene oxide)-*block*-poly(allyl glycidyl ether)-*block*-poly(glycidyl ether).

Polymer	$\overline{M}_n$ [a)]	DP[a)]	$\overline{M}_n$ [b)]	$Đ$[b)]
96a	4,400 g·mol^{-1}	9	3,000 g·mol^{-1}	1.09
96b	5,200 g·mol^{-1}	12	3,300 g·mol^{-1}	1.08
96c	6,100 g·mol^{-1}	23	3,800 g·mol^{-1}	1.11
96d	7,700 g·mol^{-1}	32	4,200 g·mol^{-1}	1.04
96e	8,200 g·mol^{-1}	39	4,500 g·mol^{-1}	1.34
96f	12,700 g·mol^{-1}	71	5,100 g·mol^{-1}	1.23
96g	14,800 g·mol^{-1}	86	5,200 g·mol^{-1}	1.22
96h	16,400 g·mol^{-1}	99	6,200 g·mol^{-1}	1.15
101a	5,700 g·mol^{-1}	13	3,500 g·mol^{-1}	1.17
101b	-	-	5,300 g·mol^{-1}	1.53
102	6,000 g·mol^{-1}	11	3,200 g·mol^{-1}	1.04

[a)] Determined by ^{1}H NMR, [b)] SEC (chloroform, PEO calibration).

5.35 Modification of Poly(ethylene oxide)-*block*-poly(allyl glycidyl ether)-*block*-poly(*tert*-butyl glycidyl ether)

5.35.1 Functionalization with Cysteamine

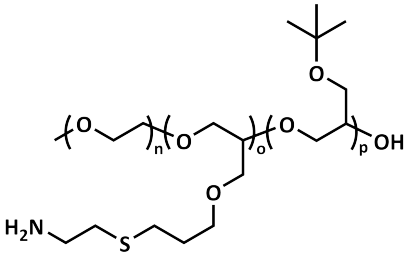

Poly(ethylene oxide)-*block*-poly(allyl glycidyl ether))-*block*-poly(*tert*-butyl glycidyl ether) was functionalized by a modified literature procedure.[215]
A solution of poly(ethylene oxide-*block*-poly(allyl glycidyl ether)-*block*-poly(*tert*-butyl glycidyl ether) (**96**), cysteamine (6.3 eq. per double bond), acetic acid and 2,2-dimethoxy-2-phenylacetophenone (0.2 eq. per double bond) in tetrahydrofuran was deoxygenated by flushing with argon for 10 minutes. The reaction mixture was irradiated with UV light for 2 hours. The polymer was purified by dialysis against water, a mixture of water and tetrahydrofuran (1:1), and finally tetrahydrofuran.

^{1}H NMR (250 MHz, $CDCl_3$, 25 °C): δ = 0.94-1.37, 1.88-2.00, 2.33-2.84, 2.84-3.12, 3.16-3.75, 3.95-4.06, 5.03-5.55, 5.76-6.02 ppm.

^{13}C NMR (63 MHz, $CDCl_3$, 25 °C): δ = 23.8-24.8, 26.9-28.2, 28.2-29.1, 29.5-30.3, 39.1-40.8, 61.6-62.6, 69.1-71.6, 72.5-73.3, 78.4-79.9, 134.7-135.2 ppm.

Table 5.32: Amine-modification of poly(ethylene oxide)-*block*-poly(allyl glycidyl ether)-*block*-poly(*tert*-butyl glycidyl ether).

Polymer	Educt	DP[a)]	Thiol	DMPA	Acid	Solvent	DoF[b)]	Yield
98a[c)]	0.539 g **96a**	9	0.708 g	0.093 g	0.75 mL	8.4 mL	92%	0.590 g
98e[c)]	0.250 g **96e**	39	0.135 g	0.021 g	0.25 mL	3.0 mL	75%	0.187 g
98h	0.297 g **96h**	99	0.115 g	0.015 g	0.75 mL	2.5 mL	56%	0.303 g

[a)] DP of the third block poly(*tert*-butyl glycidyl ether), [b)] Determined by ^{1}H NMR, [c)] Solvent mixture of THF:MeOH (2:1).

Table 5.33: SEC data of amine-modified poly(ethylene oxide)-*block*-poly(allyl glycidyl ether)-*block*-poly(glycidyl ether).

Polymer	$\overline{M}_n$[a)]	DP[a)]	$\overline{M}_n$[b)]	$Đ$[b)]
98a	5,300 g·mol^{-1}	9	2,200 g·mol^{-1}	1.12
98e	8,900 g·mol^{-1}	39	3,300 g·mol^{-1}	1.11
98h	17,000 g·mol^{-1}	99	6,100 g·mol^{-1}	1.18

[a)] Determined by ^{1}H NMR, [b)] SEC (chloroform, PEO calibration).

5.35.2 Functionalization with 3-Mercaptopropionic acid

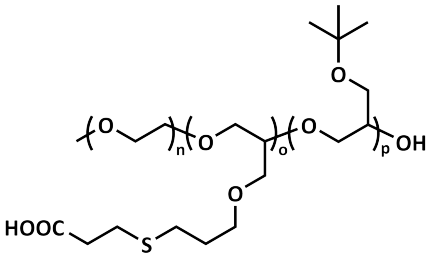

Poly(ethylene oxide)-*block*-poly(allyl glycidyl ether))-*block*-poly(*tert*-butyl glycidyl ether) was functionalized by a modified literature procedure.[215]
A solution of poly(ethylene oxide-*block*-poly(allyl glycidyl ether)-*block*-poly(*tert*-butyl glycidyl ether) (**96**), 3-mercaptopropionic acid (3.0 eq. per double bond) and 2,2-dimethoxy-2-phenylacetophenone (0.2 eq. per double bond) in tetrahydrofuran was deoxygenated by flushing with argon for 10 minutes. The reaction mixture was irradiated with UV light for 2 hours. The polymer was purified by dialysis against water, a mixture of water and tetrahydrofuran (1:1), and finally tetrahydrofuran.

^{1}H NMR (300 MHz, $CDCl_3$, 25 °C): δ = 0.98-1.39, 1.72-1.99, 2.45-2.72, 2.72-3.05, 3.08-3.98, 4.86-5.83 ppm.

^{13}C NMR (75 MHz, $CDCl_3$, 25 °C): δ = 26.6-27.2, 27.2-28.3, 28.5-29.1, 29.4-30.1, 34.7-35.3, 61.7-62.7, 69.2-71.6, 72.4-73.4, 78.5-80.1 ppm.

Table 5.34: Acid-modification of poly(ethylene oxide)-*block*-poly(allyl glycidyl ether)-*block*-poly(*tert*-butyl glycidyl ether).

Polymer	Educt	DP[a)]	Thiol	DMPA	Solvent	DoF[b)]	Yield
97a	0.515 g **96a**	9	0.36 mL	0.092 g	5.0 mL	>99%	0.662 g
97b	0.274 g **96b**	12	0.19 mL	0.044 g	2.5 mL	>99%	0.345 g
97c	1.998 g **96c**	23	1.20 mL	0.245 g	16.0 mL	>99%	2.401 g
97d	0.309 g **96d**	32	0.27 mL	0.030 g	4.0 mL	92%	0.351 g
97e	0.251 g **96e**	39	0.09 mL	0.019 g	3.0 mL	>99%	0.228 g
97f	0.300 g **96f**	71	0.16 mL	0.018 g	4.0 mL	>99%	0.322 g
97g	0.509 g **96g**	86	0.12 mL	0.029 g	5.0 mL	>99%	0.541 g
97h	0.154 g **96h**	99	0.07 mL	0.014 g	3.0 mL	>99%	0.163 g

[a)] DP of the third block poly(*tert*-butyl glycidyl ether), [b)] Determined by ^{1}H NMR.

Table 5.35: SEC data of acid-modified poly(ethylene oxide)-*block*-poly(allyl glycidyl ether)-*block*-poly(glycidyl ether).

Polymer	$\overline{M}_n$[a)]	DP[a)]	$\overline{M}_n$[b)]	$Đ$[b)]
97a	5,700 g·mol^{-1}	9	1,300 g·mol^{-1}	1.09
97c	7,300 g·mol^{-1}	23	2,000 g·mol^{-1}	1.12
97e	9,500 g·mol^{-1}	39	2,600 g·mol^{-1}	1.24
97h	17,900 g·mol^{-1}	99	4,900 g·mol^{-1}	1.48

[a)] Determined by ^{1}H NMR, [b)] SEC (THF, PEO calibration).

6 Appendix

6.1 References

[1] W. B. Jensen, *J. Chem. Educ.* **2008**, *85*, 624–625.

[2] J. J. Berzelius, *Jahres-Bericht über die Fortschritte der physischen Wissenschaften*, Heinrich Laupp, Tübingen, **1833**.

[3] H. Staudinger, *Ber. dtsch. Chem. Ges.* **1924**, *57*, 1203–1208.

[4] H. Staudinger, J. Fritschi, *Helv. Chim. Acta* **1922**, *5*, 785–806.

[5] D. Braun, *Chem. Unserer Zeit* **2012**, *46*, 310–320.

[6] D. Feldman, *Designed Monomers and Polymers* **2012**, *11*, 1–15.

[7] R. B. Seymour, *J. Macromol. Sci. Chem. A* **1989**, *26*, 1023–1032.

[8] C. Harries, *Liebigs Ann. Chem.* **1911**, *383*, 157–227.

[9] S. S. Pickles, *J. Chem. Soc. Trans.* **1910**, *97*, 1085–1090.

[10] PlasticsEurope, Plastics - the Facts 2019: An analysis of European plastics production, demand and waste data, **2019**, `https://www.plasticseurope.org/de/resources/publications/1804-plastics-facts-2019` (visited on 01/03/2021).

[11] H. Ritchie, M. Roser, Plastic Pollution, **2018**, `https://ourworldindata.org/plastic-pollution` (visited on 01/03/2021).

[12] J. R. Jambeck, R. Geyer, C. Wilcox, T. R. Siegler, M. Perryman, A. Andrady, R. Narayan, K. L. Law, *Science (New York N.Y.)* **2015**, *347*, 768–771.

[13] J. Hammer, M. H. S. Kraak, J. R. Parsons, *Rev. Environ. Contam. Toxicol.* **2012**, *220*, 1–44.

[14] L. Lebreton, B. Slat, F. Ferrari, B. Sainte-Rose, J. Aitken, R. Marthouse, S. Hajbane, S. Cunsolo, A. Schwarz, A. Levivier, K. Noble, P. Debeljak, H. Maral, R. Schoeneich-Argent, R. Brambini, J. Reisser, *Sci. Rep.* **2018**, *8*, 4666–4681.

[15] M. Eriksen, Lebreton, C. M. Laurent, H. S. Carson, M. Thiel, C. J. Moore, J. C. Borerro, F. Galgani, P. G. Ryan, J. Reisser, *PloS One* **2014**, *9*, e111913.

[16] A. Cózar, M. Sanz-Martín, E. Martí, J. I. González-Gordillo, B. Ubeda, J. Á. Gálvez, X. Irigoien, C. M. Duarte, *PloS One* **2015**, *10*, e0121762.

[17] A. L. Andrady, *Mar. Pollut. Bull.* **2011**, *62*, 1596–1605.

[18] D. K. A. Barnes, F. Galgani, R. C. Thompson, M. Barlaz, *Phil. Trans. R. Soc. B* **2009**, *364*, 1985–1998.

[19] Z. L. R. Botterell, N. Beaumont, T. Dorrington, M. Steinke, R. C. Thompson, P. K. Lindeque, *Environ. Pollut.* **2019**, *245*, 98–110.

[20] L. C. de Sá, M. Oliveira, F. Ribeiro, T. L. Rocha, M. N. Futter, *Sci. Total Environ.* **2018**, *645*, 1029–1039.

[21] Y. Zhang, S. Kang, S. Allen, D. Allen, T. Gao, M. Sillanpää, *Earth Sci. Rev.* **2020**, *203*, 103118.

[22] SAPEA, A Scientific Perspective on Microplastics in Nature and Society, **2019**, `https://doi.org/10.26356/microplastics` (visited on 01/03/2021).

[23] A. M. Mahon, B. O'Connell, M. G. Healy, I. O'Connor, R. Officer, R. Nash, L. Morrison, *Environ. Sci. Technol.* **2017**, *51*, 810–818.

[24] C. Juliano, G. Magrini, *Cosmetics* **2017**, *4*, 11–29.

[25] M. Kosuth, S. A. Mason, E. V. Wattenberg, *PLoS One* **2018**, *13*, e0194970.

[26] Q. Zhang, E. G. Xu, J. Li, Q. Chen, L. Ma, E. Y. Zeng, H. Shi, *Environ. Sci. Technol.* **2020**, *54*, 3740–3751.

[27] X. Chang, Y. Xue, J. Li, L. Zou, M. Tang, *J. Appl. Toxicol.* **2020**, *40*, 4–15.

[28] M. D. Lechner, K. Gehrke, E. Nordmeier, *Makromolekulare Chemie: Ein Lehrbuch für Chemiker, Physiker, Materialwissenschaftler und Verfahrenstechniker*, Birkhäuser Basel, 4., überarb. und erw. Aufl, **2010**.

[29] M. Szwarc, *Nature* **1956**, *178*, 1168–1169.

[30] M. Szwarc, M. Levy, R. Milkovich, *J. Am. Chem. Soc.* **1956**, *78*, 2656–2657.

[31] K. Matyjaszewski in *Encyclopedia of radicals in chemistry, biology, and materials*, (Eds.: C. Chatgilialoglu, A. Studer), John Wiley & Sons, Ltd., **2012**, pp. 1785–1812.

[32] J. Chiefari, Y. K. Chong, F. Ercole, J. Krstina, J. Jeffery, T. P. T. Le, R. T. A. Mayadunne, G. F. Meijs, C. L. Moad, G. Moad, E. Rizzardo, S. H. Thang, *Macromolecules* **1998**, *31*, 5559–5562.

[33] S. Perrier, *Macromolecules* **2017**, *50*, 7433–7447.

[34] G. Moad, E. Rizzardo, S. H. Thang, *Polymer* **2008**, *49*, 1079–1131.

[35] A. Li, J. Lu, *J. Appl. Polym. Sci.* **2009**, *114*, 2469–2473.

[36] G. Sun, C. Cheng, K. L. Wooley, *Macromolecules* **2007**, *40*, 793–795.

[37] D. J. Keddie, G. Moad, E. Rizzardo, S. H. Thang, *Macromolecules* **2012**, *45*, 5321–5342.

[38] G. Moad, *J. Polym. Sci. Part A: Polym. Chem.* **2018**, *57*, 216–227.

[39] M. Benaglia, J. Chiefari, Y. K. Chong, G. Moad, E. Rizzardo, S. H. Thang, *J. Am. Chem. Soc.* **2009**, *131*, 6914–6915.

[40] J. Gardiner, I. Martinez-Botella, T. M. Kohl, J. Krstina, G. Moad, J. H. Tyrell, M. L. Coote, J. Tsanaktsidis, *Polym. Int.* **2017**, *66*, 1438–1447.

[41] H. Willcock, R. K. O'Reilly, *Polym. Chem.* **2010**, *1*, 149–157.

[42] C. P. Jesson, C. M. Pearce, H. Simon, A. Werner, V. J. Cunningham, J. R. Lovett, M. J. Smallridge, N. J. Warren, S. P. Armes, *Macromolecules* **2017**, *50*, 182–191.

[43] M. Langer, J. Brandt, A. Lederer, A. S. Goldmann, F. H. Schacher, C. Barner-Kowollik, *Polym. Chem.* **2014**, *5*, 5330–5338.

[44] S. Perrier, P. Takolpuckdee, C. A. Mars, *Macromolecules* **2005**, *38*, 2033–2036.

[45] G. Moad, E. Rizzardo, S. H. Thang, *Polymer International* **2011**, *60*, 9–25.

[46] I.-H. Lee, E. H. Discekici, S. L. Shankel, A. Anastasaki, J. R. de Alaniz, C. J. Hawker, D. J. Lunn, *Polym. Chem.* **2017**, *8*, 7188–7194.

[47] D. Baskaran, A. H. E. Müller in *Controlled and Living Polymerizations*, (Eds.: A. H. E. Müller, K. Matyjaszewski), Wiley-VCH Verlag GmbH & Co. KGaA, Weinheim, Germany, **2009**, pp. 1–56.

[48] K. Fumino, P. Stange, V. Fossog, R. Hempelmann, R. Ludwig, *Angew. Chem. Int. Ed. Engl.* **2013**, *52*, 12439–12442.

[49] S. Carlotti, F. Peruch in *Anionic Polymerization*, (Eds.: N. Hadjichristidis, A. Hirao), Springer Japan, Tokyo, **2015**.

[50] I. E. Nifant'ev, A. V. Shlyakhtin, V. V. Bagrov, P. D. Komarov, M. A. Kosarev, A. N. Tavtorkin, M. E. Minyaev, V. A. Roznyatovsky, P. V. Ivchenko, *Polym. Chem.* **2017**, *8*, 6806–6816.

[51] T. Gleede, L. Reisman, E. Rieger, P. C. Mbarushimana, P. A. Rupar, F. R. Wurm, *Polym. Chem.* **2019**, *10*, 3257–3283.

[52] R. Luxenhofer, C. Fetsch, A. Grossmann, *J. Polym. Sci. Part A: Polym. Chem.* **2013**, *51*, 2731–2752.

[53] J. Herzberger, K. Niederer, H. Pohlit, J. Seiwert, M. Worm, F. R. Wurm, H. Frey, *Chem. Rev.* **2016**, *116*, 2170–2243.

[54] B. Esswein, M. Möller, *Angew. Chem. Int. Ed. Engl.* **1996**, *35*, 623–625.

[55] P. Verkoyen, H. Frey, *Macromol. Rapid Commun.* **2020**, *41*, e2000225.

[56] T. Yamamoto, *Polym. J.* **2013**, *45*, 711–717.

[57] B. Klumperman, *Polymer Science: A Comprehensive Reference* **2012**, *6*, 433–453.

[58] H. Feng, X. Lu, W. Wang, N.-G. Kang, J. Mays, *Polymers* **2017**, *9*, 494–525.

[59] M. Tambasco, J. E. G. Lipson, J. S. Higgins, *Macromolecules* **2006**, *39*, 4860–4868.

[60] J. N. Israelachvili, D. J. Mitchell, B. W. Ninham, *J. Chem. Soc. Faraday Trans. 2* **1976**, *72*, 1525–1568.

[61] R. Nagarajan, *Langmuir* **2002**, *18*, 31–38.

[62] M. Karayianni, S. Pispas in *Fluorescence Studies of Polymer Containing Systems*, (Ed.: K. Procházka), Springer International Publishing, Cham, **2016**, pp. 27–63.

[63] S. Y. Kim, R. A. Register in *Encyclopedia of Polymeric Nanomaterials*, (Eds.: S. Kobayashi, K. Müllen), Springer, Berlin, Heidelberg, **2021**, pp. 1–8.

[64] Y. M. A. Yamada, S. M. Sarkar, Y. Uozumi, *J. Am. Chem. Soc.* **2012**, *134*, 9285–9290.

[65] J. Lü, Y. Yang, J. Gao, H. Duan, C. Lü, *Langmuir* **2018**, *34*, 8205–8214.

[66] P. Cotanda, N. Petzetakis, R. K. O'Reilly, *MRS Commun.* **2012**, *2*, 119–126.

[67] V. Agrahari, V. Agrahari, *Drug Discovery Today* **2018**, *23*, 1139–1151.

[68] J. Líška, E. Borsig, *J. Macromol. Sci. Polym. Rev.* **1995**, *35*, 517–529.

[69] S. Koltzenburg, M. Maskos, O. Nuyken, *Polymere: Synthese, Eigenschaften und Anwendungen*, Springer, Berlin, Heidelberg, **2014**.

[70] M. L. Hallensleben, R. Fuss, F. Mummy in *Ullmann's Encyclopedia of Industrial Chemistry*, American Cancer Society, **2015**, pp. 1–23.

[71] M. A. Gauthier, M. I. Gibson, H.-A. Klok, *Angew. Chem. Int. Ed.* **2009**, *48*, 48–58.

[72] E. M. Muzammil, A. Khan, M. C. Stuparu, *RSC Adv.* **2017**, *7*, 55874–55884.

[73] A. S. Goldmann, M. Glassner, A. J. Inglis, C. Barner-Kowollik, *Macromol. Rapid Commun.* **2013**, *34*, 810–849.

[74] A. B. Lowe, *Polym. Chem.* **2010**, *1*, 17–36.

[75] S. P. S. Koo, M. M. Stamenović, R. A. Prasath, A. J. Inglis, F. E. Du Prez, C. Barner-Kowollik, W. van Camp, T. Junkers, *J. Polym. Sci. A Polym. Chem.* **2010**, *48*, 1699–1713.

[76] M. Hess, R. G. Jones, J. Kahovec, T. Kitayama, P. Kratochvíl, P. Kubisa, W. Mormann, R. F. T. Stepto, D. Tabak, J. Vohlídal, E. S. Wilks, *Pure Appl. Chem.* **2006**, *78*, 2067–2074.

[77] D. V. Pergushov, A. H. E. Müller, F. H. Schacher, *Chem. Soc. Rev.* **2012**, *41*, 6888–6901.

[78] L. García-Fernández, A. Mora-Boza, F. Reyes-Ortega in *Smart Polymers and their Applications (Second Edition)*, (Eds.: M. R. Aguilar, J. S. Román), Woodhead Publishing in Materials, Woodhead Publishing, **2019**, pp. 45–86.

[79] J. Yuan, D. Mecerreyes, M. Antonietti, *Prog. Polym. Sci.* **2013**, *38*, 1009–1036.

[80] J. Yuan, M. Antonietti, *Polymer* **2011**, *52*, 1469–1482.

[81] W. Qian, J. Texter, F. Yan, *Chem. Soc. Rev.* **2017**, *46*, 1124–1159.

[82] D. Avci, N. Mol, L. Dagasan, *Polym. Bull.* **2002**, *48*, 353–359.

[83] A. Laschewsky, *Polymers* **2014**, *6*, 1544–1601.

[84] A. B. Lowe, C. L. McCormick, *Chem. Rev.* **2002**, *102*, 4177–4190.

[85] F. Wang, J. Yang, J. Zhao, *Polym. Int.* **2015**, *64*, 999–1005.

[86] S. Minchin, J. Lodge, *Essays Biochem.* **2019**, *63*, 433–456.

[87] M. L. Edelstein, M. R. Abedi, J. Wixon, R. M. Edelstein, *J. Gene Med.* **2004**, *6*, 597–602.

[88] M. A. Mintzer, E. E. Simanek, *Chem. Rev.* **2009**, *109*, 259–302.

[89] A. Bertin in *Polyelectrolyte Complexes in the Dispersed and Solid State II: Application Aspects*, (Ed.: M. Müller), Springer, Berlin, Heidelberg, **2014**, pp. 103–195.

[90] S. Uchida, K. Kataoka, *J. Biomed. Mater. Res.* **2019**, *107*, 978–990.

[91] K. Osada, *Polym. J.* **2014**, *46*, 469–475.

[92] R. M. Pearson, H.-j. Hsu, J. Bugno, S. Hong, *MRS Bull.* **2014**, *39*, 227–237.

[93] Y.-B. Hu, E. B. Dammer, R.-J. Ren, G. Wang, *Transl. Neurodegener.* **2015**, *4*, 869.

[94] T. Bus, A. Traeger, U. S. Schubert, *J. Mater. Chem. B* **2018**, *6*, 6904–6918.

[95] C. L. Grigsby, K. W. Leong, *J. R. Soc. Interface.* **2010**, *7*, 983.

[96] C. Scholz, E. Wagner, *J. Controlled Release* **2012**, *161*, 554–565.

[97] J. Wang, Z. Lu, M. G. Wientjes, J. L.-S. Au, *AAPS J.* **2010**, *12*, 492–503.

[98] S. Soll, Q. Zhao, J. Weber, J. Yuan, *Chem. Mater.* **2013**, *25*, 3003–3010.

[99] S. Schöttler, G. Becker, S. Winzen, T. Steinbach, K. Mohr, K. Landfester, V. Mailänder, F. R. Wurm, *Nat. Nanotech.* **2016**, *11*, 372–377.

[100] M. J. Barthel, K. Babiuch, T. Rudolph, J. Vitz, S. Hoeppener, M. Gottschaldt, M. D. Hager, F. H. Schacher, U. S. Schubert, *J. Polym. Sci. A Polym. Chem.* **2012**, *50*, 2914–2923.

[101] Z. Zhang, C. Liu, C. Li, W. Wu, X. Jiang, *Research* **2019**, *2019*, 1–13.

[102] U. Günther, L. V. Sigolaeva, D. V. Pergushov, F. H. Schacher, *Macromol. Chem. Phys.* **2013**, *407*, 2202–2212.

[103] M. von der Lühe, U. Günther, A. Weidner, C. Gräfe, J. H. Clement, S. Dutz, F. H. Schacher, *RSC Adv.* **2015**, *5*, 31920–31929.

[104] P. Biehl, M. von der Lühe, S. Dutz, F. H. Schacher, *Polymers* **2018**, *10*, 91.

[105] J. B. Max, D. V. Pergushov, L. V. Sigolaeva, F. H. Schacher, *Polym. Chem.* **2019**, *10*, 3006–3019.

[106] J. B. Max, K. Kowalczuk, M. Köhler, C. Neumann, F. Pielenz, L. V. Sigolaeva, D. V. Pergushov, A. Turchanin, F. Langenhorst, F. H. Schacher, *Macromolecules* **2020**, *53*, 4511–4523.

[107] S. Asayama, T. Sekine, H. Kawakami, S. Nagaoka, *Bioconjugate Chem.* **2007**, *18*, 1662–1667.

[108] E. N. Danilovtseva, S. N. Zelinskiy, V. A. Pal'shin, G. Kandasamy, U. M. Krishnan, V. V. Annenkov, *Chin. J. Polym. Sci.* **2019**, *37*, 637–645.

[109] Y. M. A. Yamada, S. M. Sarkar, Y. Uozumi, *J. Am. Chem. Soc.* **2012**, *134*, 3190–3198.

[110] M. Takafuji, S. Ide, H. Ihara, Z. Xu, *Chem. Mater.* **2004**, *16*, 1977–1983.

[111] J.-K. Sun, Z. Kochovski, W.-Y. Zhang, H. Kirmse, Y. Lu, M. Antonietti, J. Yuan, *J. Am. Chem. Soc.* **2017**, *139*, 8971–8976.

[112] B. Wu, D. Hu, Y. Kuang, B. Liu, X. Zhang, J. Chen, *Angew. Chem. Int. Ed.* **2009**, *48*, 4751–4754.

[113] Y. Ding, A. Klyushin, X. Huang, T. Jones, D. Teschner, F. Girgsdies, T. Rodenas, R. Schlögl, S. Heumann, *Angew. Chem. Int. Ed.* **2018**, *57*, 3514–3518.

[114] W. Hou, Q. Wang, Z. Guo, J. Li, Y. Zhou, J. Wang, *Catal. Sci. Technol.* **2017**, *7*, 1006–1016.

[115] I. Yavari, H. Norouzi-Arasi, *Phosphorus Sulfur Silicon Relat. Elem.* **2002**, *177*, 87–92.

[116] B. M. Trost, G. R. Dake, *J. Am. Chem. Soc.* **1997**, *119*, 7595–7596.

[117] M. Balogh, C. Gönczi, I. Hermecz, *Stud Surf. Sci. Catal.* **1997**, *108*, 603–607.

[118] S. Santanakrishnan, R. A. Hutchinson, *Macromol. Chem. Phys.* **2013**, *214*, 1140–1146.

[119] M. H. Allen, S. T. Hemp, A. E. Smith, T. E. Long, *Macromolecules* **2012**, *45*, 3669–3676.

[120] M. Rikkou-Kalourkoti, P. A. Panteli, C. S. Patrickios, *Polym. Chem.* **2014**, *5*, 4339.

[121] B. M. Blunden, A. Rawal, H. Lu, M. H. Stenzel, *Macromolecules* **2014**, *47*, 1646–1655.

[122] D. Cordella, A. Kermagoret, A. Debuigne, C. Jérôme, D. Mecerreyes, M. Isik, D. Taton, C. Detrembleur, *Macromolecules* **2015**, *48*, 5230–5243.

[123] Z. Cui, H. Cao, Y. Ding, P. Gao, X. Lu, Y. Cai, *Polymer Chemistry* **2017**, *8*, 3755–3763.

[124] F. Zhang, W. Li, X. Zheng, P. Fang, H. Zhang, *J. Mater. Sci.* **2018**, *53*, 15784–15794.

[125] L. V. Sigolaeva, T. V. Bulko, M. S. Kozin, W. Zhang, M. Köhler, I. Romanenko, J. Yuan, F. H. Schacher, D. V. Pergushov, V. V. Shumyantseva, *Polymer* **2019**, *168*, 95–103.

[126] C. G. Overberger, N. Vorchheimer, *J. Am. Chem. Soc.* **1963**, *85*, 951–955.

[127] J. S. Tan, A. R. Sochor, *Macromolecules* **1981**, *14*, 1700–1706.

[128] C. Fodor, J. Bozi, M. Blazsó, B. Iván, *Macromolecules* **2012**, *45*, 8953–8960.

[129] K. Yao, Z. Wang, J. Wang, S. Wang, *Chem. Commun.* **2012**, *48*, 1766–1768.

[130] C. Jangu, J.-H. H. Wang, D. Wang, S. Sharick, J. R. Heflin, K. I. Winey, R. H. Colby, T. E. Long, *Macromol. Chem. Phys.* **2014**, *215*, 1319–1331.

[131] C. Jangu, J.-H. H. Wang, D. Wang, G. Fahs, J. R. Heflin, R. B. Moore, R. H. Colby, T. E. Long, *J. Mater. Chem. C* **2015**, *3*, 3891–3901.

[132] C. Rössel, M. Billing, H. Görls, G. Festag, M. Grube, P. Bellstedt, I. Nischang, F. H. Schacher, *Polymer* **2017**, *127*, 182–191.

[133] M. Riske, *Herstellung und Untersuchung von modifizierten Poly(2-(imidazol-1-yl)acrylsäureestern)*, Bachelor thesis, Friedrich-Schiller Universität Jena, **2019**.

[134] X. Wang, K. Zheng, X. Feng, C. Xu, W. Song, *Sens. Actuators B Chem.* **2015**, *219*, 361–369.

[135] S. Bellayer, J. W. Gilman, N. Eidelman, S. Bourbigot, X. Flambard, D. M. Fox, H. C. De Long, P. C. Trulove, *Adv. Funct. Mater.* **2005**, *15*, 910–916.

[136] F. Meyer, J.-M. Raquez, O. Coulembier, J. de Winter, P. Gerbaux, P. Dubois, *Chem. Commun.* **2010**, *46*, 5527–5529.

[137] M. von der Lühe, *Surface Engineering of Magnetic Nanoparticles: Synthesis, Reversibility, and Applications*, Dissertation, Friedrich-Schiller University Jena, **2018**.

[138] P. Biehl, P. Wiemuth, J. G. Lopez, M.-C. Barth, A. Weidner, S. Dutz, K. Peneva, F. H. Schacher, *Langmuir* **2020**, *36*, 6095–6105.

[139] B. L. Batchelor, S. F. Mahmood, M. Jung, H. Shin, O. V. Kulikov, W. Voit, B. M. Novak, D. J. Yang, *Carbon* **2016**, *98*, 681–688.

[140] M. Horn, K. Matyjaszewski, *Macromolecules* **2013**, *46*, 3350–3357.

[141] A. Kaur, T. G. Ribelli, K. Schröder, K. Matyjaszewski, T. Pintauer, *Inorg. Chem.* **2015**, *54*, 1474–1486.

[142] W. Tang, Y. Kwak, W. Braunecker, N. V. Tsarevsky, M. L. Coote, K. Matyjaszewski, *J. Am. Chem. Soc.* **2008**, *130*, 10702–10713.

[143] K. Gehrke, E. H. Nordmeier, M. D. Lechner, *Makromolekulare Chemie: Ein Lehrbuch für Chemiker, Physiker, Materialwissenschaftler und Verfahrenstechniker*, Birkhäuser Verlag, Basel–Boston–Berlin, 4., überarb. und erw. Aufl, **2010**.

[144] J. Qui, B. Charleux, K. Matyjaszewski, *Polimery* **2001**, *46*, 454–460.

[145] N. V. Tsarevsky, *Fundamentals of Controlled/Living Radical Polymerization*, RSC Publ., Cambridge, **2013**.

[146] S. H. Thang, Y. K. Chong, R. T. Mayadunne, G. Moad, E. Rizzardo, *Tetrahedron Lett.* **1999**, *40*, 2435–2438.

[147] M. Benaglia, E. Rizzardo, A. Alberti, M. Guerra, *Macromolecules* **2005**, *38*, 3129–3140.

[148] V. Šubr, L. Kostka, J. Strohalm, T. Etrych, K. Ulbrich, *Macromolecules* **2013**, *46*, 2100–2108.

[149] G. Ayrey, *Chem. Rev.* **1963**, *63*, 645–667.

[150] J. K. Fink, *J. Polym. Sci. Polym. Chem. Ed.* **1983**, *21*, 1445–1455.

[151] G. Moad, E. Rizzardo, D. H. Solomon, S. R. Johns, R. I. Willing, *Makromol. Chem. Rapid Commun.* **1984**, *5*, 793–798.

[152] B. Neises, W. Steglich, *Angew. Chem. Int. Ed. Engl.* **1978**, *17*, 522–524.

[153] E. E. Stache, V. Kottisch, B. P. Fors, *J. Am. Chem. Soc.* **2020**, *142*, 4581–4585.

[154] H. Wang, Z. Chen, L. Xin, J. Cui, S. Zhao, Y. Yan, *J. Polym. Sci. Part A Polym. Chem.* **2015**, *53*, 2175–2185.

[155] I. Vikholm-Lundin, S. Auer, M. Paakkunainen, J. A. Määttä, T. Munter, J. Leppiniemi, V. P. Hytönen, K. Tappura, *Sens. Actuators B Chem.* **2012**, *171-172*, 440–448.

[156] F. Falvo, L. Fiebig, M. Schäfer, *Int. J. Mass Spectrom.* **2013**, *354-355*, 26–32.

[157] O. Geraschenko, P. Khodakovskiy, O. Shishkin, P. Mykhailiuk, O. Zaporozhets, A. Tolmachev, *Synthesis* **2011**, *2011*, 1633–1637.

[158] D. Ray, J. T. Foy, R. P. Hughes, I. Aprahamian, *Nat. Chem.* **2012**, *4*, 757–762.

[159] J. D. Ha, S. J. Lee, S. Y. Nam, S. K. Kang, S. Y. Cho, J. H. Ahn, J.-K. Choi, *Tetrahedron Lett.* **2006**, *47*, 6201–6204.

[160] A. Abbotto, S. Bradamante, G. A. Pagani, *J. Org. Chem.* **1996**, *61*, 1761–1769.

[161] J. D. Martell, H. Li, T. Doukov, P. Martásek, L. J. Roman, M. Soltis, T. L. Poulos, R. B. Silverman, *J. Am. Chem. Soc.* **2010**, *132*, 798–806.

[162] M. Mishina, A. Ivanov, P. Lobanov, D. Dar'in, *Synthesis* **2016**, *48*, 2851–2862.

[163] Y. Tang, C. He, G. H. Imler, D. A. Parrish, J. M. Shreeve, *Chem. Eur. J.* **2017**, *23*, 16401–16407.

[164] M. A. Land, B. Huo, K. N. Robertson, K. E. O. Ylijoki, P. T. K. Lee, J. Areephong, D. Vidović, J. A. C. Clyburne, *Dalton Trans.* **2018**, *47*, 10195–10205.

[165] P. V. Ramachandran, D. Nicponski, B. Kim, *Org. Lett.* **2013**, *15*, 1398–1401.

[166] S. V. Mulay, R. A. Fernandes, *Chem. Eur. J.* **2015**, *21*, 4842–4852.

[167] K. Ebel in *Hetarene III*, (Ed.: E. Schaumann), Methoden der Organischen Chemie (Houben-Weyl) - Hetarene III, Georg Thieme Verlag, Stuttgart, **1994**, pp. 15–16.

[168] N. Matsunaga, T. Kaku, F. Itoh, T. Tanaka, T. Hara, H. Miki, M. Iwasaki, T. Aono, M. Yamaoka, M. Kusaka, A. Tasaka, *Bioorg. Med. Chem.* **2004**, *12*, 2251–2273.

[169] J. Krall, B. M. Brygger, S. B. Sigurðardóttir, C. K. L. Ng, C. Bundgaard, J. Kehler, B. Nielsen, T. Bek, A. A. Jensen, B. Frølund, *ChemMedChem* **2016**, *11*, 2299–2310.

[170] K. L. Seley, S. Salim, L. Zhang, *Org. Lett.* **2005**, *7*, 63–66.

[171] A. Hirsch, K. Richardson, *J. Appl. Chem.* **1969**, *19*, 83–85.

[172] G. D. Prell, *J. Labelled Compd. Radiopharm.* **1991**, *29*, 111–115.

[173] Y. He, Y. Chen, H. Du, L. A. Schmid, C. J. Lovely, *Tetrahedron Lett.* **2004**, *45*, 5529–5532.

[174] G. Agelis, A. Resvani, S. Durdagi, K. Spyridaki, T. Tůmová, J. Slaninová, P. Giannopoulos, D. Vlahakos, G. Liapakis, T. Mavromoustakos, J. Matsoukas, *Eur. J. Med. Chem.* **2012**, *55*, 358–374.

[175] J.-M. Kee, B. Villani, L. R. Carpenter, T. W. Muir, *J. Am. Chem. Soc.* **2010**, *132*, 14327–14329.

[176] M. Vuilhorgne, J. Malpart, S. Mutti, S. Mignani, *J. Heterocycl. Chem.* **2003**, *40*, 159–162.

[177] P. Wanat, S. Walczak, B. A. Wojtczak, M. Nowakowska, J. Jemielity, J. Kowalska, *Org. Lett.* **2015**, *17*, 3062–3065.

[178] T. E. McAllister, M. G. Nix, M. E. Webb, *Chem. Commun.* **2011**, *47*, 1297–1299.

[179] B. Yamada, T. Otsu, *Makromol. Chem.* **1991**, *192*, 333–340.

[180] B. Yamada, S. Kobatake, *Prog. Polym. Sci.* **1994**, *19*, 1089–1131.

[181] T. Hirano, B. Yamada, *Polymer* **2003**, *44*, 4481–4486.

[182] S. C. Warren, L. J. Mathias, *J. Polym. Sci. A Polym. Chem.* **1990**, *28*, 1637–1648.

[183] R. Fikentscher, E. Hahn, A. Kud, A. Oftring, BASF AG, US4654432, **1987**.

[184] G. F. Meijs, E. Rizzardo, S. H. Thang, *Polym. Bull.* **1990**, *24*, 501–505.

[185] D. Pasini, J .M. Klopp, J. M. J. Fréchet, *Chem. Mater.* **2001**, *13*, 4136–4146.

[186] Y. Kohsaka, Y. Matsumoto, T. Kitayama, *Polym. Chem.* **2015**, *6*, 5026–5029.

[187] G. Peer, P. Dorfinger, T. Koch, J. Stampfl, C. Gorsche, R. Liska, *Macromolecules* **2018**, *51*, 9344–9353.

[188] C. Peng, A. Joy, *Macromolecules* **2014**, *47*, 1258–1268.

[189] N. J. Warren, O. O. Mykhaylyk, D. Mahmood, A. J. Ryan, S. P. Armes, *J. Am. Chem. Soc.* **2014**, *136*, 1023–1033.

[190] R. Göschke, S. Stutz, V. Rasetti, N.-C. Cohen, J. Rahuel, P. Rigollier, H.-P. Baum, P. Forgiarini, C. R. Schnell, T. Wagner, M. G. Gruetter, W. Fuhrer, W. Schilling, F. Cumin, J. M. Wood, J. Maibaum, *J. Med. Chem.* **2007**, *50*, 4818–4831.

[191] H. Zhou, Y. Chen, C. M. Plummer, H. Huang, Y. Chen, *Polym. Chem.* **2017**, *8*, 2189–2196.

[192] F. Nagler, *Synthesis of Poly(guanidinomethylacrylic acid)*, Bachelor thesis, Friedrich Schiller University Jena, **2019**.

[193] K. D. B. Yamajala, S. Banerjee, *ChemistrySelect* **2017**, *2*, 3152–3157.

[194] W. Luo, Y. Yang, Y. Fang, X. Zhang, X. Jin, G. Zhao, L. Zhang, Y. Li, W. Zhou, T. Xia, B. Chen, *Adv. Synth. Catal.* **2019**, *361*, 4215–4221.

[195] B. Shi, M. Zheng, W. Tao, R. Chung, D. Jin, D. Ghaffari, O. C. Farokhzad, *Biomacromolecules* **2017**, *18*, 2231–2246.

[196] D. S. Shah, T. Sakthivel, I. Toth, A. T. Florence, A. F. Wilderspin, *Int. J. Pharm.* **2000**, *208*, 41–48.

[197] Y. Inoue, R. Kurihara, A. Tsuchida, M. Hasegawa, T. Nagashima, T. Mori, T. Niidome, Y. Katayama, O. Okitsu, *J. Controlled Release* **2008**, *126*, 59–66.

[198] C. Yang, N. Panwar, Y. Wang, B. Zhang, M. Liu, H. Toh, H. S. Yoon, S. C. Tjin, P. H. J. Chong, W.-C. Law, C.-K. Chen, K.-T. Yong, *Nanoscale* **2016**, *8*, 9405–9416.

[199] A. M. Nelson, A. M. Pekkanen, N. L. Forsythe, J. H. Herlihy, M. Zhang, T. E. Long, *Biomacromolecules* **2017**, *18*, 68–76.

[200] R. Lehner, K. Liu, X. Wang, M. Wolf, P. Hunziker, *Nanotechnology* **2017**, *28*, 175602.

[201] M. N. Leiske, F. H. Sobotta, F. Richter, S. Hoeppener, J. C. Brendel, A. Traeger, U. S. Schubert, *Biomacromolecules* **2018**, *19*, 748–760.

[202] A. Reschner, Y. H. Shim, P. Dubois, P. Delvenne, B. Evrard, L. Marcélis, C. Moucheron, A. Kirsch-De Mesmaeker, E. Defrancq, M. Raes, J. Piette, L. Collard, G. Piel, *J. Biomed. Nanotechnol.* **2013**, *9*, 1432–1440.

[203] A.-K. Trützschler, T. Bus, M. Reifarth, J. C. Brendel, S. Hoeppener, A. Traeger, U. S. Schubert, *Bioconjugate Chem.* **2018**, *29*, 2181–2194.

[204] S. Luo, R. Cheng, F. Meng, T. G. Park, Z. Zhong, *J. Polym. Sci. A Polym. Chem.* **2011**, *49*, 3366–3373.

[205] F. Richter, L. Martin, K. Leer, E. Moek, F. Hausig, J. C. Brendel, A. Traeger, *J. Mater. Chem. B* **2020**, *8*, 5026–5041.

[206] C. Zheng, M. Zheng, P. Gong, J. Deng, H. Yi, P. Zhang, Y. Zhang, P. Liu, Y. Ma, L. Cai, *Biomaterials* **2013**, *34*, 3431–3438.

[207] K. M. Takeda, K. Osada, T. A. Tockary, A. Dirisala, Q. Chen, K. Kataoka, *Biomacromolecules* **2017**, *18*, 36–43.

[208] M. Bauer, L. Tauhardt, H. M. L. Lambermont-Thijs, K. Kempe, R. Hoogenboom, U. S. Schubert, D. Fischer, *Eur. J. Pharm. Biopharm.* **2018**, *133*, 112–121.

[209] A. B. Cook, R. Peltier, J. Zhang, P. Gurnani, J. Tanaka, J. A. Burns, R. Dallmann, M. Hartlieb, S. Perrier, *Polym. Chem.* **2019**, *10*, 1202–1212.

[210] Y. Cheng, D. L. Sellers, J.-K. Y. Tan, D. J. Peeler, P. J. Horner, S. H. Pun, *Biomaterials* **2017**, *127*, 89–96.

[211] D. Santo, P. V. Mendonça, M. S. Lima, R. A. Cordeiro, L. Cabanas, A. Serra, Coelho, Jorge F J, H. Faneca, *Mol. Pharmaceutics* **2019**, *16*, 2129–2141.

[212] M. Hrubý, C. Konák, K. Ulbrich, *J. Controlled Release* **2005**, *103*, 137–148.

[213] M. J. Barthel, U. Mansfeld, S. Hoeppener, J. A. Czaplewska, F. H. Schacher, U. S. Schubert, *Soft Matter* **2013**, *9*, 3509–3520.

[214] T. A. Tockary, K. Osada, Q. Chen, K. Machitani, A. Dirisala, S. Uchida, T. Nomoto, K. Toh, Y. Matsumoto, K. Itaka, K. Nitta, K. Nagayama, K. Kataoka, *Macromolecules* **2013**, *46*, 6585–6592.

[215] M. J. Barthel, A. C. Rinkenauer, M. Wagner, U. Mansfeld, S. Hoeppener, J. A. Czaplewska, M. Gottschaldt, A. Träger, F. H. Schacher, U. S. Schubert, *Biomacromolecules* **2014**, *15*, 2426–2439.

[216] B. Obermeier, H. Frey, *Bioconjugate Chem.* **2011**, *22*, 436–444.

[217] Y. Zhang, P. Lundberg, M. Diether, C. Porsch, C. Janson, N. A. Lynd, C. Ducani, M. Malkoch, E. Malmström, C. J. Hawker, A. M. Nyström, *J. Mater. Chem. B* **2015**, *3*, 2472–2486.

[218] K. Hatakeyama-Sato, S. Kimura, S. Matsumoto, K. Oyaizu, *Macromol. Rapid Commun.* **2020**, *41*, e1900399.

[219] V. Loczenski Rose, S. Shubber, S. Sajeesh, S. G. Spain, S. Puri, S. Allen, D.-K. Lee, G. S. Winkler, G. Mantovani, *Biomacromolecules* **2015**, *16*, 3480–3490.

[220] S. T. Hemp, M. H. Allen, M. D. Green, T. E. Long, *Biomacromolecules* **2011**, *13*, 231–238.

[221] H. Uchida, K. Miyata, M. Oba, T. Ishii, T. Suma, K. Itaka, N. Nishiyama, K. Kataoka, *J. Am. Chem. Soc.* **2011**, *133*, 15524–15532.

[222] J. M. Chalker, L. Lercher, N. R. Rose, C. J. Schofield, B. G. Davis, *Angew. Chem. Int. Ed.* **2012**, *51*, 1835–1839.

[223] K. C. Nicolaou, J. I. Trujillo, B. Jandeleit, K. Chibale, M. Rosenfeld, B. Diefenbach, D. A. Cheresh, S. L. Goodman, *Bioorg. Med. Chem.* **1998**, *6*, 1185–1208.

[224] R. A. Moss, W. Ma, D. C. Merrer, S. Xue, *Tetrahedron Lett.* **1995**, *36*, 8761–8764.

[225] H. K. Lee, L. N. Ten, C. S. Pak, *Bull. Korean Chem. Soc.* **1998**, *19*, 1148–1149.

[226] L. Allmendinger, G. Bauschke, F. F. Paintner, *Synlett* **2005**, *17*, 2615–2618.

[227] T. R. Krishna, N. Jayaraman, *J. Org. Chem.* **2003**, *68*, 9694–9704.

[228] C. G. Radu, Z. Li, R. M. Gipson, J. Wang, N. Satyamurthy, J. M. Murphy, D. A. Nathanson, M. E. Jung, University of California, University of Illinois, WO2015-023776 A2, **2015**.

[229] J. Spychała, *Catal. Lett.* **2006**, *109*, 55–60.

[230] M. E. Jung, P. Koch, *Tetrahedron Lett.* **2011**, *52*, 6051–6054.

[231] P. G. M. Wuts, T. W. Greene, *Greene's Protective Groups in Organic Synthesis*, John Wiley & Sons, Inc, Hoboken, NJ, USA, **2006**.

[232] S. S. Husain, S. A. Forman, M. A. Kloczewiak, G. H. Addona, R. W. Olsen, M. B. Pratt, J. B. Cohen, K. W. Miller, *J. Med. Chem.* **1999**, *42*, 3300–3307.

[233] D. K. Donald, A. S. R. Jennings, N. C. Ray, F. Roussel, J. M. Sutton, P. Tisselli, M. Wilson, AstraZeneca AB, Pulmagen Therapeutics (Synergy) Limited, WO2011-048409 A1, **2011**.

[234] S. J. Dünki, M. Tress, F. Kremer, S. Y. Ko, F. A. Nüesch, C.-D. Varganici, C. Racles, D. M. Opris, *RSC Adv.* **2015**, *5*, 50054–50062.

[235] C. de Stefano, O. Giuffrè, S. Sammartano, *J. Chem. Eng. Data* **2005**, *50*, 1917–1923.

[236] S. Cren, A. Friedli, G. Rueedi, C. Zumbrunn, Actelion Pharmaceuticals Ltd., WO2016-059097 A1, **2016**.

[237] C. A. M. Afonso, N. M. T. Lourenço, A. A. Rosatella, *Molecules* **2006**, *11*, 81–102.

[238] X. Jia, Q. Huang, J. Li, S. Li, Q. Yang, *Synlett* **2007**, *2007*, 806–808.

[239] M. Krause, X. Ligneau, H. Stark, M. Garbarg, J. C. Schwartz, W. Schunack, *J. Med. Chem.* **1998**, *41*, 4171–4176.

[240] H. Peng, D. Carrico, van Thai, M. Blaskovich, C. Bucher, E. E. Pusateri, S. M. Sebti, A. D. Hamilton, *Org. Biomol. Chem.* **2006**, *4*, 1768–1784.

[241] A. V. Silamkoti, P. W. Allan, A. E. A. Hassan, A. T. Fowler, E. J. Sorscher, W. B. Parker, J. A. Secrist, *Nucleosides Nucleotides Nucleic Acids* **2005**, *24*, 881–885.

[242] E. Bedner, L. Du, F. Traganos, Z. Darzynkiewicz, *Cytometry* **2001**, *43*, 38–45.

[243] I. M. Johnson, H. Prakash, J. Prathiba, R. Raghunathan, R. Malathi, *PloS One* **2012**, *7*, e50019.

[244] J. Pandey, V. K. Tiwari, S. S. Verma, V. Chaturvedi, S. Bhatnagar, S. Sinha, A. N. Gaikwad, R. P. Tripathi, *Eur. J. Med. Chem.* **2009**, *44*, 3350–3355.

[245] C. Mattheis, H. Wang, C. Meister, S. Agarwal, *Macromol. Biosci.* **2013**, *13*, 242–255.

[246] D. J. Kim, K. H. Oh, J. K. Park, *Green Chem.* **2014**, *16*, 4098–4101.

[247] A. Pobudkowska, U. Domańska, J. A. Kryska, *J. Chem. Thermodyn.* **2014**, *79*, 41–48.

[248] J. Zhong, N. Tang, B. Asadzadeh, W. Yan, *J. Chem. Eng. Data* **2017**, *62*, 2570–2577.

[249] S. Kaga, N. P. Truong, L. Esser, D. Senyschyn, A. Sanyal, R. Sanyal, J. F. Quinn, T. P. Davis, L. M. Kaminskas, M. R. Whittaker, *Biomacromolecules* **2017**, *18*, 3963–3970.

[250] N. P. Truong, J. F. Quinn, M. R. Whittaker, T. P. Davis, *Polym. Chem.* **2016**, *7*, 4295–4312.

[251] F. M. Veronese, *Biomaterials* **2001**, *22*, 405–417.

[252] M. Brunzel, T. C. Majdanski, J. Vitz, I. Nischang, U. S. Schubert, *Polymers* **2018**, *10*, 1395.

[253] S. Falke, C. Betzel in *Radiation in Bioanalysis: Spectroscopic Techniques and Theoretical Methods*, (Eds.: A. S. Pereira, P. Tavares, P. Limão-Vieira), Springer International Publishing, Cham, **2019**, pp. 173–193.

[254] D. M. Love, K. Kim, J. T. Goodrich, B. D. Fairbanks, B. T. Worrell, M. P. Stoykovich, C. B. Musgrave, C. N. Bowman, *J. Org. Chem.* **2018**, *83*, 2912–2919.

[255] Q. Xu, L. M. Ensign, N. J. Boylan, A. Schön, X. Gong, J.-C. Yang, N. W. Lamb, S. Cai, T. Yu, E. Freire, J. Hanes, *ACS Nano* **2015**, *9*, 9217–9227.

[256] K. Rahme, L. Chen, R. G. Hobbs, M. A. Morris, C. O'Driscoll, J. D. Holmes, *RSC Adv.* **2013**, *3*, 6085–6094.

[257] P. Xu, Van Kirk, Edward A., W. J. Murdoch, Y. Zhan, D. D. Isaak, M. Radosz, Y. Shen, *Biomacromolecules* **2006**, *7*, 829–835.

[258] S. Miwa, R. Takahashi, C. Rössel, S. Matsumoto, S. Fujii, J. H. Lee, F. H. Schacher, K. Sakurai, *Langmuir* **2018**, *34*, 7813–7820.

[259] R. Takahashi, S. Miwa, C. Rössel, S. Fujii, J. H. Lee, F. H. Schacher, K. Sakurai, *Polym. Chem.* **2020**, *11*, 3446–3452.

[260] A. Toor, T. Feng, T. P. Russell, *Eur. Phys. J. E* **2016**, *39*, 57.

[261] B. M. Raycraft, J. P. MacDonald, J. T. McIntosh, M. P. Shaver, E. R. Gillies, *Polym. Chem.* **2017**, *8*, 557–567.

[262] D. M. Heinrich, J.-J. Youte, W. A. Denny, M. Tercel, *Tetrahedron Lett.* **2011**, *52*, 7000–7003.

[263] A. R. Kraska, Pfizer Inc., US4255426 A, **1981**.

[264] J. Allgaier, S. Willbold, T. Chang, *Macromolecules* **2007**, *40*, 518–525.

[265] A.-L. Brocas, C. Mantzaridis, D. Tunc, S. Carlotti, *Prog. Polym. Sci.* **2013**, *38*, 845–873.

[266] J. Blankenburg, M. Wagner, H. Frey, *Macromolecules* **2017**, *50*, 8885–8893.

[267] P. Verkoyen, T. Johann, J. Blankenburg, C. Czysch, H. Frey, *Polym. Chem.* **2018**, *9*, 5327–5338.

[268] J. K. Elter, P. Biehl, M. Gottschaldt, F. H. Schacher, *Polym. Chem.* **2019**, *10*, 5425–5439.

[269] van Nostrum, C. F., *Soft Matter* **2011**, *7*, 3246–3259.

[270] F. Q. Schafer, G. R. Buettner, *Free Radical Biol. Med.* **2001**, *30*, 1191–1212.

[271] S. McRae Page, M. Martorella, S. Parelkar, I. Kosif, T. Emrick, *Mol. Pharmaceutics* **2013**, *10*, 2684–2692.

[272] C. B. Cooley, B. M. Trantow, F. Nederberg, M. K. Kiesewetter, J. L. Hedrick, R. M. Waymouth, P. A. Wender, *J. Am. Chem. Soc.* **2009**, *131*, 16401–16403.

[273] A.-L. Zhang, Z.-d. Yu, L.-W. Yang, N.-F. Yang, *Tetrahedron: Asymmetry* **2015**, *26*, 173–179.

[274] J. Seiwert, J. Herzberger, D. Leibig, H. Frey, *Macromol. Rapid Commun.* **2017**, *38*.

[275] K. M. Zurick, M. Bernards, *J. Appl. Polym. Sci.* **2014**, *131*, n/a.

[276] M. Billing, G. Festag, P. Bellstedt, F. H. Schacher, *Polym. Chem.* **2017**, *8*, 936–945.

[277] H. E. Gottlieb, V. Kotlyar, A. Nudelman, *J. Org. Chem.* **1997**, *62*, 7512–7515.

[278] G. R. Fulmer, Miller, Alexander J. M., N. H. Sherden, H. E. Gottlieb, A. Nudelman, B. M. Stoltz, J. E. Bercaw, K. I. Goldberg, *Organometallics* **2010**, *29*, 2176–2179.

[279] C. R. Morcombe, K. W. Zilm, *J. Magn. Reson.* **2003**, *162*, 479–486.

[280] R. W. W. Hooft, *COLLECT, Data Collection Software*, Nonius BV, Delft, The Netherlands, **1998**.

[281] Z. Otwinowski, W. Minor, *Methods Enzymol.* **1997**, *276*, 307–326.

[282] *SADABS 2.10*, Bruker-AXS Inc., Madison, Wisconsin, USA, **2002**.

[283] G. M. Sheldrick, *Acta Crystallogr. Sect. A: Found. Crystallogr.* **2008**, *64*, 112–122.

[284] C. F. Macrae, P. R. Edgington, P. McCabe, E. Pidcock, G. P. Shields, R. Taylor, M. Towler, J. van de Streek, *J. Appl. Crystallogr.* **2006**, *39*, 453–457.

[285] D. Hertz, M. N. Leiske, T. Wloka, A. Traeger, M. Hartlieb, M. M. Kessels, S. Schubert, B. Qualmann, U. S. Schubert, *J. Polym. Sci. Part A: Polym. Chem.* **2018**, *56*, 1210–1224.

[286] T. R. Barlow, J. C. Brendel, S. Perrier, *Macromolecules* **2016**, *49*, 6203–6212.

[287] P. K. Singh, B. Bhattacharya, R. K. Nagarale, S. P. Pandey, K.-W. Kim, H.-W. Rhee, *Synth. Met.* **2010**, *160*, 950–954.

[288] M. Oikawa, M. Ikoma, M. Sasaki, *Eur. J. Org. Chem.* **2011**, *24*, 4654–4666.

[289] J. H. Reed, P. A. Donets, S. Miaskiewicz, N. Cramer, *Angew. Chem. Int. Ed.* **2019**, *58*, 8893–8897.

[290] X.-H. Hu, J. Zhang, X.-F. Yang, Y.-H. Xu, T.-P. Loh, *J. Am. Chem. Soc.* **2015**, *137*, 3169–3172.

[291] S. Krishnamurthy, J. Venkataprasad, T. Chand Vagvala, T. Moriguchi, A. Tsuge, *RSC Adv.* **2015**, *5*, 52154–52160.

[292] S. Breitfelder, A. C. Schuemacher, T. Rölle, M. Kikuchi, R. W. Hoffmann, *Helv. Chim. Acta* **2004**, *87*, 1202–1213.

[293] M. P. Dwyer, K. M. Keertikar, C. A. Coburn, H. Wu, B. Hu, B. Zhong, C. Zhang, Z. Dan, L. Tong, W. Yu, Merck Sharp & Dohme Corp., WO2012041227 A1, **2012**.

[294] C. Sun, X. Lin, S. M. Weinreb, *J. Org. Chem.* **2006**, *71*, 3159–3166.

[295] Y. Kohsaka, T. Kurata, T. Kitayama, *Polym. Chem.* **2013**, *4*, 5043.

[296] S. F. Reed, M. G. Baldwin, *J. Polym. Sci. A Gen. Pap.* **1964**, *2*, 1355–1363.

[297] M. Dieckmann, D. Menche, *Org. Lett.* **2013**, *15*, 228–231.

[298] P. R. Sudina, D. R. Motati, A. Seema, *J. Nat. Prod.* **2018**, *81*, 1399–1404.

[299] K. Annadi, A. G. H. Wee, *Arkivoc* **2014**, *6*, 108–126.

[300] H. Chen, B. Wang, J. Zhang, C. Nie, F. Lv, L. Liu, S. Wang, *Chem. Commun.* **2015**, *51*, 4036–4039.

6.2 List of Figures

6.3 Abbreviations

ACVA	4,4'-azobis(4-cyanovaleric acid)
AGE	allyl glycidyl ether
AIBN	azobisisobutyronitrile
aq.	aqueous
ATRP	atom transfer radical polymerization
BHT	2,6-di-*tert*-butyl-4-methylphenol
BnGE	benzyl glycidyl ether
Boc	*tert*-butyloxycarbonyl
br s	broad singlet
*n*BuLi	*n*-butyllithium
CH	cyclohexane
CPADB	4-cyano-4-(phenylcarbonothioylthio)valeric acid
CPADTTC	4-(dodecylthiocarbonothioylthio)-4-cyanovaleric acid
CPATTC	4-((((2-carboxyethyl)thio)carbonothioyl)thio)-4-cyanovaleric acid
CPzCD	2-cyanobutan-2-yl 4-chloro-3,5-dimethylpyrazole-1-carbodithioate
Cryo-TEM	cryogenic transmission electron microscopy
d	doublet
$Đ$	dispersity
DB18C6	dibenzo-18-crown-6
DCM	dichloromethane
DCC	*N*,*N*'-dicyclohexylcarbodiimide
ECH	epichlorohydrin
dd	doublet of doublet
ddd	doublet of doublet of doublet
dddd	doublet of doublet of doublet of doublet
ddt	doublet of doublet of triplet
DIPEA	Hünig's base (*N*,*N*-diisopropylethylamine)
DLS	dynamic light scattering
DMAc	*N*,*N*-dimethylacetamide
DMF	*N*,*N*-dimethylformamide
DMP	Dess–Martin periodinane
DMPA	2,2-dimethoxy-2-phenylacetophenone
DMSO	dimethyl sulfoxide
DNA	deoxyribonucleic acid
DoF	degree of functionalization
DP	degree of polymerization
dq	doublet of quartet
dt	doublet of triplet
EA	ethyl acetate
ECH	epichlorohydrin
e.g.	*exempli gratia*

EGME	2-methoxyethanol
EI-MS	electron ionization mass spectrometry
eq.	equivalent
et al.	*et alia*
HFIP	hexafluoro-2-propanol
HIm	imidazole
HMTETA	1,1,4,7,10,10-hexamethyltriethylenetetramine
IPECs	interpolyelectrolyte complexes
KHMDS	potassium bis(trimethylsilyl)amide
LAMs	less activated monomers
LGE	lauryl glycidyl ether
m	multiplet
*m*CPBA	*meta*-chloroperoxybenzoic acid
Me_4Cyclam	1,4,8,11-Tetramethyl-1,4,8,11-tetraazacyclotetradecane
Me_6TREN	tris[2-(dimethylamino)ethyl]amine
MAMs	more activated monomers
MIF	mean fluorescence intensity
MMA	methyl methacrylate
mPEO-NH_2	α-methoxy-ω-amino poly(ethylene oxide)
mRNA	messenger ribonucleic acid
Ms	mesyl
NHS	*N*-hydroxysuccinimide
NMR	nuclear magnetic resonance
MTT	3-(4,5-dimethylthiazol-2-yl)-2,5-diphenyltetrazolium bromide
p	quintet
P2VP	poly(2-vinylpyridine)
PAGE	poly(allyl glycidyl ether)
pDNA	plasmid deoxyribonucleic acid
PEI	linear poly(ethylene imine)
PEO	poly(ethylen oxide)
PG	protecting group
PMB	*para*-methoxybenzyl
PMMA	poly(methyl methacrylate)
PPFPMA	poly(pentafluorophenyl methacrylate)
ppm	parts per million
P*t*BGE	poly(*tert*-butyl glycidyl ether)
q	quartet
RAFT	reversible addition-fragmentation chain-transfer
R_f	retention factor
RFU	relative fluorescence unit
RISC	RNA-induced silencing complex
RNA	ribonucleic acid

RT	room temperature
s	singlet
SEC	size exclusion chromatography
SEM	2-(trimethylsilyl)ethoxymethyl
siRNA	small interfering ribonucleic acid
ssMAS	^{13}C solid-state magic angle spinning NMR
t	triplet
td	triplet of doublet
TBAB	tetra-*n*-butylammonium bromide
TBAF	tetra-*n*-butylammonium fluoride
TBS	*tert*-butyldimethylsilyl
TEM	transmission electron microscopy
Tf	triflyl
TFA	trifluoroacetic acid
TFE	2,2,2-trifluoroethanol
THF	tetrahydrofuran
TLC	thin-layer chromatography
TPMA	tris(2-pyridylmethyl)amine
t_R	retention time
Trt	trityl
Ts	tosyl
TTEGE	2-(tritylthio)ethyl glycidyl ether
UHPLC/HRMS	Ultra high performance liquid chromatography coupled with high resolution mass spectrometry
UV	ultraviolet

6.4 Analytical Data

6.4.1 NMR Spectra

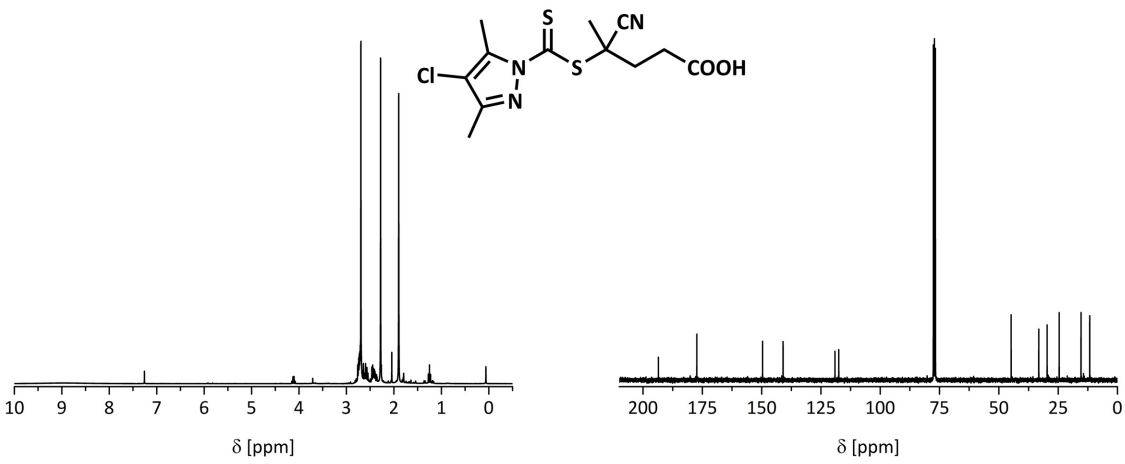

Figure 6.1: ^{1}H NMR spectrum (left) and ^{13}C NMR spectrum (right) of **12** in $CDCl_3$.

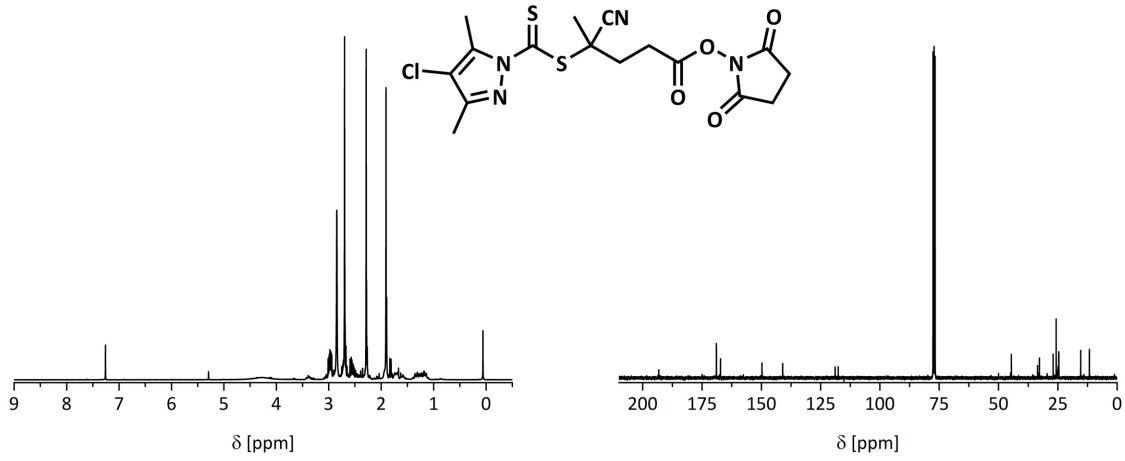

Figure 6.2: ^{1}H NMR spectrum (left) and ^{13}C NMR spectrum (right) of **13** in $CDCl_3$.

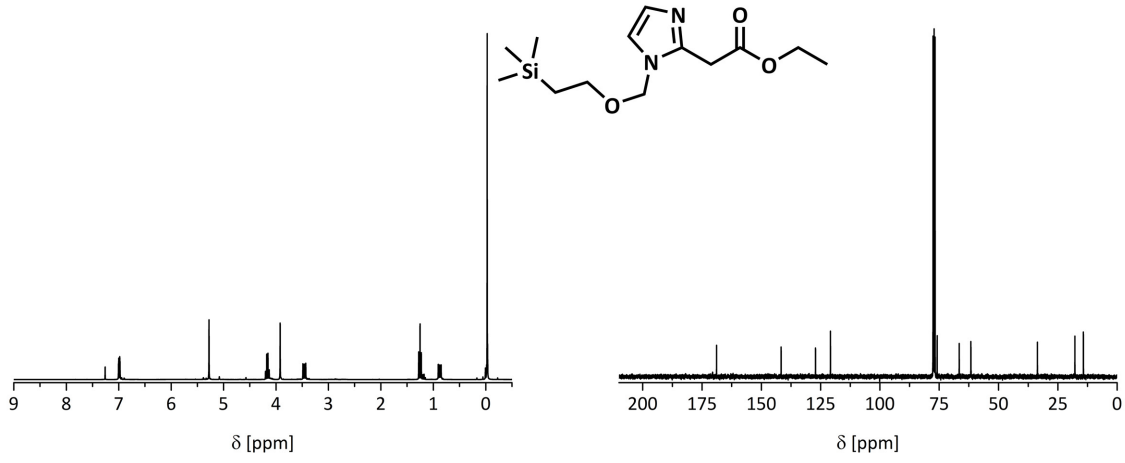

Figure 6.3: ^{1}H NMR spectrum (left) and ^{13}C NMR spectrum (right) of **29** in $CDCl_3$.

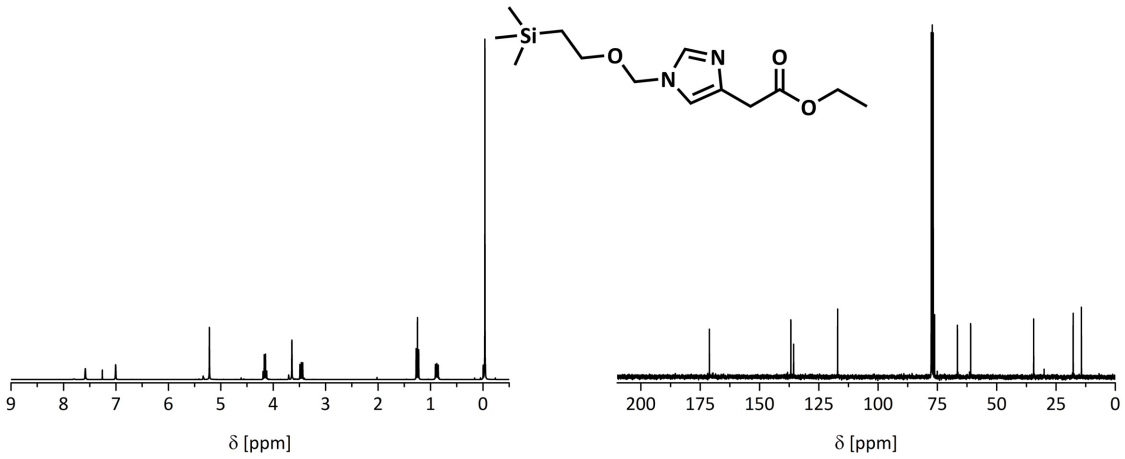

Figure 6.4: ^{1}H NMR spectrum (left) and ^{13}C NMR spectrum (right) of **40** in $CDCl_3$.

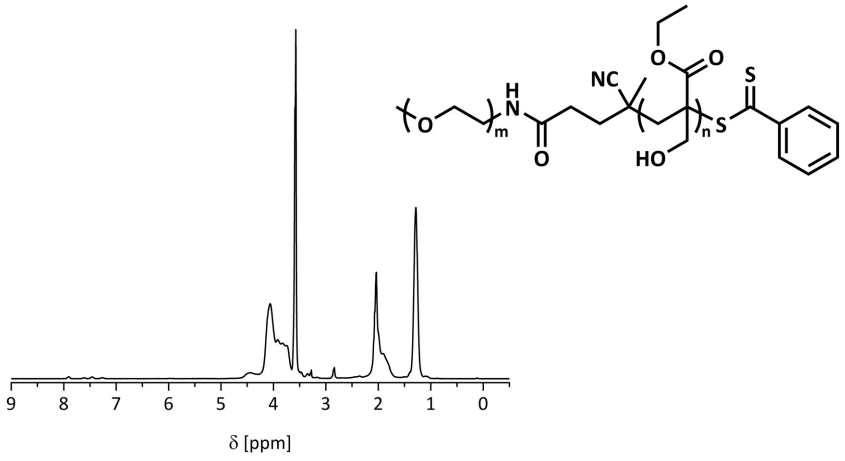

Figure 6.5: ^{1}H NMR spectrum of **54** in acetone-d_6.

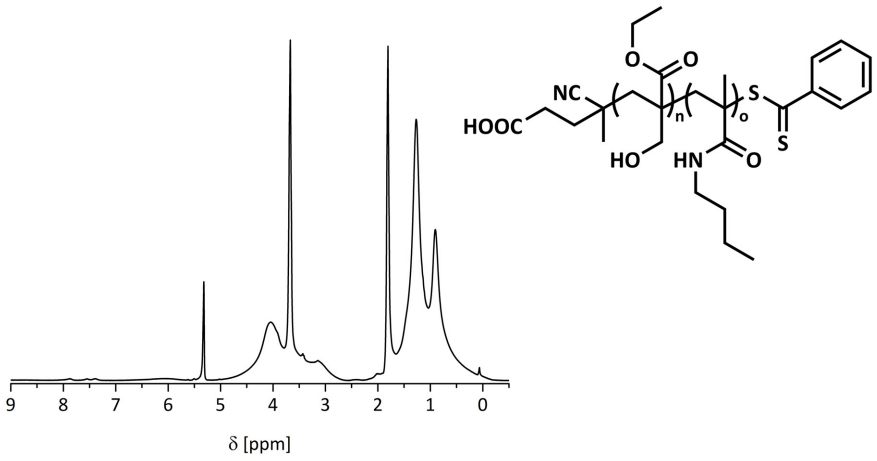

Figure 6.6: ^{1}H NMR spectrum of **56** in CD_2Cl_2.

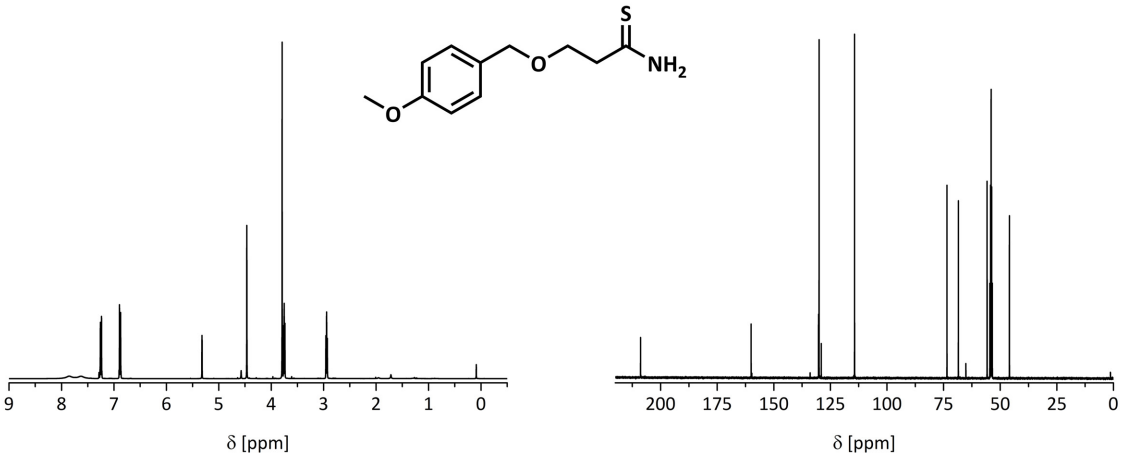

Figure 6.7: ^{1}H NMR spectrum (left) and ^{13}C NMR spectrum (right) of **68a** in CD_2Cl_2.

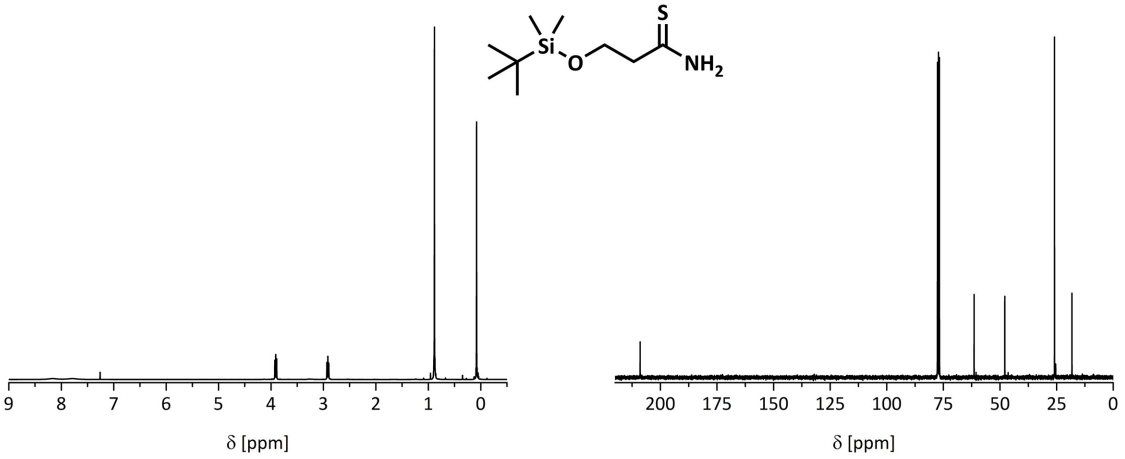

Figure 6.8: ^{1}H NMR spectrum (left) and ^{13}C NMR spectrum (right) of **68b** in $CDCl_3$.

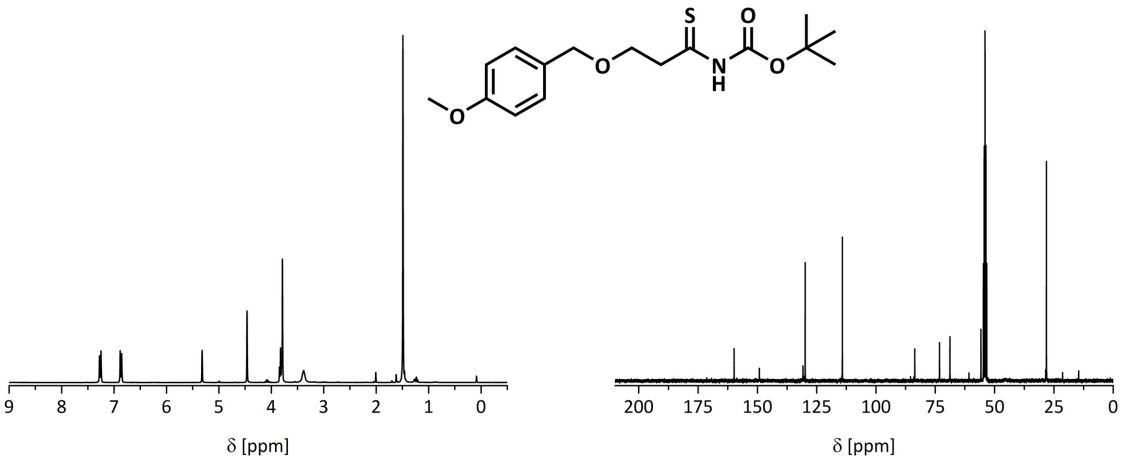

Figure 6.9: ^{1}H NMR spectrum (left) and ^{13}C NMR spectrum (right) of **69a** in CD_2Cl_2.

Figure 6.10: ^{1}H NMR spectrum (left) and ^{13}C NMR spectrum (right) of **69b** in $CDCl_3$.

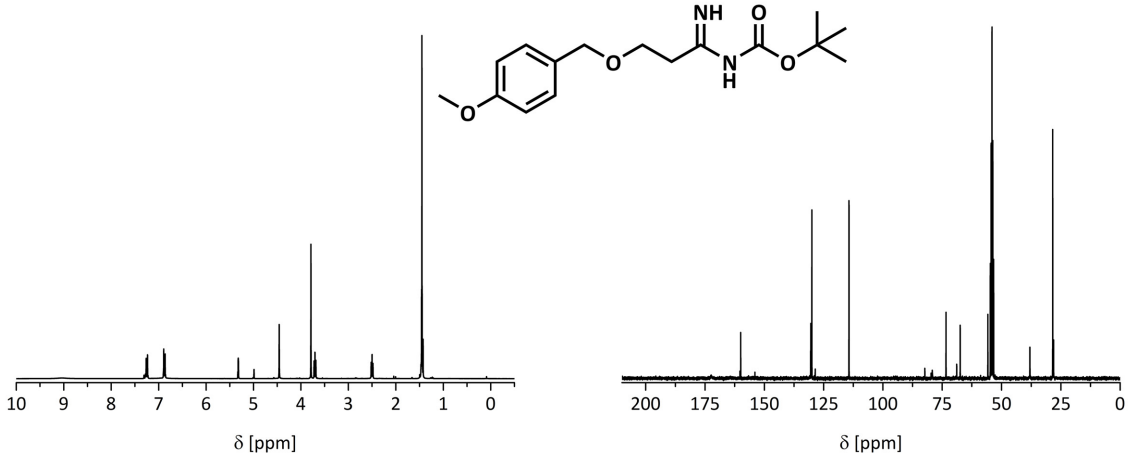

Figure 6.11: ^{1}H NMR spectrum (left) and ^{13}C NMR spectrum (right) of **70a** in CD_2Cl_2.

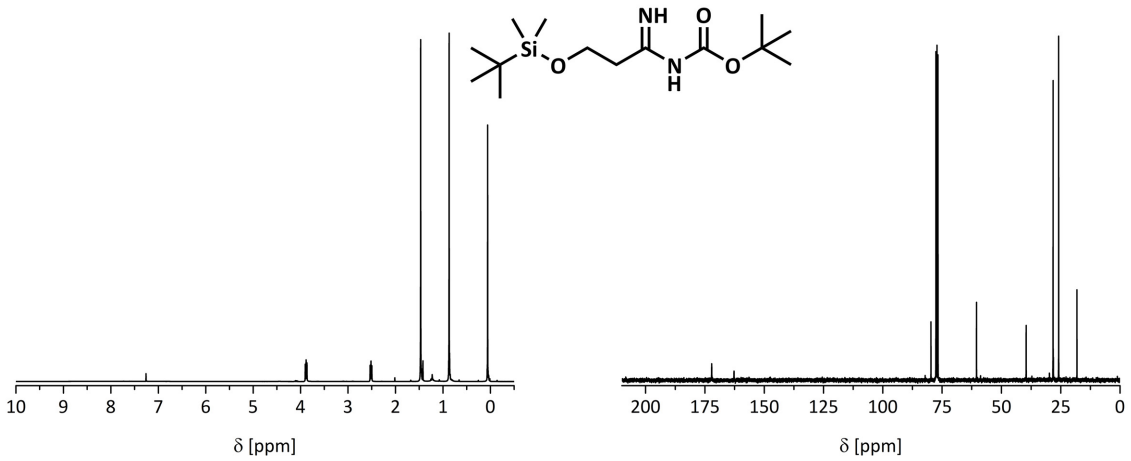

Figure 6.12: ^{1}H NMR spectrum (left) and ^{13}C NMR spectrum (right) of **70b** in $CDCl_3$.

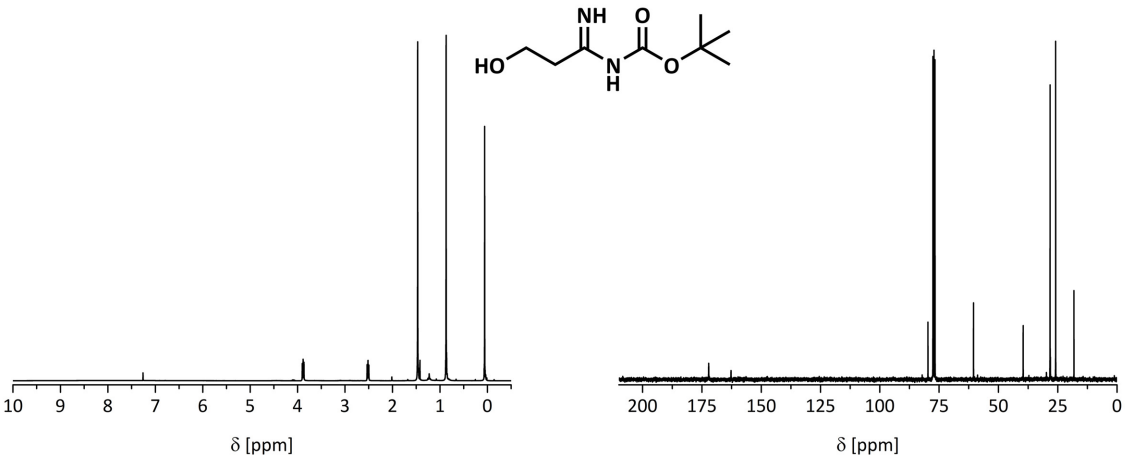

Figure 6.13: ^{1}H NMR spectrum (left) and ^{13}C NMR spectrum (right) of **71** in $CDCl_3$.

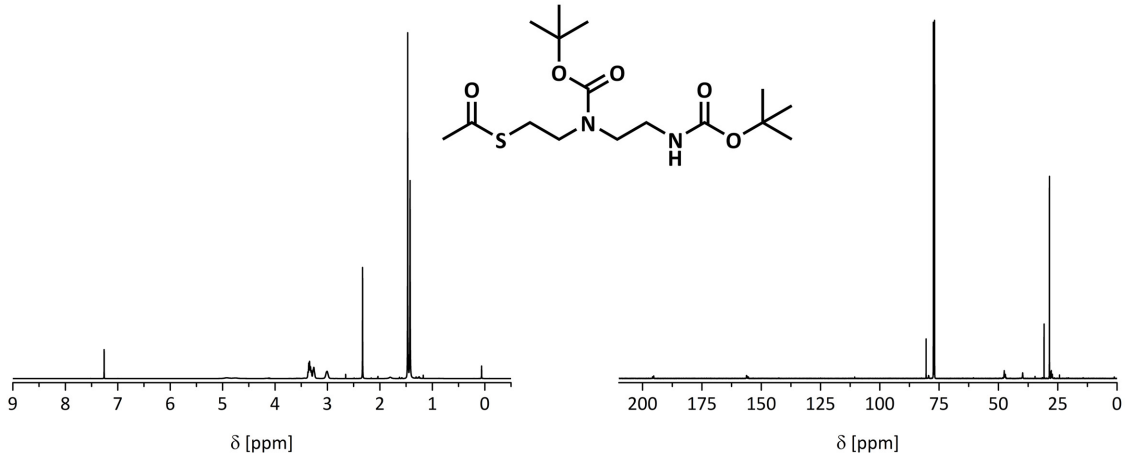

Figure 6.14: ^{1}H NMR spectrum (left) and ^{13}C NMR spectrum (right) of **75** in $CDCl_3$.

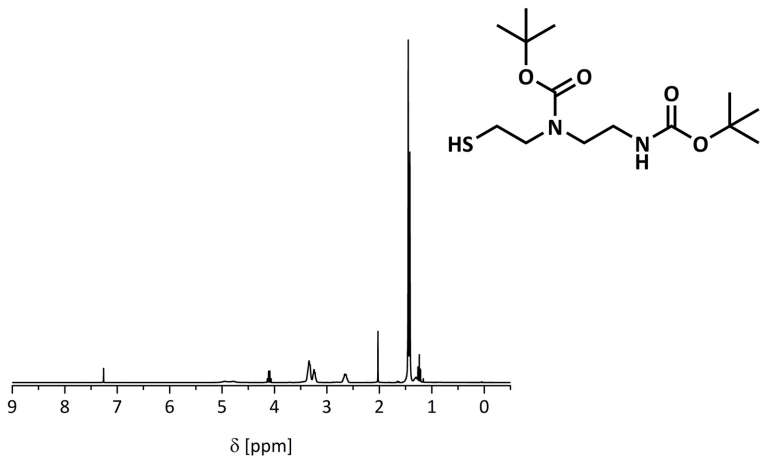

Figure 6.15: ^{1}H NMR spectrum of **76** in $CDCl_3$.

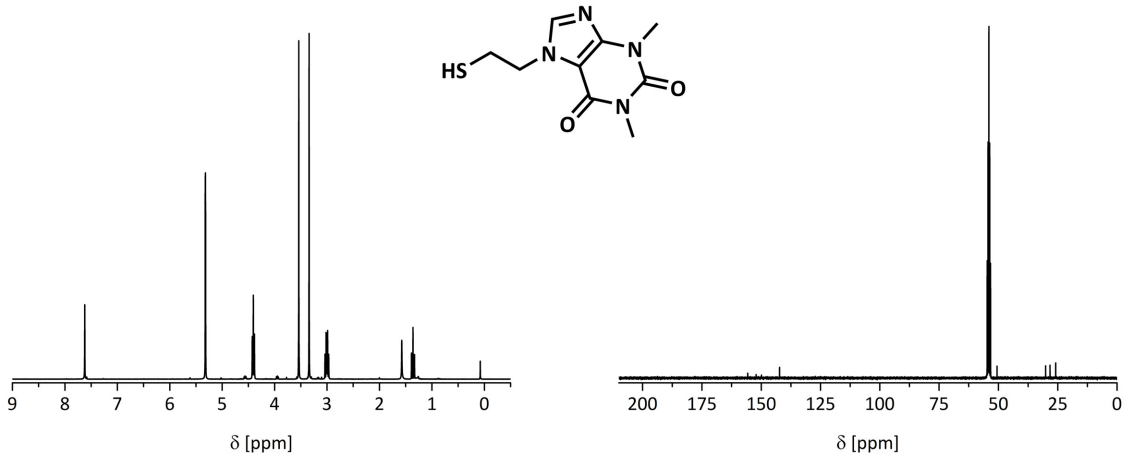

Figure 6.16: ^{1}H NMR spectrum (left) and ^{13}C NMR spectrum (right) of **83** in CD_2Cl_2.

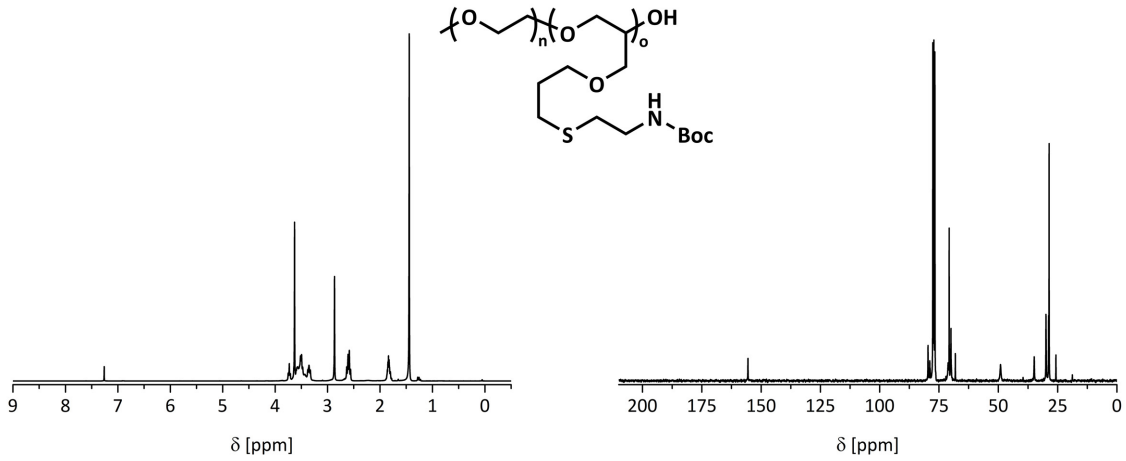

Figure 6.17: ^{1}H NMR spectrum (left) and ^{13}C NMR spectrum (right) of **84** in $CDCl_3$.

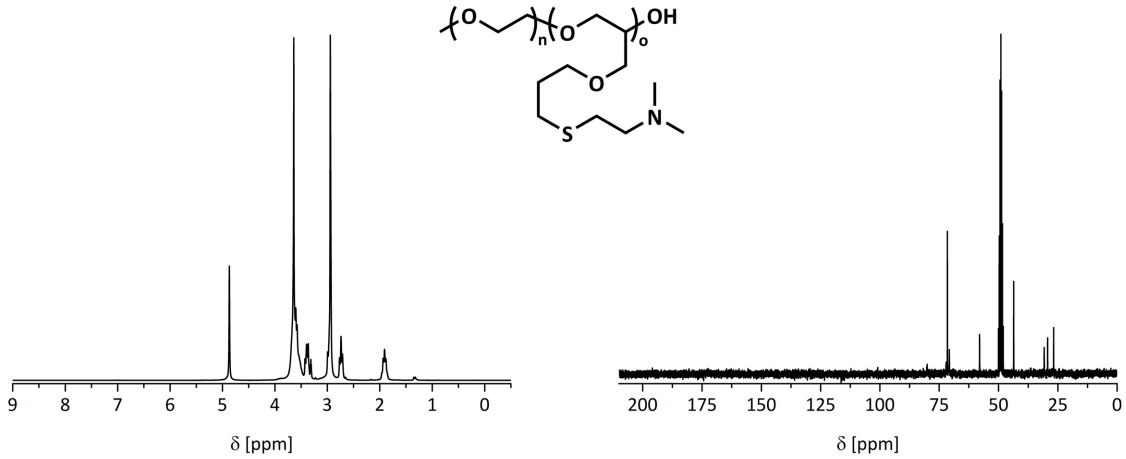

Figure 6.18: ^{1}H NMR spectrum (left) and ^{13}C NMR spectrum (right) of **85** in MeOD-d_4.

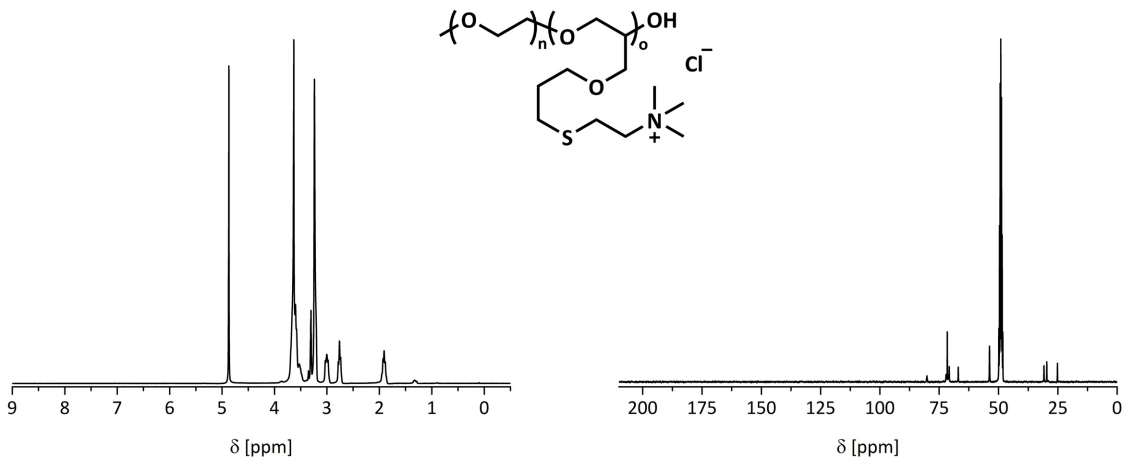

Figure 6.19: ^{1}H NMR spectrum (left) and ^{13}C NMR spectrum (right) of **86** in MeOD-d_4.

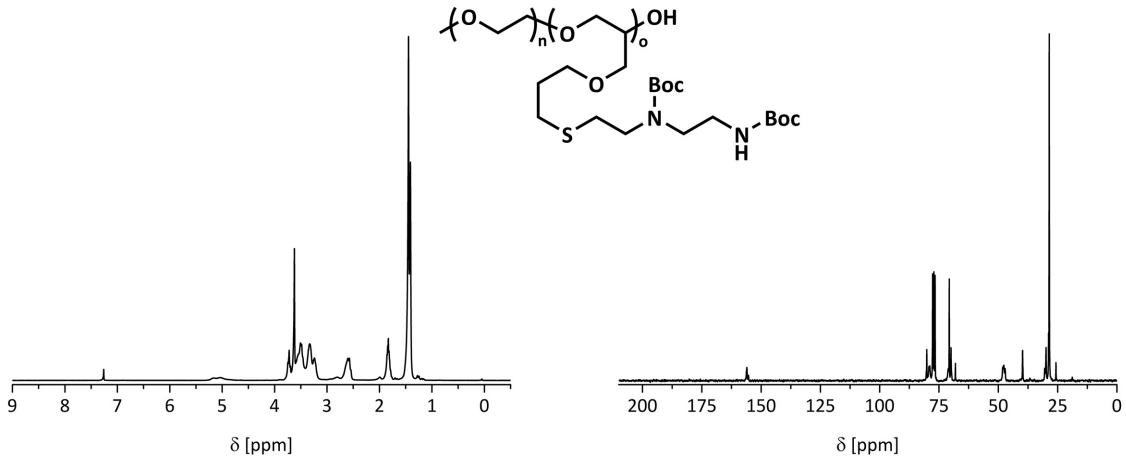

Figure 6.20: ^{1}H NMR spectrum (left) and ^{13}C NMR spectrum (right) of **87** in $CDCl_3$.

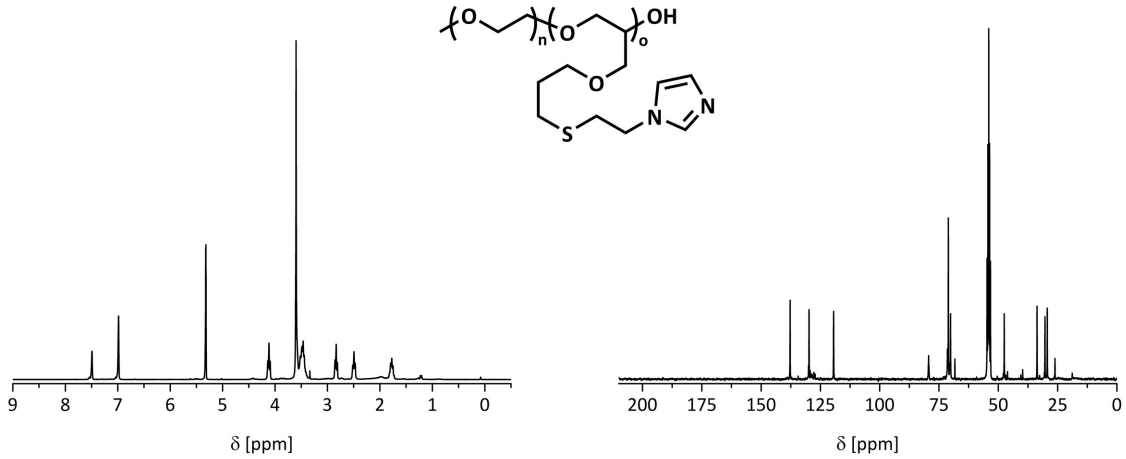

Figure 6.21: ^{1}H NMR spectrum (left) and ^{13}C NMR spectrum (right) of **89** in CD_2Cl_2.

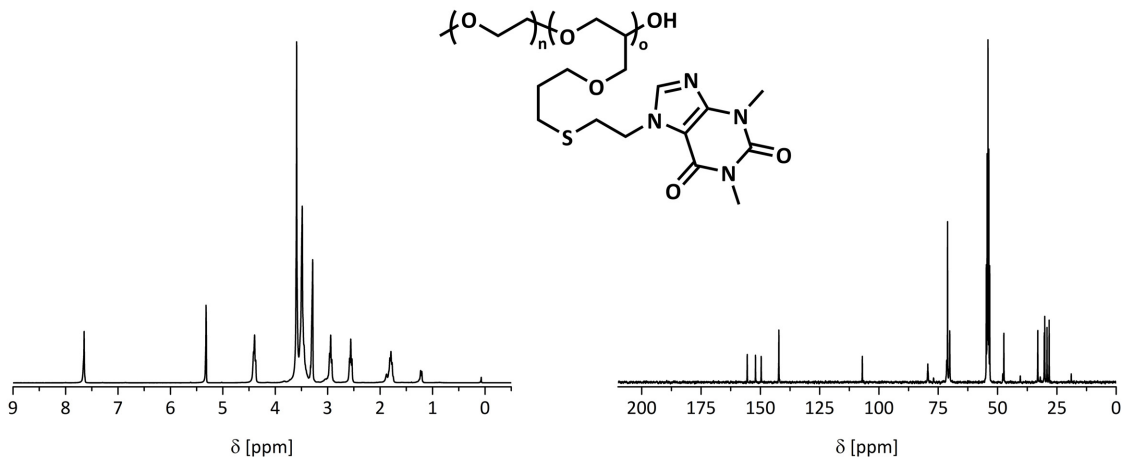

Figure 6.22: ^{1}H NMR spectrum (left) and ^{13}C NMR spectrum (right) of **91** in CD_2Cl_2.

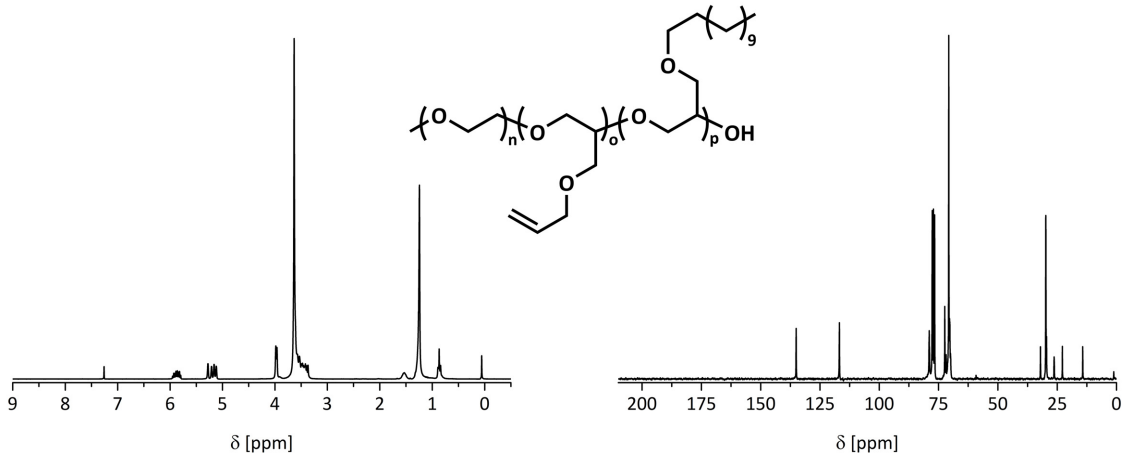

Figure 6.23: ^{1}H NMR spectrum (left) and ^{13}C NMR spectrum (right) of **102** in $CDCl_3$.

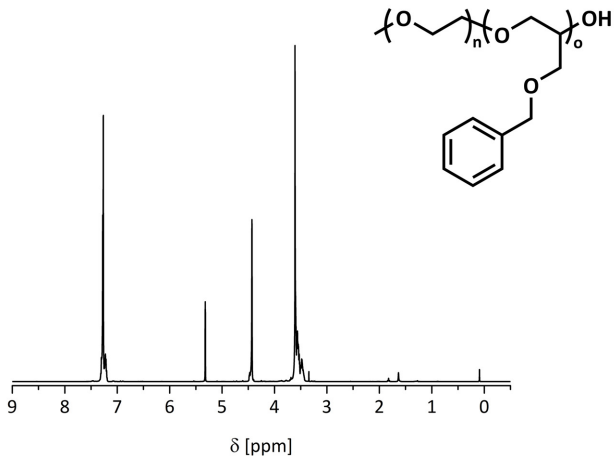

Figure 6.24: ^{1}H NMR spectrum of **103a** in CD_2Cl_2.

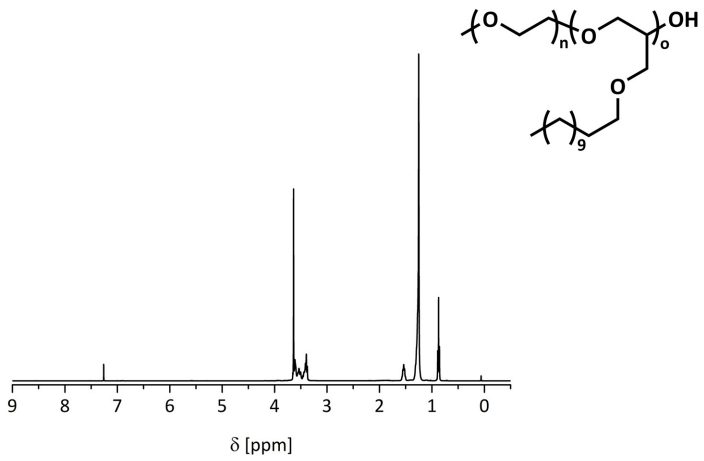

Figure 6.25: ^{1}H NMR spectrum of **104a** in $CDCl_3$.

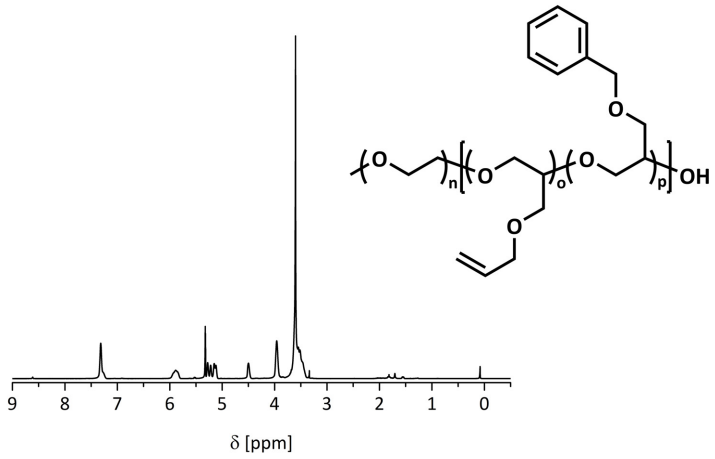

Figure 6.26: ^{1}H NMR spectrum of **105** in CD_2Cl_2.

6.4.2 Crystallographic Data of X-Ray Measurements

Substance	Ethyl 2-(1-tritylimidazol-4-yl)acrylate **41**
Sum formula	$C_{27}H_{24}N_2O_2$
Molar Mass Mr	408.48 g·mol^{-1}
Temperature	133(2) K
Wavelength	0.71073 Å
Crystal system	Monoclinic
Space group	$P2_1/n$
Unit cell dimensions	
a	8.7993(2) Å
b	26.5652(6) Å
c	9.7233(3) Å
α	90°
β	111.312(1)°
γ	90°
Volume	2117.44(9) Å^3
Z	4
Density (calculated)	1.281 Mg·m^3
Absorption coefficient	0.081 mm^{-1}
F(000)	864
Crystal size	0.144 x 0.132 x 0.102 mm
Θ range for data collection	2.92 to 27.42°
Reflections collected	14317
Independent reflections	4801 (R_{Int}=0.0273)
Completeness to Θ_{max}	99.2%
Absorption correction	Semi-empirical from equivalents
Max. and min. transmission	0.7456 and 0.6973
Refinement method	Full-matrix least-squares on F^2
Data/restraints/parameters	4801/0/376
Goodness of fit F^2	1.058
Final R Indices [$I>2\sigma(I)$]	R1=0.0393, wR2=0.0890
R Indices (all data)	R1=0.0450, wR2=0.0927
Largest diff. peak and hole	0.304 and -0.211 eÅ^{-3}

Substance	*tert*-Butyl (3-hydroxy-1-iminopropyl)carbamate (**69**)
Sum formula	$C_8H_{16}N_2O_3$
Molar Mass Mr	188.23 g·mol^{-1}
Temperature	133(2) K
Wavelength	0.71073 Å
Crystal system	Orthorhombic
Space group	P c a 21
Unit cell dimensions	
a	24.4103(7) Å
b	5.7988(2) Å
c	24.3496(6) Å
α	90°
β	90°
γ	90°
Volume	4011.5(2) Å^3
Z	16
Density (calculated)	1.247 Mg·m^3
Absorption coefficient	0.095 mm^{-1}
F(000)	1632
Crystal size	0.088 x 0.082 x 0.074 mm
Θ range for data collection	1.433 to 27.484°
Reflections collected	33215
Independent reflections	8775 (R_{Int}=0.0748)
Completeness to Θ=25.2°	99.4%
Absorption correction	Semi-empirical from equivalents
Max. and min. transmission	0.7456 and 0.5728
Refinement method	Full-matrix least-squares on F^2
Data/restraints/parameters	8775/313/481
Goodness of fit F^2	2.234
Final R Indices [$I>2\sigma(I)$]	R1=0.1755, wR2=0.4783
R Indices (all data)	R1=0.1801, wR2=0.4832
Largest diff. peak and hole	1.697 and -0.830 eÅ^{-3}

Substance	3-((*tert*-Butoxycarbonyl)amino)-3-oxopropyl thioacatate (**71**)
Sum formula	$C_{10}H_{17}NO_4S$
Molar Mass Mr	247.31 g·mol^{-1}
Temperature	133(2) K
Wavelength	0.71073 Å
Crystal system	Triclinic
Space group	$P\bar{1}$
Unit cell dimensions	
a	9.8047(3) Å
b	11.7206(4) Å
c	12.2350(4) Å
α	107.012(1)°
β	103.466(2)°
γ	97.704(1)°
Volume	1276.25(7) Å^3
Z	4
Density (calculated)	1.287 Mg·m^3
Absorption coefficient	0.253 mm^{-1}
F(000)	528
Crystal size	0.134 x 0.122 x 0.098 mm
Θ range for data collection	2.12 to 27.84°
Reflections collected	14890
Independent reflections	5794 (R_{Int}=0.0298)
Completeness to Θ_{max}	99.0%
Absorption correction	Semi-empirical from equivalents
Max. and min. transmission	0.7456 and 0.6952
Refinement method	Full-matrix least-squares on F^2
Data/restraints/parameters	5794/0/305
Goodness of fit F^2	1.052
Final R Indices [$I>2\sigma(I)$]	R1=0.0413, wR2=0.0839
R Indices (all data)	R1=0.0516, wR2=0.0892
Largest diff. peak and hole	0.298 and -0.301 eÅ^{-3}

Substance	2-(Imidazol-1-yl)ethyl thioacetate (**75**)
Sum formula	$C_7H_{10}N_2OS$
Molar Mass Mr	170.23 g·mol^{-1}
Temperature	133(2) K
Wavelength	0.71073 Å
Crystal system	Monoclinic
Space group	P21/c
Unit cell dimensions	
a	14.3232(6) Å
b	5.3128(2) Å
c	10.9732(5) Å
α	90°
β	92.328(2)°
γ	90°
Volume	834.33(6) Å^3
Z	4
Density (calculated)	1.355 Mg·m^3
Absorption coefficient	0.331 mm^{-1}
F(000)	360
Crystal size	0.088 x 0.082 x 0.078 mm
Θ range for data collection	2.847 to 27.468°
Reflections collected	6312
Independent reflections	1902 (R_{Int}=0.0262)
Completeness to Θ=25,2°	99.9%
Absorption correction	Semi-empirical from equivalents
Max. and min. transmission	0.7456 and 0.7009
Refinement method	Full-matrix least-squares on F^2
Data/restraints/parameters	1902/0/140
Goodness of fit F^2	1.061
Final R Indices [$I>2\sigma(I)$]	R1=0.0288, wR2=0.0661
R Indices (all data)	R1=0.0325, wR2=0.0680
Largest diff. peak and hole	0.257 and -0.201 eÅ^{-3}

Substance	*N*-(*tert*-Butyloxycarbonyl)-4-(2-(acetylthio)ethyl)imidazole (**78**)
Sum formula	$C_{12}H_{18}N_2O_3S$
Molar Mass Mr	270.34 g·mol^{-1}
Temperature	133(2) K
Wavelength	0.71073 Å
Crystal system	Monoclinic
Space group	$P2_1/c$
Unit cell dimensions	
a	5.8759(1) Å
b	22.0996(6) Å
c	10.5905(3) Å
α	90°
β	96.301(2)°
γ	90°
Volume	1366.92(6) Å^3
Z	4
Density (calculated)	1.314 Mg·m^3
Absorption coefficient	0.239 mm^{-1}
F(000)	576
Crystal size	0.122 x 0.102 x 0.088 mm
Θ range for data collection	2.67 to 27.48°
Reflections collected	17863
Independent reflections	3133 (R_{Int}=0.0906)
Completeness to Θ_{max}	99.8%
Absorption correction	Semi-empirical from equivalents
Max. and min. transmission	0.7456 and 0.6761
Refinement method	Full-matrix least-squares on F^2
Data/restraints/parameters	3133/0/167
Goodness of fit F^2	1.054
Final R Indices [$I>2\sigma(I)$]	R1=0.0419, wR2=0.0868
R Indices (all data)	R1=0.0530, wR2=0.0920
Largest diff. peak and hole	0.320 and -0.272 eÅ^{-3}

Substance	2-(Theophyllin-7-yl)ethyl thioacetate (**80**)
Sum formula	$C_{11}H_{14}N_4O_3S$
Molar Mass Mr	282.32 g·mol^{-1}
Temperature	133(2) K
Wavelength	0.71073 Å
Crystal system	Monoclinic
Space group	$P2_1/c$
Unit cell dimensions	
a	7.2544(1) Å
b	8.1490(2) Å
c	22.0325(6) Å
α	90°
β	90.679(1)°
γ	90°
Volume	1302.38(5) Å^3
Z	4
Density (calculated)	1.440 Mg·m^3
Absorption coefficient	0.259 mm^{-1}
F(000)	592
Crystal size	0.108 x 0.098 x 0.078 mm
Θ range for data collection	2.81 to 27.45°
Reflections collected	10209
Independent reflections	2962 (R_{Int}=0.0323)
Completeness to Θ_{max}	99.4%
Absorption correction	Semi-empirical from equivalents
Max. and min. transmission	0.7456 and 0.7088
Refinement method	Full-matrix least-squares on F^2
Data/restraints/parameters	2962/0/228
Goodness of fit F^2	1.082
Final R Indices [$I>2\sigma(I)$]	R1=0.0364, wR2=0.0896
R Indices (all data)	R1=0.0402, wR2=0.0917
Largest diff. peak and hole	0.429 and -0.303 eÅ^{-3}

Substance	2-(Tritylthio)ethyl glycidyl ether (**105**)
Sum formula	$C_{24}H_{24}O_2S$
Molar Mass Mr	376.49 g·mol^{-1}
Temperature	133(2) K
Wavelength	0.71073 Å
Crystal system	Triclinic
Space group	P$\bar{1}$
Unit cell dimensions	
a	7.7603(2) Å
b	10.2229(3) Å
c	12.4459(3) Å
α	91.892(2)°
β	97.875(2)°
γ	90.9630(10)°
Volume	977.30(4) Å^3
Z	2
Density (calculated)	1.279 Mg·m^3
Absorption coefficient	0.182 mm^{-1}
F(000)	400
Crystal size	0.108 x 0.102 x 0.088 mm
Θ range for data collection	1.99 to 27.43°
Reflections collected	5897
Independent reflections	4310 (R_{Int}=0.0165)
Completeness to Θ_{max}	96.6%
Absorption correction	Semi-empirical from equivalents
Max. and min. transmission	0.7455 and 0.6803
Refinement method	Full-matrix least-squares on F^2
Data/restraints/parameters	4310/0/254
Goodness of fit F^2	0.985
Final R Indices [$I>2\sigma(I)$]	R1=0.0431, wR2=0.1023
R Indices (all data)	R1=0.0470, wR2=0.1062
Largest diff. peak and hole	0.580 and -0.512 eÅ^{-3}

6.5 Acknowledgments

First, I would like to thank my supervisor Prof. Dr. Felix H. Schacher for the opportunity to undertake research on chargeable polymers for application in a range of areas such as gene and drug delivery in cooperation with the Institute of Biochemistry and the University hospital. Furthermore, I am grateful for his support throughout my PhD, sharing his expertise in Macromolecular Chemistry, giving different views on research, and for providing flexibility in the project structure, which resulted in a higher percentage of small molecule synthesis. I would also like to thank Felix for giving me the opportunity to attend so many conferences such as Freiburg, Mainz, and Heraklion.

I would also like to give special thanks to Dr. Jessica Tom for correcting this thesis in detail, for our fruitful discussions about the RAFT technique, interesting as well as sometimes amusing conversations in the office, and her support to further improve my English.

Furthermore, I want to thank all my project partners: Annemarie Landmann and David Hertz from the Institute of Biochemistry on the project of gene delivery; Jessica Hoff, Wanling Foo, Dr. Adrian T. Press, and Dr. Anuradha Ramoji from the University Hospitel; as well as Shotaro Miwa, Rintaro Takahashi, and Prof. Dr. Kazuo Sakurai from the University of Kitakyushu in Japan for their help on the investigation of triblock terpolymers for drug and gene delivery.

I am also grateful for the supporting work carried out by Frieda Nagler, Yannik Köster, Martin Riske, and Niklas A. Hempel in the context of either a bachelor thesis or scientific internship. It was a real pleasure to work together in the lab, and I am happy that they all endured my annoying specific questions, which hopefully expanded their knowledge.

In addition, I thank Dr. Johannes C. Brendel for all the explanations and advice concerning RAFT polymerization, which helped me gain a much deeper understanding of the kinetics and reaction mechanism. I am most grateful to Veselin Nasufovic, Frédéric Gaigne, and especially Marino Wirgenings for their help solving difficult synthetic problems. In addition to partaking in helpful scientific discussions with me, Marino helped me out when I was in desperate need of glassware or chemicals.

I would also like to thank all the members of the research group, past and present, for the great atmosphere. It was not without its ups and downs, but overall we had many interesting conversations, and quite a few fun times together. I appreciated the important distractions from the daily laboratory work in the form of coffee breaks, playing card games and table tennis. Thanks to Dr. Jessica Tom, Dr. Mark Billing, Dr. Felix Wendler, Dr. Philip Biehl, Dr. Moritz von der Lühe, Dr. Christoph Hörenz, Dr. Oliver Grimm, Dr. Iiulia Romanenko, Moritz Köhler, Johannes Max, Kathrin Kowalczuk, Peter Mons, Johanna Elter, Jonas Eichhorn, Frieda Nagler, Lisa Wiedenhöft, Oliver Eckardt, Yves Carstensen, Katja König, Viktoria Rothleitner, Barbara Werner, Robert Deubler, Afshin Nabiyan, and

Jan-Hendrik Kruse. Mark introduced me into the group and supported me at the beginning of my PhD. Philip and Moritz v.L. collaborated with me using my polyampholytes to coat iron oxide nanoparticles, and Moritz K. worked with me on the project of gene delivery. I further appreciate the TEM and cryo-TEM measurements performed by Moritz, Philip, and Moritz. I am also thankful to Dr. Grit Festag, Katja, and Barbara, for performing SEC measurements and also their maintenance of the various SEC devices.

I must also thank Dr. Helmar Görls for the single-crystal X-ray diffraction measurements and evaluation of the data. With his extensive expertise, he was also able to measure samples, which did not perfectly crystallize and which have melting points below 0 °C.

I am further grateful for the helpful lectures of the NMR staff about advanced methods, how to improve measurements, and processing of the FID to obtain better spectra or to extract further information. Moreover, I thank Dr. Peter Bellstedt, Gabriele Sentis, Friederike Pielenz, Bärbel Rambach, and Rica Patzschke for performing various NMR measurements for me, as well as their helpful discussions.

Additionally, I am thankful to Dr. Nico Ueberschaar for the UHPLC/HRMS measurements and joint evaluation that promoted the synthesis of 3-((*tert*-butoxycarbonyl)amino)-3-iminopropyl thioacatate.

For the friendly provision and permission to use the Dieter Hildebrandt caricature, I would like to thank Dieter Hanitzsch.

Finally, I am also very grateful to all my friends and family, especially my parents, sister, uncle, as well as my grandmother for giving me motivation, support, a listening ear to voice my problems to, and for their invaluable advice during my PhD.

6.6 Declaration of Authorship / Selbstständigkeitserklärung

I certify that the here presented work is, to the best of my knowledge, original and the results of my own investigations, except as acknowledged, and has not been submitted, either in part or whole, for a degree at this or any other university.

Ich erkläre, dass ich die vorliegende Arbeit selbständig und unter Verwendung der angegebenen Hilfsmittel, persönlichen Mitteilungen und Quellen angefertigt habe.

Jena, ...

Carsten Rössel